Grainy Head in Wound Healing

Maintaining Identity within Chaos

Inês Rodrigues Silva Cristo

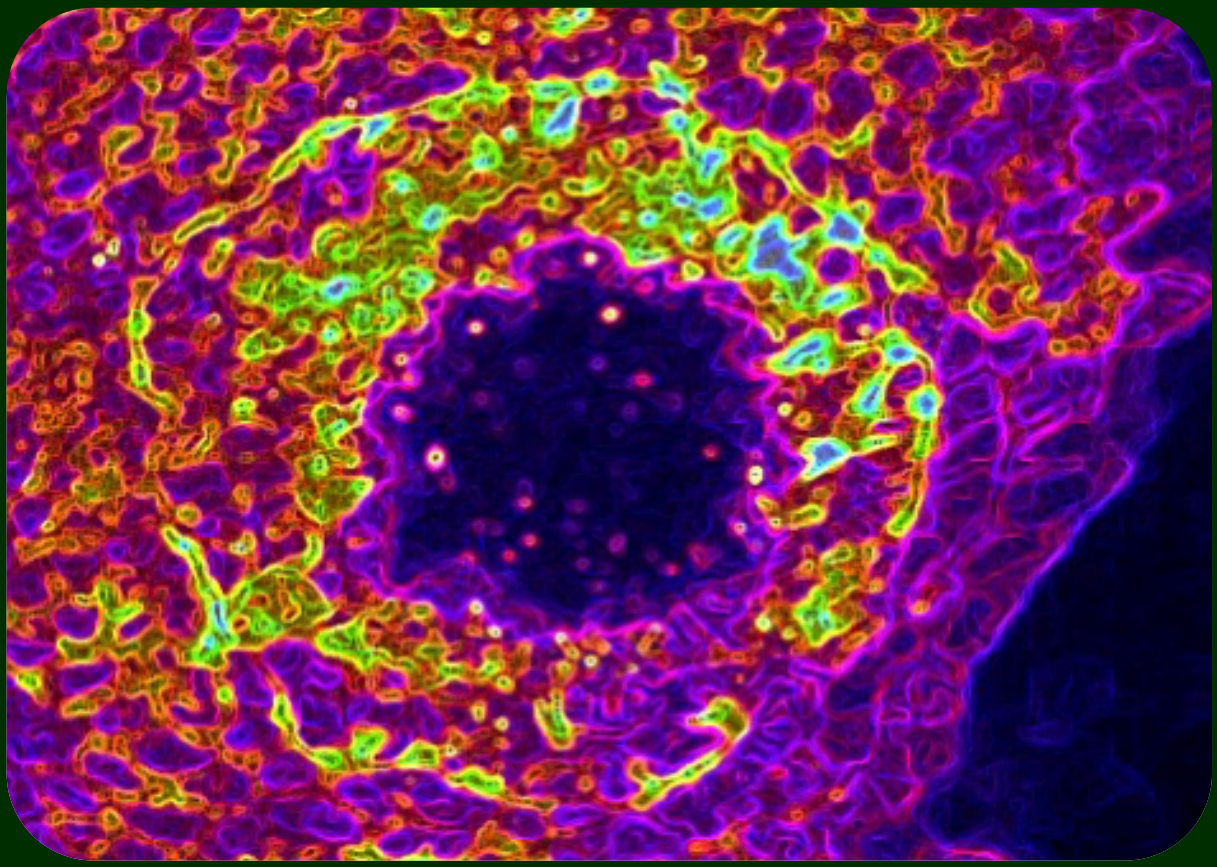

Dissertation presented to obtain the Ph.D degree in Biology

Instituto de Tecnologia Química e Biológica António Xavier | Universidade Nova de Lisboa

Oeiras,
November, 2017

UNIVERSIDADE NOVA DE LISBOA

ITQB-UNL | Av. da República, 2780-157 Oeiras, Portugal
Tel (+351) 214 469 100 | Fax (+351) 214 411 277

www.itqb.unl.pt

Grainy Head in Wound Healing

Maintaining Identity within Chaos

Inês Rodrigues Silva Cristo

Dissertation presented to obtain the Ph.D degree in Biology

Instituto de Tecnologia Química e Biológica António Xavier | Universidade Nova de Lisboa

Research work coordinated by:

Oeiras, November, 2017

The research described in the present thesis was performed at Instituto Gulbenkian de Ciência, Instituto de Medicina Molecular, Faculdade de Medicina, Universidade de Lisboa and at Chronic Diseases Research Center, NOVA Medical School, Universidade Nova de Lisboa, Lisboa, Portugal. This work was accomplished under the supervision of Dr. António Jacinto. Inês Rodrigues Silva Cristo is a student belonging to the PhD Programme at Instituto de Tecnologia Química e Biológica António Xavier (ITQB), Universidade Nova de Lisboa, Portugal.

Financial Support from **Fundação para a Ciência e Tecnologia** (FCT)

Ph.D. Fellowship: SFRH/BD/60401/2009

SUPERVISOR

António Alfredo Coelho Jacinto, PhD

Group leader at Chronic Diseases Research Center (CEDOC), NOVA Medical School, Universidade Nova de Lisboa, Lisboa, Portugal

EXAMINING COMMITTEE

Jean-Léon Maître, PhD *(Principal Examiner)*

Group leader at Genetics and Developmental Biology Unit, Institut Curie, Paris, France

Sérgio Simões, PhD *(Principal Examiner)*

Post-Doctoral Researcher at Department of Cell & Systems Biology, University of Toronto, Toronto, Canada

Rita Teodoro, PhD

Group leader at Chronic Diseases Research Center (CEDOC), NOVA Medical School, Universidade Nova de Lisboa

Pedro Domingos, PhD

Group leader at Instituto de Biologia Química e Tecnológica António Xavier (ITQB), Universidade Nova de Lisboa, Lisboa, Portugal

"*It was the best of times, it was the worst of times, it was the age of wisdom, it was the age of foolishness, it was the epoch of belief, it was the epoch of incredulity, it was the season of Light, it was the season of Darkness, it was the spring of hope, it was the winter of despair (…).*"

In A TALE OF TWO CITIES,

Charles Dickens, 1859

ACKNOWLEDGEMENTS

First of all, I would like to thank my supervisor, António Jacinto, for accepting me in his lab. Although it was a complicated start (and well, I would say a complicated finish too), we did have some fun in the middle of it all (it was a long middle). I want to thank you for teaching me how to really enjoy science, even when things weren't working; for teaching me how to be more patient (and improving my woozaahh skills, while waiting for our meetings - still to be determined if it worked); for always having your office door open and always being available for any question or problem (when you actually were in the office); for accepting everything I had to say (even if sometimes it didn't come with a smile); for saying you "really enjoy" our discussions; and finally, for helping me grow and preparing me for the next step.

I would also like to thank my Thesis Committee members, Leonor Saúde, Susana Lopes and Miguel Godinho Ferreira, for their help and wise advice.

A big thank you to Fernanda Baptista, Silvia Costa and especially Ana Roberto for all the help with the dreaded paperwork, but most importantly for getting António when we couldn't!

To my Tissue Repair peeps past and present included: I salute you in putting up with me and my complaining all this time! Thanks for all the fun and glitter, mad parties and awesome retreats of these last 6 years: to le petit Borbinha, for thinking he can actually reply to everything I say; to Ana Farinho, for her mad cutting skills and EM time; to Mr. Telmissimo, for answering all my stupid computer questions; to "Stop Stop" Paramos, we were short lived neighbors but our love of bacon and real food will endure; to Raquel, my super stylish "OCD sister"; to Marta "Tia da Póboa" Lourenço; to Papá Mesquita; to the honorary lab member "George" Costa; to Suze, I still miss your "como eu te compreendo" (hang in there!); to Sofs, my

“complaining heir”, caretaker of all the Alfredos and Albertos (babe, no fish dies in our watch!); to Miss Lara, for teaching me the wonders of Drosophila and how to deal with a Tequila hangover (both equally useful trades), and for all the help and discussions (in the end it’s always calcium)!

A special thanks to Anabela Bensimon-Brito, Lara Carvalho, Susana Ponte, Raquel Lourenço and Ana Brandão, for reading and correcting this thesis in such short notice! Your help was invaluable!

À D. Graça e ao Sr. Jorge, um muitíssimo obrigado por manterem o Indesit sempre cheio de Ucal fresquinho e Super Bock quente!

A huge shout out to the Paris crew for always having wise solutions to long distance problems: Eric, Boris, Isa, Florencia, José “The Boss” de las Heras, Stéphane, Cata and a special thanks to Diana, for all the good advice and time spent hearing me. Let’s get this party started, people!

A big thanks to the power couple Vanessa and Moritz, for all the nice dinners and awesome conversations!

Um grande obrigada aos rapazes da David de Souza (óptimo nome para o vosso futuro negócio): ao grande Chico e às suas piruetas do demo; ao Bruno e às nossas conversas sobre a filosofia da vida; ao Marco, fellow Tissue Repair member, companheiro de boa música, bons conselhos, desabafos de quem passa pelo mesmo, e aventuras!

À “mamã” Sara, ao Ricardo e ao Rafael: aos encontros de Natal e encorajamento constante, ao desanuvio e às “grandes intervenções”!

À minha trupe de metade de uma vida que vai ficar para sempre: à Rita, à Inês Morujo, à Joana, à Inês Plácido e ao Fred, Rui e Sarah, e ao meu “cachopo” João por tolerarem o facto de não compreenderem os meus horários mas mesmo assim estarem sempre lá quando é preciso!

Um grande e especial obrigada à Anabela Bensimon-Brito (olha para isto! Até levas o nome todo!): pelo “Oláááá eu sou a Inês” e “hmmm olha esta

deve ser porreira", pelas "wine hours", pelo o amor a "manteiga", pelo pragmatismo e abre-olhos, pelo karma partilhado (até dá para antecipar), pela igual satisfação em dizer uma asneira merecida, pelo sentido de justiça, pelo partilhar do pickle do meu hambúrguer, mas acima de tudo pelo teu ódio a "adhesion e cytoskeleton stuff" e por neste momento estar a poder escrever a parte final desta tese graças ao teu esforço de noites mal dormidas nestas últimas semanas. ÉS A MAIOR!

Ao meu tio, primo e avós, obrigada pelo apoio e por acreditarem em mim.

Um grande obrigada aos meus tios e prima "Thunder from Down Under", aos almoços e jantares sempre divertidos (o Cristiano continua a ser o maior!) e aos crash courses de francês em formato SMS.

Por fim, tenho que agradecer à Tríade Maravilha: obrigada por me aturarem, mal ou bem disposta (é igualmente estafante); obrigada pelas noites mal dormidas de preocupação; obrigada pelos risos de felicidade partilhados às refeições; obrigada pelas procissões quinzenais ao nosso local de reza; obrigada pelas discussões acesas e abertas; obrigada pela partilha das vossas histórias vergonhosas de adolescência; obrigada pela nossa união e amizade; obrigada por me apoiarem e acreditarem sempre que isto ia chegar ao fim; obrigada por me ensinarem a ser quem sou. Obrigada por literalmente tudo! Ao meu Pai, pelas poucas, mas sempre certeiras palavras e feitio igual ao meu; à minha Mãe, pelo apoio diário e constante preocupação materna (já não é preciso); e ao meu Irmão, a pessoa mais inteligente e divertida que conheço, pela alegria e boa disposição! Por vocês, tudo!

THESIS PUBLICATIONS

- Cristo, I., Carvalho, L., Ponte, S., Jacinto, A. **Novel role for Grainy head in the regulation of cytoskeletal and junctional dynamics during epithelial repair** (in submission)

ABSTRACT

Epithelial wound healing is an inherent ability of all organisms to deal with aggressions from the surrounding environment and maintain tissue barrier integrity. Wounds can result from accidental trauma, surgery or various pathological conditions. Independently on the cause, all wounds need to be properly solved to avoid complications, ranging from infection to fibrosis and tumour initiation. Understanding the cellular and molecular basis of wound repair is an important asset for biomedical research. The process of wound healing is attained in a highly regulated and efficient manner to ensure correct return to homeostatic conditions. Although wound repair differs in complexity between simple and stratified epithelia, both contexts involve a series of coordinated stages that unfold in a sequential manner: sensing and transmitting the wound signal; reorganizing adhesive complexes and the cytoskeleton; initiating the immune response; and closing the gap and re-establishing of the epithelial barrier. Each of these steps leads to multiple regulatory pathways and several key players converging in one single effort.

Invertebrate simple epithelia, such as in *Drosophila*, have become popular model systems since they allow high resolution live imaging and genetic manipulation. In these tissues, epithelial repair relies on the establishment of a purse string closure method, which involves cellular rearrangements promoted by adhesion and cytoskeletal remodelling and the contractile activity of an actomyosin cable formed at the wound leading edge. This mechanism is conserved in simple epithelia repair across species and it also resembles morphogenetic movements that occur during the developmental of different organisms, like dorsal closure in *Drosophila* or epiboly in Zebrafish embryos. Several regulatory pathways have been proposed to regulate wound closure in simple epithelia. Grainy head (Grh), an essential epithelial transcription factor, is known to be involved in the repair of epithelia. First described in *Drosophila*, Grh and its vertebrate homologues

(Grainyhead-like - Grhl) regulate epithelial formation and differentiation and show a conserved role in the re-establishment of the epidermal barrier upon wounding. In *Drosophila*, Grh regulates the expression of wound response genes upon wounding, to promote cuticle repair in later stages of wound healing. However, little is known about its role in other aspects of the process.

In this study, we use the pupal notum epithelium to analyse the importance of Grh in the first stages of cellular remodelling and cytoskeletal reorganization. In our model system, wounding initiates a series of coordinated flows of calcium, actomyosin filament remodelling and polymerization, and tissue contraction that lead to the formation of the actomyosin cable at the wound edge and consequent closure. We show that, upon wounding, Grh knockdown (KD) leads to defective wound closure. This phenotype correlates with impairment of cytoskeletal reorganization, leading to the formation of an ectopic actomyosin cable away from the wound edge. Moreover, Grh KD leads to the depletion of E-Cadherin (E-Cad) in the cells around the wound site. In the wild-type repair process, E-Cad needs to be downregulated at the wound edge, but only during initial stages, to promote actomyosin cable assembly. This is achieved through the activation of Dorsal (Dl), an effector of the NF-κB pathway. We have observed that, in the Grh KD, E-Cad depletion results from the hyperactivation of Dl. We propose that Grh controls Dl activity upon wounding, in order to tightly regulate the adhesion remodelling levels essential for the tissue to reorganize, while maintaining cortical stability. Furthermore, Grh KD also leads to loss of epithelial identity in cells around the wound, as these cells acquire mesenchymal traits in later stages of the wound healing process. These results uncover a new role for Grh in adhesion regulation and cytoskeletal dynamics, as well as a novel regulatory interaction with the NF-κB pathway.

Another characteristic event upon wounding of the pupal notum epithelium is the increase of intracellular calcium levels in the tissue around the wound, in a wave-like manner. Calcium is fast and pleiotropic signalling molecule, with conserved functions across species. As wound repair entails a fast response from the tissue, calcium is one of the first transcription-independent signals produced immediately after wounding. In this study, we show that the expansion of the calcium flow is a two-staged process: a first expansion that can strongly correlate with the mechanical displacement of the tissue upon wounding; and a second phase, characterized by stochastic calcium flashes that reach further in the tissue, more characteristic of biochemical signalling between cells. We show that, in the Grh KD, high intracellular calcium levels are maintained for a long period of time around the wound. To understand how this deregulation might be occurring, we performed a small screen to identify Grh direct targets that could be responsible for this deregulation. We observed that the loss-of-function of a subset of Grh target genes during wound healing also leads to impaired calcium dynamics. Moreover, calcium levels deregulation was accompanied by alterations of the actin cytoskeleton, leading to impairment in actin cable formation and consequent closure defects. These results show a novel regulation in intracellular calcium dynamics by Grh in pupal notum wound healing and introduce new players in the repair process.

Since the Grhl family of transcription factors seem to have several conserved functions between invertebrate and vertebrate organisms, we decided to characteryze their roles in vertebrate development and repair. For that, we used Zebrafish as a model organism. We first described the expression patterns of *grhl* genes during Zebrafish development, to understand the spatial and temporal distribution of the different transcription factors. Interestingly, we show for the first time the expression of a Grhl transcription factor in the notochord, floor plate and hypochord, axial support structures of the developing organism. This might point to a novel function in

organogenesis for this gene. To address the role in wound repair, we set up a new model system for vertebrate simple wound repair, through laser-based tissue wounding of the Enveloping layer (EVL), the embryonic epithelium of Zebrafish. This system resembles its invertebrate counterpart, achieving closure in a purse string manner but with much faster dynamics. Using morpholino technology, we addressed the role of *grhl2b* and *grhl3* during the repair of the EVL. We demonstrate that they are required for proper stability of the tissue and actin cytoskeletal remodelling upon wounding, as Grhl KD show a considerable delay in the closure process. Our preliminary analysis strengthens the conserved role of the Grhl family in the regulation of epithelial maintenance in homeostatic and repair conditions.

Altogether, this study highlights the importance of Grh genes across species in the maintenance and repair of simple epithelia, by unveiling new regulatory functions in the control of adhesion, cytoskeletal and calcium dynamics.

RESUMO

A cicatrização de feridas epiteliais é uma característica inerente a todos os organismos, de forma a lidar com agressões do ambiente circundante e manter a integridade da barreira epitelial. As feridas podem resultar de trauma acidental, cirurgia ou várias condições patológicas. Independentemente da causa, é necessário a sua correcta resolução de modo a evitar complicações, que podem variar entre infecção a fibrose e iniciação tumoral. Compreender as bases celulares e moleculares da reparação de feridas é um objectivo importante para a pesquisa biomédica. O processo de cicatrização é alcançado de forma altamente regulada e eficiente para assegurar o retorno correto às condições homeostáticas. Embora a reparação de feridas difira em complexidade entre epitélios simples e estratificados, ambos os contextos envolvem uma série de eventos coordenados que se desenrolam de forma sequencial: detecção e transmissão do sinal de ferida; reorganização de componentes de adesão e citoesqueleto; iniciação da resposta imune; e fecho da lacuna e restabelecimento da barreira epitelial. Cada uma destas etapas envolve múltiplas vias de sinalização e vários componentes celulares chave. Os epitélios simples de invertebrados, como *Drosophila*, tornaram-se sistemas modelo populares devido à sua acessibilidade para análise de microscopia de alta resolução em tempo real e são passíveis de manipulação genética. Nestes tecidos, a reparação epitelial depende de um método de fecho "cordão de bolsa", baseado em rearranjos celulares, promovidos pela remodelação da adesão e citoesqueleto, e a atividade contrátil de um cabo de actomiosina, formado na margem da ferida. Este mecanismo é conservado na reparação de epitélios simples em várias espécies, assemelhando-se também a movimentos morfogenéticos que ocorrem durante o desenvolvimento de diferentes organismos, como o fecho do epitélio dorsal em *Drosophila* ou epibolia em embriões de peixe-zebra.

Várias vias de sinalização regulam o fecho de feridas em epitélio simples. Grainy head (Grh), um factor de transcrição epitelial essencial, é conhecido por estar envolvido na reparação de epitélios. Descrito pela primeira vez em *Drosophila*, Grh e seus homólogos vertebrados (Grainyhead like (Grhl)) regulam a formação de epitélios e a sua diferenciação, e têm uma função conservada no restabelecimento da barreira epidérmica após a ferida. Em *Drosophila*, Grh regula a expressão de genes específicos de resposta à ferida, promovendo a reparação da cutícula nas últimas fases da cicatrização de feridas. No entanto, pouco se sabe sobre o seu papel noutros aspectos do processo de reparação. Neste estudo, utilizámos o epitélio dorsal da pupa para analisar a importância do Grh nas primeiras fases de remodelação celular e reorganização do citoesqueleto, após a ferida. Neste sistema modelo, a ferida induz uma série de eventos coordenados de aumento de cálcio, remodelação e polimerização de filamentos de actomiosina e contracção de tecido que levam à formação do cabo de actomiosina na margem da ferida e consequente fecho. Mostramos que, após a ferida, a redução da expressão (knockdown - KD) de Grh leva ao fecho defeituoso da ferida. Este fenótipo correlaciona-se com o comprometimento da reorganização do citoesqueleto, levando à formação de um cabo de actomiosina ectópico longe da margem da ferida. Adicionalmente, KD de Grh leva à depleção de E-Caderina (E-Cad) nas células em redor da ferida. No processo de reparação, E-Cad precisa ser retirada da membrana na margem da ferida, durante as fases iniciais, para promover a formação do cabo de actomiosina. Isto é conseguido através da activação de Dorsal (Dl), um efector da via de sinalização NF-κB. Observamos que, no KD de Grh, a depleção de E-Cad resulta de uma hiperactivação de Dl. Nós propomos que Grh controle a atividade Dl após a ferida, a fim de regular de forma rigorosa a remodelação de adesão essencial para a reorganização do tecido, mantendo a estabilidade cortical. Além disso, KD de Grh leva também à perda de identidade epitelial das células em redor da ferida, células essas que começam a adquirir

características mesenquimatosas em fases posteriores do processo de cicatrização da ferida. Estes resultados revelam um novo papel do Grh na regulação da dinâmica de adesão e do citoesqueleto, bem como uma nova interacção regulatória com a via de sinalização NF-κB.

Outro evento característico após a ferida do epitélio dorsal da pupa é o aumento dos níveis intracelulares de cálcio no tecido em redor da ferida, numa expansão similar a uma onda. O cálcio é uma molécula de sinalização rápida e pleiotrópica, com funções conservadas entre diferentes espécies. Como a reparação de feridas implica uma resposta rápida do tecido, o cálcio é um dos primeiros sinais, independentes de transcrição, produzidos imediatamente após a ferida. Neste estudo, mostramos que a expansão do fluxo de cálcio é um processo com duas fases: uma primeira expansão que se correlaciona fortemente com o deslocamento mecânico que o tecido sofre após a ferida; e uma segunda fase, caracterizada por flashes de cálcio estocásticos que se estendem ao longo do epitélio, mais característicos de uma reacção bioquímica de sinalização entre as células. Mostramos que, no KD de Grh, níveis elevados de cálcio intracelular são mantidos por um longo período de tempo em torno da ferida. Para entender como essa desregulação pode estar a ocorrer, realizamos uma análise genética de KD (screen genético) para identificar genes, directamente regulados por Grh, que podem ser responsáveis por essa desregulação. Observamos que a perda de função de um subconjunto de genes alvo de Grh, durante a cicatrização da ferida, também leva a uma alteração da dinâmica do cálcio. Adicionalmente, a desregulação dos níveis de cálcio foi acompanhada por alterações ao nível do citoesqueleto de actina, levando ao comprometimento da formação do cabo de actina e consequentes defeitos de fecho de ferida. Estes resultados complementam a análise da dinâmica do cálcio intracelular na cicatrização de feridas na pupa e introduzem novos elementos no processo de reparação da cicatrização de feridas.

Uma vez que a família de factores de transcrição Grhl parece ter várias funções conservadas entre organismos invertebrados e vertebrados, decidimos caracterizar a sua importância no desenvolvimento e reparação de epitélios vertebrados. Para isso, usamos o peixe-zebra como organismo modelo. Primeiro procedemos à caracterização dos padrões de expressão dos vários genes *grhl* durante o desenvolvimento do peixe-zebra, para entender a distribuição espacial e temporal dos diferentes factores de transcrição desta família, com foco nas primeiras 48 horas de desenvolvimento. Mostramos pela primeira vez a expressão de um factor de transcrição Grhl no notocorda, "floor plate" e hipocorda, estruturas de suporte axial do organismo em desenvolvimento. Estas observações sugerem uma nova função para este gene, em organogénese. Para abordar o papel na reparação de feridas, estabelecemos um novo modelo de reparação de feridas em epitélios simples vertebrados, através de da aplicação de feridas, com recurso a um laser, no "Enveloping Layer" (EVL), o epitélio embrionário do peixe-zebra. Este sistema assemelha-se ao epitélio simples invertebrado, onde o fecho ocorre através do método "cordão de bolsa", mas com uma dinâmica muito mais rápida. Usando a tecnologia morpholino, abordamos o papel de *grhl2b* e *grhl3* durante a reparação da EVL. Demonstramos que estes genes são necessários para a estabilidade do tecido e a remodelação do citoesqueleto da actina após a ferida, pois a redução da sua expressão resulta num atraso considerável no processo de fecho. A nossa análise preliminar fortalece a conservação funcional da família Grhl na regulação da manutenção epitelial em condições homeostáticas e de reparação de ferida.

Finalmente, este estudo destaca a importância de Grh, em diferentes espécies, na manutenção e reparação de epitélios simples, ao revelar novas funções regulatórias no controlo da adesão, do citoesqueleto e da dinâmica do cálcio após a ferida.

ABBREVIATIONS

Abbreviation	*Full form*
ºC	degree Celsius
α-cat	α-catenin
β-cat	β-catenin
ΔΔCt	Comparative Cycling threshold
µg	microgram(s)
µm	micrometre(s)
AJ	Adherens Junction
AnxB9	Annexin B9
AP-1	Activator Protein-1
APF	after puparium formation
aPKC	atypical Protein Kinase C
ATP	Adenosine triphosphate
Cact	Cactus
CadN	N-Cadherin
CBP	sarcoplasmic calcium-binding protein
Cdc42	Cell Division Control protein 42
cDNA	complementary Deoxyribonucleic acid
ChIP-seq	chromatin immunoprecipitation sequencing
Clic	Chloride intracellular channel
DAPI	4',6-diamidino-2-phenylindole
Ddc	Dopa decarboxylase
Dia	Diaphanous
Dl	Dorsal
DMSO	Dimethyl sulfoxide
DNA	Deoxyribonucleic acid
DUOX	NADPH Dual oxidase

Abbreviation	*Full form*
E-Cad	E-Cadherin
ECM	Extracellular Matrix
EGF	Epidermal growth factor
EGFR	Epidermal growth factor receptor
EMT	Epithelia-Mesenchymal Transition
ER	endoplasmic reticulum
ERK	Extracellular Signal–Regulated Kinase
esg	escargot
F-actin	Filamentous actin
FA	Focal Adhesions
FBS	Fetal Bovine Serum
FGF	Fibroblast growth factor
FGFR	Fibroblast growth factor receptor
G-actin	Globular actin
GAP	GTPase-activating proteins
GEF	Guanine nucleotide exchange factors
GFP	Green fluorescent protein
Grh	Grainy head
Grhl	Grainyhead-like
hpf	hours post fertilization
JNK	Jun N-Terminal Kinase
KD	knockdown
kPa	kilopascal
Lgl	Lethal (2) Giant Larvae homologue
MAPK	Mitogen Activated Protein Kinase
mey	*morpheyus*
mg	milligram(s)
MGR	Mammalian Grainy head
MHC	Myosin heavy chain

Abbreviation	*Full form*
min	minute(s)
mM	milliMolar
Mmp1	Matrix metalloproteinase 1
MO	morpholino
mpw	minutes post wounding
mRNA	messenger Ribonucleic acid
ms	millisecond(s)
N.A.	numerical aperture
nm	nanometre(s)
ON	overnight
PBS	Phosphate-buffered saline
pg	picogram(s)
pnr	pannier
psi	pounds per square inch
qPCR	quantitative real-time Polymerase Chain Reaction
RLC	regulatory light chains
RNA	Ribonucleic acid
RNAi	Ribonucleic acid interference
ROCK	Rho-associated protein kinase
ROS	Reactive Oxygen Species
RTK	Receptor Tyrosine Kinase
sec(s)	second(s)
SJ	Septate Junctions
sna	snail
SOM	Sister-of-MGR
sr	stripe
Src42A	Src oncogene at 42A
Stit	Stitcher
TF	Transcription factors

Abbreviation	*Full form*
TGFβ	Transforming growth factor-β
TJ	Tight Junctions
twi	twist
UAS	upstream activation sequence
UV	Ultraviolet
VEGFR	Vascular endothelial growth factor receptor
WASP	Wiskott-Aldrich Syndrome protein
Yki	Yorkie
ZO	Zonula Occludens

TABLE OF CONTENTS

Chapter I – Introduction

Chapter II – Grainy Head in Drosophila pupal notum repair

Chapter III – Grainy Head and calcium regulation in repair

Chapter V – General Discussion

CHAPTER I

INTRODUCTION:

A General Overview

"*The most exciting phrase to hear in science, the one that heralds new discoveries, is not "Eureka" but "That's funny…".* "

Isaac Asimov

Contents

The author of this thesis wrote this chapter based on the referred bibliography.

1. Epithelial wound healing

Every organism experiences aggressions from its surrounding environment and properly resolving any tissue discontinuity needs to be quickly and tightly regulated. This necessity has made the process of wound healing a quick and highly modulated process, requiring several players and coordination from different aspects of biological responses, in a phased and organized method. Although every structure can be affected by a wound, the importance of maintaining a defined barrier between each compartment in an organism and its constant protection is of the upmost importance and needs to be the first step in how the organism deals with a trauma. Compartmentalization maximizes and optimizes function, independently of the complexity of the respective tissue, conferring a proper barrier between different structures. This allows for the separation of the several concomitant processes necessary for development and survival of the adjoining tissues, which can be subjected to several cross-talk reactions between signalling pathways or interactions. Firm boundary between organs and structures is required for the maintenance of a tightly orchestrated routine within the organism. This physical separation is reached by the epithelial tissue and, in case of a trauma, this is the first target of the wound healing process.

1.1 The Epithelial tissue

Epithelia are the first type of organized tissues formed in an animal during the initial periods of embryogenesis and can be derived from all three embryonic layers (Alberts et al., 2007; Marchiando et al., 2010; McCaffrey and Macara, 2011). They are comprised of large sheets of cells with very few extracellular space between them, covering all structures exposed to the outside or inside lining of the organism. Epithelia act as distinctive tissue barriers in order to maintain a modular organization within an organism or a

protective layer against its surrounding, providing both defence and communication with the milieu (Wang et al., 2012). For this, epithelia rely on four simple defining characteristics: tight specialized cell-cell adhesion components, apical-basal polarization, contact to connective tissue and lack of vascularity (Alberts et al., 2007; McCaffrey and Macara, 2011; Tepass and Tanentzapf, 2001; Wang et al., 2012). Cell communication and adhesion components promote a tight bond between each cell, as well as a polarized architecture that ultimately establishes distinctive areas within each cell. These areas are characteristically defined by an apical side, in contact with the exterior, and a basal side, in contact with a basement membrane. This membrane is comprised of the basal lamina and the reticular lamina, which provides the attachment between the epithelium and the tissue it covers. Also, epithelial tissues are avascular, and nutrients and solutes are transported by diffusion or absorption between the surface and the underlying tissues. This regulated transport with adjacent tissues depends on various adhesive organizations, creating different permeability degrees. Moreover, epithelia can develop specialized structures such as microvilli or cilia that are essential for specific functions according to its localization and necessity (Alberts et al., 2007).

As mentioned before, epithelia are not only important in the separation of the individual and the surrounding exterior environment but also between different organs of the organism itself. Epithelial tissues are found in the external protective barrier (commonly denominated skin) but also in the lining of the gastrointestinal system, respiratory tract or the lining of blood vessels (endothelium) and surrounding glandular organs (glandular epithelium) (Alberts et al., 2007). Although all epithelia share some important structural and functional features, their localization inherently affects their principal functions: protection from microorganisms or physical and chemical trauma by repair mechanisms; provision of tact and sensation in association with the nervous system; regulation of solute exchange

between different compartments affecting blood circulation, respiration or digestion with different permeability degrees and specialized structures that expand the contact area and maximize efficiency of exchange (like microvilli in the intestinal tract or cilia in the respiratory system); or the secretion of hormones to the circulatory system and enzymes to the gastrointestinal tract (Alberts et al., 2007). All these different functions result from subtle but crucial differences in the composition and morphology of the epithelial tissue.

The classification of each type of epithelial tissue can be done according to two different aspects regarding its structure: the morphology of the cells that comprise it and how they are organised to form the tissue (Fig.1).
Epithelial cells can be classified in three different types according to their morphology: squamous, cuboidal or columnar. This categorization is mainly based on the distribution and extent of their polarized areas. Squamous cells have a larger apical perimeter and almost no lateral area, forming a very thin cell layer, normally associated with high solute exchange through diffusion (such as the endothelium). Cuboidal cells show a similar distribution between the apical and lateral sides (forming a cube) and are normally associated with epithelial duct tissues, where absorption and secretion are necessary. Columnar cells present a higher lateral than apical side and are generally associated with metabolite production and secretion as well as structure and protection (Alberts et al., 2007). The different distributions of these types of cells within the epithelium are responsible for the classification of this tissue regarding its structure. Epithelial tissues can be formed by a single (simple epithelia) or several layers of cells (stratified epithelia). A third denomination arises from a differential positioning of the nuclei of columnar cells that, despite corresponding only to one cell layer, give rise to a pseudostratified epithelium (nuclei at different levels give the impression of several cell layers) (Fig. 1).

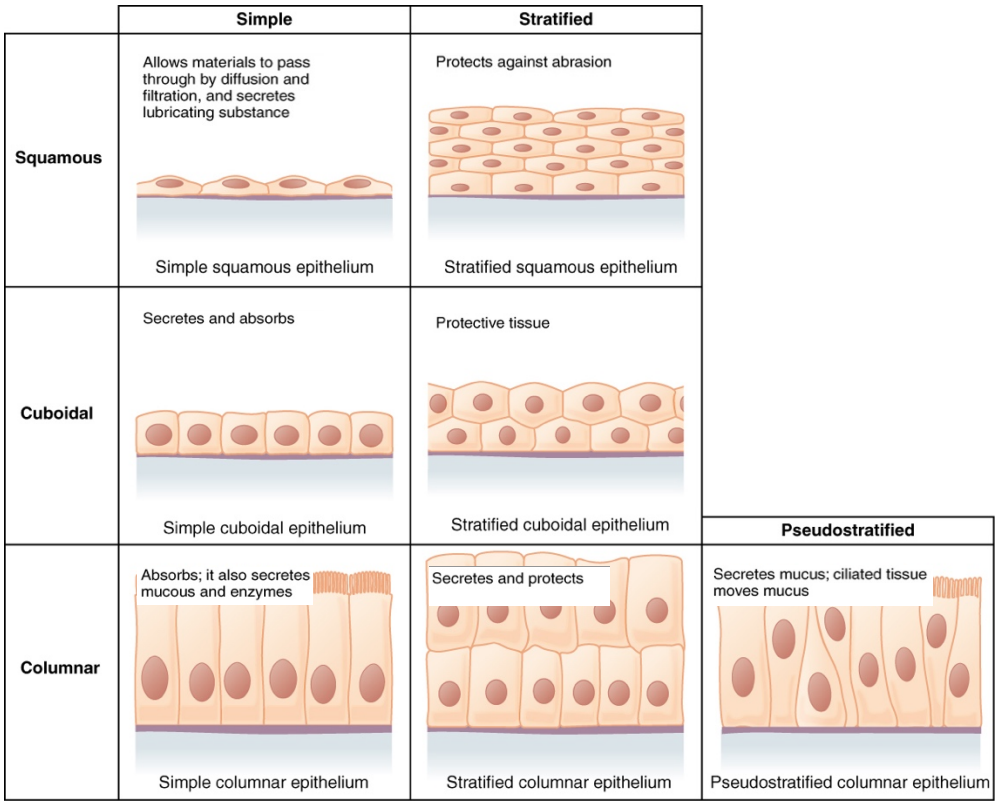

Figure 1. Types of epithelial tissues and their functions. Each type of epithelial tissue is given by its predominant type of cell (described in left row by squamous, cuboidal or columnar) and number of cell layers that constitute the tissue (simple – one cell layer; stratified – several cell layers). The pseudostratified epithelial tissue is neither a simple or stratified epithelium since, although constituted by only one cell layer, the cell nuclei are not aligned in one row, giving the morphological impression of more than one cell layer. Each morphology is associated with specific roles (Adapted from OpenStax, Anatomy & Physiology. OpenStax CNX. http://cnx.org/).

Another exception to the classification of epithelia is the transitional epithelium, a stratified epithelium constituted by columnar and cuboidal epithelial cells that can stretch and change morphology. This epithelium is commonly associated with the urinary organs as they require the capacity of inflation and deflation (Alberts et al., 2007).

1.2 The Epithelial Cell

Epithelial cells are characterized by the polarized distribution of different cellular components and composition of the plasma membrane. This creates distinct domains within the plasma membrane that exert different functions in the overall structure of the tissue. The maintenance of polarity requires the interaction between different components and cellular machineries, such as polarized distribution of adhesive contacts, polarized vesicle trafficking, and polarized activity of cytoskeletal filaments within the cell. This results from the consorted regulation of polarity proteins in distinctive domains of the cellular membrane (Martin-Belmonte and Perez-Moreno, 2011). These cell polarity complexes, first identified in invertebrate model organisms, are highly evolutionarily conserved. Polarity determination depends on the asymmetric segregation of proteins and lipids to the correct membrane domains (Martin-Belmonte and Mostov, 2008). Three major polarity complexes have been identified: the PAR/aPKC complex, consisting of Par3 (Bazooka in *Drosophila*), Par6, atypical Protein Kinase C (aPKC) and Cell Division Control protein 42 (CDC42), which mark the apical-basolateral membrane border; the Crumbs (CRB) complex, consisting mainly of Crumbs, PALS1 (Stardust in *Drosophila*) and PALS1-associated Tight Junction Protein (PATJ), responsible for defining the apical side of the cell membrane; and the Scribble homologue (SCRIB), Lethal (2) Giant Larvae homologue (Lgl in *Drosophila*; also known as LLGL) and the Discs-large homologue (DLG) that are responsible for the definition of the basal domain of the cell membrane (Martin-Belmonte and Mostov, 2008; Martin-Belmonte and Perez-Moreno, 2011) (Fig. 2).

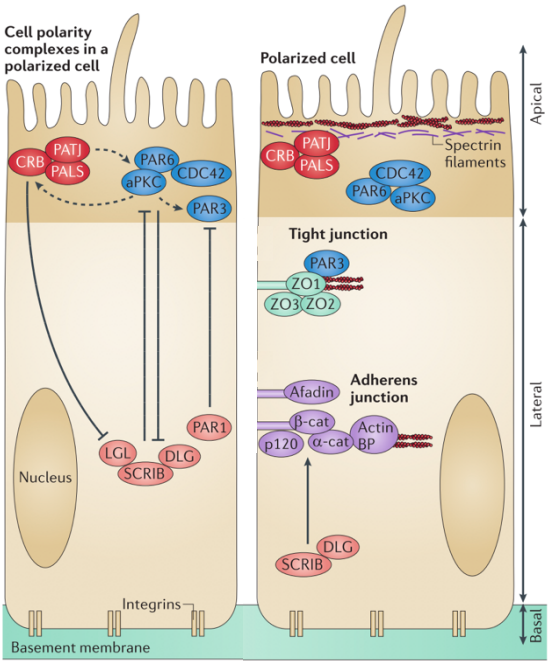

Figure 2. Polarization complexes determine different domains in the cell membrane. Three distinct polarity complexes determine apical-basal polarity in the epithelial cell: the CRB complex (shown in red) defines the apical side along with the associated cytoplasmic proteins PALS1 and PATJ; the PAR complex (PAR3, PAR6, aPKC and CDC42) (shown in blue) determines the boundary between apical and lateral sides of the membrane; the SCRIB complex (SCRIB, LGL, DLG) (shown in orange) defines the basolateral plasma membrane. These interactions will lead to differential accumulation of the adhesion molecules and the maturation of the different adhesion areas. α-cat, α-catenin; actin BP, actin-binding protein; β-cat, β-catenin; p120, p120-catenin; ZO, zonula occludens protein (Adapted from Martin-Belmonte and Perez-Moreno, 2011)

The distribution of these factors is regulated through a series of sequential inhibitory interactions between the different complexes and adhesion molecules like Adherens (AJs) and Tight Junctions (TJs). The process of polarity establishment starts with PAR3 driving the recruitment of the AJ E-Cadherin (E-Cad) and other junctional molecules to the cell cortex through

the localization of Afadin. This promotes adhesive homophilic interactions between neighbouring cells. The consequent separation of the different adhesion molecules is done by the exclusion of PAR3 from this primordial adhesion site. This exclusion delocalizes tight junction-associated proteins to a more subapical region, where PAR3 exclusion happens once again due to aPKC phosphorylation activity, to permit junction maturation. In *Drosophila,* the determination of this boundary through PAR3-aPKC interaction, leading to apical and lateral domain, is very similar to the vertebrate process (Morais-de-Sá et al., 2010). The SCRIB complex then controls the determination of the basolateral domain, while the CRB complex interacts with supra apical cytoskeletal components to define the apical area. By regulating adhesion proteins and the cytoskeleton to define the polarity axis of the cell, these polarity complexes lead to the formation of roughly four distinct regions in the membrane: supra-apical, apical, lateral and basal (Knust, 2002; Rodriguez-Boulan and Macara, 2014; St Johnston and Sanson, 2011; Tepass, 2012).

At the supra apical domain, the cell faces the exterior, and can organize special functional structures already previously referred, like microvilli and cilia, supported by a highly dense actin filament meshwork (Alberts et al., 2007). At the apical and lateral domains, adhesive and communicating structures are also present promoting the attachment to the underlying actin cytoskeleton and link to the neighbouring cells (Cavey and Lecuit, 2009; Getsios et al., 2004; Zihni et al., 2016). Finally, the basal side of the cell promotes the contact between the cells and the basement membrane and extracellular matrix (ECM) (Fig. 3). All other organelles are also polarized within the cytoplasm, with the nucleus occupying the basal side and the secretory machinery and other functional organelles occupying the remaining space (Alberts et al., 2007).

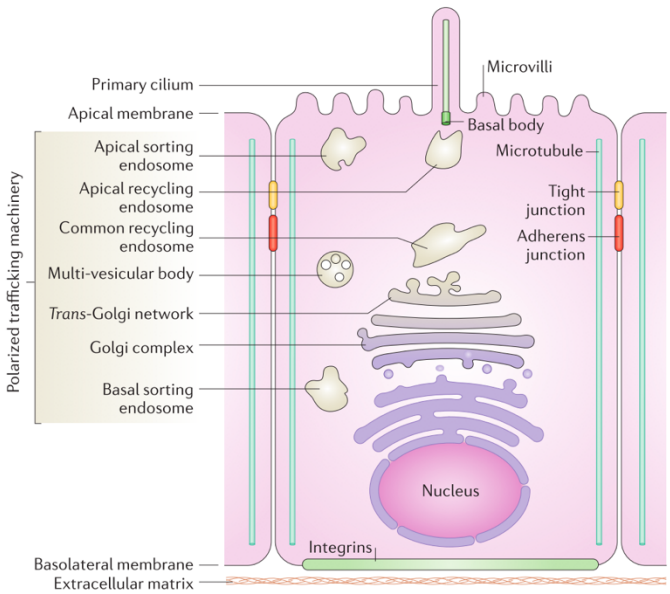

Figure 3. Polarized distribution of epithelial cell components and organelles. Schematic representation of a vertebrate epithelial cell, showing the polarized distribution of the different cellular components, a specialized structure formed at the supra apical part (cilium), the different vesicle sorting machinery distributed along the cell body and the nucleus at a more basal position. The junctional complexes are depicted along the cellular membrane with Tight and Adherens Junctions at the apical lateral membrane and the integrins at the basal side in contact with the basal membrane and ECM. (Adapted from Rodriguez-Boulan and Macara, 2014)

1.2.1 Cell junction and communication components

Different and abundant adhesion complexes are one of the most relevant characteristics of epithelial cells. As referred previously, several types of adhesion components are distributed along the cell membrane in a polarized manner. Their maturation occurs in a sequential process. Each of these adhesion complexes has a particular structure and function, involved in cell communication, paracellular transport or barrier. They can be divided

in three different groups: occluding junctions, communicating junctions and anchoring junctions (Alberts et al., 2007) (Fig. 4).

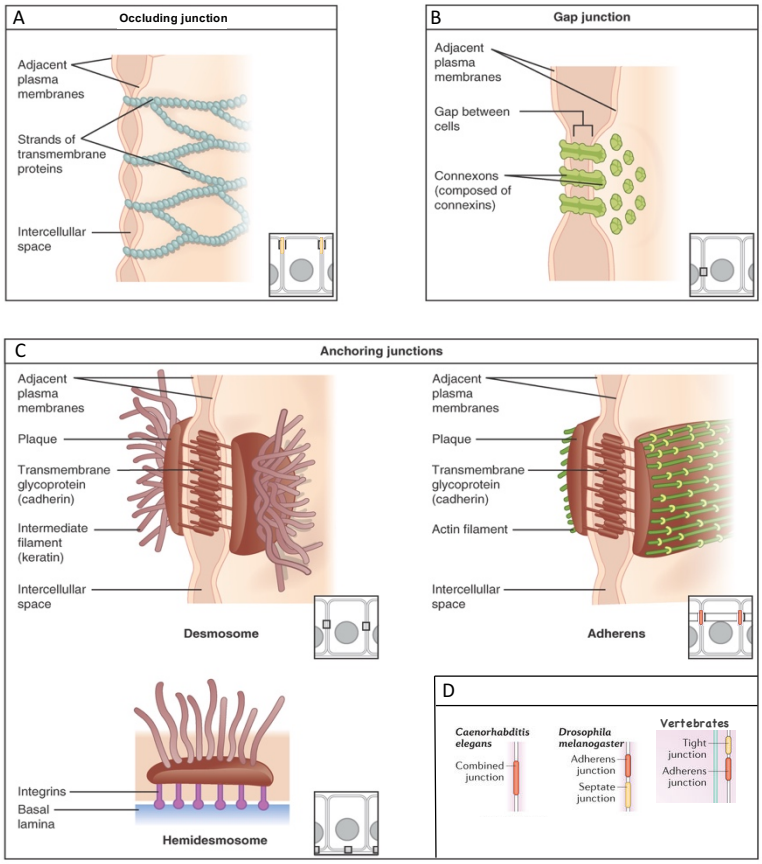

Figure 4. Different adhesion complexes present in epithelial cells. Schematic representation of three types of adhesion molecules in epithelial tissue: (A) occluding junctions, (B) gap junctions and (C) anchoring junctions. (D) Occluding junctions are Tight Junctions in vertebrates and Septate Junctions in invertebrates, and their relative distribution in the apical lateral membrane regarding Adherens Junctions varies across species: in vertebrates, Tight Junctions are more apical than Adherens Junctions; in invertebrates (such as *Drosophila*), Adherens Junctions are more apical than Septate Junctions, and in *C. elegans* both Adherens and Occluding Junctions form one complex named combined junction (D) (Adapted from OpenStax, Anatomy & Physiology. OpenStax CNX. http://cnx.org/ and Rodriguez-Boulan and Macara, 2014).

Occluding junctions (OJs) include TJs in vertebrates and Septate Junctions (SJs) in invertebrates. They are composed of claudins, occludins and Junction Adhesion Molecules (JAMs), which interact with scaffolding proteins like Zonula Occludens proteins (ZOs) and the cytoskeleton, functioning as signalling hubs. They provide a strong contact between neighbour cells and regulate the paracellular permeability barrier. Their distribution is different between vertebrates (more apical) and invertebrates (below Adherens junctions) (Matter and Balda, 2003; Zihni et al., 2016) (Fig. 4A and D).

Communicating junctions (gap junctions) are plasma membrane complexes of channel proteins (connexins in vertebrates and innexins in invertebrates). These junctions facilitate the passage and transport of small molecules and ions between neighbouring cells, permitting a rapid and easy distribution of solutes between adjacent cytosols. Although their function is not directly related to adhesion, these complexes allow the rapid distribution of electrical and chemical signals, while metabolically coupling adjacent cells and coordinating overall function in a large group of tightly linked cells (Evans and Martin, 2002) (Fig. 4B).

Anchoring junctions are comprised of Desmosomes, Hemidesmosomes and AJs. Desmosomes are responsible for mediating mechanical coupling between neighbouring cells. They are intercellular junctional complexes composed of cadherins and plakins, stabilizing the link to intermediate filaments between cells, which strengthens the adhesion across the tissue. These structures, as well as intermediate filaments, are absent in *Drosophila* epithelia (Getsios et al., 2004). Hemidesmosomes are also classified as anchoring junctions despite their localization on the basal side of the cell. Their function is to link the cell to the basement membrane, through binding to its ECM components like laminin or fibronectin. These junctions, along with intermediate filaments, integrins and Focal Adhesions (FAs) strengthen the bound of the epithelium to the underlying connective

tissue (Borradori and Sonnenberg, 1999; Lee and Streuli, 2014; Zhang and Labouesse, 2010). FAs are multiprotein complexes, composed of several adhesion and adaptor proteins, such as integrins, talin, vinculin or paxillin. They connect the actin cytoskeleton to the basal membrane and ECM, with important mechanosensing and force transmission functions, especially for the process of cell migration (Wozniak et al., 2004; Wu, 2007).

The AJs are composed of Cadherin molecules which mediate calcium-dependent homophilic interactions between adjacent cells. Like OJs, AJs are also distributed differently between vertebrate and invertebrates, with a more apical localization in the latter systems, compared to its vertebrates counterparts (Knust, 2002) (Fig. 4C and D). Focusing on epithelial Cadherin (E-Cadherin, E-Cad), this molecule forms complexes with β-catenin (β-cat), p120-catenin and α-catenin (α-cat), adaptor proteins closely connected to the actin cytoskeleton and actin binding proteins (Fig. 5). E-cad is localized at the membrane, stabilized by p120-catenin, and its cytoplasmic tail directly binds β-cat. This bound enables the recruitment of α-cat to this complex, essential for the stability of the junction (Bajpai et al., 2008; Takeichi, 2014). Although p120-catenin plays a supporting role in cell adhesion, it is worth noting that its role as a link to the cytoskeleton and its regulation are less defined in *Drosophila*. In this organism, p120-catenin is not an essential component for AJ function, but is suggested to be important for regulating E-Cad endocytosis and turnover (Bulgakova and Brown, 2016; Myster et al., 2003). In turn, the direct link with the actin cytoskeleton is done through α-cat. This is essential to firmly link plasma membranes and bind to actin binding proteins, namely EPLIN, Vinculin, α-Actinin, Formin1, Afadin and ZO-1. These provide access to additional regulatory cascades for the modification of the actin network organization at the AJs, as well as its attachment to the AJs complexes (Leckband and de Rooij, 2014; Takeichi, 2014).

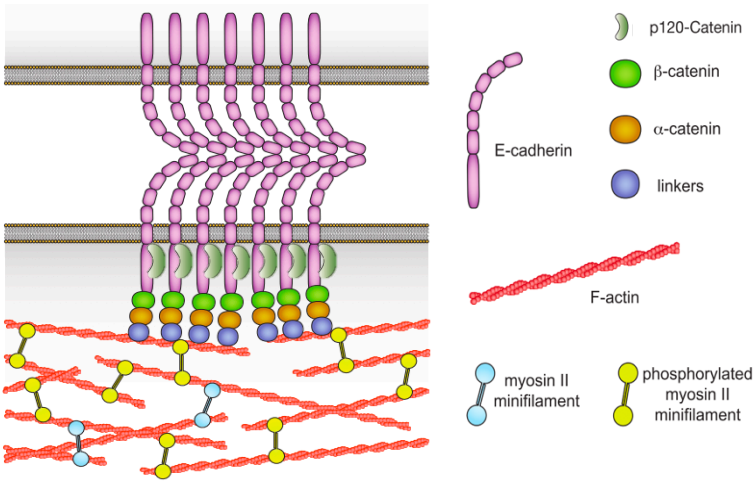

Figure 5. Adherens Junctions complex. Schematic representation of the Adherens Junctions complex and its components. Homophilic interaction between transmembrane E-Cad molecules of adjacent epithelial cells are stabilized at the membrane by adaptor proteins p120-catenin, β-cat and α-cat. α-cat also binds to several actin binding proteins promoting the link between the AJ and the actin cytoskeleton (Adapted from Engl et al., 2014).

In recent years, the modulation of the link between the AJs and the cytoskeleton by α-cat has been under debate, regarding its capabilities to bind directly or not to the AJ complex and the actin filaments. It was shown *in vitro* that α-cat can bind both the E-Cad-β-cat complex and filamentous actin (F-actin) in mutually exclusive manner. This work showed α-cat monomers preferentially bind to β-cat, while the dimeric form has a higher affinity to bind to F-actin. These findings lead to a revised model where a highly dynamic and transient modification in α-cat form would be necessary to mediate both interactions with the AJ complex and the cytoskeleton (Drees et al., 2005; Yamada et al., 2005). More recently, this model has been abandoned as it was shown that, under tension, α-cat undergoes a conformational change in its structure, allowing the binding to both β-cat and F-actin (Buckley et al., 2014). Therefore, differences in low and high force in

the structure of the molecule are essential to create the conformational change necessary to accommodate the interactions with both the adherens complex and F-actin. Since this change is dependent on physical forces, these findings could not be addressed *in vitro*. Nevertheless, this model correlates nicely with several *in vivo* analysis showing the need for a physical connection between all these components, in order to maintain structural integrity of the AJs and the transduction of mechanical signals into the cell (Desai et al., 2013; Pacquelet and Rorth, 2005; Sarpal et al., 2012; Twiss et al., 2012). The interactions between the different AJ components provide a platform for cell signalling at the membrane domain and transduction to the cell skeletal structure. This is crucial to convert mechanical inputs to chemical and biological responses at a cellular level. Hence, the dynamic and continuous turnover of AJ components facilitates their role in cell shape changes and tissue remodelling (Ladoux et al., 2015; Niessen, 2007; Niessen et al., 2011; Tepass, 2012; Yonemura et al., 2010).

1.2.2 The Actomyosin Cytoskeleton

Although cell communication is important for tissues, the epithelial cell depends on its skeletal components to confer a proper structural basis. There are three types of cytoskeletal components: microtubules, intermediate filaments and microfilaments (actin filaments) (Alberts et al., 2007). The first two are important for several structural functions, cell division processes and transport within the cell (Alberts et al., 2007). Nevertheless, this study will focus only on the actin cytoskeleton, along with the motor protein myosin, comprising the actomyosin cytoskeleton. Its function and regulation is intrinsically linked with epithelial cell dynamics and regulatory processes. Actin monomers (G-actin) are some of the most abundant proteins in every cell. Its organisation is highly dynamic, dependent on actin regulator proteins that promote stabilization,

polymerization or severing of the actin cytoskeleton (Table 1), essential for the modulation of rapid and orchestrated processes within the cell.

Table 1. Actin regulator proteins. Actin regulator proteins grouped according to function, with homologue components in vertebrates and invertebrates systems (*H. sapiens* and *D. melanogaster*) (Adapted from Siripala and Welch, 2007).

Protein Family		Biochemical Function	*H. sapiens*	*D. melanogaster*
Actin Nucleators				
Formins		associates with barbed ends, promotes nucleation	*hDia1, 2, 3, FHOD1, 2, 3, 4, DAAM1, 2, FMN1, 2, FRL1, 2, 3, INF1, 2, Delphilin	Diaphanous/Dia, Cappucino/FMN, DAAM, FRL, FHOD, INF
Spir		nucleates unbranched filaments	Spir-1, Spir-2	Spir/spire
Arp2/3 complex		polymerizes Y-branched filament networks	ARP2, ARP3, ARPC1A, 1B, 2, 3, 4, 5, 5L	ARP2, ARP3, ARPC1, 2, 3A, 3B, 4, 5, 5L
Arp2/3 complex regulators	**CARMIL**	links capping protein, Arp2/3 and myosin I	CARMIL	DCarmil
	Coronin	binds F-actin and Arp2/3 complex, enhances actin depolymerization	coronin 1A, B, C; 2A, B; 7	Coro/Coronin, Dpod1
	Cortactin	activates/modulates Arp2/3 complex, binds F-actin	cortactin, HS1	DCortactin
	SCAR/WAVE family	activates Arp2/3 complex	SCAR1, SCAR2, SCAR3	SCAR
	WASP family	activates Arp2/3 complex	*WASP, N-WASP	WASp
G-Actin Binding Proteins				
CAP/Srv2		recycles actin monomers	CAP1, CAP2	Act up/Capulet
Profilin		promotes actin monomer addition at barbed ends	profilin 1, 2, 3, 4	Chickadee
Thymosin β4		sequesters G-actin	thymosin β4	Ciboulot
Verprolin/WIP		binds actin monomers, WASP	WIP, WIRE/WICH, CR16	†Q8MLU0
F-Actin Binding Proteins				
Ena/VASP family		antagonizes CapZ capping at filament ends, recruits profilin	Mena, VASP, EVL	Enabled
MIM		binds both G- and F-actin, may regulate nucleation-promoting factors	MIM	
Pointed End Capping Proteins				
Tropomodulin/ Tmod		caps pointed ends, binds tropomyosin	Tmod1, 2, 3, 4, Lmod1, 2, 3	Sanpodo

Barbed End Capping Proteins			
AIP1	promotes depolymerization by ADF/ cofilin	AIP1/WDR1	Aip1
CapG	caps barbed ends (calcium-dependent)	capG	CapG
CapZ/capping protein/β-actinin	heterodimer caps barbed ends	capZ (A1-3, B1-2)	CapZ (cpa, cpb)
Eps8	caps barbed ends, involved in Rac signalling	Eps8, Eps8L1, 2, 3	Arouser, †Q95TJ6
Actin Depolymerizing/Severing Proteins			
ADF/cofilin	promotes actin filament disassembly	cofilin1, cofilin2, ADF	Cofilin/Twinstar
Gelsolin/villin superfamily	severs actin filaments	gelsolin, adseverin/ scinderin, villin, advillin, supervillin, flightless I	Gelsolin, Villin-like/ Quail, Flightless I
Twinfilin	inhibits actin nucleotide exchange, severs actin	twinfilin-1/A6, twinfilin-2	Twinfilin
Actin Bundling/Crosslinking Proteins			
α-actinin	connects and organizes actin filaments	α-actinin1-4	α-actinin/Flightless A
EPLIN	stabilizes and bundles actin filaments	EPLIN	
Espin	forms parallel actin bundles	*espin	Forked
Fascin	bundles actin filaments	fascin 1, 2, 3	Singed
Filamin	orthogonally crosslinks actin filaments	filamin *A, *B, C	Jitterbug, Cheerio
Fimbrin/plastin	bundles actin filaments	plastin 1-3 (I, L, T)	Fimbrin

Actin polymerizes into filaments (F-actin) that are involved in several functions of the cell, as mechanical support, tracks for movements of intracellular materials, and force to drive cell shape changes and movements (Pollard and Cooper, 2009). Their polymerization occurs in an ATP-dependent manner, consisting in the formation of actin dimers/trimers with the help of different actin nucleators according to the type of filaments that will be assembled (Table 1 and Fig. 6). The spontaneous polymerization of F-actin is a highly unstable process, which leads to the maintenance of a pool of unassembled monomers in the cytosol, to ensure quick remodelling of the actin cytoskeleton. This is achieved by the binding of Profilin to the actin monomers, inhibiting the spontaneous formation of actin dimers or trimers, essential for nucleation (Blanchoin et al., 2014; Pollard et al., 2000) (Fig. 6A).

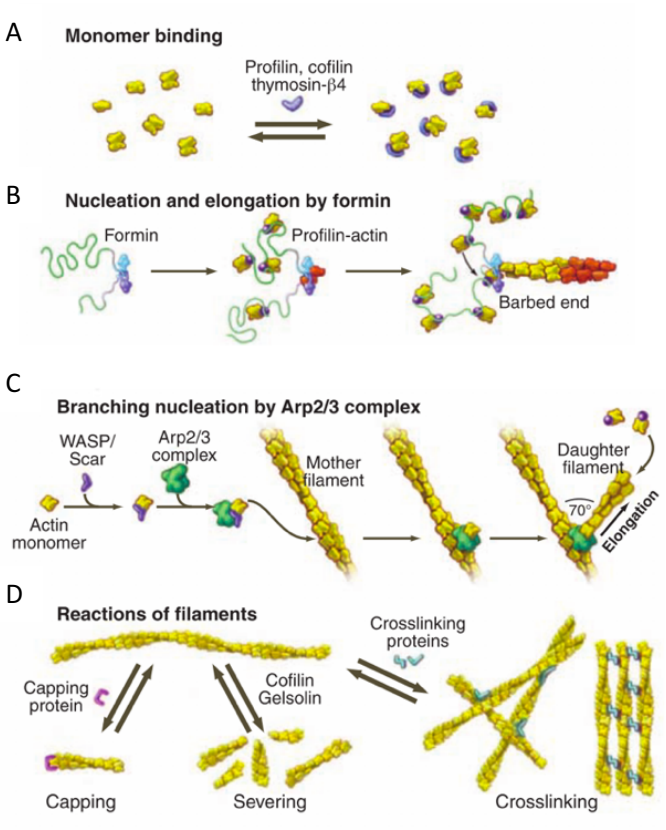

Figure 6. Actin nucleation reactions. (A) G-actin (monomer) is maintained by the association of Profilin to each unit. (B) Nucleation and filament elongation can be achieved by the support of formins and (C) branching is done through the activation of Arp2/3 Complex. (D) Capping proteins also assist in the maturation of the branched network, by limiting the elongation of each branch indefinitely. Branching is achieved by polymerization but also severing processes at the filaments, by Cofilin or Gelsolin, promoting the creation of new branching nodes. Cross-linking of filaments and bundles is also necessary to confer rigidity to the cytoskeletal structure, which is also mediated by adaptor proteins between the filaments (Adapted from Pollard and Cooper, 2009).

F-actin filaments are assembled in an asymmetrical structure, with a fast growing end (barbed-end) and a slower growing end (pointed-end). The addition of G-actin to the barbed-end is ten times faster than the

depolymerization rate at the pointed-end. This highly dynamic polymerization/depolymerization process is named *treadmilling* (Blanchoin et al., 2014; Pollard and Cooper, 2009). The active nucleation process is assisted by formins and the Arp2/3 complex, activated by the Wiskott-Aldrich Syndrome protein (WASP)/WAVE family of proteins (in case of branched nucleation) (Blanchoin et al., 2014; Machesky and Insall, 1998) (Fig. 6B and C). The branched actin network, commonly associated with motility patterns and the expansion of cellular protrusions, like lamellipodia, is important for the generation of a rigid and stable mesh to support tissue force and tension (Vinzenz et al., 2012). However, to promote the required stability for efficient force production, branching needs to be coupled and limited by capping events in the filament tips to prevent continuous polymerization in one unique direction. This is done by capping proteins, that consequently promote branching in other areas of the meshwork, creating stable subnets and rigidity in the structure (Akin and Mullins, 2008; Blanchoin et al., 2014) (Fig. 6D). Cross-linking of parallel actin bundles and filaments is also necessary to promote stiffness and robustness of the meshwork, being essential for the stabilization of the cortical actin network of the cell. This is achieved by adaptor cross-linker proteins, like α-Actinin, Filamin or Fascin (Table 1) (Blanchoin et al., 2014). Moreover, parallel actin bundles are essential for the formation of filopodia, structures important in the sensing of cell environment, initiation of cell contacts, and transmission of cell-cell signals (Blanchoin et al., 2014). To ensure dynamic turnover, many actin filaments suffer depolymerization or severing events. These are promoted by other actin regulators like Cofilin, Gelsolin and Twinfilin (Table 1) (Blanchoin et al., 2014; Okada et al., 2006). This abrupt remodelling of the actin network permits fast paced changes in the macrostructure of the cytoskeleton to accommodate cell shape changes and cellular dynamics. This can observed in the process of retrograde flow in the leading edge of migrating/extending cells (Blanchoin et al., 2014).

Like the denomination suggests, the actomyosin cytoskeleton is also constituted by the motor protein Myosin. In this study, only non-muscle Myosin II (myosin from now on) will be addressed, as a core component of the contractile machinery of the epithelial cell. Myosin is composed of two heavy chains (MHCs) (*Drosophila* only has one MHC – Zipper), two essential light chains (ELCs) and two regulatory light chains (RLCs) (Levayer and Lecuit, 2011). As a motor protein, myosin has the capability of binding and sliding on actin filaments, in an ATP-dependent process. It produces internal stress within the cross-linked networks, contributing to structural stiffening (Levayer and Lecuit, 2011; Vicente-Manzanares et al., 2009). To achieve this, myosin undergoes dynamic assembly and disassembly steps, similar to the actin cytoskeleton. These events are associated with rounds of phosphorylation and dephosphorylation, allowing temporal and spatial control of its contractile properties. Regulation of myosin activation is done through the concerted action of different Rho GTPase molecules (Rho, Rac and Cdc42), their regulators Guanine nucleotide exchange factors (GEFs) and GTPase-activating proteins (GAPs), and Rho downstream target kinases (like Rho-associated protein kinase, ROCK) (Sit and Manser, 2011; Tybulewicz and Henderson, 2009). Myosin interacts with F-actin through the generation of bipolar and highly processive minifilaments. They produce contractility by pulling on actin filaments of opposite polarity (antiparallel), resultant from contraction and extension periods within the cytoskeleton (Levayer and Lecuit, 2011) (Fig. 7). The interactions between the different structures created by the actin cytoskeleton and the engaging of myosin in this network promotes a contractile network all around the cell. Its organization and connection to adjacent cells and ECM supports applied forces to the tissue and also transmits relevant signals through the tissue. This entails a dynamic cooperation between the adhesion components, referred in the previous section, and all the machinery that activates or relaxes the cytoskeleton. All

these intricate procedures need to be tightly regulated to assure proper function and remodelling of the epithelial cell.

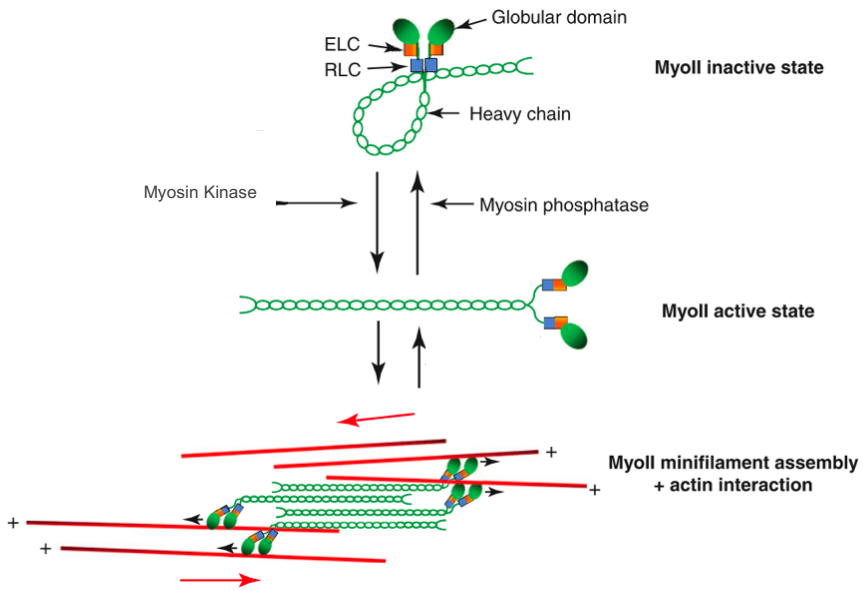

Figure 7. Actomyosin contractility through myosin (MyoII) activation and filament assembly. Myosin is activated by the phosphorylation of its RLC, acquiring a conformation susceptible for binding anti-parallel actin filaments (in red) through its globular domain, while forming minifilaments with the interaction of its heavy chain. The ATP-dependent sliding on the actin filaments generates contractility and expansion of the cytoskeletal network (Adapted from Levayer and Lecuit, 2011).

1.2.3 Epithelial cohesion and mechanotransduction

Epithelia undergo continuous rearrangements to accommodate the development of the organism. The regulation of epithelial cohesiveness and integrity is a common feature across several biological situations: from regular morphogenetic movements (Lecuit et al., 2011; Martin et al., 2010; Rauzi et al., 2010), to collective migration or cell shape rearrangement

during wound healing (Garcia-Fernandez et al., 2009; Trepat et al., 2009; Wood et al., 2002), maintenance of epithelial barrier (Twiss et al., 2012) or cancer progression (Friedl et al., 2004). Its integrity is mainly achieved by the interplay of the adhesion molecules and the cytoskeleton, in order to deal with the spatiotemporal regulation of the mechanical forces inherent in all these mechanisms (Heisenberg and Bellaïche, 2013). Therefore, the generation of contractile forces within the cell needs to occur in a concerted manner to accommodate the necessity of the modifying tissue without losing integrity. F-actin and myosin are the responsible drivers of such forces, regulating both cortical and cytoplasmic (medial pool) regions to sustain a balanced mechanical force. Although a balanced tension is maintained across the whole tissue, this is invariantly a highly dynamic process, where peaks of local tension can induce small changes and rearrangements. For example, small isotropic accumulations of myosin in the medial pool have been related to apical constriction, while anisotropic accumulation at cell-cell junctions has been proposed to drive shortening of cell junctions (Fig. 8) (Heisenberg and Bellaïche, 2013).

The differences in distribution of the contractile cytoskeletal components within the cell lead to the formation of actomyosin pulses and flows within the cell, resulting in cell constriction, cellular intercalation rearrangements, and tissue spreading or collective tissue migration (Collinet and Lecuit, 2013; Heisenberg and Bellaïche, 2013; Levayer and Lecuit, 2011; Murrell et al., 2015). Although their contractile properties depend on the activation by GTPases and kinases, like RhoA, Cdc42 and ROCK (Heisenberg and Bellaïche, 2013; Levayer and Lecuit, 2011), the polarized distribution and directionality of these pulses and flows determine the spatial orientation of the cell deformation. This directionality is dependent on the anisotropic distribution of Cadherin-catenin complexes in cell junctions (Collinet and Lecuit, 2013; Rauzi et al., 2010).

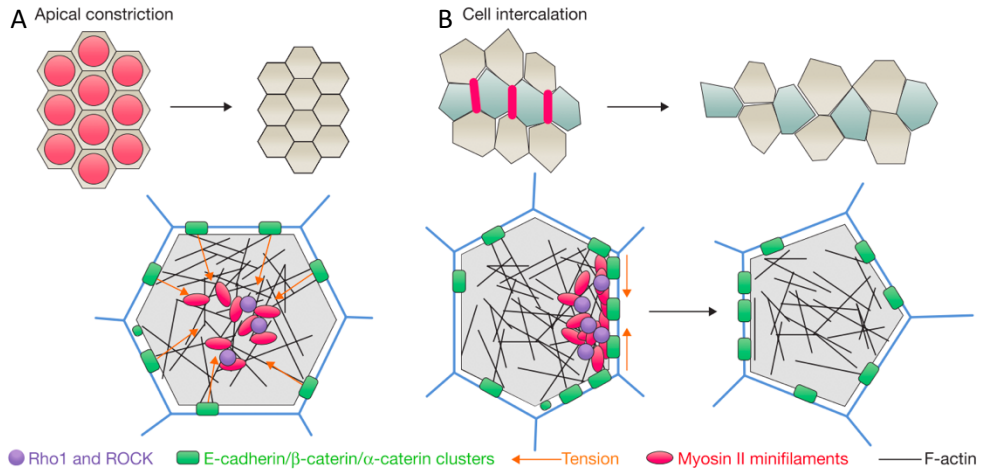

Figure 8. Actomyosin contractility within cells leads to tissue scale rearrangements. Apical constriction and cell intercalation are two of the possible tissue modifications resulting from actomyosin pulses and flows within the cells. (A) Apical constriction leads to the reduction of the apical area of the cells. This results from an isotropic accumulation at the medial pool of contractile actomyosin pulses. The network exerts traction forces against E-cadherin complexes at cell–cell contacts, leading to constriction of the apical poles of the cells. The contractility is promoted by the activation of Rho and ROCK and consequent myosin phosphorylation. (B) In cell intercalation events, cells exchange neighbours due to junction remodelling promoted by polarized actomyosin flows within the cells. Shrinking junctions (in red) deform due to anisotropic accumulations of myosin at the cell contacts. Tension transmission is achieved by the AJs complexes, which lead to cell rearrangements and neighbour exchange (Adapted from Lecuit and Yap, 2015).

Although these processes might seem small at the tissue scale, their combined action leads to rather drastic morphogenetic events (like *Drosophila* germ-band extension or vertebrate neural tube folding) (Heisenberg and Bellaïche, 2013; Nishimura et al., 2012; Rauzi et al., 2008). The epithelial tissue has to be prepared to deal with anomalies regarding tissue tension. Excess tension in a tissue can lead to the rupture of cell

adhesive contacts (Sahai and Marshall, 2002). The loss of the characteristic adhesion complexes poses a threat to the epithelial identity maintenance of the tissue, as it can trigger a differentiation mechanism known as Epithelial-Mesenchymal Transition (EMT) (Nieto et al., 2016). Within this process, epithelial tissue loses its defining characteristics and functions giving place to a mesenchymal tissue. Although this process takes place during certain stages of development (like gastrulation), its occurrence in differentiated epithelia in adult tissues is normally associated with cancer and tumour progression (Baum et al., 2008; Nieto et al., 2016; Thiery et al., 2009). Therefore, the resolution of any tissue or tension discontinuity within an epithelium needs to be quickly and tightly resolved.

1.3 Wound healing

Epithelia prevent the unregulated mixing and leakage of materials between adjacent tissues and/or the environment. Injury leads to barrier breaching, compromising this compartmental distribution. Since epithelia are constantly damaged by the environment or intrinsic defects, re-establishment of its integrity needs to be a robust mechanism in order to eliminate the damaged tissue and restore its continuity. Although wound healing can differ in complexity and players involved between different organisms, repair mechanisms are extremely conserved across species (Abreu-Blanco et al., 2012; Bement and Capco, 1991; Galko and Krasnow, 2004; Mandato and Bement, 2001; Martin and Lewis, 1992; Niethammer et al., 2009; Ting et al., 2005a; Xu and Chisholm, 2011). Wound healing occurs in a highly regulated and sequential manner: recognition of injury through damage signals; closure of the gap through the rapid reorganization of the cytoskeletal components; infection treatment; re-establishment of barrier function; and restoration of tissue architecture. The repair program scales according to the size of the injury and complexity of the tissues affected (Cordeiro and

Jacinto, 2013; Sonnemann and Bement, 2011). Despite the differences between simple and stratified epithelia, most of the key players are common to all repair processes. In this study, we focused on a cellular level approach to understand the recovery of the simple epithelial tissue, which heals in a scar-free manner. Nevertheless, it is important to note the main differences between simple and stratified epithelia tissue repair. Simple epithelia rely on the formation of actomyosin contractile structures to close the gap. This is the first step after acknowledgment of the injury by the system. After this, and while the discontinuity is being resolved, immune cells are recruited to fight the infection and eliminate any present cellular debris. The wound closure process relies on a fundamental mechanism, called purse string, that leads to wound closure through the contractile ability of a supracellular actomyosin cable assembled at the wound margin. During the final stages, leading edge cells promote the formation of specialized actin structures (lamellipodia and filopodia) that help the formation of contacts between opposing margins and lead to the zippering closure of the gap without leaving a scar (Cordeiro and Jacinto, 2013) (Fig. 9A).

In complex epithelia, upon injury and spread of the damage signals, platelet aggregation occurs at the wound site. The consequent secretion of several factors leads to the formation of a protective clot, that plugs the hole and impairs blood loss. During this time, immune system cells are recruited (as in simple epithelia) promoting the cleaning of the wound site from pathogens and debris. Concomitantly, angiogenesis begins. Then, proliferation of epithelial cells and consequent migration cover the epithelial tissue discontinuity. With the help of fibroblasts and the deposition of new ECM elements, wound re-epithelization occurs. After closure is achieved at a much slower pace than in simple epithelia, immune cells secret new factors that will help reduce the granulation tissue formed during closure and promote scar tissue formation (Cordeiro and Jacinto, 2013; Martin, 1997; Redd et al., 2004) (Fig. 9B).

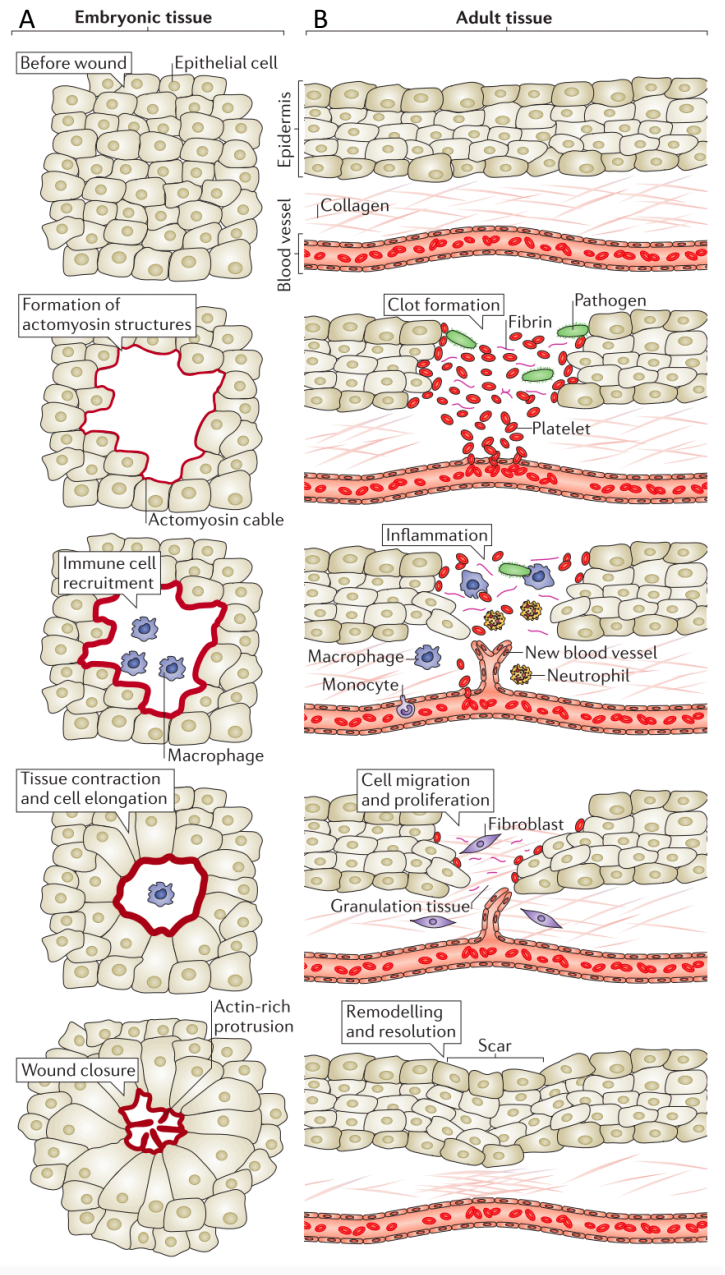

Figure 9. Wound healing phases. Differences between wound repair stages between (A) embryonic tissues (simple epithelia) and (B) adult tissues (stratified epithelia) (Adapted from Cordeiro and Jacinto, 2013).

Considering the common features between the two processes, we will take advantage of the simplicity of simple epithelia. Within this study, we will focus on the common players and stages, namely damage signal release, cytoskeletal and cellular rearrangements, activation of canonical stress response pathways and inflammatory response that ultimately lead to closure of the wound.

1.3.1 Release of damage signals and wound sensing

As soon as injury occurs, cells need to quickly signal the non-compromised tissue to react and establish integrity. This needs to be achieved in a transcription-independent manner in order to get a fast alert of the whole tissue to initiate the repair process. Fast diffusible molecules and ions, like calcium, hydrogen peroxide (H_2O_2) and other Reactive Oxygen Species (ROS) are involved in the immediate response of wound healing (Antunes et al., 2013; Moreira et al., 2010; Niethammer et al., 2009; Xu and Chisholm, 2011; Yoo et al., 2012). Calcium is a well studied messenger in a variety of biological processes (Berridge et al., 2000; Cheng et al., 2015). Upon injury, its intracellular concentration rapidly increases, extending to the tissue surrounding the wound. Calcium relevance besides signalling has been linked to activation of the immune response (Razzell et al., 2013) and cytoskeletal reorganization and contractile machinery (Antunes et al., 2013; Benink and Bement, 2005). Calcium increase upon wounding results from plasma membrane damage and subsequent activation of calcium channels present at the damaged membrane (Xu and Chisholm, 2011). Moreover, ATP release into the extracellular space, due to cell lysis, activates G-protein coupled receptors in neighbouring cells that lead to inositol triphosphate (IP_3) production, which in turn leads to calcium release from intracellular stores, like the endoplasmic reticulum (ER) or the mitochondria (Berridge, 1997; Fonteriz et al., 2016; Tsai et al., 2015). These feedback

processes, the numerous calcium channels present in cell membranes and the fast diffusion of calcium signalling through gap junctions make the expansion of the calcium signalling increase exponentially in order to cover the necessary range of the tissue to promote effective response (Balaji et al., 2017; Cordeiro and Jacinto, 2013; Enyedi and Niethammer, 2015; Zhang et al., 2006).

ROS also function as fast signalling molecules, spreading across the tissue similar to calcium intracellular increase. H_2O_2 is formed due to oxidative metabolism and can be either deadly to the cell (in high concentrations) or function as a signalling molecule (Dickinson and Chang, 2011). Its release can happen from the fission of mitochondria upon wounding (Muliyil and Narasimha, 2014; Xu and Chisholm, 2014) and its function can modulate protein reactivity to its downstream targets, alter phosphorylation states or induce other post-translational changes in other proteins (for example, it is known to affect kinase signalling in the leading edge of migrating cells) (Hurd et al., 2012). All these functions are important for wound healing, specifically regarding chemoattractant functions, immune cell activation or modulation of cell adhesion and migration (Cordeiro and Jacinto, 2013; Dunnill et al., 2017; Hurd et al., 2012; Moreira et al., 2010; Niethammer et al., 2009; Xu and Chisholm, 2014; Yoo et al., 2012). More importantly, it was shown in *Drosophila* embryos that inhibiting H_2O_2 production upon wounding (by knocking down NADPH Dual oxidase, DUOX) leads to the decrease of migration of the immune cells to the wound site (Moreira et al., 2010). Additionally, calcium increased has been shown to be involved in production of H_2O_2 by DUOX (Razzell et al., 2013; Xu and Chisholm, 2014).

Nucleotides can also function as signalling molecules. Adenosine triphosphate (ATP) has also been shown to be involved in the sensing of epithelial wound healing. Studies of wound repair in corneal and bronchial human epithelia show a rapid release of ATP to the extracellular medium upon cell lysis. These molecules then interact with receptors from

neighbouring cells that ultimately lead to release of Epidermal Growth Factor (EGF) ligands involved in the regulation of cell proliferation, adhesion and migration. Most importantly, ATP might also increase the uptake of calcium in the context of wound healing, giving yet another evidence of the multiple feedback loops involved in the primary stages of wound sensing (Cordeiro and Jacinto, 2013; Enyedi and Niethammer, 2015; Yin et al., 2007).

Besides these examples of fast signalling methods, wound healing also relies on Damaged-Associated Molecular Patterns (DAMPs), nitric oxide (NO) and electrical fields to signal the presence of an injury in the tissue. As the other small molecules previously described, all these components act immediately upon wounding in order to better orchestrate and modulate the repair process (Cordeiro and Jacinto, 2013; Enyedi and Niethammer, 2015; Kono and Rock, 2008; Leoni et al., 2015; Luo and Chen, 2005; Zhao, 2009).

1.3.2 Cytoskeletal and cell rearrangements

One of the common features across species in epithelial wound repair is the reorganization of the actomyosin cytoskeleton at the wound edge, specially in, although not limited to simple epithelia (Abreu-Blanco et al., 2012; Begnaud et al., 2016; Bement et al., 1993; Danjo and Gipson, 1998; Galko and Krasnow, 2004; Ting et al., 2005a; Wood et al., 2002). Even in amoeba and algae, cytoskeletal reorganization seems to happen upon damage (La Claire II, 1989; Jeon and Jeon, 1975). The assembly of contractile actomyosin cable and the development of specialized actin structures essential for the zippering between wound edges is necessary for proper closure of the gap and rapid resolve of tissue integrity (Begnaud et al., 2016; Cordeiro and Jacinto, 2013; Garcia-Fernandez et al., 2009; Jacinto et al., 2001). This purse string closure mechanism closely resembles other

developmental processes that occur in different species, like dorsal closure in *Drosophila* embryos, epiboly in Zebrafish embryogenesis or cellular extrusion of apoptotic cells (Köppen et al., 2006; Rosenblatt et al., 2001; Wood et al., 2002). All these events involve common players and structures and may be of important value to understand how this event is regulated at a molecular and mechanical levels (Fig. 10).

Most of the cellular analysis of the repair process using live imaging techniques has been done in *Drosophila*. This approach allowed to follow the repair process and formation of the contractile structures, together with the cell shape changes necessary to accommodate the closure without the need for cell proliferation (Antunes et al., 2013; Wood et al., 2002). Nevertheless, we now know that these mechanisms are conserved across species, such as *Xenopus* (Benink and Bement, 2005), mice (Caddy et al., 2010) or chick (Brock et al., 1996).

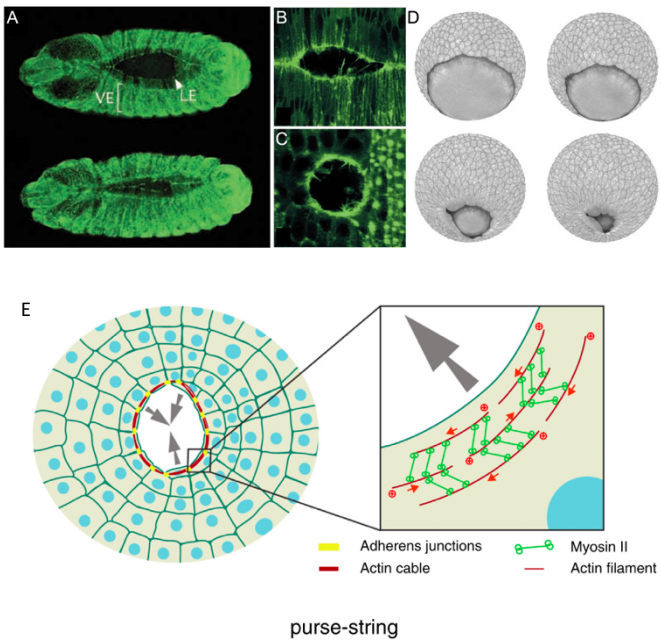

Figure 10. Gap resolution is achieved by purse string closure across different species and different biological processes. The formation of an actomyosin contractile cable at the

leading edge of an epithelial tissue in order to close a discontinuity through tissue contraction and purse string effect is conserved across different morphogenetic events. This structure is important for (A and B) dorsal closure in *Drosophila* embryos, (C) epithelial wound healing in *Drosophila* or (D) epiboly in Zebrafish embryos. (E) The cable is formed through the polymerization of actomyosin filaments at the tissue edge, acquiring contractile capabilities, which drive gap closure. E-Cad is removed of the tissue edge to permit cable assembly, remaining only at the vertices of the leading edge cells (Adapted from http://ist.ac.at/fileadmin/user_upload/pictures/Press_pictures/121011_Heisenberg_Science/1210_HeisenbergGastrulationPhases.jpg; Begnaud et al., 2016; Martin and Parkhurst, 2004).

The formation of the contractile cable at the leading edge soon after wounding (Antunes et al., 2013; Martin and Lewis, 1992; Wood et al., 2002) relies on rapid polymerization of the actomyosin cytoskeleton, through the activation of the small GTPases Rho, Rac and Cdc42 (Benink and Bement, 2005; Tapon and Hall, 1997). Among these factors, Rho is responsible for the formation of the leading edge cable, Rac is involved in the formation of lamellipodia and Cdc42 regulates the formation of filopodia (Cordeiro and Jacinto, 2013; Garcia-Fernandez et al., 2009; Jacinto et al., 2002; Sonnemann and Bement, 2011; Wood et al., 2002; Woolner et al., 2005). Calcium waves within the tissue also correlate with the initiation of actin cytoskeleton polymerization through the regulation of Rho GTPase activity, including its regulators RhoGEFs (Benink and Bement, 2005; Rossman et al., 2005; Xu and Chisholm, 2011). Moreover, increase in intracellular calcium leads to the activation of other actin binding proteins with severing functions (Gelsolin) that can increase the pool of actin monomers. This promotes a bigger and faster wave of actin polymerization through Rho to form the contractile cable (Antunes et al., 2013; Cordeiro and Jacinto, 2013; Robinson, 1999). AJs also play a role in the promotion of the cellular changes. As previously referred in this study, AJs and cytoskeleton maintain a tight communication and mechanical sensing function. Apart from the

normal turnover necessary to accommodate the tension disruption upon injury, it has also been shown that, in *Drosophila* embryos, the downregulation and controlled turnover of E-Cad at the Adherens complexes is required for actin polymerization and bundle formation. Ultimately this process leads to the assembly of the contractile cable around the wound margin (Carvalho et al., 2014; Hunter et al., 2015; Matsubayashi et al., 2015). Integrating all these processes in a coordinated manner promotes the cytoskeletal modifications necessary to lead to the cell shape changes, including first tissue contraction and later cell elongation, to facilitate the rapid closure of the injury and rectifying tissue integrity.

1.3.3 Signalling pathways activated upon wounding

Along with the activation of small GTPases involved in the remodelling of the cytoskeleton of the affected tissue, injury also triggers the activation of other signalling pathways involved in transcription-dependent modulation of the tissue repair process. This modulation is achieved by the activation of key Transcription Factors (TFs), like Grainy Head, c-JUN, FOS, SMAD or STAT3 (Leoni et al., 2015; Mace et al., 2005; Redd et al., 2004; Schäfer and Werner, 2007; Schiller et al., 2004; Ting et al., 2005a; Zenz et al., 2003). These TFs are then responsible for differential gene expression profiles that, although cell type specific, are characteristic of the wound healing process (Sonnemann and Bement, 2011). Additionally, growth factors like transforming growth factor-β (TGFβ), hepatocyte growth factor (HGF), fibroblast growth factor (FGF), platelet derived growth factor (PDGF) or epidermal growth factor (EGF) (Ullrich and Schlessinger, 1990; Werner and Grose, 2003) are released at the wound site, activating intracellular signalling pathways. These growth factors are important in the activation of signalling cascades (normally phosphorylation cascades) that are commonly associated with the initiation of the wound repair mechanism. Receptor

Tyrosine Kinases (RTKs) (Lemmon and Schlessinger, 2010) at the cell membrane recognize the wound signals. These cell surface receptors control several cellular processes fundamental for wound repair, such as proliferation and differentiation, cell survival and metabolism, cell migration, and cell-cycle control (Lemmon and Schlessinger, 2010; Ullrich and Schlessinger, 1990). The overall activation and function of RTKs are highly conserved across different species, in accordance to their important role in cell signalling (Lemmon and Schlessinger, 2010). Several RTKs have been shown to be important for the wound healing process (Müller et al., 2012). The Epidermal growth factor receptor (EGFR) (Shilo, 2005) has been described to be necessary for wound repair in different systems, acting in cytoskeletal remodelling, cell migration and proliferation through crosstalk with ERK signalling (Abu-Humaidan et al., 2014; Geiger et al., 2011; Nakamura et al., 2001; Pastore et al., 2008; Tsarouhas et al., 2014). Fibroblast growth factor receptor (FGFR) and Vascular endothelial growth factor receptor (VEGFR) have also been addressed in the context of wound healing (Bao et al., 2010; Komi-Kuramochi et al., 2005; Werner and Grose, 2003), although their regulation seems to be more important for complex epithelia repair and re-epithelialization stages, especially VEGFR which is linked to angiogenesis. In *Drosophila,* two other RTKs have been shown to be important for repair: Pvr, a member of the PDGF Receptor family, essential for re-epithelialization during larval stages (Wu et al., 2009); and Stitcher (Stit), a RET RTK, that is important for actin remodelling and purse string closure (Wang et al., 2009).

RTKs initiate the signalling cascade that is often relayed to Mitogen Activated Protein Kinase (MAPK) signalling cascades, in an intracellular crosstalk, leading to rapid relay of the wound repair signal. The previously referred ERK signalling pathway, the p38 MAPK (Ono and Han, 2000) and the Jun N-Terminal Kinase (JNK) cascade (Weston and Davis, 2002) are all MAPK involved in the signal transmission and activation of cellular

processes necessary for wound closure and injury resolution. ERK signalling has been proven to be necessary for wound healing and regeneration, namely for migration and actin cytoskeleton remodelling in different systems like *Drosophila*, *Xenopus,* Zebrafish or human cell culture (Geiger et al., 2011; Li et al., 2013; Matsubayashi et al., 2004; Tsarouhas et al., 2014; Wang et al., 2009; Yoo et al., 2012). p38 MAPK has been shown to be involved in the regulation of migration and proliferation during the repair process of corneal epithelial mouse cells (Saika et al., 2004; Sharma et al., 2003; Terai et al., 2011). JNK is also involved in the process of tissue repair in different stages of *Drosophila* development, by directly controlling the activation of specific TFs like Jun, puckered or Fos (Campos et al., 2010; Galko and Krasnow, 2004; Rämet et al., 2002). Interestingly, JNK is also essential for dorsal closure (Jacinto et al., 2002), which supports the existence of common features between this process and wound healing. Overall, most of these signalling cascades cross-talk with each other, resulting in various specific processes within the cell, to ensure tight regulation of the different reactions necessary to achieve the healed tissue.

1.3.4 Immune Response activation

Immune response activation is important to ensure proper wound healing of the injury tissue, regulating the inflammatory process that leads to clot formation and degranulation of the tissue at later stages. Though this process may be more relevant in the repair of complex epithelia, immune cell recruitment also happens in simple/embryonic epithelia. Its main role is to promote debris removal, pathogen clean up and acceleration of tissue closure (Redd et al., 2004; Sonnemann and Bement, 2011). Within the context of this study, only immune cell recruitment in simple epithelia will be discussed, focusing on *Drosophila* wound healing.

Drosophila macrophage-like cells, the hemocytes, migrate to the wound site in a chemoattractant dependent manner (Evans and Wood, 2014; Tepass et al., 1994). These highly motile cells are able to polarize upon sensing the chemotactic gradient, pursuing a direct migration to the source local (Weiner, 2002; Wood et al., 2006). This migration is dependent on phosphatidylinositol3-kinase (PI3K) (Wood et al., 2006) and activation of small GTPases to regulate the formation of actin protrusions and confer motility (Stramer et al., 2005). Moreover, they have the ability to prioritize between stress sensing and development cues (Moreira et al., 2010). In wound repair, H_2O_2 acts as the chemoattractant for these cells (Moreira et al., 2010; Razzell et al., 2013), leading them to the wound edge, where they can engulf damaged epithelial cells and pathogens, clearing the way for proper tissue contraction and closure. This ROS also has the same role in Zebrafish (Niethammer et al., 2009). H_2O_2 production at the wound site is promoted by DUOX (Moreira et al., 2010; Niethammer et al., 2009), which is in turn activated by the rise of intracellular calcium concentration (Razzell et al., 2013). Therefore, this adds up another function for calcium function during the repair process, as the trigger factor for immune cell recruitment in *Drosophila* wound healing.

1.3.5 When Wound Healing fails

The study of wound healing is obviously an interesting issue from the biomedical point of view. Wounds are major routes for the entry of pathogens that lead to potentially damaging infections. Burn injuries or chronic open wounds in diabetic patients, as well as scar formation and fibrosis, can result in complicated and dangerous medical situations, aggravating the clinical state of the patients (Frykberg and Banks, 2015; Greenhalgh, 2003; Sonnemann and Bement, 2011). Moreover, wounds are known to facilitate tumour initiation and progression. Morphogen distribution

and gene expression patterns during wound repair are very similar to the tumour progression microenvironment (Arwert et al., 2012). Epithelial cancers account for the majority of all human cancers. Wound repair of epithelial tissues relies on several mechanisms to restitute cell polarity and adhesion, hallmarks of epithelial cells. Interestingly, the proteins that convey these characteristics can act as tumour suppressors or proto-oncogenes (Martin-Belmonte and Perez-Moreno, 2011). Loss of adhesion cohesiveness in AJs and TJs complexes, with associated depolarization of the cell, can promote the gain of mesenchymal, migratory and invasive characteristics of cells (Jeanes et al., 2008; Lee and Vasioukhin, 2008). This EMT process can be promoted by key TFs (Martin-Belmonte and Perez-Moreno, 2011; Moreno-Bueno et al., 2008), exacerbating epithelial identity loss and paving the way for tumour initiation. Therefore, understanding the molecular basis of epithelial repair is of the upmost importance. Due to the conserved factors upon wound healing across species and scar free manner of resolving tissue discontinuities, simple epithelia are great candidates to understand the dynamics of tissue repair in a cellular level. This model may bring new insights into the tissue behaviour and possible regulatory points.

2. *Drosophila* Epithelial Repair

Drosophila, a well known model organism in genetics and developmental biology, which has been used as a model system for biomedical research for several years now. The analysis of its whole genome as made it possible to analyse the high degree of conservation between *Drosophila* and vertebrates at the level of the molecular players involved in key biochemical pathways (Gonzalez, 2013; Jennings, 2011; Wangler et al., 2015). The absence of genome duplication in *Drosophila* simplifies the analysis of molecular pathways, since most of its components present only a single gene copy. Moreover, the fast and easy maintenance of these animals,

combined with powerful genetic and molecular tools make it a perfect candidate to dissect the molecular basis of biological processes. Wound healing is one of the areas of research where *Drosophila* studies have proven to be crucial for the understanding of the cellular and molecular alterations that occur and how they are regulated (Belacortu and Paricio, 2011; Razzell et al., 2011). The use of insects to study this process dates back to the early twentieth century (Wigglesworth, 1937). The similarity of wound healing with morphogenetic epithelial events that occur during the development of *Drosophila* makes it a strong case for the importance and conservation of these processes (Belacortu and Paricio, 2011; Wood et al., 2002). Despite the obvious differences between the complex mammalian epidermis and the single cell layer epidermis in *Drosophila* (Harden, 2005; Segre, 2003), both entail a similar response mechanism to promote wound closure: reaction to transcription-independent signals like calcium or H_2O_2 (Klepeis et al., 2001; Muliyil and Narasimha, 2014; Niethammer et al., 2009; Razzell et al., 2013); activation of Rho GTPases and kinase signalling cascades, like RTKs and JNK pathways to promote active participation of the leading edge cells in the closure process (Caddy et al., 2010; Galko and Krasnow, 2004; Wood et al., 2002; Woolner et al., 2005); and conserved TFs involved in the modulation of the wound response (Mace et al., 2005; Ting et al., 2005a).

Another advantage of *Drosophila* in wound healing studies is that this process can be studied throughout all developmental stages of the organism. As an holometabolous insect, *Drosophila* undergoes a four-stage metamorphic life cycle divided in embryo, larva, pupa, and the adult fly. It is possible to conduct wound healing analysis at each one of these different stages, assessing differences in developmental periods and players, as well as differential contributions of each part of the system (Fig. 11). For example, while in embryonic and pupal stages no proliferation is necessary

for wound closure nor there is a significant inflammatory response, in larval and adult stages both processes occur (Belacortu and Paricio, 2011).

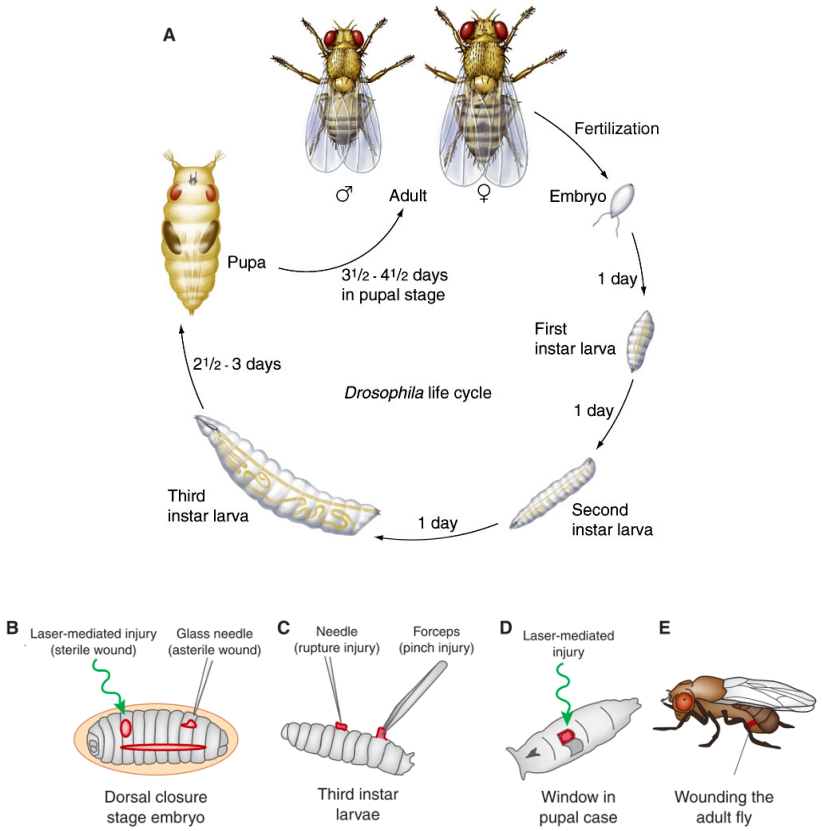

Figure 11. *Drosophila* life cycle and methods to study wound healing at different stages of the organism development. (A) *Drosophila* develops through four different stages (embryo, larva, pupa and adult) that last a period of 10 days (at 25ºC). Embryogenesis occurs in one day, transitioning to a larval stage. The larva grows continuously during three different phases called instars. Pupariation follows, where the organism turns into an immotile pupa, that undergoes metamorphosis to give rise to the adult fly. Wound healing studies can be done in these four different stages, through the application of different methods. (B) In embryos, both sterile and asterile wounding methods can be used (laser ablation and glass needle puncture). (C) In larval stages, rupture or pinch injury can be applied to analyse the wound response. (D) During pupal stages, laser induced wounds are achieved through the prior opening of the pupal case. (E) Adult flies can be

easily injured through mechanical disruption of the tissue or amputation (Adapted from ©The McGraw-Hill Companies, Inc; Razzell et al., 2011).

2.1 Pupal Notum Epithelium formation

In this study, I focus on wound healing dynamics of the pupal epithelium. The formation of this tissue actually starts in the larval stages. During the larval stage, specialized epithelial structures named imaginal discs develop, and ultimately give rise to the definitive adult form. These imaginal discs consist of pairs of highly proliferative epithelial sacs, derived from internal invaginations of the body wall. They are composed of a columnar epithelium, covered by a squamous epithelial peripodial membrane, which is attached to the larval epidermis through a peripodial stalk. During pupal stages, the embryonic and larval remains are destroyed, and these epithelial structures undergo morphogenetic movements of eversion, where the sac turns inside out, and fuse to form the structure that will give rise to the adult form (Fig. 12). This happens during the first 12 hours after puparium formation (APF) (Fristrom and Fristrom, 1993; Zeitlinger and Bohmann, 1999). The pupal epithelium, that will give rise to the adult thorax, derives from the wing imaginal disc (Lawrence and Morata, 1977). One of the morphogenetic events that takes place in the early pupal stages is the junction of both wing imaginal discs. This event is called thorax closure and depends on JNK dependent activation of puckered and Fos, to promote attachment and fusion of both epithelial parts. This is done through the formation of specialized actin structures in the wing disc epithelium, resembling the molecular machinery necessary for embryonic dorsal closure (Martin-Blanco et al., 2000) (Fig. 12).

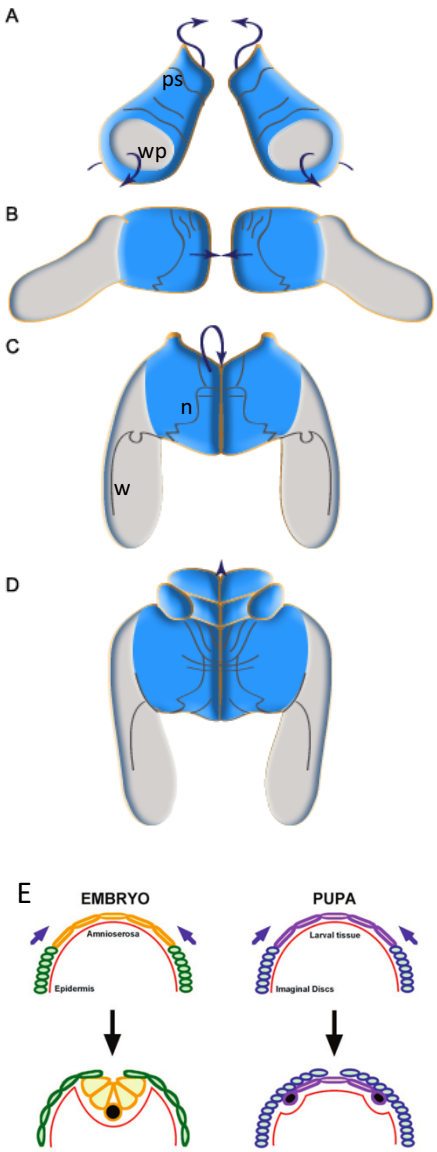

Figure 12. Wing Imaginal discs give rise to the pupal notum and wing. Schematic representation of the morphogenetic event that leads to the formation of the pupal thorax area. The wing disc is attached to the larval epidermis though the peripodial stalk (ps). (A) During pupariation, this structure widens and spreads inside the pupal case (upper arrows). At the same time, the wing pouch (wp; marked in gray) folds on itself (lower arrows) through the invagination of the disc epithelium. (B) The dorsal parts of the discs (marked in blue) then approach and attach to each other in a fusion/closure process, forming the notum (n) and the wing (w). (C) After the closure process, the anterior part folds to contact the eye-antennal imaginal disc (arrow) and, later on, (D) head eversion occurs. (E) In the embryo, dorsal closure promotes the closure of a gap by overlapping the amnioserosa cells (in yellow) with the epidermal cells (in green), which resembles the process of thorax closure in the pupa, where wing disc cells (in blue) close the gap by overlapping the larval tissue cells (in purple). Both amnioserosa and larval cells delaminate and undergo apoptosis (in black) (Adapted from Martin-Blanco et al., 2000; Zeitlinger and Bohmann, 1999).

2.2 Wound healing in pupal stages

The *Drosophila* pupal notum epithelia has proven to be a powerful and efficient model to study morphogenetic movements and epithelial properties (Bosveld et al., 2012; Herszterg et al., 2013; Langevin et al., 2005; Pinheiro et al., 2017). Its accessibility and amenability to genetic manipulation increased its popularity for live imaging analysis of dynamic cellular processes. The analysis by Antunes *et al.* of the wound healing process in this system has greatly improved our understanding of the cytoskeletal dynamics that take place across the tissue upon injury (Antunes et al., 2013). The process of wound repair in the pupa epithelium shows the same characteristics as the repair of simple epithelia in other systems, with the increase of intracellular calcium, reorganization of the actomyosin cytoskeleton to form a contractile actin cable at the wound edge. This cable is capable of contractile force to close the gap, with the aid of filopodia and lamellipodia in the final stages of epithelial resealing (Antunes et al., 2013; Garcia-Fernandez et al., 2009). In this system, it was possible for the first time to observe and understand how all these biomechanical processes are sequentially coordinated at the tissue scale to form the necessary contractile structure and resolve the tissue discontinuity (Fig. 13).

Upon wounding, a rapid and dramatic cytoskeleton remodelling takes place, consisting in a pulse of actomyosin filaments (Munro et al., 2004). This pulse starts several cell rows away from the wound edge, and is then directed cell-to-cell towards the wound site. This creates a flow effect that travels across the tissue, resulting in contractile cable formation. This flow is a consequence of the intracellular increase of calcium that is observed in the tissue, the earliest event observed. The calcium increase propagates from the wound edge, affecting also several cell rows, coinciding with the area that responds to the cytoskeletal reorganization.

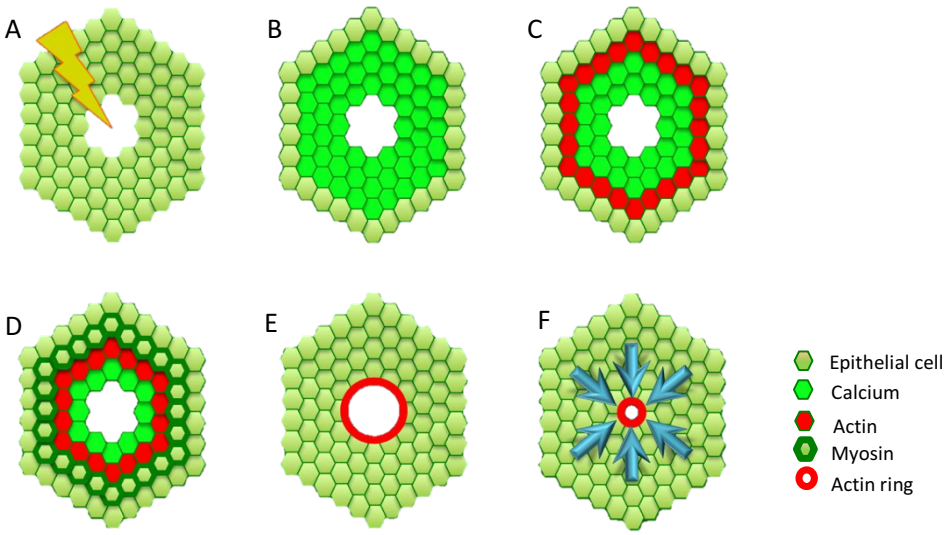

Figure 13. Coordinated events that lead to contractile cable formation in the *Drosophila* pupal notum epithelium. Schematic representation of the process of pupal wound closure. (A) Upon wounding, tissue displacement occurs. (B) It is then followed by an increase of intracellular calcium in several cell rows around the wound (in bright green). (C) As the intracellular calcium wave diminishes in the tissue, directionally towards the wound edge cells, an actin polymerization wave follows (in red). (D) This is accompanied by myosin polymerization and tissue contraction wave (cells delineate in dark green), that ultimately lead to (E) formation of the leading edge contractile actomyosin cable (red circle) and (F) purse string closure of the wound (blue arrows).

The area of the responsive tissue highly correlates with the size of the wound, pointing to a link between tissue displacement and cellular signalling in a mechanosensing process. This tissue displacement and tension disruption may also be important in the mechanical induction of actin monomer release from filaments, that will then be used for repolymerization (Antunes et al., 2013; Higashida et al., 2013; Leckband, 2013). The high levels of actin polymerization that follow, require a considerable pool of actin monomers to permit the increased formin activity. Moreover, in order to

increase the G-actin pool necessary, the intracellular calcium wave is also important in the activation of the actin-severing protein Gelsolin. Similar to wound healing in *C. elegans* (Xu and Chisholm, 2011), transient receptor potential channel M (TRPM) seems to be involved in the start and propagation of the wound response. Along with the actomyosin flow, and as a consequence of its activity, a wave of apical contraction also affects the tissue in the same directional manner promoting the cell shape rearrangements necessary to cover the wound gap. Both these flows are regulated by the Rho GTPase target ROCK and the nucleation activity of the formin Diaphanous (Dia). The propagation of the polymerization event across the tissue points to a mechanical coupling between adjacent cells in order to relay the contractile signal (Martin et al., 2010). The anisotropy of this actomyosin flow is briefly addressed in this study and linked to a slight decrease of E-Cad levels in the junctions parallel to the wound edge, due to stretching and possible redistribution of the adhesion components. This correlation is based on previous studies that show directed actomyosin flows within cells as a response of differential junctional E-Cad levels (Lecuit et al., 2011; Levayer et al., 2011; Rauzi et al., 2010). The coordinated processes that lead to wound closure in the *Drosophila* pupal notum epithelium give a better understanding of the interconnection of all signalling mechanisms. This system can prove to be useful in the identification of new players in the wound healing process.

3. Grainy head family of Transcription Factors

Although the mechanism of wound closure initiation relies on the fast and precise action of transcription-independent signalling, tissue repair ultimately depends on the remodelling of gene expression to restore tissue integrity. For that, several TFs are necessary for the differential activation of wound response genes (Schäfer and Werner, 2007; Sonnemann and Bement,

2011). Several TFs families are activated upon wounding, such as: the Activator Protein-1 (AP-1) TFs, like Fos, Jun and CREB/ATF families, important for the expression of ECM and adhesion components; Myc and the E2F TFs family, that are involved in cell proliferation regulation; or the SMAD proteins, involved in the regulation of migration (Schäfer and Werner, 2007).

One of the most commonly associated TFs families with the process of wound healing, as a conserved player in the activation of wound response genes and re-establishment of the epidermal barrier in vertebrates and invertebrates, is the Grainy head (Grh) family (Mace et al., 2005; Ting et al., 2005a). This family is subdivided in the Grainyhead-like (Grhl) and the CP2 subfamilies (Wang and Samakovlis, 2012). Grh, originally named Elf-1/ NTF-1, was first described in *Drosophila* (Bray and Kafatos, 1991; Bray et al., 1989; Dynlacht et al., 1989). Homologues have since forth been described across a wide and diverse range of animal organisms, from nematodes to higher vertebrates (Janicke et al., 2010; Lim et al., 1992; Murata et al., 1998; Venkatesan et al., 2003; Wang and Samakovlis, 2012; Wilanowski et al., 2002). Grh TFs have also been identified in unicellular organisms, like choanoflagellates and fungi, although with no distinct determination to any of the subfamilies previously referred, which can indicate this phylogenetic division might have occurred later in evolution (Traylor-Knowles et al., 2010). The Grh proteins are characterized by an isoleucine-rich activation domain, a unique DNA-binding motif and a dimerization domain (Attardi et al., 1993; Uv et al., 1994; Venkatesan et al., 2003), as these TFs function as dimers for the binding of a conserved consensus sequence in the DNA regulatory regions. Flies and nematodes present only one Grh gene, while vertebrates have three homologues belonging to the Grhl gene family (Grhl1-3) (Zebrafish has four genes, resultant from the genomic duplication). These TFs can control gene expression as activators or repressors, depending on developmental context

and interaction/competition with other TFs binding partners (Attardi et al., 1993; Bray and Kafatos, 1991; Harrison et al., 2010; Huang et al., 1995; Liaw et al., 1995; Wang and Samakovlis, 2012). Grh has been shown to form complexes with Polycomb TFs, facilitating their respective binding to the DNA sequence (Blastyák et al., 2006; Tuckfield et al., 2002). Moreover, its function can be modified post-translationally, through regulation by upstream signalling pathways (like RTKs, FGF or BMP signalling), leading to differential activation of Grh target genes (Kim and McGinnis, 2011; Liaw et al., 1995; Mace et al., 2005; Tao et al., 2005). Adding to this, alternative splicing in the *Drosophila* Grh can also result in tissue specific isoforms (Uv et al., 1997). Combining all these regulatory processes, Grh TFs sum up a huge list of target genes, conditioned to different biological processes and developmental stages (Wang and Samakovlis, 2012). Several genome wide analysis studies, specially in *Drosophila,* have been done to identify this multitude of target genes (Nevil et al., 2017; Paré et al., 2012; Potier et al., 2014; Yao et al., 2017)

3.1 Grainy head in *Drosophila*

Since *Drosophila* contains only one *grh* gene, this makes it a very attractive system to study how this TF regulates gene expression across the development of the organism. It was named due to its mutant phenotype, an embryo with a grainy head skeleton and a fragile epidermal cuticle (Nüsslein-Volhard et al., 1984), and it was first identified through its ability to bind a cis-element in the *Dopa decarboxylase* (*Ddc*) gene that regulates larval epidermal expression (Bray and Kafatos, 1991; Bray et al., 1989; Johnson et al., 1989). Its expression has been observed in the epidermal tissue, the tracheal airways, foregut and hindgut, as well as in the embryonic central nervous system (CNS), larval neuroblasts and imaginal discs (Bray and Kafatos, 1991; Hemphälä et al., 2003; Uv et al., 1997; Wang and

Samakovlis, 2012). The splicing isoform Grh-O is expressed in the CNS, while the rest of the epithelial tissues express the Grh-N isoform (Uv et al., 1997). Its broad distribution correlates with the numerous processes that it can regulate, such as: epidermal differentiation (Bray et al., 1989; Dynlacht et al., 1989; Johnson et al., 1989), epidermal barrier formation (Mace et al., 2005), tracheal tube size control (Hemphälä et al., 2003), CNS development (Almeida and Bray, 2005; Baumgardt et al., 2014) and establishment of wing hair polarity (Lee and Adler, 2004). Due to the large number of target genes, I will give a few examples of Grh activity across distinct regulatory processes focusing on epithelial development.

One of the most characteristic functions of Grh is the activation of *Ddc* and *pale* (*ple*), genes encoding enzymes necessary for cuticle formation and maturation (Wang and Samakovlis, 2012). Grh has also been shown to regulate adhesion molecules in different contexts: overexpression of Grh in the amnioserosa cells during embryonic dorsal closure leads to the upregulation of SJ components (Narasimha et al., 2008); and the regulation of E-Cad levels by Grh is essential for post-embryonic neuroblast differentiation, serving as a terminal embryonic CNS lineage marker (Almeida and Bray, 2005). At the membrane receptor level, Grh is known to regulate the expression of RTKs, namely Stit, which in turn is responsible for Grh phosphorylation in wound repair (through ERK activation), leading to a regulatory feedback loop (Wang et al., 2009). But *stit* mutants do not show any defects during embryogenesis, which might suggest that Stit is an effector of Grh function only in certain developmental and biological contexts. This proves to be a good example of the highly different functions of Grh across the regulatory network along development. Regarding organ size and morphology control, Grh is the only TF linked to gene regulation during tracheal tube size control (Hemphälä et al., 2003; Yao et al., 2017). In this system, Grh is important in regulating cuticle deposition, epithelial cell shape and apical cell membrane expansion in order to properly form the

tubular epithelial structure. In the adult tissue, Grh is involved in the differentiation of the adult epidermis and polarized hair formation (Lee and Adler, 2004). Here, Grh regulates the expression of Starry night (Stan), an AJ component involved in the regulation of planar cell polarity (PCP) in the tissue. All these different regulation processes derive from a highly modulated function of a single TF (Wang and Samakovlis, 2012).

3.2 Grainyhead-like family in vertebrates

In vertebrates, the Grhl family of TFs is composed of several genes, contrasting to the single copy in the *Drosophila* genome. Mammals have 3 Grh homologues: Grhl-1 (also known as Mammalian Grainy head (MGR)/LBP-32/TFCP2L2), Grhl-2 (Brother-of-MGR (BOM)/TFCP2L3), and Grhl-3 (Sister-of-MGR (SOM)/ Grainy head-like epithelial activator (GET-1)/TFCP2L4) (Wang and Samakovlis, 2012). In Zebrafish, Grhl-2 suffered a duplication along the evolution, giving rise to Grhl2a and Grhl2b, adding to a total of four Grhl TFs. Although there is a high degree of conservation and similarity between their sequences, *GRHL* genes have differential expression patterns and do not seem to be fully redundant during development (Auden et al., 2006; Boglev et al., 2011). In addition, they can form homo or heterodimers to bind DNA and induce/repress gene expression, depending on the context. Grhl TFs are expressed in the epidermis and other epithelial tissue linings, like the oral cavity, urogenital bladder or the gastrointestinal tract (Auden et al., 2006; Wang and Samakovlis, 2012). All three Grhl forms have been associated across different species with epithelial differentiation, barrier function, as well as with morphogenetic movements of ectodermal derived structures, like the neural tube or eyelid closure (Boglev et al., 2011; Gustavsson et al., 2008; Janicke et al., 2010; Mlacki et al., 2014; Rifat et al., 2010; Ting et al., 2005a, 2005b; Wilanowski et al., 2008; Yu et al., 2006). This evident epidermal

maintenance function has also been reported in *Xenopus*, where Grhl-1 was shown to be important for the terminal differentiation of keratinized epidermal structures (Tao et al., 2005). These are a few examples of the multiple functions these TFs can have in epithelial homeostasis and repair.

More recently, specially due to its major importance in the establishment of epithelial identity and development, Grhl deregulation has been observed in tumour formation and cancer progression (Bhandari et al., 2013; Fabian et al., 2014; Kang et al., 2009). Furthermore, their function in regulating epithelial cell adhesion molecules, while repressing mesenchymal markers (Werth et al., 2010), and their involvement in the regulation of EMT (Cieply et al., 2012, 2013), have led some authors to consider these genes as tumour suppressors (Frisch et al., 2017; Ma et al., 2017). This specific function in cancer is still focus of some debate, due to conflicting results about overexpression or downregulation of these TFs in different cancerous contexts (Werner et al., 2013).

3.3 Conserved Functions in Epithelial Regulation

Grh TFs are major determinants of epithelial identity maintenance. Despite the differences in complexity between invertebrate and vertebrate systems, these proteins still display conserved function in the regulation of several biological processes across the different species. Both in *Drosophila* and mice, this TF family shows a restricted expression pattern during embryogenesis, with important roles in organogenesis and epidermal maturation, as development proceeds. Grh TFs have been shown to be important for regulation of cell adhesion (Lee and Adler, 2004; Narasimha et al., 2008; Werth et al., 2010; Yu et al., 2006), an important characteristic of epithelial tissues. Moreover, although the structure of the mammalian skin differs in complexity and components from the insect epidermis, the integrity

of both tissues and the maintenance of the epidermal barrier is promoted and regulated by Grh TFs (Harden, 2005; Jane et al., 2005; Mace et al., 2005; Moussian and Uv, 2005; Ting et al., 2005a). Mouse transglutaminase 1 (TGase1) is a direct target of Grhl3, while in *Drosophila*, Grh regulates the expression of Ddc (Bray and Kafatos, 1991; Ting et al., 2005b). Both proteins are important enzymes in the process of keratin and chitin cross-linking, forming the keratinized structure and cuticle. These are fundamental structures that build a proper epidermal barrier in vertebrates and invertebrates.

It is also worth noting, that although function conservation has not been proven yet, Grh TFs have been linked to the PCP pathway in both invertebrate and vertebrate systems: in flies, the regulation of Stan, through the cooperation with Frizzled, leads to the formation of planar polarized structures in the epidermis of the adult organism (Lee and Adler, 2004); in *Xenopus*, Grhl3 was shown to regulate directly RhoGEF19, a RhoA activator involved in planar polarization during epidermal wound repair (Caddy et al., 2010). Another example of possible function conservation is the formation and maintenance of epithelial characteristics in tubular structures. In *Drosophila*, Grh is associated with tube size control in the tracheal system, while Grhl TFs have been linked to several tubular tissues undergoing branching morphogenesis, such as the lungs or the kidney (Auden et al., 2006; Aue et al., 2015; Hemphälä et al., 2003).

This homology between several different processes strengthens the Grh family of TFs as a highly conserved player in epithelial regulation.

The conserved functions of Grh in the maintenance of epidermal barrier and in wound repair are the focus of this study.

3.4 Grainy head and Wound healing

Although epithelial tissues have many functions related to compartmentalization, the permeability barrier needs to be established soon enough to allow the development and survival of the organism. Depending on the complexity of the animal, its permeability barrier can be defined by different specialized layers of epithelial cells. This includes the keratinized cover of the mammalian skin (Feingold and Denda, 2012) or the chitin cuticle structure that protects the outer epithelium in insects (Pesch et al., 2016). Disruption of this permeability barrier can result in rapid deregulation of the internal cellular environment, which is why the repair process is quickly activated in the affected epithelium and, consequently, in the underlying tissue (Feingold and Denda, 2012; Marchiando et al., 2010). Grh TFs are known to be important regulators of this structure (Moussian and Uv, 2005).

Grh has long been known to be essential for the repair of the protective cuticle layer of *Drosophila* in the later stages of wound repair (Mace et al., 2005). For this, Grh activates a group of wound response genes, responsible for restoring this structure (Mace et al., 2005; Pearson et al., 2009). During the repair process, ERK phosphorylates Grh to drive the expression of the target genes (Kim and McGinnis, 2011). It has been shown that phosphorylation is only necessary for Grh functions in the wound repair process but not for developmental homeostatic regulation of other targets. More recently, it was shown that Grh is also involved in the control of the actin cytoskeleton and the formation of the characteristic contractile actomyosin cable at the leading edge of the wound (Wang et al., 2009). Here, the RTK Stit (also known as Cad96Ca) activates ERK at the wound site and consequent phosphorylation of Grh (Fig. 14). In turn, Grh activates epidermal Stit expression. Thus, Stit acts upstream and downstream of Grh, in a positive feedback loop where signalling amplification ensures the

efficient triggering and resolution of wound repair. The link to the cytoskeleton is also through Stit, as mutants for this RTK fail to assemble a proper cable and show a delay in tissue closure (Wang et al., 2009).

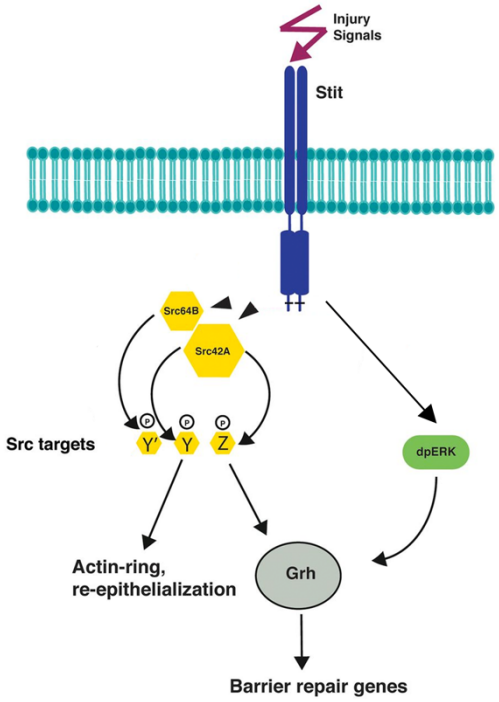

Figure 14. Grh phosphorylation upon injury. Proposed model for phosphorylation of Grh and wound response genes activation. Grh is phosphorylated by ERK or Src42A. The activation of both kinases is dependent on the RTK Stit, itself a transcriptional target of Grh. Src42A is also responsible for actin cytoskeleton remodelling upon Stit activation (Adapted from Tsarouhas et al., 2014).

The regulation of the actin remodelling is done through the activation of Src42A, a downstream target of Stit. In turn, Src42A is also capable of phosphorylating Grh in order to promote further wound response gene activation (Tsarouhas et al., 2014). An additional regulation step is the potential activation of ERK through EGFR, another RTK pathway (Geiger et al., 2011). This shows an indirect link between actin remodelling and Grh function (through the regulation of Stit). However in *Xenopus* it was shown that Grhl3 can also control actin cytoskeleton remodelling through the regulation of the direct target small GTPase RhoGEF19 (Caddy et al., 2010).

The combination of all these studies suggests a key role for Grh in wound repair, besides the later stage processes of cuticle remodelling.

4. Aims and Scope

Withstanding aggression comes at a cost for the integrity of the protective epithelial tissue of any organism. Any discontinuity needs to be fast and properly resolved, in order to restore normal development or homeostasis. For this, wound healing relies on the coordination of numerous integrated signalling machineries. It is of the upmost importance to understand the processes that occur within each reactive cell, their regulation and how they are transmitted to the adjacent neighbours leading to a concerted tissue response. Grh TFs, regulators of epithelial identity, are crucial for the coordination of the wound repair response, and given the size of the regulatory network they control, many of their targets will undoubtedly be necessary for this process.

This PhD thesis aims to better understand the role of Grh in wound healing of simple epithelia, by analysing several aspects of the regulation of the process in which Grh is potentially involved. For that, I made use of fast live imaging analysis in the *Drosophila* pupal notum epithelium and the Zebrafish embryonic epithelium to assess how Grh is regulating cellular dynamics in wound repair.

In Chapter II, I intended to unveil how Grh directly modulates the cellular response during early repair stages, prior to cuticle restoration. For this I made use of high resolution live imaging of the repair process in the *Drosophila* pupal notum epithelium.

In Chapter III, I wanted to understand the influence of Grh in calcium dynamics and regulation, through a genetic screen of Grh targets and the

analysis of their importance in the early response of the repair process using the same approach as in Chapter II.

In Chapter IV, I wanted to complement my analysis in Drosophila with a perspective of Grh roles in a vertebrate system. For that, I decide to use Zebrafish to characterize the expression of the different Grhl TFs during development. Moreover, I aimed to set a new wound healing assay in the Zebrafish embryonic epithelium, and perform a preliminary analysis of the importance of Grhl TFs in vertebrate embryonic wound repair.

Finally, in Chapter V, I integrate all the resulting work, correlating it to what is now known in the field, in order to propose future perspectives for the study of Grh in wound healing and its role as a general epithelial stress manager.

5. References

Abreu-Blanco, M.T., Verboon, J.M., Liu, R., Watts, J.J., and Parkhurst, S.M. (2012). Drosophila embryos close epithelial wounds using a combination of cellular protrusions and an actomyosin purse string. J. Cell Sci. *125*, 5984–5997.

Abu-Humaidan, A.H.A., Ananthoju, N., Mohanty, T., Sonesson, A., Alberius, P., Schmidtchen, A., Garred, P., and Sorensen, O.E. (2014). The Epidermal Growth Factor Receptor Is a Regulator of Epidermal Complement Component Expression and Complement Activation. J. Immunol. *192*, 3355–3364.

Akin, O., and Mullins, R.D. (2008). Capping Protein Increases the Rate of Actin-Based Motility by Promoting Filament Nucleation by the Arp2/3 Complex. Cell *133*, 841–851.

Alberts, B., Johnson, A., Lewis, J., Martin, R., Roberts, K., and Walter, P. (2007). Molecular Biology of the Cell (New York: Garland Science).

Almeida, M.S., and Bray, S.J. (2005). Regulation of post-embryonic neuroblasts by Drosophila Grainyhead. Mech. Dev. *122*, 1282–1293.

Antunes, M., Pereira, T., Cordeiro, J. V., Almeida, L., and Jacinto, A. (2013). Coordinated waves of actomyosin flow and apical cell constriction immediately after wounding. J. Cell Biol. *202*, 365–379.

Arwert, E.N., Hoste, E., and Watt, F.M. (2012). Epithelial stem cells, wound healing and cancer. Nat. Rev. Cancer *12*, 170–180.

Attardi, L.D., Von Seggern, D., and Tjian, R. (1993). Ectopic expression of wild-type or a dominant-negative mutant of transcription factor NTF-1 disrupts normal Drosophila development. Proc. Natl. Acad. Sci. U. S. A. *90*, 10563–10567.

Auden, A., Caddy, J., Wilanowski, T., Ting, S.B., Cunningham, J.M., and

Jane, S.M. (2006). Spatial and temporal expression of the Grainyhead-like transcription factor family during murine development. Gene Expr. Patterns *6*, 964–970.

Aue, A., Hinze, C., Walentin, K., Ruffert, J., Yurtdas, Y., Werth, M., Chen, W., Rabien, A., Kilic, E., Schulzke, J.-D., et al. (2015). A Grainyhead-Like 2/Ovo-Like 2 Pathway Regulates Renal Epithelial Barrier Function and Lumen Expansion. J. Am. Soc. Nephrol. *26*, 2704–2715.

Bajpai, S., Correia, J., Feng, Y., Figueiredo, J., Sun, S.X., Longmore, G.D., Suriano, G., and Wirtz, D. (2008). alpha-Catenin mediates initial E-cadherin-dependent cell-cell recognition and subsequent bond strengthening. Proc. Natl. Acad. Sci. U. S. A. *105*, 18331–18336.

Balaji, R., Bielmeier, C., Harz, H., Bates, J., Stadler, C., Hildebrand, A., and Classen, A.-K. (2017). Calcium spikes, waves and oscillations in a large, patterned epithelial tissue. Sci. Rep. *7*, 42786.

Bao, P., Kodra, A., Tomic-canic, M., Golinko, M.S., Ehrlich, H.P., and Brem, H. (2010). The role of vascular endothelial groth factor in wound healing. J. Surg. Res. *153*, 347–358.

Baum, B., Settleman, J., and Quinlan, M.P. (2008). Transitions between epithelial and mesenchymal states in development and disease. Semin. Cell Dev. Biol. *19*, 294–308.

Baumgardt, M., Karlsson, D., Salmani, B.Y., Bivik, C., MacDonald, R.B., Gunnar, E., and Thor, S. (2014). Global Programmed Switch in Neural Daughter Cell Proliferation Mode Triggered by a Temporal Gene Cascade. Dev. Cell *30*, 192–208.

Begnaud, S., Chen, T., Delacour, D., Mège, R.M., and Ladoux, B. (2016). Mechanics of epithelial tissues during gap closure. Curr. Opin. Cell Biol. *42*, 52–62.

Belacortu, Y., and Paricio, N. (2011). Drosophila as a model of wound

healing and tissue regeneration in vertebrates. Dev. Dyn. *240*, 2379–2404.

Bement, W.M., and Capco, D.G. (1991). Analysis of inducible contractile rings suggests a role for protein kinase C in embryonic cytokinesis and wound healing. Cell Motil. Cytoskeleton *20*, 145–157.

Bement, W.M., Forscher, P., and Mooseker, M.S. (1993). A novel cytoskeletal structure involved in purse string wound closure and cell polarity maintenance. J. Cell Biol. *121*, 565–578.

Benink, H.A., and Bement, W.M. (2005). Concentric Zones of Active RhoA and Cdc42 around Single Cell Wounds. J. Cell Biol. *168*, 429–439.

Berridge, M.J. (1997). Elementary and global aspects of calcium signalling. J. Physiol. *499*, 291–306.

Berridge, M.J., Lipp, P., and Bootman, M.D. (2000). The versatility and universality of calcium signalling. Nat. Rev. Mol. Cell Biol. *1*, 11–21.

Bhandari, A., Gordon, W., Dizon, D., Hopkin, A.S., Gordon, E., Yu, Z., and Andersen, B. (2013). The Grainyhead transcription factor Grhl3/Get1 suppresses miR-21 expression and tumorigenesis in skin: modulation of the miR-21 target MSH2 by RNA-binding protein DND1. Oncogene *32*, 1497–1507.

Blanchoin, L., Boujemaa-Paterski, R., Sykes, C., and Plastino, J. (2014). Actin Dynamics, Architecture, and Mechanics in Cell Motility. Physiol. Rev. *94*, 235–263.

Blastyák, A., Mishra, R.K., and Karch, F. (2006). Efficient and Specific Targeting of Polycomb Group Proteins Requires Cooperative Interaction between Grainyhead and Pleiohomeotic Efficient and Specific Targeting of Polycomb Group Proteins Requires Cooperative Interaction between Grainyhead and Pleiohome. *26*, 1434–1444.

Boglev, Y., Wilanowski, T., Caddy, J., Parekh, V., Auden, A., Darido, C., Hislop, N.R., Cangkrama, M., Ting, S.B., and Jane, S.M. (2011). The unique

and cooperative roles of the Grainy head-like transcription factors in epidermal development reflect unexpected target gene specificity. Dev. Biol. *349*, 512–522.

Borradori, L., and Sonnenberg, A. (1999). Structure and function of hemidesmosomes: More than simple adhesion complexes. J. Invest. Dermatol. *112*, 411–418.

Bosveld, F., Bonnet, I., Guirao, B., Tlili, S., Wang, Z., Petitalot, A., Marchand, R., Bardet, P.-L.P.-L., Marcq, P., Graner, F., et al. (2012). Mechanical control of morphogenesis by Fat/Dachsous/Four-Jointed planar cell polarity pathway. Science *336*, 724–727.

Bray, S.J., and Kafatos, F. (1991). Developmental function of Elf-1: an essential transcription factor during embryogenesis in Drosophila. Genes Dev. *5*, 1672–1683.

Bray, S.J., Burke, B., Brown, N.H., and Hirsh, J. (1989). Embryonic expression pattern of a family of Drosophila proteins that interact witn a central nervous system regulatory element. Genes Dev. *1019*, 1130–1145.

Brock, J., Midwinter, K., Lewis, J., and Martin, P. (1996). Healing of Incisional Wounds in the Embryonic Chick Wing Bud: Characterization of the Actin Purse-String and Demonstration of a Requirement for Rho Activation. J. Cell Biol. *135*, 1097–1107.

Buckley, C.D., Tan, J., Anderson, K.L., Hanein, D., Volkmann, N., Weis, W.I., Nelson, W.J., and Dunn, a. R. (2014). The minimal cadherin-catenin complex binds to actin filaments under force. Science *346*, 1254211–1254211.

Bulgakova, N.A., and Brown, N.H. (2016). Drosophila p120catenin is critical for endocytosis of the dynamic E-cadherin-Bazooka complex. J. Cell Sci. *129*, 477–482.

Caddy, J., Wilanowski, T., Darido, C., Dworkin, S., Ting, S.B., Zhao, Q.,

Rank, G., Auden, A., Srivastava, S., Papenfuss, T. a, et al. (2010). Epidermal wound repair is regulated by the planar cell polarity signaling pathway. Dev. Cell *19*, 138–147.

Campos, I., Geiger, J. a, Santos, A.C., Carlos, V., and Jacinto, A. (2010). Genetic screen in Drosophila melanogaster uncovers a novel set of genes required for embryonic epithelial repair. Genetics *184*, 129–140.

Carvalho, L., Jacinto, A., and Matova, N. (2014). The Toll/NF-κB signaling pathway is required for epidermal wound repair in Drosophila. Proc. Natl. Acad. Sci. U. S. A. *111*, E5373-82.

Cavey, M., and Lecuit, T. (2009). Molecular Bases of Cell – Cell Junctions Stability and Dynamics. Cold Spring Harb. Perspect. Biol. *1*, 1–19.

Cheng, X., Zhang, X., Yu, L., and Xu, H. (2015). Calcium signaling in membrane repair. Semin. Cell Dev. Biol. *45*, 24–31.

Cieply, B., Riley, P., Pifer, P.M., Widmeyer, J., Addison, J.B., Ivanov, A. V, Denvir, J., and Frisch, S.M. (2012). Suppression of the Epithelial-Mesenchymal Transition by Grainyhead-Like-2. Cancer Res. *72*, 2440–2453.

Cieply, B., Farris, J., Denvir, J., Ford, H.L., and Frisch, S.M. (2013). Epithelial-mesenchymal transition and tumor suppression are controlled by a reciprocal feedback loop between ZEB1 and Grainyhead-like-2. Cancer Res. *73*, 6299–6309.

La Claire II, J.W. (1989). Actin cytoskeleton in intact and wounded coenocytic green algae. Planta *177*, 47–57.

Collinet, C., and Lecuit, T. (2013). Stability and dynamics of cell-cell junctions (Elsevier Inc.).

Cordeiro, J. V, and Jacinto, A. (2013). The role of transcription-independent damage signals in the initiation of epithelial wound healing. Nat. Rev. Mol. Cell Biol. *14*, 249–262.

Danjo, Y., and Gipson, I.K. (1998). Actin “purse string” filaments are anchored by E-cadherin-mediated adherens junctions at the leading edge of the epithelial wound, providing coordinated cell movement. J. Cell Sci. *111 (Pt22)*, 3323–3332.

Desai, R., Sarpal, R., Ishiyama, N., Pellikka, M., Ikura, M., and Tepass, U. (2013). Monomeric α-catenin links cadherin to the actin cytoskeleton. Nat. Cell Biol. *15*, 261–273.

Dickinson, B.C., and Chang, C.J. (2011). Chemistry and biology of reactive oxygen species in signaling or stress responses. Nat. Chem. Biol. *7*, 504–511.

Drees, F., Pokutta, S., Yamada, S., Nelson, W.J., and Weis, W.I. (2005). Alpha-catenin is a molecular switch that binds E-cadherin-beta-catenin and regulates actin-filament assembly. Cell *123*, 903–915.

Dunnill, C., Patton, T., Brennan, J., Barrett, J., Dryden, M., Cooke, J., Leaper, D., and Georgopoulos, N.T. (2017). Reactive oxygen species (ROS) and wound healing: the functional role of ROS and emerging ROS-modulating technologies for augmentation of the healing process. Int. Wound J. *14*, 89–96.

Dynlacht, B.D., Attardi, L.D., Admon, A., Freeman, M., and Tjian, R. (1989). Functional analysis of NTF-1, a developmentally regulated Drosophila transcription factor that binds neuronal cis elements. Genes Dev. *3*, 1677–1688.

Engl, W., Arasi, B., Yap, L.L., Thiery, J.P., and Viasnoff, V. (2014). Actin dynamics modulate mechanosensitive immobilization of E-cadherin at adherens junctions. Nat. Cell Biol *16*, 584–591.

Enyedi, B., and Niethammer, P. (2015). Mechanisms of epithelial wound detection. Trends Cell Biol. *25*, 398–407.

Evans, I.R., and Wood, W. (2014). Drosophila blood cell chemotaxis. Curr.

Opin. Cell Biol. *30*, 1–8.

Evans, W.H., and Martin, P.E.M. (2002). Gap junctions: structure and function (Review). Mol. Membr. Biol. *19*, 121–136.

Fabian, J., Lodrini, M., Oehme, I., Schier, M.C., Thole, T.M., Hielscher, T., Kopp-Schneider, A., Opitz, L., Capper, D., Von Deimling, A., et al. (2014). GRHL1 acts as tumor suppressor in neuroblastoma and is negatively regulated by MYCN and HDAC3. Cancer Res. *74*, 2604–2616.

Feingold, K.R., and Denda, M. (2012). Regulation of permeability barrier homeostasis. Clin. Dermatol. *30*, 263–268.

Fonteriz, R., Matesanz-Isabel, J., Arias-del-Val, J., Alvarez-Illera, P., Montero, M., and Alvarez, J. (2016). Modulation of Calcium Entry by Mitochondria. In Calcium Entry Pathways in Non-Excitable Cells., J. Rosado, ed. (Springer International Publishing), pp. 405–421.

Friedl, P., Hegerfeldt, Y., and Tusch, M. (2004). Collective cell migration in morphogenesis and cancer. Int. J. Dev. Biol. *48*, 441–449.

Frisch, S.M., Farris, J.C., and Pifer, P.M. (2017). Roles of Grainyhead-like transcription factors in cancer. Oncogene *96*, 1200–1209.

Fristrom, D., and Fristrom, J.W. (1993). The metamorphic development of the adult epidermis. In The Development of Drosophila Melanogaster., M. Bate, and A. Martinez-Arias, eds. (Cold Spring Harbor Laboratory Press.), p.

Frykberg, R.G., and Banks, J. (2015). Challenges in the Treatment of Chronic Wounds. Adv. Wound Care *4*, 560–582.

Galko, M.J., and Krasnow, M. a (2004). Cellular and genetic analysis of wound healing in Drosophila larvae. PLoS Biol. *2*, E239.

Garcia-Fernandez, B., Campos, I., Geiger, J., Santos, A.C., and Jacinto, A. (2009). Epithelial resealing. Int. J. Dev. Biol. *53*, 1549–1556.

Geiger, J. a, Carvalho, L., Campos, I., Santos, A.C., and Jacinto, A. (2011).

Hole-in-one mutant phenotypes link EGFR/ERK signaling to epithelial tissue repair in Drosophila. PLoS One *6*, e28349.

Getsios, S., Huen, A.C., and Green, K.J. (2004). Working out the strength and flexibility of desmosomes. Nat. Rev. Mol. Cell Biol. *5*, 271–281.

Gonzalez, C. (2013). Drosophila melanogaster: a model and a tool to investigate malignancy and identify new therapeutics. Nat. Rev. Cancer *13*, 172–183.

Greenhalgh, D.G. (2003). Wound healing and diabetes mellitus. Clin. Plast. Surg. *30*, 37–45.

Gustavsson, P., Copp, A.J., and Greene, N.D.E. (2008). Grainyhead genes and mammalian neural tube closure. Birth Defects Res. A. Clin. Mol. Teratol. *82*, 728–735.

Harden, N. (2005). Of Grainy Heads and Broken Skins. Science *308*, 364–365.

Harrison, M.M., Botchan, M.R., and Cline, T.W. (2010). Grainyhead and Zelda compete for binding to the promoters of the earliest-expressed Drosophila genes. Dev. Biol. *345*, 248–255.

Heisenberg, C.P., and Bellaïche, Y. (2013). Forces in tissue morphogenesis and patterning. Cell *153*, 948–962.

Hemphälä, J., Uv, A., Cantera, R., Bray, S., and Samakovlis, C. (2003). Grainy head controls apical membrane growth and tube elongation in response to Branchless/FGF signalling. Development *130*, 249–258.

Herszterg, S., Leibfried, A., Bosveld, F., Martin, C., and Bellaiche, Y. (2013). Interplay between the dividing cell and its neighbors regulates adherens junction formation during cytokinesis in epithelial tissue. Dev. Cell *24*, 256–270.

Higashida, C., Kiuchi, T., Akiba, Y., Mizuno, H., Maruoka, M., Narumiya, S.,

Mizuno, K., and Watanabe, N. (2013). F- and G-actin homeostasis regulates mechanosensitive actin nucleation by formins. Nat. Cell Biol. *15*, 395–405.

Huang, J., Dubnicoff, T., Liaw, G., Bai, Y., Valentine, S.A., Shirokawa, J.M., Lengyel, J.A., and Courey, A.J. (1995). Binding sites for transcription factor repression of decapentaplegic. 3177–3189.

Hunter, M. V., Lee, D.M., Harris, T.J.C., and Fernandez-Gonzalez, R. (2015). Polarized E-cadherin endocytosis directs actomyosin remodeling during embryonic wound repair. J. Cell Biol. *210*, 801–816.

Hurd, T.R., DeGennaro, M., and Lehmann, R. (2012). Redox regulation of cell migration and adhesion. Trends Cell Biol. *22*, 107–115.

Jacinto, A., Martinez-Arias, A., and Martin, P. (2001). Mechanisms of epithelial fusion and repair. Nat. Cell Biol. *3*, E117-123.

Jacinto, A., Wood, W., Woolner, S., Hiley, C., Turner, L., Wilson, C., Martinez-Arias, A., and Martin, P. (2002). Dynamic analysis of actin cable function during Drosophila dorsal closure. Curr. Biol. *12*, 1245–1250.

Jane, S.M., Ting, S.B., and Cunningham, J.M. (2005). Epidermal impermeable barriers in mouse and fly. Curr. Opin. Genet. Dev. *15*, 447–453.

Janicke, M., Renisch, B., and Hammerschmidt, M. (2010). Zebrafish grainyhead-like1 is a common marker of different non-keratinocyte epidermal cell lineages, which segregate from each other in a Foxi3-dependent manner. Int. J. Dev. Biol. *54*, 837–850.

Jeanes, A., Gottardi, C.J., and Yap, A.S. (2008). Cadherins and cancer: how does cadherin dysfunction promote tumor progression? Oncogene *27*, 6920–6929.

Jennings, B.H. (2011). Drosophila - a versatile model in biology & medicine. Mater. Today *14*, 190–195.

Jeon, K.W., and Jeon, M.S. (1975). Cytoplasmic filaments and cellular wound healing in amoeba proteus. J. Cell Biol. *67*, 243–249.

Johnson, W. a., McCormick, C. a., Bray, S.J., and Hirsh, J. (1989). A neuron-specific enhancer of the Drosophila dopa decarboxylase gene. Genes Dev. *3*, 676–686.

Kang, X., Chen, W., Kim, R.H., Kang, M.K., and Park, N.-H. (2009). Regulation of the hTERT promoter activity by MSH2, the hnRNPs K and D, and GRHL2 in human oral squamous cell carcinoma cells. Oncogene *28*, 565–574.

Kim, M., and McGinnis, W. (2011). Phosphorylation of Grainy head by ERK is essential for wound-dependent regeneration but not for development of an epidermal barrier. Proc. Natl. Acad. Sci. U. S. A. *108*, 650–655.

Klepeis, V.E., Cornell-Bell, A., and Trinkaus-Randall, V. (2001). Growth factors but not gap junctions play a role in injury-induced Ca2+ waves in epithelial cells. J. Cell Sci. *114*, 4185–4195.

Knust, E. (2002). Composition and Formation of Intercellular Junctions in Epithelial Cells. Science *298*, 1955–1959.

Komi-Kuramochi, A., Kawano, M., Oda, Y., Asada, M., Suzuki, M., Oki, J., and Imamura, T. (2005). Expression of fibroblast growth factors and their receptors during full-thickness skin wound healing in young and aged mice. J. Endocrinol. *186*, 273–289.

Kono, H., and Rock, K.L. (2008). How dying cells alert the immune system to danger. Nat. Rev. Immunol. *8*, 279–289.

Köppen, M., Fernández, B.G., Carvalho, L., Jacinto, A., and Heisenberg, C.-P. (2006). Coordinated cell-shape changes control epithelial movement in zebrafish and Drosophila. Development *133*, 2671–2681.

Ladoux, B., Nelson, J., Yan, J., and Mège, R.-M. (2015). The mechanotransduction machinery at work at adherens junctions. Integr. Biol.

7, 1109–1119.

Langevin, J., Morgan, M.J., Rossé, C., Racine, V., Sibarita, J.-B., Aresta, S., Murthy, M., Schwarz, T., Camonis, J., and Bellaïche, Y. (2005). Drosophila Exocyst Components Sec5, Sec6, and Sec15 Regulate DE-Cadherin Trafficking from Recycling Endosomes to the Plasma Membrane. Dev. Cell *9*, 365–376.

Lawrence, P.A., and Morata, G. (1977). The early development of mesothoracic compartments in Drosophila. An analysis of cell lineage and fate mapping and an assessment of methods. Dev. Biol. *56*, 40–51.

Leckband, D. (2013). Formin' cables under stress. Nat. Cell Biol. *15*, 345–346.

Leckband, D.E., and de Rooij, J. (2014). Cadherin Adhesion and Mechanotransduction. Annu. Rev. Cell Dev. Biol. *30*, 291–315.

Lecuit, T., and Yap, A.S. (2015). E-cadherin junctions as active mechanical integrators in tissue dynamics. Nat. Cell Biol. *17*, 533–539.

Lecuit, T., Lenne, P.-F., and Munro, E. (2011). Force generation, transmission, and integration during cell and tissue morphogenesis. Annu. Rev. Cell Dev. Biol. *27*, 157–184.

Lee, H., and Adler, P.N. (2004). The grainy head transcription factor is essential for the function of the frizzled pathway in the Drosophila wing. Mech. Dev. *121*, 37–49.

Lee, J.L., and Streuli, C.H. (2014). Integrins and epithelial cell polarity. J. Cell Sci. *127*, 3217–3225.

Lee, M., and Vasioukhin, V. (2008). Cell polarity and cancer - cell and tissue polarity as a non-canonical tumor suppressor. J. Cell Sci. *121*, 1141–1150.

Lemmon, M.A., and Schlessinger, J. (2010). Cell signaling by receptor tyrosine kinases. Cell *141*, 1117–1134.

Leoni, G., Neumann, P.-A., Sumagin, R., Denning, T.L., and Nusrat, A. (2015). Wound repair: role of immune–epithelial interactions. Mucosal Immunol. *8*, 959–968.

Levayer, R., and Lecuit, T. (2011). Biomechanical regulation of contractility: spatial control and dynamics. Trends Cell Biol. *22*, 61–81.

Levayer, R., Pelissier-Monier, A., and Lecuit, T. (2011). Spatial regulation of Dia and Myosin-II by RhoGEF2 controls initiation of E-cadherin endocytosis during epithelial morphogenesis. Nat. Cell Biol. *13*, 529–540.

Li, J., Zhang, S., Soto, X., Woolner, S., and Amaya, E. (2013). ERK and phosphoinositide 3-kinase temporally coordinate different modes of actin-based motility during embryonic wound healing. J. Cell Sci. *126*, 5005–5017.

Liaw, G.J., Rudolph, K.M., Huang, J.D., Dubnicoff, T., Courey, A.J., and Lengyel, J.A. (1995). The torso response element binds GAGA and NTF-1/Elf-1, and regulates tailless by relief of repression. Genes Dev. *9*, 3163–3176.

Lim, L.C., Swendeman, S.L., and Sheffery, M. (1992). Molecular Cloning of the oL-Globin Transcription Factor CP2. Mol. Cell. Biol. *12*, 828–835.

Luo, J.D., and Chen, A.F. (2005). Nitric oxide: A newly discovered function on wound healing. Acta Pharmacol. Sin. *26*, 259–264.

Ma, L., Yan, H., Zhao, H., and Sun, J. (2017). Grainyhead-like 2 in development and cancer. Tumor Biol. *39*, 101042831769837.

Mace, K.A., Pearson, J.C., and McGinnis, W. (2005). An epidermal barrier wound repair pathway in Drosophila is mediated by grainy head. Science *308*, 381–385.

Machesky, L.M., and Insall, R.H. (1998). Scar1 and the related Wiskott–Aldrich syndrome protein, WASP, regulate the actin cytoskeleton through the Arp2/3 complex. Curr. Biol. *8*, 1347–1356.

Mandato, C.A., and Bement, W.M. (2001). Contraction and polymerization cooperate to assemble and close actomyosin rings around Xenopus oocyte wounds. J. Cell Biol. *154*, 785–797.

Marchiando, A.M., Graham, W.V., and Turner, J.R. (2010). Epithelial barriers in homeostasis and disease. Annu. Rev. Pathol. *5*, 119–144.

Martin, P. (1997). Wound Healing - Aiming for Perfect Skin Regeneration. Science *276*, 75–81.

Martin, P., and Lewis, J. (1992). Actin cables and epidermal movement in embryonic wound healing. Nature *360*, 179–183.

Martin, P., and Parkhurst, S.M. (2004). Parallels between tissue repair and embryo morphogenesis. Development *131*, 3021–3034.

Martin, A.C., Gelbart, M., Fernandez-Gonzalez, R., Kaschube, M., and Wieschaus, E.F. (2010). Integration of contractile forces during tissue invagination. J. Cell Biol. *188*, 735–749.

Martin-Belmonte, F., and Mostov, K. (2008). Regulation of cell polarity during epithelial morphogenesis. Curr. Opin. Cell Biol. *20*, 227–234.

Martin-Belmonte, F., and Perez-Moreno, M. (2011). Epithelial cell polarity, stem cells and cancer. Nat. Rev. Cancer *12*, 23–38.

Martin-Blanco, E., Pastor-Pareja, J.C., and Garcia-Bellido, a (2000). JNK and decapentaplegic signaling control adhesiveness and cytoskeleton dynamics during thorax closure in Drosophila. Proc. Natl. Acad. Sci. U. S. A. *97*, 7888–7893.

Matsubayashi, Y., Ebisuya, M., Honjoh, S., and Nishida, E. (2004). ERK Activation Propagates in Epithelial Cell Sheets and Regulates Their Migration during Wound Healing. Current *14*, 731–735.

Matsubayashi, Y., Coulson-Gilmer, C., and Millard, T.H. (2015). Endocytosis-dependent coordination of multiple actin regulators is required

for wound healing. J. Cell Biol. *210*, 419–433.

Matter, K., and Balda, M.S. (2003). Signalling to and from tight junctions. Nat. Rev. Mol. Cell Biol. *4*, 225–236.

McCaffrey, L.M., and Macara, I.G. (2011). Epithelial organization, cell polarity and tumorigenesis. Trends Cell Biol. *21*, 727–735.

Mlacki, M., Darido, C., Jane, S.M., and Wilanowski, T. (2014). Loss of grainy head-like 1 is associated with disruption of the epidermal barrier and squamous cell carcinoma of the skin. PLoS One *9*, e89247.

Morais-de-Sá, E., Mirouse, V., and St Johnston, D. (2010). aPKC Phosphorylation of Bazooka Defines the Apical/Lateral Border in Drosophila Epithelial Cells. Cell *141*, 509–523.

Moreira, S., Stramer, B., Evans, I., Wood, W., and Martin, P. (2010). Prioritization of Competing Damage and Developmental Signals by Migrating Macrophages in the Drosophila Embryo. Curr. Biol. *20*, 464–470.

Moreno-Bueno, G., Portillo, F., and Cano, A. (2008). Transcriptional regulation of cell polarity in EMT and cancer. Oncogene *27*, 6958–6969.

Moussian, B., and Uv, A.E. (2005). An ancient control of epithelial barrier formation and wound healing. BioEssays *27*, 987–990.

Muliyil, S., and Narasimha, M. (2014). Mitochondrial ROS Regulates Cytoskeletal and Mitochondrial Remodeling to Tune Cell and Tissue Dynamics in a Model for Wound Healing. Dev. Cell *28*, 239–252.

Müller, A.K., Meyer, M., and Werner, S. (2012). The roles of receptor tyrosine kinases and their ligands in the wound repair process. Semin. Cell Dev. Biol. *23*, 963–970.

Munro, E., Nance, J., and Priess, J.R. (2004). Cortical flows powered by asymmetrical contraction transport PAR proteins to establish and maintain anterior-posterior polarity in the early C. elegans embryo. Dev. Cell *7*, 413–

424.

Murata, T., Nitta, M., and Yasuda, K. (1998). Transcription factor CP2 is essential for lens-specific expression of the chicken ??A-crystallin gene. Genes to Cells *3*, 443–457.

Murrell, M., Oakes, P.W., Lenz, M., and Gardel, M.L. (2015). Forcing cells into shape: the mechanics of actomyosin contractility. Nat. Rev. Mol. Cell Biol. *16*, 486–498.

Myster, S.H., Cavallo, R., Anderson, C.T., Fox, D.T., and Peifer, M. (2003). Drosophila p120catenin plays a supporting role in cell adhesion but is not an essential adherens junction component. J. Cell Biol. *160*, 433–449.

Nakamura, Y., Sotozono, C., and Kinoshita, S. (2001). The epidermal growth factor receptor (EGFR): role in corneal wound healing and homeostasis. Exp. Eye Res. *72*, 511–517.

Narasimha, M., Uv, A., Krejci, A., Brown, N.H., and Bray, S.J. (2008). Grainy head promotes expression of septate junction proteins and influences epithelial morphogenesis. J. Cell Sci. *121*, 747–752.

Nevil, M., Bondra, E.R., Schulz, K.N., Kaplan, T., and Harrison, M.M. (2017). Stable Binding of the Conserved Transcription Factor Grainy Head to its Target Genes Throughout Drosophila melanogaster Development. Genetics *205*, 605–620.

Niessen, C.M. (2007). Tight junctions/adherens junctions: basic structure and function. J. Invest. Dermatol. *127*, 2525–2532.

Niessen, C.M., Leckband, D., and Yap, A.S. (2011). Tissue organization by cadherin adhesion molecules: dynamic molecular and cellular mechanisms of morphogenetic regulation. Physiol. Rev. *91*, 691–731.

Niethammer, P., Grabher, C., Look, A.T., and Mitchison, T.J. (2009). A tissue-scale gradient of hydrogen peroxide mediates rapid wound detection in zebrafish. Nature *459*, 996–999.

Nieto, M.A., Huang, R.Y.Y.J., Jackson, R.A.A., and Thiery, J.P.P. (2016). Emt: 2016. Cell *166*, 21–45.

Nishimura, T., Honda, H., and Takeichi, M. (2012). Planar cell polarity links axes of spatial dynamics in neural-tube closure. Cell *149*, 1084–1097.

Nüsslein-Volhard, C., Wieschaus, E., and Kluding, H. (1984). Mutations affecting the pattern of the larval cuticle in Drosophila melanogaster I. Zygotic loci on the second chromosome. Roux's Arch Dev Biol *193*, 267–282.

Okada, K., Ravi, H., Smith, E.M., and Goode, B. (2006). Aip1 and Cofilin Promote Rapid Turnover of Yeast Actin Patches and Cables: A Coordinated Mechanism for Severing and Capping Filaments. Mol. Biol. Cell *17*, 2855–2868.

Ono, K., and Han, J. (2000). The p38 signal transduction pathway: activation and function. Cell Signal *12*, 1–13.

Pacquelet, A., and Rorth, P. (2005). Regulatory Mechanisms Required for DE-Cadherin Function in Cell Migration and Other Types of Adhesion. J. Cell Biol. *170*, 803–812.

Paré, A., Kim, M., Juarez, M.T., Brody, S., and McGinnis, W. (2012). The functions of Grainy Head-like proteins in animals and fungi and the evolution of apical extracellular barriers. PLoS One *7*, e36254.

Pastore, S., Mascia, F., Mariani, V., and Girolomoni, G. (2008). The Epidermal Growth Factor Receptor System in Skin Repair and Inflammation. J. Invest. Dermatol. *128*, 1365–1374.

Pearson, J.C., Juarez, M.T., Kim, M., Drivenes, Ø., and McGinnis, W. (2009). Multiple transcription factor codes activate epidermal wound-response genes in Drosophila. Proc. Natl. Acad. Sci. U. S. A. *106*, 2224–2229.

Pesch, Y.-Y., Riedel, D., Patil, K.R., Loch, G., and Behr, M. (2016).

Chitinases and Imaginal disc growth factors organize the extracellular matrix formation at barrier tissues in insects. Sci. Rep. *6*, 18340.

Pinheiro, D., Hannezo, E., Herszterg, S., Bosveld, F., Gaugue, I., Balakireva, M., Wang, Z., Cristo, I., Rigaud, S.U., Markova, O., et al. (2017). Transmission of cytokinesis forces via E-cadherin dilution and actomyosin flows. Nature *545*, 103–107.

Pollard, T.D., and Cooper, J.A. (2009). Actin, a Central Player in Cell Shape and Movement. Science *326*, 1208–1212.

Pollard, T.D., Blanchoin, L., and Mullins, R.D. (2000). Molecular Mechanisms controlling Actin Filament Dynamics in Nonmuscle Cells. Annu. Rev. Biophys. Biomol. Struct. *29*, 545–576.

Potier, D., Davie, K., Hulselmans, G., NavalSanchez, M., Haagen, L., Huynh-Thu, V.A., Koldere, D., Celik, A., Geurts, P., Christiaens, V., et al. (2014). Mapping Gene Regulatory Networks in Drosophila Eye Development by Large-Scale Transcriptome Perturbations and Motif Inference. Cell Rep. *9*, 2290–2303.

Rämet, M., Lanot, R., Zachary, D., and Manfruelli, P. (2002). JNK signaling pathway is required for efficient wound healing in Drosophila. Dev. Biol. *241*, 145–156.

Rauzi, M., Verant, P., Lecuit, T., and Lenne, P.-F. (2008). Nature and anisotropy of cortical forces orienting Drosophila tissue morphogenesis. Nat. Cell Biol. *10*, 1401–1410.

Rauzi, M., Lenne, P.-F., and Lecuit, T. (2010). Planar polarized actomyosin contractile flows control epithelial junction remodelling. Nature *468*, 1110–1114.

Razzell, W., Wood, W., and Martin, P. (2011). Swatting flies: modelling wound healing and inflammation in Drosophila. Dis. Model. Mech. *4*, 569–574.

Razzell, W., Evans, I.R., Martin, P., and Wood, W. (2013). Calcium Flashes Orchestrate the Wound Inflammatory Response through DUOX Activation and Hydrogen Peroxide Release. Curr. Biol. *23*, 424–429.

Redd, M.J., Cooper, L., Wood, W., Stramer, B., and Martin, P. (2004). Wound healing and inflammation: embryos reveal the way to perfect repair. Philos. Trans. R. Soc. Lond. B. Biol. Sci. *359*, 777–784.

Rifat, Y., Parekh, V., Wilanowski, T., Hislop, N.R., Auden, A., Ting, S.B., Cunningham, J.M., and Jane, S.M. (2010). Regional neural tube closure defined by the Grainy head-like transcription factors. Dev. Biol. *345*, 237–245.

Robinson, R.C. (1999). Domain Movement in Gelsolin: A Calcium-Activated Switch. Science *286*, 1939–1942.

Rodriguez-Boulan, E., and Macara, I.G. (2014). Organization and execution of the epithelial polarity programme. Nat. Rev. Mol. Cell Biol. *15*, 225–242.

Rosenblatt, J., Raff, M.C., and Cramer, L.P. (2001). An epithelial cell destined for apoptosis signals its neighbors to extrude it by an actin- and myosin-dependent mechanism. Curr. Biol. *11*, 1847–1857.

Rossman, K.L., Der, C.J., and Sondek, J. (2005). GEF means go: turning on RHO GTPases with guanine nucleotide-exchange factors. Nat. Rev. Mol. Cell Biol. *6*, 167–180.

Sahai, E., and Marshall, C.J. (2002). Rho–GTPases and Cancer. Nat. Rev. Cancer *2*, 133–142.

Saika, S., Okada, Y., Miyamoto, T., Yamanaka, O., Ohnishi, Y., Ooshima, A., Liu, C.-Y., Weng, D., and Kao, W.W.-Y. (2004). Role of p38 MAP kinase in regulation of cell migration and proliferation in healing corneal epithelium. Invest. Ophthalmol. Vis. Sci. *45*, 100–109.

Sarpal, R., Pellikka, M., Patel, R.R., Hui, F.Y.W., Godt, D., and Tepass, U. (2012). Mutational analysis supports a core role for Drosophila α-Catenin in

adherens junction function. J. Cell Sci. *125*, 233–245.

Schäfer, M., and Werner, S. (2007). Transcriptional control of wound repair. Annu. Rev. Cell Dev. Biol. *23*, 69–92.

Schiller, M., Javelaud, D., and Mauviel, A. (2004). TGF-β-induced SMAD signaling and gene regulation: Consequences for extracellular matrix remodeling and wound healing. J. Dermatol. Sci. *35*, 83–92.

Segre, J. (2003). Complex redundancy to build a simple epidermal permeability barrier. Curr. Opin. Cell Biol. *15*, 778–784.

Sharma, G.-D., He, J., and Bazan, H.E.P. (2003). p38 and ERK1/2 coordinate cellular migration and proliferation in epithelial wound healing: evidence of cross-talk activation between MAP kinase cascades. J. Biol. Chem. *278*, 21989–21997.

Shilo, B.-Z. (2005). Regulating the dynamics of EGF receptor signaling in space and time. Development *132*, 4017–4027.

Siripala, A.D., and Welch, M.D. (2007). SnapShot: Actin Regulators. Cell *128*, 626, 1014.

Sit, S.-T., and Manser, E. (2011). Rho GTPases and their role in organizing the actin cytoskeleton. J. Cell Sci. *124*, 679–683.

Sonnemann, K.J., and Bement, W.M. (2011). Wound repair: toward understanding and integration of single-cell and multicellular wound responses. Annu. Rev. Cell Dev. Biol. *27*, 237–263.

St Johnston, D., and Sanson, B. (2011). Epithelial polarity and morphogenesis. Curr. Opin. Cell Biol. *23*, 540–546.

Stramer, B., Wood, W., Galko, M.J., Redd, M.J., Jacinto, A., Parkhurst, S.M., and Martin, P. (2005). Live imaging of wound inflammation in Drosophila embryos reveals key roles for small GTPases during in vivo cell migration. J. Cell Biol. *168*, 567–573.

Takeichi, M. (2014). Dynamic contacts: rearranging adherens junctions to drive epithelial remodelling. Nat. Rev. Mol. Cell Biol. *15*, 397–410.

Tao, J., Kuliyev, E., Wang, X., Li, X., Wilanowski, T., Jane, S.M., Mead, P., and Cunningham, J.M. (2005). BMP4-dependent expression of Xenopus Grainyhead-like 1 is essential for epidermal differentiation. Development *132*, 1021–1034.

Tapon, N., and Hall, A. (1997). Rho, Rac and Cdc42 GTPases regulate the organization of the actin cytoskeleton. Curr. Opin. Cell Biol. *9*, 86–92.

Tepass, U. (2012). The Apical Polarity Protein Network in *Drosophila* Epithelial Cells: Regulation of Polarity, Junctions, Morphogenesis, Cell Growth, and Survival. Annu. Rev. Cell Dev. Biol. *28*, 655–685.

Tepass, U., and Tanentzapf, G. (2001). Epithelial Cell Polarity and Cell Junctions in Drosophila. Annu. Rev. Genet. *35*, 747–784.

Tepass, U., Fessler, L.I., Aziz, a, and Hartenstein, V. (1994). Embryonic origin of hemocytes and their relationship to cell death in Drosophila. Development *120*, 1829–1837.

Terai, K., Call, M.K., Liu, H., Saika, S., Liu, C.Y., Hayashi, Y., Chikama, T.I., Zhang, J., Terai, N., Kao, C.W.C., et al. (2011). Crosstalk between TGF-β and MAPK Signaling during Corneal Wound Healing. Investig. Ophthalmol. Vis. Sci. *52*, 8208–8215.

Thiery, J.P., Acloque, H., Huang, R.Y.J., and Nieto, M.A. (2009). Epithelial-Mesenchymal Transitions in Development and Disease. Cell *139*, 871–890.

Ting, S.B., Caddy, J., Hislop, N., Wilanowski, T., Auden, A., Zhao, L.-L., Ellis, S., Kaur, P., Uchida, Y., Holleran, W.M., et al. (2005a). A homolog of Drosophila grainy head is essential for epidermal integrity in mice. Science *308*, 411–413.

Ting, S.B., Caddy, J., Wilanowski, T., Auden, A., Cunningham, J.M., Elias, P.M., Holleran, W.M., and Jane, S.M. (2005b). The Epidermis of Grhl3-Null

Mice Displays Altered Lipid Processing and Cellular Hyperproliferation Stephen. Organogenesis *2*, 33–35.

Traylor-Knowles, N., Hansen, U., Dubuc, T.Q., Martindale, M.Q., Kaufman, L., and Finnerty, J.R. (2010). The evolutionary diversification of LSF and Grainyhead transcription factors preceded the radiation of basal animal lineages. BMC Evol. Biol. *10*, 101.

Trepat, X., Wasserman, M.R., Angelini, T.E., Millet, E., Weitz, D.A., Butler, J.P., and Fredberg, J.J. (2009). Physical forces during collective cell migration. Nat. Phys. *5*, 426–430.

Tsai, F., Kuo, G., Chang, S., and Tsai, P. (2015). Ca 2 + Signaling in Cytoskeletal Reorganization, Cell Migration, and Cancer Metastasis. Biomed Res. Int. *2015*, 409245.

Tsarouhas, V., Yao, L., and Samakovlis, C. (2014). Src kinases and ERK activate distinct responses to Stitcher receptor tyrosine kinase signaling during wound healing in Drosophila. J. Cell Sci. *127*, 1829–1839.

Tuckfield, A., Clouston, D.R., Wilanowski, T.M., Zhao, L.L., Cunningham, J.M., and Jane, S.M. (2002). Binding of the RING polycomb proteins to specific target genes in complex with the grainyhead-like family of developmental transcription factors. Mol Cell Biol *22*, 1936–1946.

Twiss, F., Le Duc, Q., Van Der Horst, S., Tabdili, H., Van Der Krogt, G., Wang, N., Rehmann, H., Huveneers, S., Leckband, D.E., and De Rooij, J. (2012). Vinculin-dependent Cadherin mechanosensing regulates efficient epithelial barrier formation. Biol. Open *1*, 1128–1140.

Tybulewicz, V.L.J., and Henderson, R.B. (2009). Rho family GTPases and their regulators in lymphocytes. Nat. Rev. Immunol. *9*, 630–644.

Ullrich, A., and Schlessinger, J. (1990). Signal transduction by receptors with tyrosine kinase activity. Cell *61*, 203–212.

Uv, A.E., Harrison, E.J., and Bray, S.J. (1997). Tissue-Specific Splicing and

Functions of the Drosophila Transcription Factor Grainyhead. Mol. Cell. Biol. *17*, 6727–6735.

Uv, a E., Thompson, C.R., and Bray, S.J. (1994). The Drosophila tissue-specific factor Grainyhead contains novel DNA-binding and dimerization domains which are conserved in the human protein CP2. Mol. Cell. Biol. *14*, 4020–4031.

Venkatesan, K., McManus, H.R., Mello, C.C., Smith, T.F., and Hansen, U. (2003). Functional conservation between members of an ancient duplicated transcription factor family, LSF/Grainyhead. Nucleic Acids Res. *31*, 4304–4316.

Vicente-Manzanares, M., Ma, X., Adelstein, R.S., and Horwitz, A.R. (2009). Non-muscle myosin II takes centre stage in cell adhesion and migration. Nat. Rev. Mol. Cell Biol. *10*, 778–790.

Vinzenz, M., Nemethova, M., Schur, F., Mueller, J., Narita, A., Urban, E., Winkler, C., Schmeiser, C., Koestler, S.A., Rottner, K., et al. (2012). Actin branching in the initiation and maintenance of lamellipodia. J. Cell Sci. *125*, 2775–2785.

Wang, S., and Samakovlis, C. (2012). Grainy head and its target genes in epithelial morphogenesis and wound healing. In Current Topics in Developmental Biology, S. Plaza, and F. Payre, eds. (Amsterdam: Elsevier Inc.), pp. 35–63.

Wang, C., Jamal, L., and Janes, K.A. (2012). Normal morphogenesis of epithelial tissues and progression of epithelial tumors. Wiley Interdiscip Rev Syst Biol Med *4*, 51–78.

Wang, S., Tsarouhas, V., Xylourgidis, N., Sabri, N., Tiklová, K., Nautiyal, N., Gallio, M., and Samakovlis, C. (2009). The tyrosine kinase Stitcher activates Grainy head and epidermal wound healing in Drosophila. Nat. Cell Biol *11*, 890–895.

Wangler, M.F., Yamamoto, S., and Bellen, H.J. (2015). Fruit Flies in Biomedical Research. Genetics *199*, 639–653.

Weiner, O.D. (2002). Regulation of cell polarity during eukaryotic chemotaxis: The chemotactic compass. Curr. Opin. Cell Biol. *14*, 196–202.

Werner, S., and Grose, R. (2003). Regulation of wound healing by growth factors and cytokines. Physiol Rev. *83*, 835–870.

Werner, S., Frey, S., Riethdorf, S., Schulze, C., Alawi, M., Kling, L., Vafaizadeh, V., Sauter, G., Terracciano, L., Schumacher, U., et al. (2013). Dual roles of the transcription factor grainyhead-like 2 (GRHL2) in breast cancer. J. Biol. Chem. *288*, 22993–23008.

Werth, M., Walentin, K., Aue, A., Schönheit, J., Wuebken, A., Pode-Shakked, N., Vilianovitch, L., Erdmann, B., Dekel, B., Bader, M., et al. (2010). The transcription factor grainyhead-like 2 regulates the molecular composition of the epithelial apical junctional complex. Development *137*, 3835–3845.

Weston, C.R., and Davis, R.J. (2002). The JNK signal transduction pathway. Curr. Opin. Genet. Dev. *12*, 14–21.

Wigglesworth, V.B. (1937). Wound Healing in an Insect (Rhodnius prolixus Hemiptera). J. Exp. Biol. *14*, 365–381.

Wilanowski, T., Tuckfield, A., Cerruti, L., O'Connell, S., Saint, R., Parekh, V., Tao, J., Cunningham, J.M., and Jane, S.M. (2002). A highly conserved novel family of mammalian developmental transcription factors related to Drosophila grainyhead. Mech. Dev. *114*, 37–50.

Wilanowski, T., Caddy, J., Ting, S.B., Hislop, N.R., Cerruti, L., Auden, A., Zhao, L.-L., Asquith, S., Ellis, S., Sinclair, R., et al. (2008). Perturbed desmosomal cadherin expression in grainy head-like 1-null mice. EMBO J. *27*, 886–897.

Wood, W., Jacinto, A., Grose, R., Woolner, S., Gale, J., Wilson, C., and

Martin, P. (2002). Wound healing recapitulates morphogenesis in Drosophila embryos. Nat. Cell Biol. *4*, 907–912.

Wood, W., Faria, C., and Jacinto, A. (2006). Distinct mechanisms regulate hemocyte chemotaxis during development and wound healing in Drosophila melanogaster. J. Cell Biol. *173*, 405–416.

Woolner, S., Jacinto, A., and Martin, P. (2005). The small GTPase Rac plays multiple roles in epithelial sheet fusion--dynamic studies of Drosophila dorsal closure. Dev. Biol. *282*, 163–173.

Wozniak, M.A., Modzelewska, K., Kwong, L., and Keely, P.J. (2004). Focal adhesion regulation of cell behavior. Biochim. Biophys. Acta - Mol. Cell Res. *1692*, 103–119.

Wu, C. (2007). Focal Adhesion. Cell Adh. Migr. *1*, 13–18.

Wu, Y., Brock, A.R., Wang, Y., Fujitani, K., Ueda, R., and Galko, J. (2009). A blood-borne PDGF/VEGF-like ligand initiates wound-induced epidermal cell migration in Drosophila larvae. Curr. Biol. *19*, 1473–1477.

Xu, S., and Chisholm, A.D. (2011). A Gα(q)-Ca(2+) Signaling Pathway Promotes Actin-Mediated Epidermal Wound Closure in C. elegans. Curr. Biol. *21*, 1960–1967.

Xu, S., and Chisholm, A.D. (2014). C. elegans Epidermal Wounding Induces a Mitochondrial ROS Burst that Promotes Wound Repair. Dev. Cell *31*, 48–60.

Yamada, S., Pokutta, S., Drees, F., Weis, W.I., and Nelson, W.J. (2005). Deconstructing the cadherin-catenin-actin complex. Cell *123*, 889–901.

Yao, L., Wang, S., Orzechowski-Westholm, J., Dai, Q., Matsuda, R., Hosono, C., Bray, S., Lai, E.C., and Samakovlis, C. (2017). Genome-wide identification of Grainy head targets in Drosophila reveals regulatory interactions with the POU-domain transcription factor, Vvl. Development *144*, 3145–3155.

Yin, J., Xu, K., Zhang, J., Kumar, A., and Yu, F.-S.X. (2007). Wound-induced ATP release and EGF receptor activation in epithelial cells. J. Cell Sci. *120*, 815–825.

Yonemura, S., Wada, Y., Watanabe, T., Nagafuchi, A., and Shibata, M. (2010). alpha-Catenin as a tension transducer that induces adherens junction development. Nat. Cell Biol. *12*, 533–542.

Yoo, S.K., Freisinger, C.M., LeBert, D.C., and Huttenlocher, a. (2012). Early redox, Src family kinase, and calcium signaling integrate wound responses and tissue regeneration in zebrafish. J. Cell Biol. *199*, 225–234.

Yu, Z., Lin, K.K., Bhandari, A., Spencer, J. a, Xu, X., Wang, N., Lu, Z., Gill, G.N., Roop, D.R., Wertz, P., et al. (2006). The Grainyhead-like epithelial transactivator Get-1/Grhl3 regulates epidermal terminal differentiation and interacts functionally with LMO4. Dev. Biol. *299*, 122–136.

Zeitlinger, J., and Bohmann, D. (1999). Thorax closure in Drosophila: involvement of Fos and the JNK pathway. Development *126*, 3947–3956.

Zenz, R., Scheuch, H., Martin, P., Frank, C., Eferl, R., Kenner, L., Sibilia, M., and Wagner, E.F. (2003). c-Jun regulates eyelid closure and skin tumor development through EGFR signaling. Dev. Cell *4*, 879–889.

Zhang, H., and Labouesse, M. (2010). The making of hemidesmosome structures in vivo. Dev. Dyn. *239*, 1465–1476.

Zhang, B.-X., Ma, X., Shu, Z., Yeh, C.-K., Swerdlow, R.H., and Katz, M.S. (2006). Differential regulation of intracellular calcium oscillations by mitochondria and gap junctions. Cell Biochem. Biophys. *44*, 187–203.

Zhao, M. (2009). Electrical fields in wound healing-An overriding signal that directs cell migration. Semin. Cell Dev. Biol. *20*, 674–682.

Zihni, C., Mills, C., Matter, K., and Balda, M.S. (2016). Tight junctions: from simple barriers to multifunctional molecular gates. Nat. Rev. Mol. Cell Biol. *17*, 564–580.

CHAPTER II

GRAINY HEAD IN DROSOPHILA PUPAL NOTUM REPAIR:

Actin it up, Cadherin it down

This chapter is based on the following manuscript:

Novel role for Grainy head in the regulation of cytoskeletal and junctional dynamics during epithelial repair

Inês Cristo, Lara Carvalho, Susana Ponte and António Jacinto (in submission)

“ *Phenomenal cosmic powers! Itty bitty living space!* ”

Genie,

in *Aladdin*

Contents

The author of this thesis performed all the experiments. The thesis author, Lara Carvalho and António Jacinto contributed to the experimental conception and design. Lara Carvalho and Susana Ponte collected specimens for qPCR analysis and helped with *Drosophila* crosses. Yorkie analysis was done in collaboration with Telmo Pereira, who performed the quantification and graphical analysis for that experiment. All other data analysis was done by the author of this thesis.

1. Summary

During life, tissue repair is critical to maintain epithelial integrity and permeability. The repair of simple epithelia relies on a combination of collective cell movements and the action of a contractile actomyosin cable forming at the wound edge that together promote the fast and efficient closure of tissue discontinuities. Grainy head (Grh) is an essential transcription factor that has been implicated both in the development and repair of epithelia. However, the genes and the molecular mechanisms that it controls remain poorly understood. Using the *Drosophila* pupa epithelial tissue, we combined live imaging and genetics to show that Grh knockdown disrupts actomyosin dynamics upon injury. This leads to the formation of an ectopic actomyosin cable away from the wound edge and impaired wound closure. We also uncovered that E-Cadherin is downregulated in the Grh-depleted tissue around the wound, likely as a consequence of Dorsal/NF-κB misregulation, which also affects actomyosin cable formation. Moreover, Grh seems to be involved in later stages of wound healing, as Grh deficient cells around the wound acquire mesenchymal traits, such as loss of adherens junctions, in what resembles an EMT-like event. Our work highlights the importance of Grh as a stress response factor and its central role in the maintenance of epithelial characteristics for tissue repair by regulating cytoskeleton and E-Cadherin dynamics.

1.1 Keywords

Grainy head, epithelia, wound healing, E-Cadherin, cytoskeleton

2. Introduction

Epithelia are the first line of defence against the surrounding environment in most multicellular organisms. As barrier maintenance is critical for survival, epithelia need to be able to self-repair. Multiple molecular mechanisms are used during a wound response that differ depending on the species and developmental stage (Garcia-Fernandez et al., 2009). Injured simple epithelia efficiently close small holes relying mostly on cellular cytoskeleton dynamics, in particular through the formation of an actomyosin contractile cable at the wound edge. Such structure functions as a purse-string that brings cells together. This mechanism has been first dissected in *Drosophila* (Wood et al., 2002) but is also conserved in vertebrate systems, such as humans, mice and zebrafish (Bement et al., 1993; Danjo and Gipson, 1998; Martin and Lewis, 1992; Mateus et al., 2012). The *Drosophila* pupa notum epithelium is an excellent system to study cellular dynamics (Antunes et al., 2013; Bosveld et al., 2012; Herszterg et al., 2013), being highly amenable to genetic manipulation and live imaging. We have previously shown that, in this system, the rapid formation of the actomyosin cable upon injury is preceded by a set of coordinated flows of calcium, actin and myosin, and apical cell constriction across the tissue (Antunes et al., 2013). The first signal detected upon tissue damage is an increase in intracellular calcium, which induces a flow of actomyosin polymerization and cell constriction from a few cell rows away of the wound toward the wound edge. Notably, rearrangement of junctional complexes takes place during the propagation of these flows (Antunes et al., 2013). E-Cadherin (E-Cad), one of the major components of the Adherens Junctions (AJs), is highly regulated upon injury. E-Cad turnover and recycling are important in accommodating cell shape changes, as well as actomyosin flow formation and directionality (Antunes et al., 2013; Pinheiro et al., 2017; Rauzi et al., 2010). It has recently been shown in *Drosophila* embryos that inhibition of E-Cad turnover

leads to an impairment in actin cable formation and wound closure (Carvalho et al., 2014; Hunter et al., 2015; Matsubayashi et al., 2015). Therefore, it is critical to understand how E-Cad is regulated during wound repair to modulate actomyosin dynamics and promote an efficient repair.

Grainy head (Grh) is an essential transcription factor (TF) expressed in virtually all epithelial tissues. This gene was first identified in *Drosophila* (Bray et al., 1989; Dynlacht et al., 1989) and is conserved in vertebrates within the *grainyhead-like* (*grhl*) gene family (Janicke et al., 2010; Sueyoshi et al., 1995; Venkatesan et al., 2003; Wang and Samakovlis, 2012; Wilanowski et al., 2002). Interestingly, the evolution of this gene family seems to match the evolutionary origin of the epithelium itself (Traylor-Knowles et al., 2010), highlighting its importance as an epithelial master regulator. Grh TFs can act as activators or repressors according to the developmental context (Attardi and Tjian, 1993; Bray and Kafatos, 1991; Huang et al., 1995). In *Drosophila*, Grh is necessary during embryonic development, epidermal differentiation, central nervous system specification, and epithelial repair (Attardi et al., 1993; Bray et al., 1989; Brody and Odenwald, 2000). During repair of the *Drosophila* embryonic epidermis, Grh induces the expression of genes associated with cuticle repair (Bray and Kafatos, 1991; Mace et al., 2005) as well as the activation of the receptor tyrosine kinase Stitcher, which in turn regulates actomyosin cable formation (Wang et al., 2009). In mammals, *grhl3* mutants fail to repair the epidermis upon injury (Ting et al., 2005) and cultured keratinocytes from these animals present actin polymerization defects upon wounding (Caddy et al., 2010). The conserved involvement of the *grh* genes in tissue repair across different model systems suggests that this gene family is essential for the regulation of cytoskeletal dynamics and junctional complexes during tissue repair.

In this study, we uncover a novel and central role for Grh in integrating AJ and actomyosin dynamics while maintaining epithelial identity during wound

repair. We show that Grh is required both for the early cellular events after injury, such as the actomyosin flow and actin cable formation, and for the maintenance of epithelial characteristics of cells at the wound edge. Moreover, we demonstrate that Grh acts by orchestrating a tight balance of E-Cad dynamics which is crucial for the proper repair of the injured epithelium.

3. Materials and Methods

3.1 *Drosophila* lines and genetics

Flies were cultured and maintained on standard conditions. Actin expression in the notum epithelium was assessed by expressing *UAS-mcherry::moesin* (Millard and Martin, 2008) under the control of the *pnr-GAL4* driver (Calleja et al., 1996) or *sqh-utrophin::GFP* (Förster and Luschnig, 2012). *sqh-sqh::GFP* (Royou et al., 2002) was used to access myosin expression. To analyse E-Cadherin expression, *DE-Cadherin::mtomato* (Huang et al., 2009) or *ubi-e-cadherin::GFP* flies (Oda and Tsukita, 2001) were crossed with *sr-GAL4* (Usui et al., 2004) recombined with *UAS-mcherry::moesin*. α-catenin (α-cat) dynamics was assessed expressing UAS-Dα-cat::GFP (Oda and Tsukita, 1999) under the *pnr-GAL4* driver.

To knockdown Grh expression, *UAS-grh-RNAi* KK (Dietzl et al., 2007) (Vienna Drosophila Resource Center) and *UAS-grh-RNA*i VALIUM10 TRiP (Transgenic RNAi Project, Bloomington Drosophila Stock Center) were used. Downregulation of endogenous Grh expression was assessed through the use of a *BAC-grh::GFP* line (Spokony insertions, Bloomington Drosophila Stock Center).

UAS-shg-RNAi VALIUM 20 TRiP (Transgenic RNAi Project, Bloomington Drosophila Stock Center) was crossed with *pnr-GAL4,UAS-mcherry::moesin* to analyse actin flow dynamics in a *shg/e-cad* knockdown background. *UAS-shg* (Sarpal et al., 2012) was crossed with *pnr-GAL4,UAS-mcherry::moesin* to analyse actin flow dynamics in a *shg/e-cad* overexpression.

dl reporter analysis was performed using the transgenic line *dl::GFP* (DeLotto et al., 2007) on a *Dif dl/+* background (Matova and Anderson, 2006) crossed with *pnr-GAL4,UAS-mcherry::moesin*. For overexpression of

Dl and Cact knockdown, *UAS-dl* (Matova and Anderson, 2006) and *UAS-cact*-RNAi VALIUM20 TRiP (Transgenic RNAi Project, Bloomington Drosophila Stock Center), respectively, were crossed with *pnr-GAL4, UAS-mcherry::moesin* for F-actin flow analysis and *w; ubi-e-cad::GFP; sr-GAL4*, *UAS-mcherry::moesin* for E-Cad dynamics analysis.

UAS-Yki-GFP (Oh and Irvine, 2008) was crossed with *pnr-GAL4,UAS-mcherry::moesin* to analyse Yki dynamics in notum epithelium during wound healing in the wild type and with *UAS-grh-RNAi* in Grh knockdown background.

Transheterozygotes embryos resulting from two P-element insertions, grh^{06850} and grh^{s2140} (Hemphälä et al., 2003; Spradling et al., 1999) were used for gene expression analysis in *grh* mutant.

Due to lethality of phenotypes in some experiments, *pnr-GAL4* was replaced by *sr-GAL4*, which shows a more restricted expression domain and weaker expression levels, allowing the survival of the organism.

Crosses were performed at 22ºC (crosses with *UAS-shg-RNAi* and *dl::GFP* on a *Dif dl/+* background), 25ºC (crosses with *UAS-grh-RNAi and UAS-Yki-GFP*) or at 29°C (crosses with *UAS-shg, UAS-dl* and *UAS-cact-RNAi*) to maximize RNAi expression and viability using the UAS/GAL4 system (Brand and Perrimon, 1993).

3.2 Permeability assay

Control and Grh KD (*UAS-grh-RNAi; pnr-GAL4)* pupae were staged at 13 hours APF and mounted on slides with double-sided sticky tape, with clearance of the full puparium case along the dorsal side of the pupae. Slides with the pupae where then immersed in a Petri dish containing a solution of 1% Rhodamine B (Sigma) diluted in distilled water, for 5 minutes

with moderate agitation. This incubation was followed by several washes in distilled water, during a period of 30 minutes. Excess water was carefully removed around the organisms and imaged in a stereoscope (V12 Lumar; Carl Zeiss) equipped with a Zeiss digital camera. Pupae were then mounted as previously described (Antunes et al., 2013) and imaged in a confocal laser-scanning microscope (LSM710; Carl Zeiss), through a C-Apochromat 40x water (N.A. 1.2; Zeiss).

3.3 Wounding assay and live-imaging

Pupae were staged at 13h APF (after puparium formation) (Bainbridge and Bownes, 1981). Pupae were mounted, dorsal side facing upwards, on double-sided tape on top of a slide, with the anterior part of the puparium removed with the help of scalpel and forceps, exposing the head and notum of the pupae. A small drop of Halocarbon 700 oil (Sigma-Aldrich) was added on top of the pupae to improve imaging quality. Two spacers made of five coverslips each were used as bridge for a coverslip placed on top of the notum (previously described in Antunes et al., 2013). Laser wounding and live imaging were performed as previously described (Antunes et al., 2013). Wounds were performed on the pupal notum epithelium using a MicroPoint (Andor Technology) UV nitrogen-pumped dye laser (435 nm). Live imaging was performed using a Nikon/Andor Revolution spinning disk system with an EMCCD Camera (iXon 897; Andor Technology) at 25ºC, using the iQ software (Andor Technology). Z-stacks were acquired with a Plan Apo VC PFS 60× objective (NA 1.40; Nikon) every: 10s for F-actin/Myosin movies; 30s for E-Cad and F-actin/F-actin and Myosin movies; every 60s for *dl::GFP* movies.

3.4 Image Analysis

Raw data was processed using Fiji (Schindelin et al., 2012) to obtain maximum intensity projections and orthogonal views. Kymographs were made using a 1 pixel-width line. Quantification of F-actin fluorescence intensity along time was obtained by averaging each cell row, according to its distance from the wound margin. To quantify Myosin and E-Cad fluorescence intensity and junctional length, 10 cells from each row (for each movie) were selected and intensity plots were obtained for cortical and medial areas of each cell. Relative Intensity values along time were obtained by normalizing each time point to average values before wound. In Yki intensity quantification, nuclear tracking was done manually by selecting nuclear centroids in Fiji using the Point Marker tool. Nuclear centre coordinates were exported to Matlab to process intensity data. A custom Matlab script was developed to find nuclear boundaries starting from nuclear centre. Images were processed using a median filter with a disk kernel with a radius of 3. A seeded (nuclear centres) watershed algorithm was used next. Binary masks were applied to original mCherry::Moesin and Yki-GFP images and intensity information was extracted. Resultant Intensity data was normalized to mCherry::Moesin and Yki-GFP average intensity values before wound, respectively. All other quantifications were done manually using Fiji.

3.5 RNA extraction and Quantitative real-time PCR

Wild type (*w1118*) and *grh* mutant embryos at stage 16 were collected and dechorionated. RNA extraction was performed with the RNeasy Plus Micro Kit (Qiagen). Total RNA (1 µg) was reverse-transcribed using the Transcriptor High Fidelity cDNA Synthesis kit (Roche). Quantitative real-time

PCR (qPCR) was performed by using the Fast Green Master Mix (Roche) and the Roche LightCycler 480. Normalization of gene expression values was done regarding the *βTub56* housekeeping gene expression levels and the fold change was calculated through the ΔΔCT method (Livak and Schmittgen, 2001). *Dopa decarboxilase* (*Ddc*), a known transcriptional target of Grh (Bray et al., 1989), and *grh* were used as negative controls for the experiment. Four biological replicates (50 embryos each) and two technical replicates were analysed for each condition. Primers were the following:

βTub56 Fwd -5′- CGGCCAACTGAACGCTGAT-3′;

βTub56 Rev -5′- GCGGCCATCATGTTCTTGG-3′;

shg Fwd -5′- CGACCTTGGCAGGCGACTA -3′;

shg Rev -5′- GGTCGACGGCCTCTACGG -3′.

grh Fwd -5′- CCTCACCGTTCCTGCTCCA -3′;

grh Rev -5′- GTCATCCTGCCGCGCTTC -3′;

ddc Fwd -5′- GCCCACATCCGCAGACAC -3′;

ddc Rev -5′- GGCCGCGTCCATTGATTC -3′;

dl Fwd -5′- CGGCAGGAAAGGCGCTAA -3′;

dl Rev -5′- GCAGCCCTCCTTGCCAAC -3′;

dif Fwd -5′- CCCGAGCCAAGTGCAAGA -3′;

dif Rev -5′- GCTCGTCGCTCGTCACACA -3′;

sna Fwd -5′- CAGCAGCGGTGCCAGTGTA -3′;

sna Rev -5′- ACAGGCCCATCGAGGTGG -3′;

esg Fwd -5′- CATGGCTGCTGCAAGGACA -3′;

esg Rev -5′- TCCGCCCTCTGAATGCTTG -3′;

CadN Fwd -5′- TCGTTCGCGATCGGACTG -3′;

CadN Rev -5′- GCCGCCCACGATTGAAAG -3′;

Mmp1 Fwd -5′- CACCCGTTTCCACCACCAC -3′;

Mmp1 Rev -5′- AGTCCCGCGAAGCTTTGG -3′;

Twi Fwd -5′- TGTCGCCCAAAGTGCTGC -3′;

Twi Rev -5′- GCGTACTGGGCATGCTGC -3′;

wor Fwd -5′- GGGAGTGCCGCGATACCA -3′;

wor Rev -5′- AGGAGCCATGGTCGCGA -3′.

3.6 Statistical analysis

Statistical analysis was performed using Prism (GraphPad Software). Error bars in graphs correspond to the standard deviation or standard error of the mean, as stated in figure legends. Statistical analysis parameters and tests used to assess significance are stated in each figure legend.

4. Results

4.1 E-Cadherin dynamics are compromised during wound repair upon Grh depletion

To better understand the roles of Grh in cytoskeletal dynamics, cell-to-cell communication and tissue movement during epithelial repair, we made use of the *Drosophila* pupal notum epithelium and a laser ablation set-up and live imaging protocol previously established in our lab (Antunes et al., 2013). Since known *grh* mutations are embryonic lethal (Bray and Kafatos, 1991), we explored the possibility of inducing *grh* mutant clones in the notum Unfortunately, *grh* somatic clones could not be recovered. As an alternative, we manipulated Grh function by expressing double-stranded RNAi through the GAL4/UAS system (Brand and Perrimon, 1993; Dietzl et al., 2007), knocking down Grh expression in a tissue-specific and time-controlled manner. We validated the *grh* knockdown (KD) by observing the reduced expression of the *grh* gene in a *BAC-grh-GFP* transgenic line expressing *grh dsRNA* under the control of the pupal notum driver *stripe*-GAL4 (*sr*-GAL4) (Usui et al., 2004) (Fig. 1).

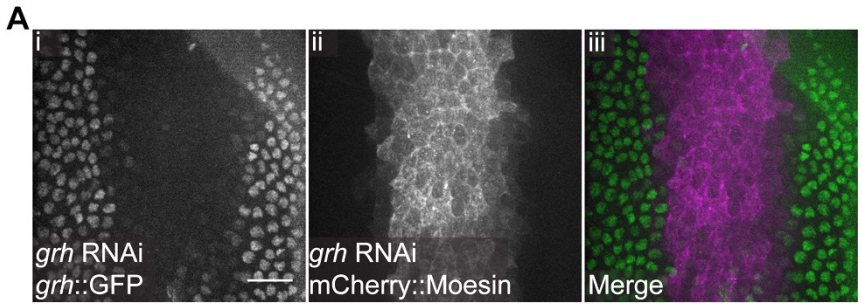

Figure 1. Validation of Grh RNAi efficiency. (**A**) Pupal notum epithelium expressing BAC-Grh-GFP (Ai), and UAS-Grh RNAi (VDRC KK) and UAS-mCherry::Moesin under the *sr*-GAL4

driver (Aii). The downregulation of Grh::GFP is visible in the cells expressing Grh RNAi (Ai-iii). Scale bar: 20 μm.

We started by assessing the integrity of the permeability barrier in the Grh KD. Grh and its orthologues are known to be involved in the regulation of different junctional components across species important in the maintenance of this barrier (Moussian and Uv, 2005; Wang and Samakovlis, 2012). *grh* mutant embryos show misregulation of the formation of the cuticle permeability barrier (Bray and Kafatos, 1991) leading to a defective permeable structure. We tested whether our Grh KD had a similar effect in the barrier maintenance through the incubation in 1% Rhodamine B solution, to assess if the fluorescent dye would penetrate the barrier and reach the epithelial cells in the Grh KD (Fig. 2). In the wild type pupa, no increase in fluorescence is seen at macroscopic level (Fig. 2Ai), while in the Grh KD, the Rhodamine B signal is visible in the notum of the pupa, where the driver of the RNAi is expressed (Fig. 2Ai'). Looking at higher resolution in a confocal microscope, it is possible to observe dye remnants on top of the cuticle of the wild type pupa (Fig. 2Aii-iii). Grh KD pupa shows the epithelial cell cytoplasm with the Rhodamine B fluorescent signal (Fig. 2Aii-iii). This shows the KD is also targeting Grh functions.

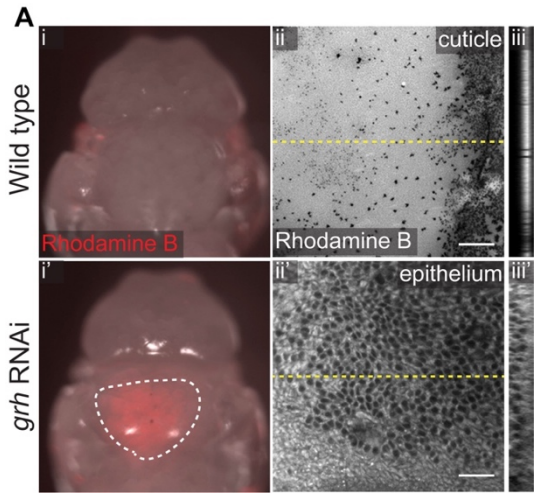

Figure 2. Grh is necessary for the formation of a proper permeability barrier of the *Drosophila* notum epithelium. (**A**) Brightfield images of pupae after permeability assay with Rhodamine B. Control pupa (Ai) does not show fluorescent signal while Grh KD pupa shows an increase in red fluorescence in the region of *pnr* domain (represented by the white dashed line) (Ai'). Image of Rhodamine B fluorescence on

top of the cuticle of a control pupa (Aii) and image of Rhodamine B distribution in the cytoplasm of notum epithelial cells in the Grh KD (Aii'). Orthogonal analysis (yellow dashed line in Aii,ii') shows the localization in the z plane of Rhodamine B signal on top of the notum cuticle in control pupa (Aiii) while in the grh KD, Rhodamine B is distributed within the intracellular milieu (Aiii'). Scale bars: 20 μm. (not included in manuscript)

We then proceed our analysis of *grh* phenotype by comparing the localization of E-Cad (E-Cad::tomato or E-Cad::GFP) (Huang et al., 2009; Oda and Tsukita, 2001) and actomyosin (Utrophin::GFP, mCherry::Moesin and Spaghetti-squash::GFP) (Förster and Luschnig, 2012; Millard and Martin, 2008; Royou et al., 2002) in wild type and *grh* KD pupae before wounding. The effects on E-Cad were analysed by expressing *grh* dsRNA under the control *sr*-GAL4, which is expressed in a subset of cells in the notum (Usui et al., 2004), allowing us to compare wild type and Grh KD cells in the same pupa. We observed that E-Cad protein levels were increased when *grh* was knocked down compared to control pupae, but the subcellular localization of E-Cad and the integrity of the epithelium were maintained (Fig. 3Ai,ii). In agreement with this E-Cad increase, we observed that E-Cad (*shg*) mRNA levels were also increased in *grh* mutant embryos when compared to wild type (Fig. 3Aiii). Regarding actin and myosin, the results were similar: levels of F-actin and Myosin II were elevated and their apical basal distribution appears normal when *grh* is knocked down when compared to wild type (Fig. 3B,B').

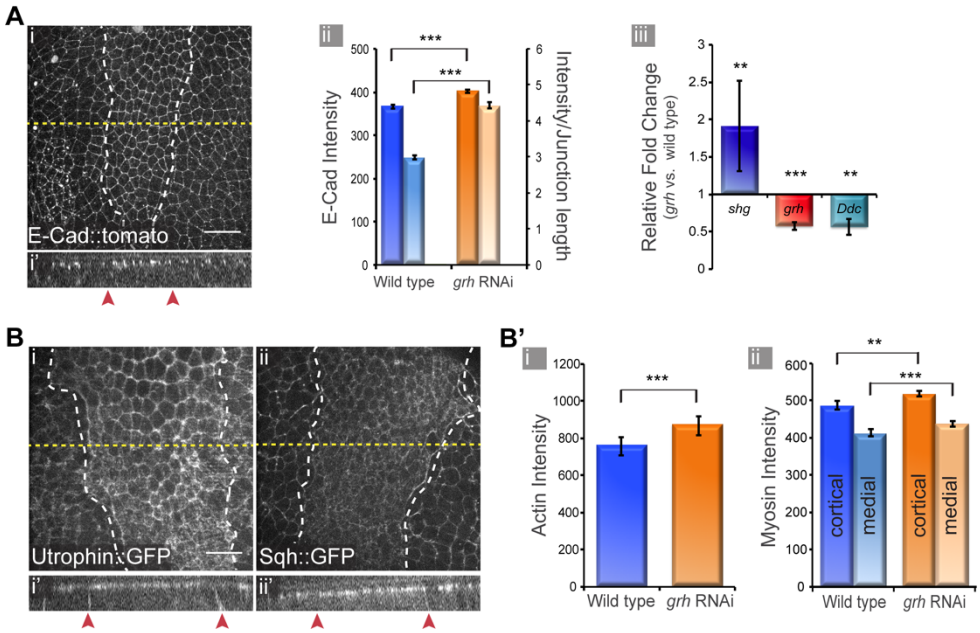

Figure 3. Grh KD phenotype in the homeostasis of the *Drosophila* notum epithelium. (**A**) Movie still of a pupal notum epithelium expressing E-Cad::tomato and UAS-Grh RNAi under the *sr*-GAL4 driver (Ai). (Ai') Orthogonal analysis (yellow dashed line in Bi) shows no difference in apico-basal distribution of E-Cad between Grh KD (between red arrowheads) and wild type tissue. (Aii) Quantification of E-Cad cortical intensity (darker colour, left bars) and intensity levels normalized to cell apical perimeter (lighter colour, right bars) show slight increase in E-Cad levels in the Grh KD in comparison to wild type. Error bars represent standard error of the mean; n=40 cells from 4 pupae for each condition. ***P value < 0.0001; Two-tailed Paired *t* test was performed to test for significant differences between conditions. (Aiii) qPCR analysis of *shg*, *grh* and *Ddc* mRNA levels in *grh* mutant embryos versus wild type embryos. *Ddc* is used here as control for Grh KD. Error bars represent standard error of the mean. **P value < 0.01, ***P value = 0.001; two tailed, nonparametric paired Wilcoxon test was performed to test for significant differences between conditions. (**B**) Movie stills of pupal notum epithelia before wounding expressing UAS-Grh RNAi under the *sr*-GAL4 driver and Utrophin::GFP (Bi) or Sqh::GFP (Bii). F-actin (Bi) and myosin (Bii) localization and intensity differ in the cells expressing Grh RNAi compared to wild type tissue (area limited by the white dashed lines; outside is the wild type tissue). Orthogonal analysis of the tissue

(represented by yellow dashed lines in Bi-ii) shows that F-actin and myosin localization (Bi'-ii') is mainly apical both in wild type and Grh KD cells. Quantification of F-actin and myosin intensity (B'i-ii) shows higher levels in the Grh KD in comparison to wild type cells. For myosin, this increase is observed both in the cortical and medial regions of the cells. Error bars represent standard error of the mean; n=4 pupae for F-actin quantification and n=30 cells from 3 pupae for myosin quantification, for each condition. **P value < 0.01, ***P value < 0.001; Two-tailed Paired *t* tests were performed to determine statistical differences between conditions. Red arrowheads mark knockdown region. Scale bars: 20 μm.

While the mild changes in adhesion and cytoskeletal components observed in the absence of Grh did not appear to cause major changes in tissue organization, we observed that Grh KD had a striking effect upon wounding (Fig. 4; Video S1). We found that in the Grh KD pupae, E-Cad membrane levels were strongly and permanently reduced. This was observed in the first four to six cell rows around the wound, when compared to levels pre-wound and to cell rows further away from the wound site after injury (Fig. 4Ai'-iv',B). In contrast, wild type pupae showed no drastic variation in E-Cad levels (Fig. 4Ai-iv). Quantification of E-Cad::GFP levels in the Grh KD showed the clear and rapid decrease in intensity in the first minutes after wounding, which becomes more gradual 15 minutes post wounding (mpw, Fig. 4Aii'-iv', 4B).

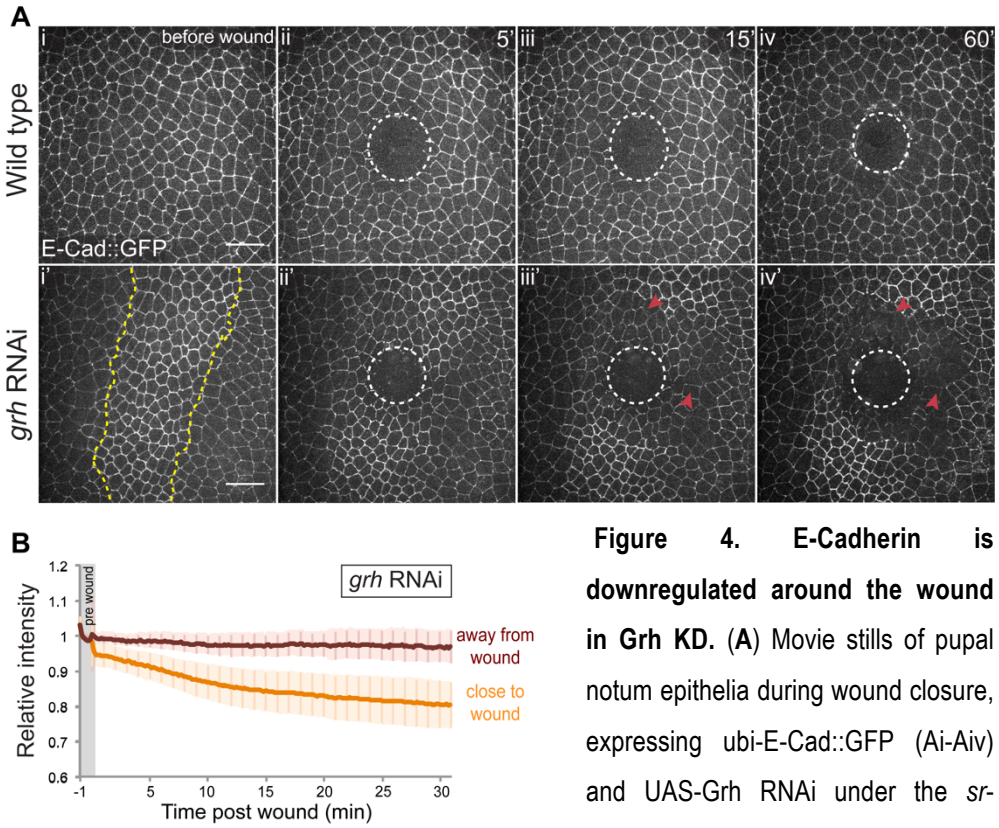

Figure 4. E-Cadherin is downregulated around the wound in Grh KD. (**A**) Movie stills of pupal notum epithelia during wound closure, expressing ubi-E-Cad::GFP (Ai-Aiv) and UAS-Grh RNAi under the *sr*-GAL4 driver (Ai'-iv') (Video S1). In Grh KD (Ai'-iv') E-Cad levels decrease in cells around the wound (red arrowheads) in contrast to wild type (Ai-iv). Area between yellow dashed lines represents *sr*-GAL4 expression domain. White dashed circle represents wound margin. Scale bars: 20 μm. (**B**) Graphical analysis of E-Cad relative intensity in Grh KD cells. E-Cad intensity decreases in cells close to the wound in contrast to cells away from the wound (lighter area in each curve represents the standard deviation; n=30 cells from 3 pupae for each condition).

The same phenotype was observed when using another reporter for E-Cad under control of its endogenous promoter (E-Cad::tomato) (Huang et al., 2009) (Fig. 5). Our analysis shows that, in spite of having only a modest effect in the expression of E-Cad/Shg in notum epithelial cells before wound,

Grh is essential for correct E-Cad dynamics occurring at the wound periphery upon injury.

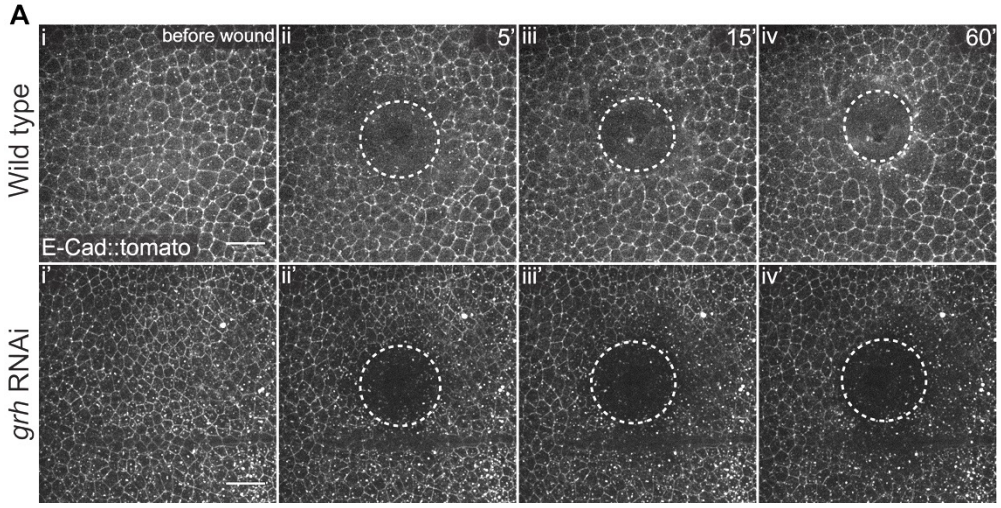

Figure 5. E-Cad dynamics observed through the expression of an E-Cad fusion protein under control of the endogenous promoter are also affected in Grh KD. (**A**) Movie stills of pupal notum epithelia expressing E-Cad::tomato (Ai-iv) and UAS-Grh RNAi under the *pnr*-GAL4 driver (Ai'-iv') show that E-Cad::tomato levels decrease in cells around the wound in the Grh KD when compared to wild type (Ai-iv) (similar to ubi-E-Cad::GFP shown in Figure 2). White dashed circle represents wound margin. Scale bars: 20 μm.

4.2 Grh is required for proper actin dynamics upon wounding

Having observed a change in E-Cad dynamics during wound closure in Grh KD, we wanted to understand whether this was associated with changes in actomyosin dynamics. In the wild type, the typical actomyosin flow occurs shortly upon laser ablation, initiates between four to six cell rows away from the leading edge, and propagates towards the wound edge, leading to the formation of an actomyosin cable (Fig. 6Ai-iv).

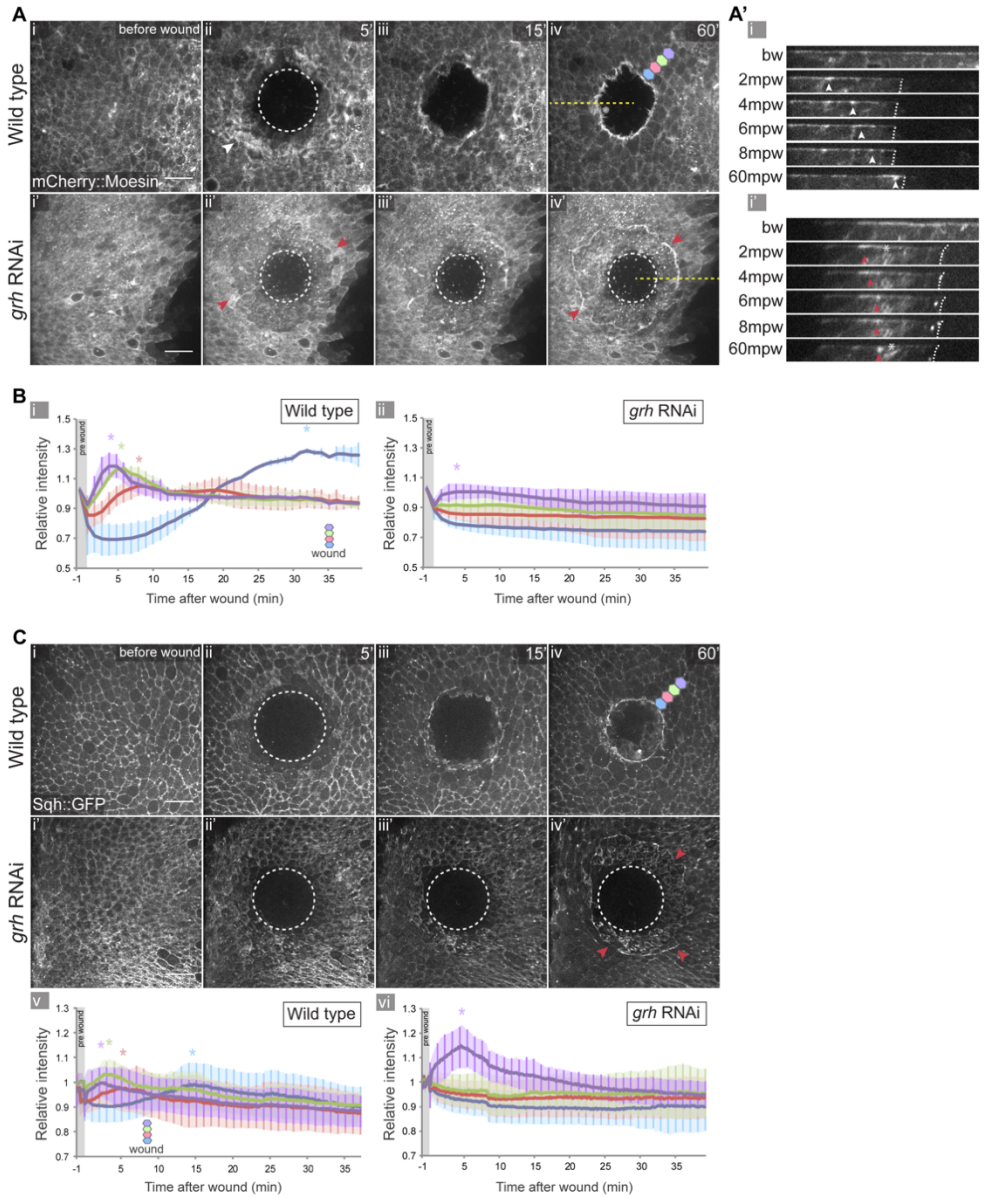

Figure 6. Grh is important for proper cytoskeletal dynamics during wound closure. (**A**) Movie stills of F-actin dynamics during wound closure in pupal notum epithelia expressing UAS-mCherry::Moesin in wild type (Ai-iv) and UAS-Grh RNAi (Ai'-iv') (Video S2) under the control of *pnr*-GAL4 driver. In control conditions a characteristic actin flow (white arrowhead in Aii) is followed by the formation of a cable at the wound edge (Aiv). Grh KD impairs the propagation of the actin flow, despite the initiation of polymerization observed at 5 mpw (red arrowheads in Aii'), leading to the formation of an ectopic cable (red arrowheads in Aiv'). (A'i-

i') Orthogonal analysis of the tissue around the wound (dashed yellow lines in Aiv and Aiv') in wild type (A'i) and Grh KD (A'i'). (A'i') In the wild type, the actin wave progresses along the apical surface leading to cable formation (white arrowheads), while in the Grh KD the apical F-actin accumulation is still visible but its progression is stalled (red arrowheads); in Grh KD F-actin also accumulates latero-basally in contrast to wild type (white asterisks). Bw represents before wound. White dashed line represents the wound margin. (**B**) Graphical analysis of F-actin intensity over time in four cell rows around the wound (colour coding according to representation in Aiv). (Bi) In the wild type, each asterisk marks the peak of F-actin relative intensity representing the progression of the actin wave. (Bii) In the Grh KD, only the furthest cell row enhances the F-actin expression (purple asterisk), but still shows no wave profile. Error bars represent standard deviation; grey shadow represents pre-wound period; n=3 pupae for each condition. (**C**) Movie stills of Myosin II dynamics during wound closure of pupal notum epithelia, expressing Sqh::GFP in wild type (Ci-iv) and UAS-Grh RNAi under the control of *pnr*-GAL4 (Ci'-iv') (Video S3). Myosin shows a similar pattern to the one described for F-actin expression, both in wild type and in Grh KD (red arrowheads in Ciii' show ectopic myosin accumulation in Grh KD). Myosin relative intensity profiles in wild type (Cv) and Grh KD (Cvi) are similar to their respective F-actin profiles (coloured asterisks represent peaks of myosin relative intensity; error bars represent standard deviation; grey shadow represents pre-wound period; n=30 cells from 3 pupae for each condition). White dashed circle represents wound margin. Scale bars: 20 μm.

By contrast, in Grh KD the propagation of the actin flow was stalled and ectopic actin cables formed within the tissue surrounding the wound, a few cell rows away from the wound margin (red arrowheads; Fig. 6Ai'-iv'; Video S2). This behaviour was also confirmed using a different Grh dsRNA line (Fig. 7B).

To better understand the defects associated with this phenotype, we quantified the peaks of F-actin intensity in the four cell rows around the wound, which results in a clear profile of the sequential reaction of the cells. Whereas in the wild type the peaks of intensity are consecutively attained

starting from the cells furthest away from the wound to the cells at the wound edge (Fig. 6Bi, asterisks), in Grh KD F-actin intensity increased in the fourth cell row away from the wound, but not in the three cell rows closer to the wound margin (Fig. 6Bii, asterisk). The ectopic actin cable in Grh KD typically formed at the boundary between these two tissue regions that exhibit contrasting behaviours. Interestingly, the cells that lie between the ectopic cable and the wound margin are the same cells that show a strong reduction in E-Cad (Fig. 7A). To look in more detail at the actin flow in Grh KD pupae, we analysed YZ sections of the tissue surrounding the wound site during the first 60 mpw. In the wild type, F-actin concentrated in the apical side of the cell during flow propagation, whereas in Grh KD this polarization seemed to be partially lost and F-actin localized not only apically but also along the whole apical-basal axis (Fig. 6A'i,i', white asterisk).

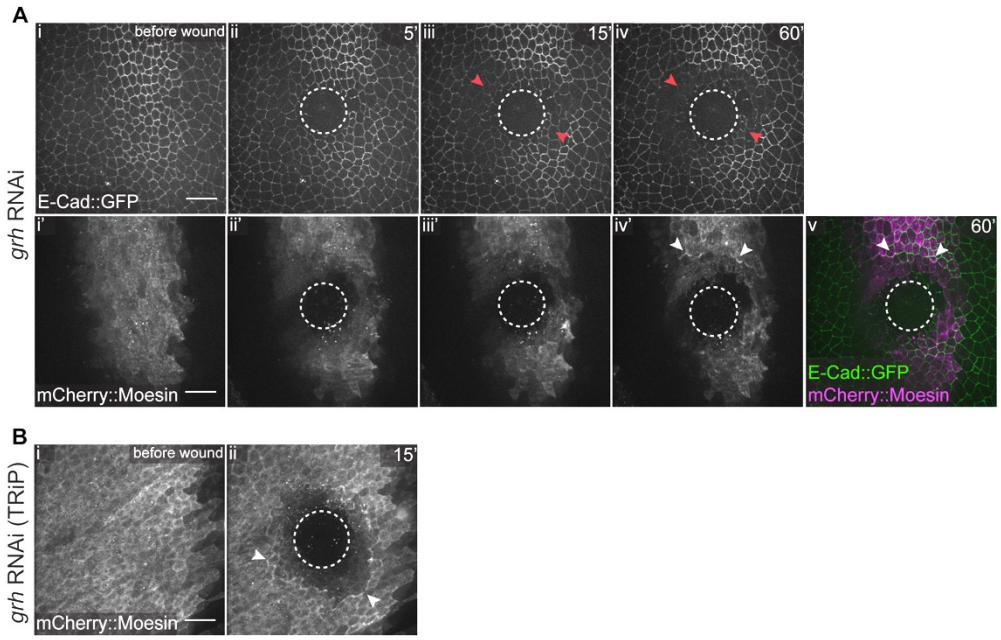

Figure 7. Ectopic accumulation of F-actin coincides with E-Cad downregulation in Grh KD upon wounding. (**A**) Movie stills of pupal notum epithelium during wound closure, expressing ubi-E-Cad::GFP (Ai-Aiv) and UAS-mCherry::Moesin (Ai'-iv') and UAS-Grh RNAi

under the *sr*-GAL4 driver. In Grh KD (Ai'-iv') E-Cad levels decrease in cells around the wound (red arrowheads in Aiii-iv). These cells localize between the wound edge and the F-actin ectopic accumulation (white arrowheads mark actin accumulation in Aiv'). (Av) Merge image showing decrease in F-actin and E-Cad at the wound edge (white arrowheads). (**B**) Grh KD phenotype reproducibility. Movie stills of pupal notum epithelium expressing UAS-mCherry::Moesin and UAS-Grh RNAi (TRiP valium 10) under the control of *pnr*-GAL4. The phenotype is similar to the one achieved with the first Grh RNAi presented (VDRC KK): ectopic actin accumulates within the tissue upon wounding (white arrowheads in Bii). White dashed circle represents wound margin. Scale bars: 20 μm.

We detected similar dynamics for non-muscle myosin II (Royou et al., 2002), whereas the wild type presented a flow of apical myosin that propagated from cells away from the wound towards cells at the wound edge (Fig. 6Ci-v; Video S3), in Grh KD this flow was stalled in the third cell row (Fig. 6Ci'-iv',vi, Video S3). Furthermore, similar to F-actin, myosin ectopically accumulated away from the wound in Grh KD, instead of forming the typical myosin cable at the wound edge observed in the wild type (Fig. 6Civ,iv', arrowheads; Video S3).

Together, our results show that Grh regulates the dynamics of the actin and myosin cytoskeletons during repair. Grh is key for the correct propagation of actin and myosin flows and for the formation of a proper actomyosin cable at the leading edge of the wound.

4.3 Actin flow propagation requires proper regulation of cortical E-Cadherin

E-Cad establishes a link between cell adhesion and cytoskeleton components that is essential for tissue-level responses (Martin et al., 2010).

Moreover, the regulation of E-Cad dynamics is crucial for maintaining the directionality of intracellular actomyosin flows (Lecuit et al., 2011; Rauzi et al., 2010). To test the hypothesis that the observed E-Cad downregulation phenotype in the Grh KD is linked to the defects in actin flow propagation, we knocked down E-Cad and analysed F-actin dynamics upon wounding in notum epithelial cells. We reduced E-Cad levels by expressing E-Cad RNAi under the *sr*-GAL4 driver and imaged F-actin using the mCherry::Moesin reporter. We found that the propagation of the actin flow was clearly impaired in E-Cad KD cells and the actin cable failed to assemble at the wound edge (Fig. 8A; Video S4).

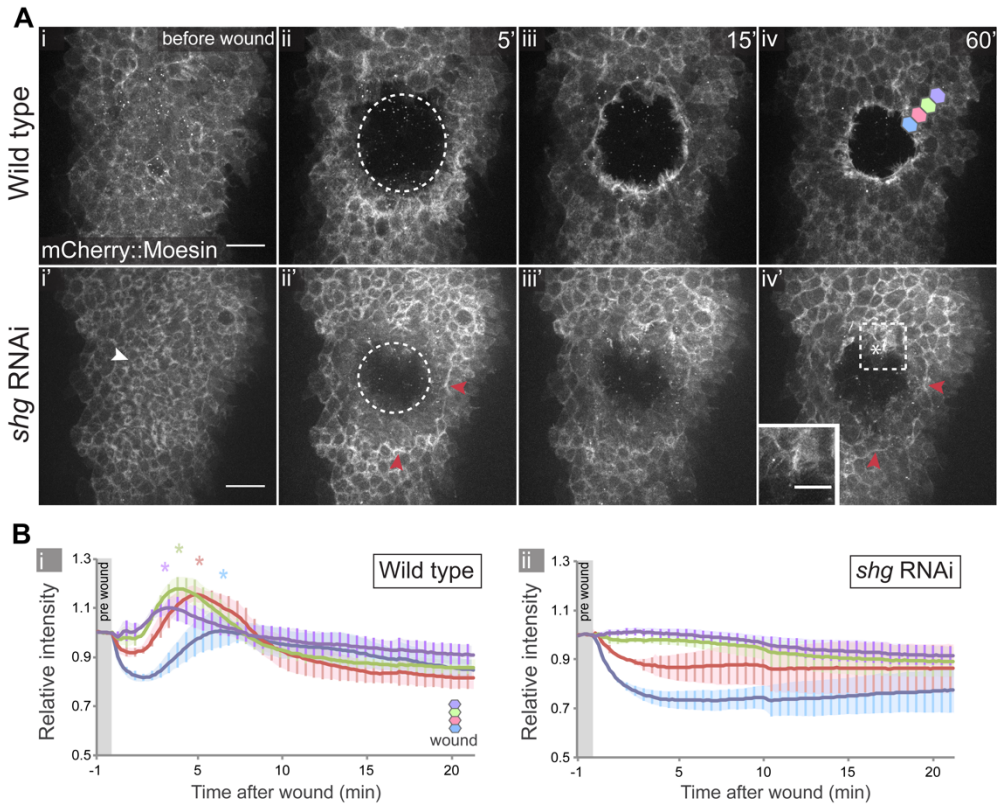

Figure 8. E-Cad/Shg knockdown impairs F-actin wave progression. (**A**) Movie stills of wound closure in pupal notum epithelia expressing UAS-mCherry::Moesin under the *sr*-GAL4 driver in wild type (Ai-iv) and together with UAS-Shg RNAi (Ai'-iv') (Video S4). Shg KD cells appear rounder than wild type, with compromised adhesion (white arrowhead in Ai'). Wound

closure is impaired and F-actin accumulation spots are visible in cells away from the wound (red arrowheads in Aii',iv'). Filopodia at the wound edge appear more prominent in Shg KD than in the wild type (white asterisk in Aiv'; inset) (zoomed area represented in dashed square). White dashed circle represents wound margin. Scale bars: 20 μm and 10 μm in zoomed area. (**B**) Quantification of F-actin relative intensity in four cell rows around the wound (colour coding according to diagram in Aiv; n=4 pupae for each condition), in wild type (Bi) and in UAS-Shg RNAi (Bii), shows that no actin wave occurs in E-Cad KD. Error bars represent standard deviations. Grey shadows mark the pre-wound period.

In addition, the E-Cad KD epithelium was more disorganized and cells exhibited more irregular and rounded shapes than wild type cells (Fig. 8Ai', white arrowhead). We also found that, in these pupae, ectopic actin accumulations similar to Grh KD formed a few cell rows away from the wound edge, although not as strong (Fig. 8Aii'-iv', red arrowheads). At 60 mpw, the E-Cad KD cells closer to the wound edge seemed to form longer and larger numbers of actin protrusions than in the wild type (Fig. 8Aiv', white asterisk and insert). When quantifying the F-actin levels in several cell rows around the wound, it is clear that the actin flow was abolished, as actin intensity levels in the E-Cad KD did not show the characteristic intensity peaks observed in the wild type (Fig. 8B).

To find whether the higher levels of E-Cad observed in *grh* depleted tissue before wounding (Fig. 3Ai') could also be responsible for the phenotypes observed during wound closure in Grh KD, we looked at wound closure upon E-Cad overexpression under the control of the *pnr*-GAL4 driver. The results showed that E-Cad overexpression did not affect the epithelial structure of the notum before wounding and did not prevent the actin flow or the formation of the actomyosin cable upon wounding (Fig. 9). These results support our hypothesis (or suggest) that it is the loss of E-Cad in Grh KD that causes defects in F-Actin/Myosin propagation upon wounding.

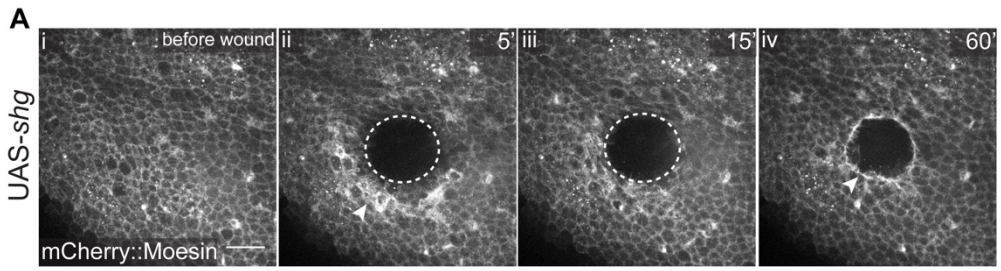

Figure 9. Overexpression of E-Cad does affect wound closure process. (**A**) Movie stills of pupal notum epithelium during wound closure expressing UAS-mCherry::Moesin and UAS-*shg* under the *pnr*-GAL4 driver (Ai-iv). In Shg overexpression (UAS-*shg*), the characteristic actin flow (white arrowhead in Aii) and the formation of the actin cable at the leading edge (white arrowhead in Aiv) are observed, leading to a normal wound closure process. This phenotype is similar to the wild type condition (shown in Fig. 3Ai-iv). White dashed circle represents wound margin. Scale bar: 20 µm.

4.4 *dl* regulation is impaired during closure in Grh KD

We next investigated how Grh loss-of-function impairs E-Cad dynamics during wounding and thus the repair process. It has been shown that, in *Drosophila* embryos, the downregulation and controlled turnover of E-Cad at the adherens complexes is required for actin polymerization and bundle formation, leading to the assembly of the contractile cable around the wound margin (Carvalho et al., 2014; Hunter et al., 2015; Matsubayashi et al., 2015). Moreover, the Toll/NF-κB signalling pathway is required for the E-Cad turnover process during wound closure. Namely, the NF-κB transcription factors Dif and Dorsal (Dl), which act as effectors of the pathway, the membrane receptor Toll, and the inhibitor Cactus (Cact) have all been implicated in this process. In *Dif dl* and *Toll* mutants, as well as in Cact overexpressing embryos, E-Cad is stabilized at the junctions in cells at the wound edge thus impairing actin cable formation (Carvalho et al., 2014).

This link led us to investigate if the molecular mechanism of Grh function during wound closure is related to the NF-κB pathway, by assessing whether *Dif* and/or *dl* misregulation could be playing a part in the reduction of E-Cad levels in a Grh KD context upon wounding. We addressed this at the transcriptional level by quantifying *Dif* and *dl* mRNA levels in *grh* mutant embryos through quantitative real-time PCR. These data showed an increase of *dl* (but not *Dif*) expression in the mutants in comparison to wild type (Fig. 10A), suggesting that Grh might promote the downregulation of *dl* expression. Dl activation involves its translocation from the cytoplasm to the nucleus (Roth et al., 1989; Steward, 1989). Using a *dl*::GFP line as a reporter (DeLotto et al., 2007), we showed that in a wild type pupal notum epithelium, Dl nuclear translocation begins soon after wounding (7 mpw) in some cells (Fig. 10ii'), later spreading to the whole tissue around the wound (Fig. 10Biii'; Video S5). This is similar to what has been shown for embryonic stages (Carvalho et al., 2014).

Therefore, taking into account the transcriptional upregulation of *dl* in *grh* mutant embryos and its activation upon wounding, it is possible that this factor is overactivated in the Grh KD notum epithelium. This could lead to the defective E-Cad downregulation and impaired F-actin dynamics. To test this, we overexpressed *dl* using UAS-*dl* under the control of *pnr*-GAL4 (Fig. 10C-C'; Video S6). Upon wounding, F-actin dynamics and flow propagation were impaired and ectopic F-actin accumulated further away from the wound margin in these pupae (Fig. 10Cii-iv, red arrowheads), similar to the Grh KD (Fig. 6Ai'-iv'). Plotting the F-actin intensity for each cell row around the wound showed that the characteristic intensity peaks representing the wave propagation were missing (Fig. 10Cv). Regarding E-Cad, its intensity was reduced in the cells around the wound overexpressing Dl (yellow dashed line) (Fig. 10C'i-iii), between the ectopic actin accumulation spots (white arrowheads) and the wound margin (Fig. 10C'iv), similar to Grh KD (Fig. 4Ai'-iv'). Quantification of E-Cad intensity levels during wound closure

showed the clear decrease in the cells near the wound site when compared to cells further away from the wound (Fig. 10C'v).

To further address the impact of *dl* overexpression and activation in wound closure, we knocked down its known inhibitor, Cactus (Cact). This IκB homologue inhibits the Toll signalling pathway by binding to Dl, thereby impairing its dimerization and consequently its activation (Belvin et al., 1995; Geisler et al., 1992; Roth et al., 1991). By knocking down *cact* through the expression of *UAS-cact-RNAi* under the control of the *pnr*-GAL4 driver (Fig. 10D-D'), we observed that the actin flow propagation and actin cable formation were impaired (Fig. 10Di-iv). This was also evident after quantifying F-actin intensities in the cells around the wound along time (Fig. 10Dv). E-Cad dynamics was also affected around the wound (Fig. 10D'i-iii). The decrease in the intensity levels of E-Cad was similar to what was observed for *dl* overexpression (compare Fig. 10D'v and Fig. 10C'v).

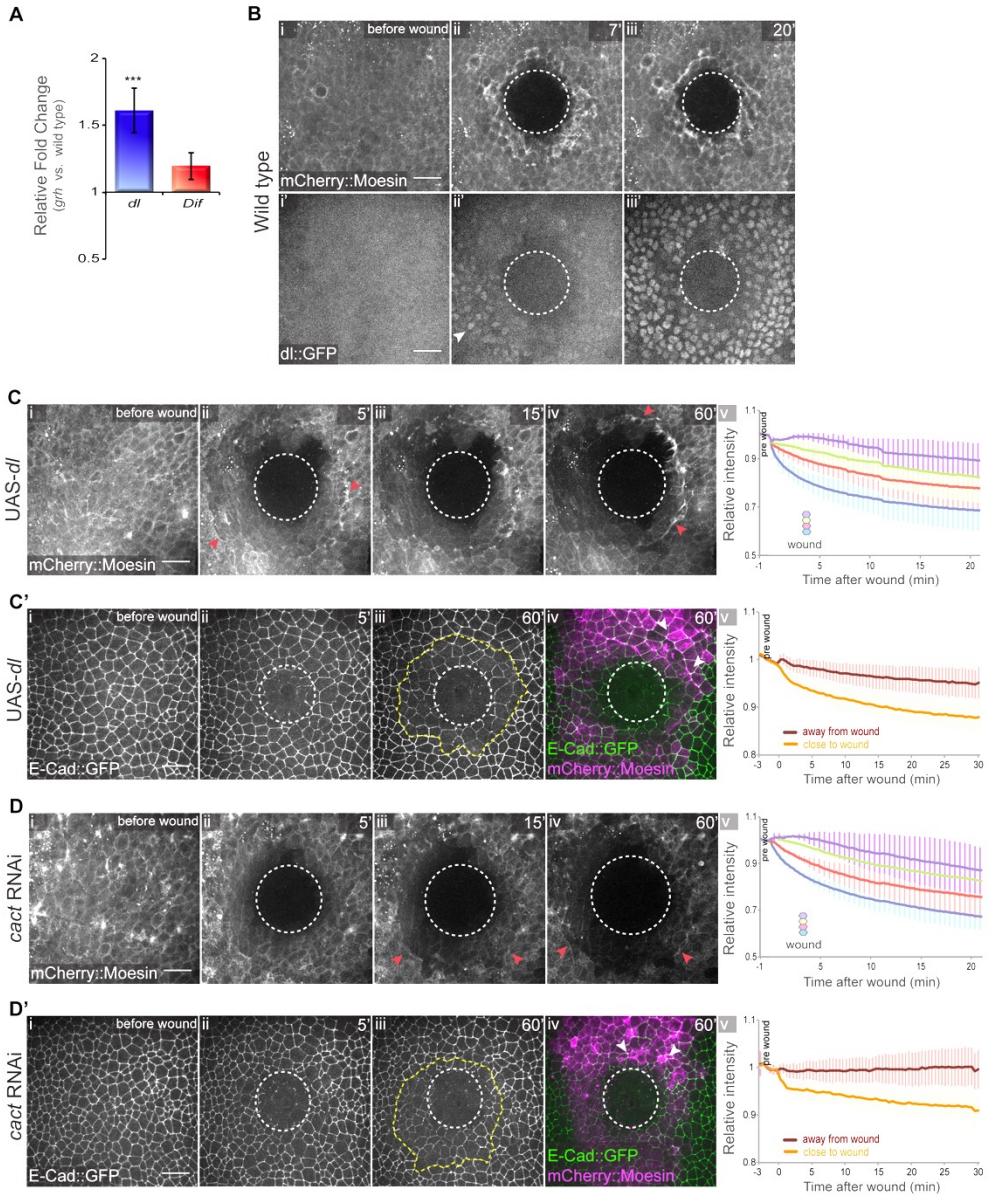

Figure 10. Grh possibly acts through Dorsal to regulate wound closure. (**A**) qPCR analysis of *dl* and *Dif* mRNA levels in *grh* mutant embryos versus wild type embryos shows that *dl* relative expression is higher in *grh* mutants than in wild type whereas *Dif* relative expression is similar. Error bars represent standard error of the mean. ***P value = 0.0005; two tailed, nonparametric paired Wilcoxon test was used to determine the statistical significance between conditions. (**B**) Movie stills of wound closure in a pupal notum

epithelium expressing UAS-mCherry::Moesin under the control of the *pnr*-GAL4 driver (Bi-iii) and Dl::GFP (Bi´-iii´) (Video S5). Dl nuclear translocation is observed as early as 7 mpw in a few cells close to the wound (white arrowhead); at 20 mpw, Dl is inside the nucleus in the all the cells around the wound. (**C**) Movie stills of wound closure of pupal notum epithelium expressing UAS-mCherry::Moesin and UAS-Dl under the *pnr*-GAL4 driver (Ci-iv) (Video S6) and quantification of F-actin wave progression profile in four cell rows around the wound (Cv) (n=3 pupae). Dl overexpression leads to wave impairment and actin ectopic accumulation (red arrowheads). (C') Movie stills of wound closure of pupal notum epithelium expressing ubi-E-Cad::GFP, UAS-mCherry::Moesin and UAS-Dl, under the *sr*-GAL4 driver (C'i-iv) (Video S6). Cells closer to the wound show decrease in E-Cad expression (limited by yellow dashed line). These cells are limited by actin accumulation spots (C'iv, white arrowheads). Graphical analysis of E-Cad relative intensity in Dl overexpressing epithelium shows a decrease in E-Cad intensity in cells close to the wound in contrast to cells away from the wound margin (C'v) (n=40 cells from 4 pupae for each condition). (**D**) Movie stills of wound closure of pupal notum epithelium expressing UAS-mCherry::Moesin and UAS-Cact RNAi under the *pnr*-GAL4 driver (Di-iv) and quantification of F-actin wave progression profile in four cell rows around the wound (Dv) (n=3 pupae). Cact KD also leads to F-actin wave flow impairment, visible by the absence of intensity peaks in graph shown in Dv, and ectopic actin accumulation in cells away from the wound (red arrowheads in Diii,iv). (D') Movie stills of wound closure of pupal notum epithelium expressing ubi-E-Cad::GFP, UAS-mCherry::Moesin and UAS-Cact RNAi under the *sr*-GAL4 driver (D'i-iv). Cells closer to the wound show a decrease in E-Cad intensity (limited by yellow dashed line). Ectopic actin accumulation is present, although less noticeable than in Grh RNAi (D'iv, white arrowheads). Graphical analysis of E-Cad relative intensity in Cact KD shows a decrease in E-Cad intensity cells close to the wound when compared to cells away from the wound (n=30 cells from 3 pupae for each condition) (D'v). Error bars in Cv,C'v,Dv,D'v represent standard deviation. White dashed circle represents wound margin. Scale bars: 20 μm.

These data show that the deregulation of Dl affects F-actin and E-Cad dynamics during the wound closure process in a similar manner as the

reduction of Grh. This points to a possible regulatory role for Grh in NF-κB signalling during wound healing.

4.5 Loss of epithelial identity and cortical stability in cells around the wound

To investigate the long-term consequence of the impairment of E-Cad and actomyosin dynamics on epithelial repair, we tracked wound recovery up until 12 hours post wounding. Wound closure was not achieved (Fig. 12A), which was expected as the cable plays a critical role in this process (Martin and Lewis, 1992; Wood et al., 2002). Surprisingly, after the ectopic cable is fully established in Grh KD (around 60 mpw), cells localized between the cable and the wound margin remained in the tissue but their phenotypic characteristics changed dramatically regarding AJs and cytoskeletal dynamics. One known component that acts as a bridge between the adherens complexes and the cytoskeleton is α-catenin (α-cat) (Kobielak and Fuchs, 2004; Rimm et al., 1995). We analysed α-cat dynamics in the cells located between the ectopic cable and the wound margin, through the expression of UAS-*α-cat*::GFP under the control of the *pnr*-GAL4 driver (Fig. 11A; Video S7).

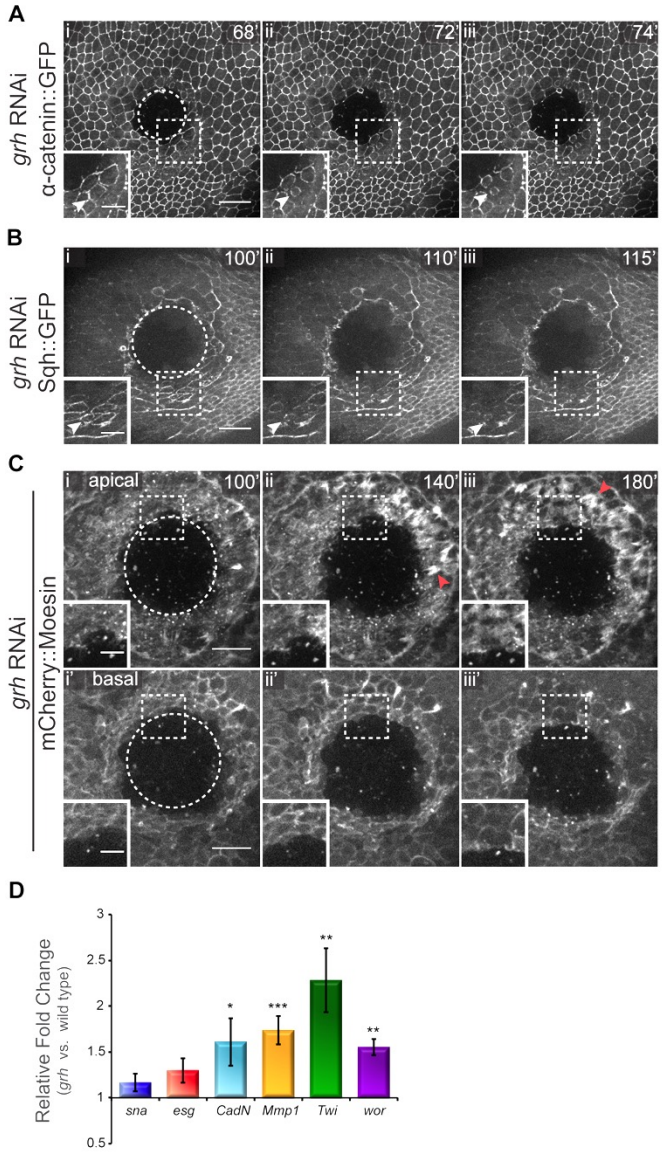

Figure 11. Grh knockdown leads to wound closure failure and loss of cortical stability in the cells around the wound. (**A**) Movie stills of wound closure of pupal notum epithelium expressing UAS-α-Cat::GFP and UAS-Grh RNAi under the *pnr*-GAL4 driver (Ai-iii) (Video S7). Cortical α-Cat in cells around the wound collapses to the apical centre of the cell (white arrowheads in zoomed area represented in dashed square). (**B**) Movie stills of wound closure of pupal notum epithelium expressing Sqh::GFP and UAS-Grh RNAi under the *pnr*-GAL4 driver (Bi-iii) (Video S8). The same collapsing effect is observed in the myosin cortical

cytoskeleton (white arrowheads in zoomed area represented in the dashed area). Scale bars: 20 μm and 10 μm in zoomed areas. (**C**) Movie stills of wound closure of pupal notum epithelium expressing UAS-mCherry::Moesin and UAS-Grh RNAi under the *pnr*-GAL4 driver (Video S9). Apical (Ci-iii) and basal (Ci'-iii') distribution of F-actin in Grh KD cells localized between the ectopic cable and the wound margin. These cells extend filopodia (red arrowheads) and their basal cortex rounds up (zoomed areas represented in dashed square). Scale bars: 15 μm and 7 μm in zoomed areas. White dashed circles in A-C represent wound margin. (**D**) qPCR analysis of EMT markers *sna, esg, CadN, Mmp1, Twi* and *wor* in *grh* mutant embryos versus wild type embryos. Error bars represent standard error of the mean. *P value < 0.05, **P value < 0.01, ***P value = 0.001; two tailed, nonparametric paired Wilcoxon test was performed to test for significant differences.

While in wild type the integrity of the epithelium around the wound was maintained during the entire closure process, in the Grh KD cortical α-cat detached from neighbours and quickly collapsed to the apical centre of the cells (Fig. 11A, white arrowheads). This extremely fast behaviour was also observed for myosin (Fig. 11B; Video S8) and F-actin (Fig. 11C; Video S9), although for the latter this was not as evident due to the several F-actin populations existent in each cell. All these events occurred simultaneously between two and three hours post wounding. After the collapse of the cortical components, large sets of filopodia formed at the apical side (Fig. 11Ci-iii; red arrowheads) whereas the basal side of the cells rounded up (Fig. 11Ci'-iii'; Video S9). When labelling myosin and F-actin simultaneously, we observed that these filopodia only started to form after the cortical collapse (Fig. 12B; Video S10). We tested if the observed phenotypes were recapitulated by Dl overexpression, since in these conditions E-Cad dynamics is also compromised around the wound. These experiments importantly revealed that the cortical collapse and filopodia formation did not occur upon Dl overexpression (Fig. 12C), suggesting these phenotypes might be directly linked to Grh KD independently of Dl deregulation.

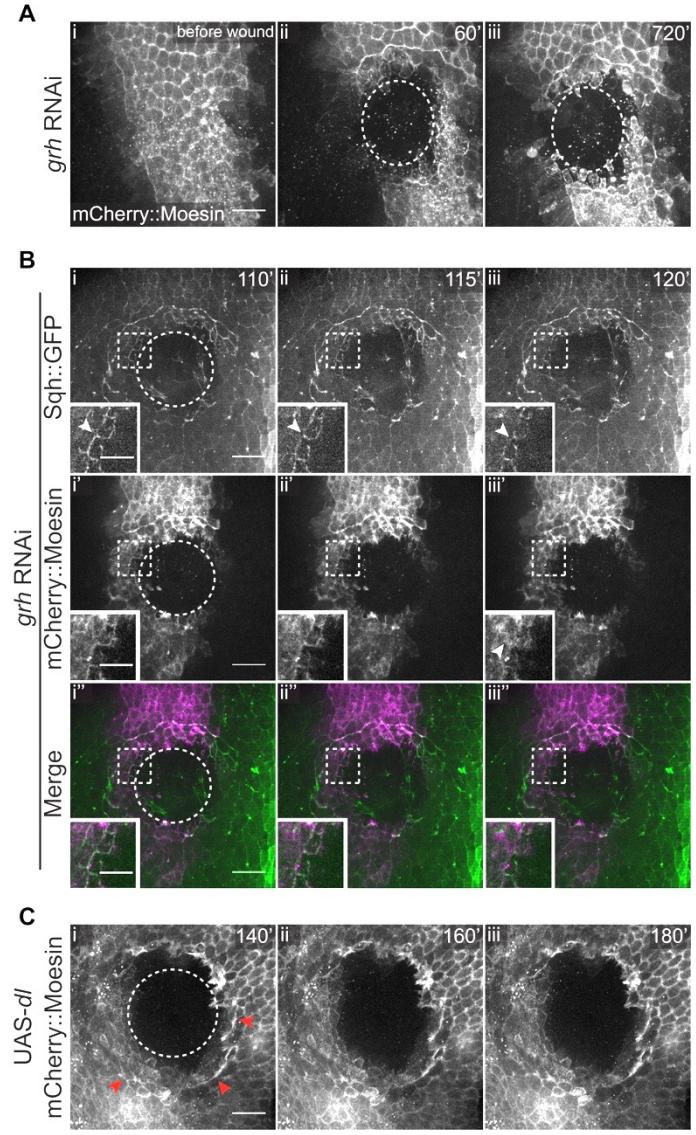

Figure 12. Wounds in Grh-depleted tissue do not close and cells positioned between the ectopic cable and the wound margin emit filopodia soon after cortical collapse occurs. (**A**) Movie stills of wound closure of pupal notum epithelium expressing UAS-mCherry::Moesin and UAS-Grh RNAi under the *sr*-GAL4 driver until 12 hours (720 min) post wounding (Ai-iii). (**B**) Movie stills of wound closure of pupal notum epithelium expressing Sqh::GFP (Bi-iii), UAS-mCherry-Moesin (Bi'-iii') and UAS-Grh RNAi under the *sr*-GAL4 driver (merge Bi''-iii'') (Video S10). Insets show zoomed regions marked by the squares. When cortical myosin starts to disappear (white arrowheads in zoomed areas of Bi-iii), filopodia

start emerging in these cells (white arrowhead in zoomed area of Biii'). (**C**) Movie stills of wound closure of pupal notum epithelium expressing UAS-mCherry::Moesin and UAS-Dl under the *pnr*-GAL4 driver (Ci-iii) show no cortex detachment or filopodia formation in cells localized between ectopic actin accumulation (red arrowheads in Ci) and wound margin, at similar time points where this phenotype is visible in Grh KD epithelia. White dashed circle represents wound margin. Scale bars: 20 µm and 10 µm in zoomed areas.

These data suggest that in Grh KD the cells remaining between the ectopic cable and the wound margin develop mesenchymal traits, uncharacteristic of an epithelial tissue. Epithelial cells, in certain developmental or disease contexts, can transition into mesenchymal cells, in a reversible manner, in a partial or full term (Baum et al., 2008; Lim and Thiery, 2012). This conserved process, called Epithelial-to-Mesenchymal Transition (EMT), is characterized by the loss of tight epithelial adhesion and polarity, the reorganization of the cytoskeleton and the expression of new regulatory pathways, which can lead to increased cell motility and invasiveness (Greenburg and Hay, 1982; Hay, 1995; Lamouille et al., 2014). Altogether, this led us to hypothesize that the lack of Grh might induce a mesenchymal transcriptional program independently of the overactivation of Toll/NF-κB signalling. Several conserved genes linked to the mesenchymal phenotype have been classically used as markers to detect EMT, not only during developmental processes but also in disease contexts. Many of these genes belong to the conserved Snail family of transcription factors, such as *snail* (*sna*), *twist* (*twi*), *escargot* (*esg*) and *worniu* (*wor*). In addition, the upregulation of *Matrix metalloproteinase 1* (*Mmp1*), a regulator of extracellular matrix composition, and *N-Cadherin* (*CadN*), an AJ protein, has also been associated with the EMT phenotype in *Drosophila* (Oda et al., 1998; Stevens and Page-McCaw, 2012; Vicidomini et al., 2015).

To understand if Grh is required to maintain the epithelial characteristics of the cells surrounding the wound, we investigated whether its depletion affects the expression of the EMT-related genes previously mentioned. For this, we quantified their expression in wild type and *grh* mutant embryos through real-time PCR. Although *sna* and *esg* were not significantly altered, *CadN*, *Mmp1*, *twi* and *wor* increased their expression significantly in *grh* mutants when compared to wild type embryos (Fig. 11D). These data shows that cells lacking Grh upregulate the expression of genes typical of a mesenchymal phenotype and involved in EMT.

Another important transcription factor that has been linked to EMT is Yorkie (Yki, or YAP/TAZ in mammals). This transcriptional co-activator is a key downstream mediator of the conserved Hippo signalling pathway (Lin et al., 2014; Overholtzer et al., 2006), known to regulate organ size, tissue repair and stem cell maintenance (Genevet and Tapon, 2011). The deregulation of this pathway is very frequently observed in multiple types of human cancers (including liver, colon, cervical, ovarian, lung, gastric, breast, and pancreatic) (Pfleger, 2017). The sub-cellular localization of Yki, and consequently its activation/function, is regulated by a kinase cascade. When Hippo is active, this cascade promotes the sequestration of Yki in the cytoplasm in its inactive, phosphorylated form; when Hippo is inactive, Yki is dephosphorylated and able to enter the nucleus and induce transcription of its targets.

To find whether Yki activation is affected by the absence of Grh during wound closure, we looked at the expression of Yki::GFP (Oh and Irvine, 2008) in wild type and Grh RNAi pupal notum epithelia. Our data show that in the wild type Yki localization is dynamic during wound closure: while in the unwounded pupal epithelium Yki is mainly restricted to the cytoplasm (Fig.13Ai'), in its inactive form, this molecule translocates to the nucleus within seconds after wounding (arrowheads in Fig. 13ii'; Video S11), reaching a peak of nuclear accumulation around 5 mins after wounding (Fig.

13Aiii and Fig. 13B). Interestingly, this peak of nuclear Yki immediately precedes the typical peak of apical actin filament polymerization in the same cells (Fig.13Bvi). After this intensity peak of F-actin, nuclear/cytoplasm ratio of Yki intensity lowers coming back to pre wound levels (Fig. 13Av,vi). In the Grh KD, the nuclear translocation still happens, but Yki accumulation in the nuclei is still visible in time points where the wild type pre wound levels are already restored (Fig. 13C and Video S12). This uncharacteristic persistence of nuclear Yki might lead to the transcription of pro-apoptotic and migration linked genes, which might contribute to induce the mesenchymal-like phenotype of these cells.

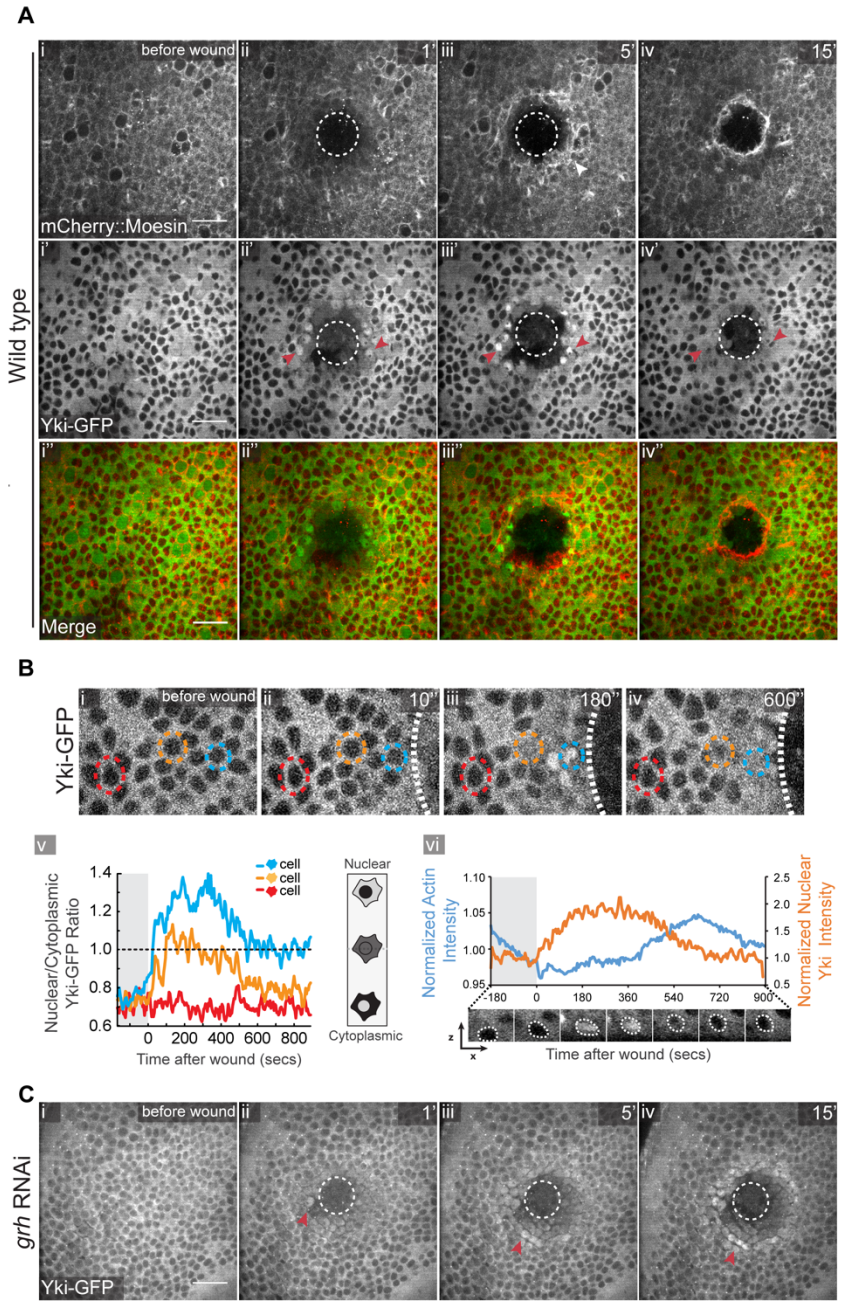

Figure 13. Yorkie dynamics in wild type and Grh KD pupal wound healing (**A**) Movie stills of wound closure of pupal notum epithelium expressing UAS-mCherry::Moesin (Ai-iv) and UAS-Yki-GFP (Ai'-iv') under the *pnr*-GAL4 driver until 15 minutes post wounding (Video S11). Upon wounding, Yki rapidly translocates to the nucleus (red arrowheads in Aii'). After

the actin polymerization propagates to the leading edge and the actin cable is formed (white arrowhead in Aiii), Yki translocates back to cytoplasm (red arrowheads in Aiv') (merge in Ai''-iv''). (**B**) Zoomed images of wound closure of pupal notum epithelium expressing UAS-Yki::GFP under the *pnr*-Gal4 driver (Bi-iv). Colour dashed circles represent cells analysed in Bv, regarding their nuclear/cytoplasmic intensity ratio of Yki::GFP and their distance to the wound edge. A representative scheme of Yki distribution shows the gradual ratio achieved in Yki intensity. By quantifying actin intensity (blue line in Bvi) in the apical side of the cells and Yki intensity (orange line in Bvi) at the nuclear level, we can observe that the increase in Yki intensity correlates to the decrease in actin intensity and vice-versa (Bvi). Insets below graphical analysis show Yki dynamics during the analysed process. (**C**) Movie stills of wound closure of pupal notum epithelium expressing UAS-Yki-GFP and UAS-Grh-RNAi under the *pnr*-GAL4 driver (Ci-iv) that Yki translocates to the nucleus during the first minutes after wounding in the absence of Grh (red arrowheads in Cii-iii), but remains in the nuclei for a longer period of time (red arrowhead in Civ), in contrast to what is observed in the wild type. White dashed circle and lines represent wound margin. Scale bars: 20 μm. (not included in the manuscript).

Our results indicate that knocking down Grh leads to cortical instability and loss of epithelial identity upon wounding. Cells close to the wound margin lose E-Cad and α-cat at their AJs, affecting the attachment of the cortical cytoskeleton, which might induce them to acquire mesenchymal-like properties. Furthermore, the upregulation of mesenchymal markers in *grh* embryos and the persistence of nuclear Yki upon wounding supports our hypothesis that Grh is needed to maintain the epithelial phenotype of cells upon injury.

5. Discussion

The Grh family of transcription factors has been previously linked to epithelial repair not only in *Drosophila* but also in vertebrates (Ting et al., 2005). In *Drosophila,* Grh function has been mainly linked to the activation of wound response genes necessary for cuticle repair (Mace et al., 2005). Here we propose a novel function for Grh at the early stages of wound closure, by regulating cytoskeletal and junctional dynamics. Moreover, we show the importance of this factor in the maintenance of epithelial identity during the wound repair response.

By knocking down Grh using tissue-specific RNAi, we uncovered the importance of this factor in regulating the cellular dynamics necessary to attain tissue closure in the pupa notum epithelium. Upon wounding, Grh-depleted tissue is incapable of forming the characteristic contractile actomyosin cable at the wound edge and achieve wound closure. Instead, the actomyosin flow does not propagate and leads to formation of cable-like structures at ectopic locations. The location of these ectopic cables seems to depend on where the actomyosin flow starts; bigger wounds tend to induce the actomyosin flow and the ectopic cables further away from the wound edge. This is likely a result of the tissue displacement and tension release caused by injury (Antunes et al., 2013). Notably, knocking down E-Cad in the notum epithelium leads to a similar phenotype as Grh loss-of-function. This lead us to hypothesize that the Grh KD phenotype is related to the impairment of E-Cad dynamics in the cells around the wound.

E-Cad transmembrane clusters are central components of AJs, essential for the communication of forces and signals that enable cells to work collectively. Typically, AJs respond to mechanical cues that are transmitted to the interior of the cell through a series of actin-binding proteins, thereby leading to cytoskeletal rearrangements (Martin et al., 2010; Michael and

Yap, 2013; Sawyer et al., 2009). These cellular events have consequences at the tissue level, resulting in coordinated cell rearrangements that are at the basis of epithelial morphogenesis, including epithelial repair (Gustafson and Wolpert, 1962; Holtfreter, 1943). In these processes, AJs localization and turnover are very dynamic and their regulation is crucial (Gumbiner, 2005; Lecuit and Lenne, 2007). In fact, it has recently been described that the regulated removal of junctional E-Cad from the wound margin is necessary for the formation of the actomyosin cable in the *Drosophila* embryonic epidermis (Carvalho et al., 2014; Hunter et al., 2015). Moreover, in the pupal notum epithelium, the tissue displacement caused by wounding leads to the redistribution of E-cad in cells around the wound (Antunes et al., 2013). Here, we have confirmed and extended these findings by showing that Grh plays a key role in the regulation of tissue dynamics through E-Cad. Upon wounding, Grh KD cells that are in the proximity of the wound fail to properly regulate E-Cad levels, leading to a progressive and irreversible loss of this cortical component. Without E-Cad, affected cells possibly lose an important communication channel, becoming unable to transduce the tension cues necessary for the propagation of the actomyosin flow, formation of the contractile cable and eventually wound closure.

Although E-Cad levels severely diminish upon wounding, we should not forget that in the Grh KD, E-Cad appears to be upregulated in unwounded tissue, suggesting that during homeostasis Grh acts as a negative regulator of this protein (Fig. 14Ai). Such regulation is likely to be at the expression level as *grh* embryos exhibit an increase of *shg* mRNA levels. This role of Grh does not come as a surprise as both *Drosophila* Grh and at least one of its vertebrate homologs (*Grhl2*) regulate the expression of *e-cad* in neuroblasts and different types of epithelia (Almeida and Bray, 2005; Pyrgaki et al., 2011; Werth et al., 2010). Nevertheless, the repression effects that Grh exerts in E-Cad in undamaged epithelia are dramatically reverted during the wound closure process, where Grh becomes essential to

maintain E-Cad levels at the junctions. Our current model is that upon wounding Grh acts, at least in part, through Dl, the effector of the Toll/NF-κB signalling pathway (Fig. 14Aii). This pathway has been extensively studied in *Drosophila* and is conserved in vertebrates, with important roles in the initiation of the inflammatory response, morphogenesis and early embryo patterning (Matova and Anderson, 2006; Valanne et al., 2011). More recently, we showed that *dl* activation (in combination with *Dif*) is responsible for regulating E-cad dynamics and downregulation at the wound margin in *Drosophila* embryos during the closure process. This seems to occur via a two-tiered mechanism: in the early stages of closure, Dl regulates E-Cad at the post-transcriptional level; in later stages, Dl represses the transcription of *shg*, thereby contributing to the sustained E-Cad downregulation at the wound edge (Carvalho et al., 2014). Here, we show that *dl* expression is increased in *grh* embryos, suggesting that Grh might directly repress *dl*. This is supported by other studies showing that the transcription starting site of the *dl* gene contains a presumptive binding domain for Grh (Potier et al., 2014), and that the expression of *Drosomycin*, a *bona fide* target of Dl, is increased in *grh* mutant embryos in comparison to wild type (Nevil et al., 2017; Paré et al., 2012). The regulation of Dl by Grh might be especially relevant during wound healing. In agreement with those results, we show that overexpressing Dl or knocking down its inhibitor Cact lead to phenotypes similar to Grh loss-of-function, regarding both F-actin and E-Cad dynamics. It is possible that the increase of *dl* transcripts in the Grh KD leads to the hyperactivation of this pathway, upon activation of its membrane receptor Toll upon injury, resulting in the uncontrolled depletion of junctional E-Cad in the cells surrounding the wound. The mechanism by which this depletion occurs is still unknown, but recent studies point to the importance of E-Cad endocytosis during wound healing (Hunter et al., 2015; Matsubayashi et al., 2015). We also show that, both in Grh loss-of-function and Dl overexpression, a specific range of cells around the wound are affected in terms of F-actin dynamics and loss of AJs. This

might be related to the gradient of tension disruption sensed by the tissue, conveyed by the size of the wound (Antunes et al., 2013). Although our Dl reporter analysis shows that this factor translocates to the nucleus in several cell rows away from the wound edge, the effect on junctional E-Cad could obey a signalling threshold that we cannot measure with the currently available tools.

Grh has already been shown to act through specific pathways in a stress response context. Upon injury, Grh is phosphorylated by ERK and this modification is required for the activation of the wound response genes but not for the homeostatic processes where Grh participates (Kim and McGinnis, 2011). Therefore, it is possible that this phosphorylation is important for the inhibitory interaction between Grh and Dl in the nucleus of the cells affected by a wound. More experiments are necessary to prove this link, especially regarding protein-protein interactions and/or transcription regulation of Dl by Grh, but altogether this work points to a novel regulatory function for Grh in the epithelial stress response.

5.1 Grh maintains epithelial identity during tissue closure

Wound closure is impaired in the absence of Grh. Nevertheless, the cells located between the ectopic cable and the wound margin remain alive and active. These cells lose junctional E-Cad and α-cat, having thus to accommodate their internal cytoskeletal forces without the normal membrane anchoring of an epithelial cell. α-cat links E-Cad to the F-actin cytoskeleton and plays an important role in mechanotransduction and tension sensing (Buckley et al., 2014; Kobielak and Fuchs, 2004; Rimm et al., 1995; Yonemura et al., 2010). The cortical actomyosin cytoskeleton ring also quickly collapses in the cells around the wound margin in Grh KD. This event may be a response to the exacerbated cortical tension caused by the

increased apical cytoskeletal meshwork we observe previous to wounding. This collapse also resembles the epithelial tears seen in *β-catenin/armadillo* mutant embryos during high tension morphogenetic movements (Martin et al., 2010). Adding to this, the formation of numerous filopodia in these cells after the collapse occurs, as well as the rounding of their basal side, suggest they could be undergoing an EMT-like process. Indeed, loss of E-Cad has been linked to the initiation of this type of transition (Thiery and Sleeman, 2006) and in *Drosophila* embryogenesis this process is controlled by Dl activation (Baum et al., 2008; Leptin, 1991). The possible deregulation of Yki signalling we observe around the wound can also contribute to the acquisition of the mesenchymal-like phenotype of these cells (Lin et al., 2014). Recently, extracellular matrix stiffness and tension across the tissue have been proposed as key factors in the growth and propagation of tumour cells (DuFort et al., 2011), linking mechanical control of Hippo signalling with tumour progression. Interestingly, we found a correlation between the actin wave progression and the translocation of Yki to the nucleus in the wild type. This correlaction might be a result of the different actin distribution along the apical-basal axis of the cell. Previous studies, in cultured cells, have shown that the YAP activation can be a direct result of the remodelling of the actin cytoskeleton, where the response to mechanical stimuli appears to be an essential aspect of Hippo regulation (Aragona et al., 2013; Dupont et al., 2011; Gaspar and Tapon, 2014). In the pupal notum epithelium, as the actin polymerization wave reaches a certain cell, its F-actin pool needs to be fully localized to the apical side, leaving the basal side, where the nucleus is located, with less F-actin (Antunes et al., 2013). This F-actin local dynamics might be important in the inactivation of Yki, as the link between actin polymerization and Yki dynamics have been intensively addressed in recent years (Gaspar and Tapon, 2014). In the Grh KD, the lingering of nuclear Yki can be due to the absence of this polymerization dynamics and impairment of actin wave propagation, observed in this phenotype.

As a master regulator of epithelial determination and maintenance, Grh not only activates the expression of characteristic epithelial components but also transcriptionally represses mesenchymal genes, such as *sna*, *twi*, *esg* and *wor*. These mesenchymal factors are involved in EMT events both during development and in the context of diseases such as cancer (Barrallo-Gimeno and Nieto, 2005; Leptin, 1991). Our results show that in *grh* embryos two of these factors, *twi* and *wor*, are upregulated, indicating that in the absence of Grh cells might be more prone to undergo an EMT-like event. Supporting this hypothesis, two other EMT-related genes, *Mmp1* and *CadN*, are also upregulated in *grh* embryos. Mmp1 is an enzyme important for the remodeling of the basement membrane during the transition to a more motile phenotype (Stevens and Page-McCaw, 2012; Vicidomini et al., 2015). The upregulation of *CadN*, a characteristic adhesion component of neuronal tissues (Iwai et al., 1997), coincides with *shg/e-cad* downregulation and the onset of EMT-like processes (Oda et al., 1998). A question that remains is how are EMT markers behaving in Grh-depleted cells in the notum upon wounding. So far, we have not been able to address this in the notum due to technical hurdles, but this should be pursued in future studies.

In vertebrates, TFs of the Grhl family, homologues of Grh, have been shown to be important in preventing EMT (Cieply et al., 2013; Farris et al., 2016; Ray and Niswander, 2016) and their misregulation has been observed in different types of tumors (Cieply et al., 2012; Mlacki et al., 2015). It is still not well understood how Grhl TFs regulate these events, but a link to AJs is likely. Interestingly, it has been shown that in *grhl2* mutant mice epithelia, the depletion of E-Cad is accompanied by an increase of CadN (Werth et al., 2010).

The relevance of EMT to wound healing has already been reported, with the inflammatory response as a key mediator (Lee and Nelson, 2012). In more complex systems such as vertebrates, promptly inflammation responses are essential for proper wound closure. Although *Drosophila* tissue repair is

achieved in a scar-free manner, the inflammatory response in vertebrate systems leads to the onset of fibrosis, which in extreme cases can lead to cancer (Coussens and Werb, 2002; López-Novoa and Nieto, 2009). Interestingly, this process has been linked to NF-κB over-activation, and inhibiting this pathway can diminish the fibrotic reaction (Kuwabara et al., 2006), demonstrating the importance of regulating these pathways. Grh could play a role in the regulation of this response.

According to our model, Grh is a negative regulator of E-Cad in the notum epithelium in homeostatic conditions (Fig. 14Ai). Upon wounding, Dl is activated during the closure response and leads to the fast downregulation of E-Cad at the AJs in an early stage of the process (Fig. 14B, full line). The weakening of the epithelial junctions is likely to be necessary to facilitate tissue repair movements and resembles the EMT processes that have been associated with vertebrate skin wound healing. However, this regulation needs to be tuned down quickly as repair proceeds, so that the tissue can regain epithelial integrity. The activation of Grh plays a key role in this process by limiting Dl action at the proper time and acting as a stop signal for the wound response (Fig. 14Aii) at a later phase of the repair process. In the absence of the Grh brake, the downregulation of E-Cad by Dl is exacerbated leading to the impairment of the tissue repair process (Fig. 14B, dashed line). The interaction between Grh and Dl may be of general importance for tissue homeostasis. While Dl promotes the tissue movements necessary for repair, Grh prevents an excessive response that might otherwise result in malignant processes.

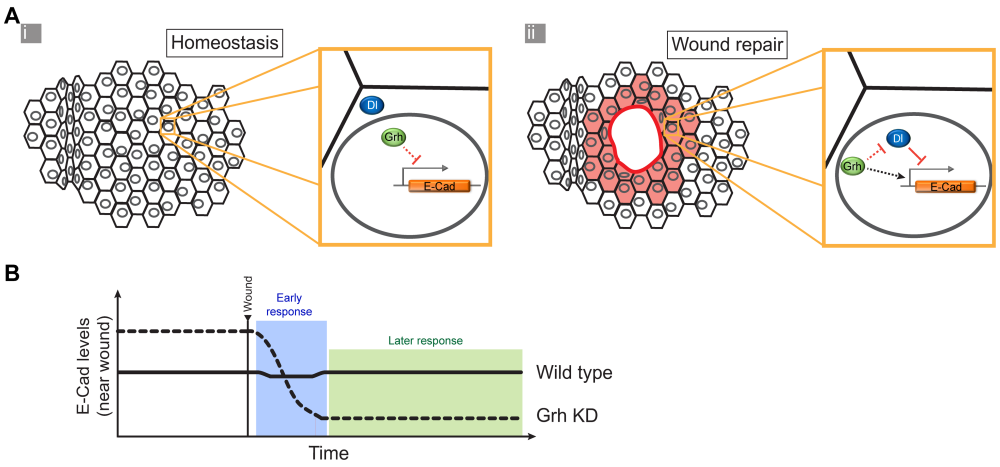

Figure 14. Schematic models for Grh function in wound healing. (**A**) Schematic representation of the proposed function for Grh in simple epithelia. Each cell is a black hexagon; orange highlight depicts one cell. In homeostasis (i), Grh (green circle) regulates E-Cad levels at the transcriptional level (gray circle), directly or indirectly (red dashed inhibitory line), while Dl (blue circle) remains in the cytoplasm. Upon wounding (ii), Grh acts as a stress response manager. Several rows of cells are affected by wound signals (cells in red), which react instantly to form a proper contractile cable (red line at wound margin). In these cells, AJs need to be rapidly and properly regulated. On one hand, Dl quickly translocates to the nucleus, inducing the downregulation of E-Cad levels (red inhibitory line); on the other hand, Grh negatively regulates Dl activity (red dashed inhibitory line) to prevent total E-Cad depletion, resulting in an indirect upregulation of this AJ protein (black dashed arrow). (**B**) Graphic model for E-Cad levels pre- and post-wound in the notum epithelium. In wild type wound repair (black line), E-Cad levels need to be tightly regulated to accommodate for cytoskeletal and tissue rearrangements that occur during the early phase response (blue area). Upon cable formation and to allow tissue closure, E-Cad levels are restored to maintain epithelial integrity as closure proceeds, corresponding to a later phase response (green area). In the Grh KD tissue (black dashed line), E-Cad levels are upregulated pre-wound when compared to wild type, but drop dramatically and rapidly after wounding during the early phase response. These levels are not restored in the later phase. These events point to a two-phase regulation of E-Cad during repair process: the early phase, where a highly regulated dynamic process is necessary to redistribute E-Cad at the membrane level,

probably through post-translational regulation; and a second phase, where these levels are restored to pre-wound levels, in order to maintain epithelial integrity and identity, likely through additional transcriptional regulation. Grh appears to be essential for both these steps of regulation.

In conclusion, our results show that Grh participates in both early and late stages of wound response, regulating the cellular components and transcriptional identity of the epithelium. Future studies analysing the functional interactions between the vertebrate homologues of these TFs, Grhl and NF-κB, might help to better understand how wound healing occurs at the cellular level in more complex epithelia. Grh factors might thus be central regulators of homeostasis in epithelial tissues, not only by controlling cytoskeletal and cell-cell interactions but also by maintaining epithelial identity.

6. References

Almeida, M.S., and Bray, S.J. (2005). Regulation of post-embryonic neuroblasts by Drosophila Grainyhead. Mech. Dev. *122*, 1282–1293.

Antunes, M., Pereira, T., Cordeiro, J. V., Almeida, L., and Jacinto, A. (2013). Coordinated waves of actomyosin flow and apical cell constriction immediately after wounding. J. Cell Biol. *202*, 365–379.

Aragona, M., Panciera, T., Manfrin, A., Giulitti, S., Michielin, F., Elvassore, N., Dupont, S., and Piccolo, S. (2013). A mechanical checkpoint controls multicellular growth through YAP/TAZ regulation by actin-processing factors. Cell *154*, 1047–1059.

Attardi, L.D., and Tjian, R. (1993). Drosophila tissue-specific transcription factor NTF-1 contains a novel isoleucinerich activation motif. Genes Dev. *7*, 1341–1353.

Attardi, L.D., Von Seggern, D., and Tjian, R. (1993). Ectopic expression of wild-type or a dominant-negative mutant of transcription factor NTF-1 disrupts normal Drosophila development. Proc. Natl. Acad. Sci. U. S. A. *90*, 10563–10567.

Bainbridge, S.P., and Bownes, M. (1981). Staging the metamorphosis of Drosophila melanogaster. J. Embryol. Exp. Morphol. *66*, 57–80.

Barrallo-Gimeno, A., and Nieto, M.A. (2005). The Snail genes as inducers of cell movement and survival: implications in development and cancer. Development *132*, 3151–3161.

Baum, B., Settleman, J., and Quinlan, M.P. (2008). Transitions between epithelial and mesenchymal states in development and disease. Semin. Cell Dev. Biol. *19*, 294–308.

Belvin, M.P., Jin, Y., and Anderson, K. V. (1995). Cactus protein degradation mediates Drosophila dorsal-ventral signaling. Genes Dev. *9*,

783–793.

Bement, W.M., Forscher, P., and Mooseker, M.S. (1993). A novel cytoskeletal structure involved in purse string wound closure and cell polarity maintenance. J. Cell Biol. *121*, 565–578.

Bosveld, F., Bonnet, I., Guirao, B., Tlili, S., Wang, Z., Petitalot, A., Marchand, R., Bardet, P.-L.P.-L., Marcq, P., Graner, F., et al. (2012). Mechanical control of morphogenesis by Fat/Dachsous/Four-Jointed planar cell polarity pathway. Science *336*, 724–727.

Brand, A.H., and Perrimon, N. (1993). Targeted gene expression as a means of altering cell fates and generating dominant phenotypes. Development *118*, 401–415.

Bray, S.J., and Kafatos, F. (1991). Developmental function of Elf-1: an essential transcription factor during embryogenesis in Drosophila. Genes Dev. *5*, 1672–1683.

Bray, S.J., Burke, B., Brown, N.H., and Hirsh, J. (1989). Embryonic expression pattern of a family of Drosophila proteins that interact witn a central nervous system regulatory element. Genes Dev. *1019*, 1130–1145.

Brody, T., and Odenwald, W.F. (2000). Programmed Transformations in Neuroblast Gene Expression during Drosophila CNS Lineage Development. Dev. Biol. *226*, 34–44.

Buckley, C.D., Tan, J., Anderson, K.L., Hanein, D., Volkmann, N., Weis, W.I., Nelson, W.J., and Dunn, a. R. (2014). The minimal cadherin-catenin complex binds to actin filaments under force. Science *346*, 1254211–1254211.

Caddy, J., Wilanowski, T., Darido, C., Dworkin, S., Ting, S.B., Zhao, Q., Rank, G., Auden, A., Srivastava, S., Papenfuss, T. a, et al. (2010). Epidermal wound repair is regulated by the planar cell polarity signaling pathway. Dev. Cell *19*, 138–147.

Calleja, M., Moreno, E., Pelaz, S., and Morata, G. (1996). Visualization of gene expression in living adult Drosophila. Science *274*, 252–255.

Carvalho, L., Jacinto, A., and Matova, N. (2014). The Toll/NF-κB signaling pathway is required for epidermal wound repair in Drosophila. Proc. Natl. Acad. Sci. U. S. A. *111*, E5373-82.

Cieply, B., Riley, P., Pifer, P.M., Widmeyer, J., Addison, J.B., Ivanov, A. V, Denvir, J., and Frisch, S.M. (2012). Suppression of the Epithelial-Mesenchymal Transition by Grainyhead-Like-2. Cancer Res. *72*, 2440–2453.

Cieply, B., Farris, J., Denvir, J., Ford, H.L., and Frisch, S.M. (2013). Epithelial-mesenchymal transition and tumor suppression are controlled by a reciprocal feedback loop between ZEB1 and Grainyhead-like-2. Cancer Res. *73*, 6299–6309.

Coussens, L.M., and Werb, Z. (2002). Inflammation and cancer. Nature *420*, 860–867.

Danjo, Y., and Gipson, I.K. (1998). Actin “purse string” filaments are anchored by E-cadherin-mediated adherens junctions at the leading edge of the epithelial wound, providing coordinated cell movement. J. Cell Sci. *111 (Pt22)*, 3323–3332.

DeLotto, R., DeLotto, Y., Steward, R., and Lippincott-Schwartz, J. (2007). Nucleocytoplasmic shuttling mediates the dynamic maintenance of nuclear Dorsal levels during Drosophila embryogenesis. Development *134*, 4233–4241.

Dietzl, G., Chen, D., Schnorrer, F., Su, K.-C., Barinova, Y., Fellner, M., Gasser, B., Kinsey, K., Oppel, S., Scheiblauer, S., et al. (2007). A genome-wide transgenic RNAi library for conditional gene inactivation in Drosophila. Nature *448*, 151–156.

DuFort, C.C., Paszek, M.J., and Weaver, V.M. (2011). Balancing forces:

architectural control of mechanotransduction. Nat. Rev. Mol. Cell Biol. *12*, 308–319.

Dupont, S., Morsut, L., Aragona, M., Enzo, E., Giulitti, S., Cordenonsi, M., Zanconato, F., Le Digabel, J., Forcato, M., Bicciato, S., et al. (2011). Role of YAP/TAZ in mechanotransduction. Nature *474*, 179–183.

Dynlacht, B.D., Attardi, L.D., Admon, A., Freeman, M., and Tjian, R. (1989). Functional analysis of NTF-1, a developmentally regulated Drosophila transcription factor that binds neuronal cis elements. Genes Dev. *3*, 1677–1688.

Farris, J.C., Pifer, P.M., Zheng, L., Gottlieb, E., Denvir, J., and Frisch, S.M. (2016). Grainyhead-like 2 reverses the metabolic changes induced by the oncogenic Epithelial-Mesenchymal Transition: effects on anoikis. Mol. Cancer Res. *14*, 528–538.

Förster, D., and Luschnig, S. (2012). Src42A-dependent polarized cell shape changes mediate epithelial tube elongation in Drosophila. Nat. Cell Biol. *14*, 526–534.

Garcia-Fernandez, B., Campos, I., Geiger, J., Santos, A.C., and Jacinto, A. (2009). Epithelial resealing. Int. J. Dev. Biol. *53*, 1549–1556.

Gaspar, P., and Tapon, N. (2014). Sensing the local environment: actin architecture and Hippo signalling. Curr. Opin. Cell Biol. *31*, 74–83.

Geisler, R., Bergmann, A., Hiromi, Y., and Nüsslein-Volhard, C. (1992). cactus, a gene involved in dorsoventral pattern formation of Drosophila, is related to the I??B gene family of vertebrates. Cell *71*, 613–621.

Genevet, A., and Tapon, N. (2011). The Hippo pathway and apico-basal cell polarity. Biochem. J. *436*, 213–224.

Greenburg, G., and Hay, E.D. (1982). Epithelia suspended in collagen gels can lose polarity and express characteristics of migrating mesenchymal cells. J. Cell Biol. *95*, 333–339.

Gumbiner, B.M. (2005). Regulation of cadherin-mediated adhesion in morphogenesis. Nat Rev Mol Cell Biol *6*, 622–634.

Gustafson, T., and Wolpert, L. (1962). Cellular mechanisms in the morphogenesis of the sea urchin larva: change in shape of cell sheets. Exp. Cell Res. *27*, 260–279.

Hay, E.D. (1995). An Overview of Epithelio-Mesenchymal Transformation. Cells Tissues Organs *154*, 8–20.

Hemphälä, J., Uv, A., Cantera, R., Bray, S., and Samakovlis, C. (2003). Grainy head controls apical membrane growth and tube elongation in response to Branchless/FGF signalling. Development *130*, 249–258.

Herszterg, S., Leibfried, A., Bosveld, F., Martin, C., and Bellaiche, Y. (2013). Interplay between the dividing cell and its neighbors regulates adherens junction formation during cytokinesis in epithelial tissue. Dev. Cell *24*, 256–270.

Holtfreter, J. (1943). A study of the mechaniscs of gastrulation. J. Exp. Zool. *94*, 269–319.

Huang, J., Zhou, W., Dong, W., Watson, A.M., and Hong, Y. (2009). Directed, efficient, and versatile modifications of the Drosophila genome by genomic engineering. Proc. Natl. Acad. Sci. U. S. A. *106*, 8284–8289.

Huang, J.D., Dubnicoff, T., Liaw, G.J., Bai, Y., Valentine, S. a, Shirokawa, J.M., Lengyel, J. a, and Courey, a J. (1995). Binding sites for transcription factor NTF-1/Elf-1 contribute to the ventral repression of decapentaplegic. Genes Dev. *9*, 3177–3189.

Hunter, M. V., Lee, D.M., Harris, T.J.C., and Fernandez-Gonzalez, R. (2015). Polarized E-cadherin endocytosis directs actomyosin remodeling during embryonic wound repair. J. Cell Biol. *210*, 801–816.

Iwai, Y., Usui, T., Hirano, S., Steward, R., Takeichi, M., and Uemura, T. (1997). Axon patterning requires DN-cadherin, a novel neuronal adhesion

receptor, in the drosophila embryonic CNS. Neuron *19*, 77–89.

Janicke, M., Renisch, B., and Hammerschmidt, M. (2010). Zebrafish grainyhead-like1 is a common marker of different non-keratinocyte epidermal cell lineages, which segregate from each other in a Foxi3-dependent manner. Int. J. Dev. Biol. *54*, 837–850.

Kim, M., and McGinnis, W. (2011). Phosphorylation of Grainy head by ERK is essential for wound-dependent regeneration but not for development of an epidermal barrier. Proc. Natl. Acad. Sci. U. S. A. *108*, 650–655.

Kobielak, A., and Fuchs, E. (2004). α-Catenin: at the junction of intercellular adhesion and actin dynamics. Nat Rev Mol Cell Biol *5*, 614–625.

Kuwabara, N., Tamada, S., Iwai, T., Teramoto, K., Kaneda, N., Yukimura, T., Nakatani, T., and Miura, K. (2006). Attenuation of renal fibrosis by curcumin in rat obstructive nephropathy. Urology *67*, 440–446.

Lamouille, S., Xu, J., and Derynck, R. (2014). Molecular mechanisms of epithelial-mesenchymal transition. Natl. Rev. Mol. Cell Biol. *15*, 178–196.

Lecuit, T., and Lenne, P.-F. (2007). Cell surface mechanics and the control of cell shape, tissue patterns and morphogenesis. Nat. Rev. Mol. Cell Biol. *8*, 633–644.

Lecuit, T., Lenne, P.-F., and Munro, E. (2011). Force generation, transmission, and integration during cell and tissue morphogenesis. Annu. Rev. Cell Dev. Biol. *27*, 157–184.

Lee, K., and Nelson, C.M. (2012). New insights into the regulation of epithelial-mesenchymal transition and tissue fibrosis. In International Review of Cell and Molecular Biology, K.W. Jeon, ed. (Amsterdam: Elsevier Inc.), pp. 171–221.

Leptin, M. (1991). twist and snail as positive and negative regulators during Drosophila mesoderm development. Genes Dev. *5*, 1568–1576.

Lim, J., and Thiery, J.P. (2012). Epithelial-mesenchymal transitions: insights from development. Development *139*, 3471–3486.

Lin, T.H., Yeh, T.H., Wang, T.W., and Yu, J.Y. (2014). The hippo pathway controls border cell migration through distinct mechanisms in outer border cells and polar cells of the drosophila ovary. Genetics *198*, 1087–1099.

Livak, K.J., and Schmittgen, T.D. (2001). Analysis of relative gene expression data using real-time quantitative PCR and the 2(-Delta Delta C(T)) Method. Methods *25*, 402–408.

López-Novoa, J.M., and Nieto, M.A. (2009). Inflammation and EMT: An alliance towards organ fibrosis and cancer progression. EMBO Mol. Med. *1*, 303–314.

Mace, K.A., Pearson, J.C., and McGinnis, W. (2005). An epidermal barrier wound repair pathway in Drosophila is mediated by grainy head. Science *308*, 381–385.

Martin, P., and Lewis, J. (1992). Actin cables and epidermal movement in embryonic wound healing. Nature *360*, 179–183.

Martin, A.C., Gelbart, M., Fernandez-Gonzalez, R., Kaschube, M., and Wieschaus, E.F. (2010). Integration of contractile forces during tissue invagination. J. Cell Biol. *188*, 735–749.

Mateus, R., Pereira, T., Sousa, S., de Lima, J.E., Pascoal, S., Saúde, L., and Jacinto, A. (2012). In vivo cell and tissue dynamics underlying zebrafish fin fold regeneration. PLoS One *7*, e51766.

Matova, N., and Anderson, K. V (2006). Rel/NF-kappaB double mutants reveal that cellular immunity is central to Drosophila host defense. Proc. Natl. Acad. Sci. U. S. A. *103*, 16424–16429.

Matsubayashi, Y., Coulson-Gilmer, C., and Millard, T.H. (2015). Endocytosis-dependent coordination of multiple actin regulators is required for wound healing. J. Cell Biol. *210*, 419–433.

Michael, M., and Yap, A.S. (2013). The regulation and functional impact of actin assembly at cadherin cell-cell adhesions. Semin. Cell Dev. Biol. *24*, 298–307.

Millard, T.H., and Martin, P. (2008). Dynamic analysis of filopodial interactions during the zippering phase of Drosophila dorsal closure. Development *135*, 621–626.

Mlacki, M., Kikulska, A., Krzywinska, E., Pawlak, M., and Wilanowski, T. (2015). Recent discoveries concerning the involvement of transcription factors from the Grainyhead-like family in cancer. Exp. Biol. Med. *240*, 1396–1401.

Moussian, B., and Uv, A.E. (2005). An ancient control of epithelial barrier formation and wound healing. BioEssays *27*, 987–990.

Nevil, M., Bondra, E.R., Schulz, K.N., Kaplan, T., and Harrison, M.M. (2017). Stable binding of the conserved transcription factor Grainy Head to its target genes throughout Drosophila melanogaster development. Genetics *205*, 605–620.

Oda, H., and Tsukita, S. (1999). Dynamic features of adherens junctions during Drosophila embryonic epithelial morphogenesis revealed by a Dalpha-catenin-GFP fusion protein. Dev. Genes Evol. *209*, 218–225.

Oda, H., and Tsukita, S. (2001). Real-time imaging of cell-cell adherens junctions reveals that Drosophila mesoderm invagination begins with two phases of apical constriction of cells. J. Cell Sci. *114*, 493–501.

Oda, H., Tsukita, S., and Takeichi, M. (1998). Dynamic behavior of the cadherin-based cell-cell adhesion system during Drosophila gastrulation. Dev. Biol. *203*, 435–450.

Oh, H., and Irvine, K.D. (2008). In vivo regulation of Yorkie phosphorylation and localization. Development *135*, 1081–1088.

Overholtzer, M., Zhang, J., Smolen, G.A., Muir, B., Li, W., Sgroi, D.C.,

Deng, C.-X., Brugge, J.S., and Haber, D.A. (2006). Transforming properties of YAP, a candidate oncogene on the chromosome 11q22 amplicon. Proc. Natl. Acad. Sci. USA *103*, 12405–12410.

Paré, A., Kim, M., Juarez, M.T., Brody, S., and McGinnis, W. (2012). The functions of Grainy Head-like proteins in animals and fungi and the evolution of apical extracellular barriers. PLoS One *7*, e36254.

Pfleger, C.M. (2017). The Hippo Pathway: A Master Regulatory Network Important in Development and Dysregulated in Disease (Elsevier Inc.).

Pinheiro, D., Hannezo, E., Herszterg, S., Bosveld, F., Gaugue, I., Balakireva, M., Wang, Z., Cristo, I., Rigaud, S.U., Markova, O., et al. (2017). Transmission of cytokinesis forces via E-cadherin dilution and actomyosin flows. Nature *545*, 103–107.

Potier, D., Davie, K., Hulselmans, G., NavalSanchez, M., Haagen, L., Huynh-Thu, V.A., Koldere, D., Celik, A., Geurts, P., Christiaens, V., et al. (2014). Mapping Gene Regulatory Networks in Drosophila Eye Development by Large-Scale Transcriptome Perturbations and Motif Inference. Cell Rep. *9*, 2290–2303.

Pyrgaki, C., Liu, A., and Niswander, L. (2011). Grainyhead-like 2 regulates neural tube closure and adhesion molecule expression during neural fold fusion. Dev. Biol. *353*, 38–49.

Rauzi, M., Lenne, P.-F., and Lecuit, T. (2010). Planar polarized actomyosin contractile flows control epithelial junction remodelling. Nature *468*, 1110–1114.

Ray, H.J., and Niswander, L.A. (2016). Grainyhead-like 2 downstream targets act to suppress EMT during neural tube closure. Development *143*, 1192–1204.

Rimm, D.L., Koslov, E.R., Kebriaei, P., Cianci, C.D., and Morrow, J.S. (1995). Alpha(1)(E)-Catenin Is an actin-binding and actin-bundling protein

mediating the attachment of F-Actin to the membrane adhesion complex. Proc. Natl. Acad. Sci. U. S. A. *92*, 8813–8817.

Roth, S., Stein, D., and Nüsslein-Volhard, C. (1989). A gradient of nuclear localization of the dorsal protein determines dorsoventral pattern in the Drosophila embryo. Cell *59*, 1189–1202.

Roth, S., Hiromi, Y., Godt, D., and Nüsslein-Volhard, C. (1991). cactus, a maternal gene required for proper formation of the dorsoventral morphogen gradient in Drosophila embryos. Development *112*, 371–388.

Royou, A., Sullivan, W., and Karess, R. (2002). Cortical recruitment of nonmuscle myosin II in early syncytial Drosophila embryos: Its role in nuclear axial expansion and its regulation by Cdc2 activity. J. Cell Biol. *158*, 127–137.

Sarpal, R., Pellikka, M., Patel, R.R., Hui, F.Y.W., Godt, D., and Tepass, U. (2012). Mutational analysis supports a core role for Drosophila α-Catenin in adherens junction function. J. Cell Sci. *125*, 233–245.

Sawyer, J.K., Harris, N.J., Slep, K.C., Gaul, U., and Peifer, M. (2009). The Drosophila afadin homologue Canoe regulates linkage of the actin cytoskeleton to adherens junctions during apical constriction. J. Cell Biol. *186*, 57–73.

Schindelin, J., Arganda-Carreras, I., Frise, E., Kaynig, V., Longair, M., Pietzsch, T., Preibisch, S., Rueden, C., Saalfeld, S., Schmid, B., et al. (2012). Fiji: an open-source platform for biological-image analysis. Nat. Methods *9*, 676–682.

Spradling, A.C., Stern, D., Beaton, A., Rhem, E.J., Laverty, T., Mozden, N., Misra, S., and Rubin, G.M. (1999). The Berkeley Drosophila Genome Project gene disruption project: Single P-element insertions mutating 25% of vital Drosophila genes. Genetics *153*, 135–177.

Stevens, L.J., and Page-McCaw, A. (2012). A secreted MMP is required for

reepithelialization during wound healing. Mol. Biol. Cell *23*, 1068–1079.

Steward, R. (1989). Relocalization of the dorsal protein from the cytoplasm to the nucleus correlates with its function. Cell *59*, 1179–1188.

Sueyoshi, T., Kobayashi, R., Nishio, K., Aida, K., Moore, R., Wada, T., Handa, H., and Negishi, M. (1995). A nuclear factor (NF2d9) that binds to the male-specific P450 (Cyp 2d-9) gene in mouse liver. Mol. Cell. Biol. *15*, 4158–4166.

Thiery, J.P., and Sleeman, J.P. (2006). Complex networks orchestrate epithelial-mesenchymal transitions. Nat. Rev. Mol. Cell Biol. *7*, 131–142.

Ting, S.B., Caddy, J., Hislop, N., Wilanowski, T., Auden, A., Zhao, L.-L., Ellis, S., Kaur, P., Uchida, Y., Holleran, W.M., et al. (2005). A homolog of Drosophila grainy head is essential for epidermal integrity in mice. Science *308*, 411–413.

Traylor-Knowles, N., Hansen, U., Dubuc, T.Q., Martindale, M.Q., Kaufman, L., and Finnerty, J.R. (2010). The evolutionary diversification of LSF and Grainyhead transcription factors preceded the radiation of basal animal lineages. BMC Evol. Biol. *10*, 101.

Usui, K., Pistillo, D., and Simpson, P. (2004). Mutual exclusion of sensory bristles and tendons on the notum of dipteran flies. Curr. Biol. *14*, 1047–1055.

Valanne, S., Wang, J.-H., and Rämet, M. (2011). The Drosophila Toll signaling pathway. J. Immunol. *186*, 649–656.

Venkatesan, K., McManus, H.R., Mello, C.C., Smith, T.F., and Hansen, U. (2003). Functional conservation between members of an ancient duplicated transcription factor family, LSF/Grainyhead. Nucleic Acids Res. *31*, 4304–4316.

Vicidomini, R., Di Giovanni, A., Petrizzo, A., Iannucci, L.F., Benvenuto, G., Nagel, a C., Preiss, A., and Furia, M. (2015). Loss of Drosophila

pseudouridine synthase triggers apoptosis-induced proliferation and promotes cell-nonautonomous EMT. Cell Death Dis. *6*, e1705.

Wang, S., and Samakovlis, C. (2012). Grainy head and its target genes in epithelial morphogenesis and wound healing. In Current Topics in Developmental Biology, S. Plaza, and F. Payre, eds. (Amsterdam: Elsevier Inc.), pp. 35–63.

Wang, S., Tsarouhas, V., Xylourgidis, N., Sabri, N., Tiklová, K., Nautiyal, N., Gallio, M., and Samakovlis, C. (2009). The tyrosine kinase Stitcher activates Grainy head and epidermal wound healing in Drosophila. Nat. Cell Biol *11*, 890–895.

Werth, M., Walentin, K., Aue, A., Schönheit, J., Wuebken, A., Pode-Shakked, N., Vilianovitch, L., Erdmann, B., Dekel, B., Bader, M., et al. (2010). The transcription factor grainyhead-like 2 regulates the molecular composition of the epithelial apical junctional complex. Development *137*, 3835–3845.

Wilanowski, T., Tuckfield, A., Cerruti, L., O'Connell, S., Saint, R., Parekh, V., Tao, J., Cunningham, J.M., and Jane, S.M. (2002). A highly conserved novel family of mammalian developmental transcription factors related to Drosophila grainyhead. Mech. Dev. *114*, 37–50.

Wood, W., Jacinto, A., Grose, R., Woolner, S., Gale, J., Wilson, C., and Martin, P. (2002). Wound healing recapitulates morphogenesis in Drosophila embryos. Nat. Cell Biol. *4*, 907–912.

Yonemura, S., Wada, Y., Watanabe, T., Nagafuchi, A., and Shibata, M. (2010). alpha-Catenin as a tension transducer that induces adherens junction development. Nat. Cell Biol. *12*, 533–542.

7. Acknowledgements

I would like to thank Anabela Bensimon-Brito for advice on qPCR analysis and critical manuscript review; Yohanns Bellaiche and José de las Heras Chanes for helpful discussion and manuscript review; Anabela Bensimon-Brito, Marco Antunes, Ana Brandão and Francisca Vasconcelos for helpful discussions; Telmo Pereira for advice on imaging and data analysis; Robert DeLotto for the *dl::GFP* transgene; Yohanns Bellaiche for the DE-cad::tomato transgene; TRiP at Harvard Medical School (NIH/NIGMS R01-GM084947) and VDRC for providing transgenic RNAi fly stocks used in this study and the Bloomington Stock Center for other *Drosophila* lines.

8. Supplementary Data

8.1 Video Legends

Video S1. E-Cad dynamics during wound closure in wild type and Grh KD. Notum epithelia expressing E-Cad::GFP, labelling E-Cad. Wild type shown on left and Grh KD shown on the right. Red arrowheads show decrease of E-Cad cortical levels on the right. Images were acquired using a spinning disk imaging system (Revolution XD; Andor Technology). Frames were taken every 1 min. Scale bar: 20 μm.

Video S2. Actin dynamics in wild type and Grh KD. Notum epithelia expressing mCherry::Moesin under the control of *pnr*-GAL4 driver labelling F-actin. Wild type shown on left and Grh KD shown on the right. White arrowhead shows progression of actin flow and cable formation in wild type. Red arrowhead shows progression of actin flow and ectopic cable formation in Grh KD. Images were acquired using a spinning disk imaging system (Revolution XD; Andor Technology). Frames were taken every 1 min. Scale bar: 20 μm.

Video S3. Myosin dynamics in wild type and Grh KD. Notum epithelia expressing Sqh::GFP labelling myosin. Wild type shown on left and Grh KD shown on the right. White arrowhead shows progression of myosin flow and cable formation in wild type. Red arrowhead shows progression of myosin flow and ectopic cable formation in Grh KD. Images were acquired using a spinning disk imaging system (Revolution XD; Andor Technology). Frames were taken every 1 min. Scale bar: 20 μm.

Video S4. Actin dynamics in wild type and Shg KD. Notum epithelia expressing mCherry::Moesin under the control of *pnr*-GAL4 driver labelling F-actin. Wild type shown on left and Shg KD shown on the right. Red arrowhead shows lack of progression of actin flow

in Shg KD. Images were acquired using a spinning disk imaging system (Revolution XD; Andor Technology). Frames were taken every 1 min. Scale bar: 20 μm.

Video S5. Dl nuclear translocation during wound closure in wild type. Notum epithelium expressing *dl*::GFP and mCherry::Moesin under the control of *pnr*-GAL4 driver labelling Dl and F-actin, respectively. Dl is shown on the left (green in merge), F-actin in the middle (magenta in merge) and merged image on the right. Images were acquired using a spinning disk imaging system (Revolution XD; Andor Technology). Frames were taken every 1 min. Scale bar: 20 μm.

Video S6. Actin and E-Cad dynamics during wound closure in Dl overexpression. Left-most panel - Notum epithelium expressing mCherry::Moesin and UAS-Dl under the control of *pnr*-GAL4 driver, labelling F-actin. Red arrowheads show F-actin accumulation at ectopic location. Right-most panels - Notum epithelium expressing E-Cad::GFP, mCherry::Moesin and UAS-Dl under the control of *sr*-GAL4 driver, labelling E-Cad and F-actin, respectively. E-Cad is shown on the left (green in merge), F-actin in the middle (magenta in merge) and merged image on the right. Images were acquired using a spinning disk imaging system (Revolution XD; Andor Technology). Frames were taken every 1 min. Scale bar: 20 μm.

Video S7. α-catenin dynamics in later stages of Grh KD wound closure. Notum epithelium expressing α-catenin::GFP under the control of *pnr*-GAL4 driver, labelling α-catenin. Zoomed area represents portion limited by dashed white square, showing the cortical collapse of the cells. Movie starts 30 mpw. Images were acquired using a spinning disk imaging system (Revolution XD; Andor Technology). Frames were taken every 1 min. Scale bars: 20 μm and 10 μm in zoomed area.

Video S8. Myosin dynamics in later stages of Grh KD wound closure. Notum epithelium expressing Sqh::GFP, labelling myosin. Zoomed area represents portion limited by dashed

white square, showing the cortical collapse of the cells. Movie starts 30 mpw. Images were acquired using a spinning disk imaging system (Revolution XD; Andor Technology). Frames were taken every 1 min. Scale bars: 20 µm and 10 µm in zoomed area.

Video S9. Apical and basal actin dynamics in later stages of Grh KD wound closure. Notum epithelium expressing mCherry::Moesin under the control of *pnr*-GAL4 driver, labelling F-actin. Apical (top image) and basal (bottom image) sides of area within the ectopic cable. Zoomed areas represent portions limited by dashed white square, showing cells emitting filopodia (apical) as they round up (basal). Movie starts 30 mpw. Images were acquired using a spinning disk imaging system (Revolution XD; Andor Technology). Frames were taken every 1 min. Scale bars: 15 µm and 7 µm in zoomed area.

Video S10. Actin and myosin dynamics during cortical collapse in Grh KD. Notum epithelia expressing Sqh::GFP, and mCherry::Moesin under the control of *sr*-GAL4 driver, labelling myosin and F-actin, respectively. Myosin is shown on the left (green in merge), F-actin in the middle (magenta in merge) and merged image on the right. Zoomed areas represent portions limited by dashed white square, showing decrease in cortical myosin (left image) is followed by emerging filopodia (middle image). Movie starts 60 mpw. Images were acquired using a spinning disk imaging system (Revolution XD; Andor Technology). Frames were taken every 1 min. Scale bar: 20 µm and 10 µm in zoomed areas.

Video S11. Yorkie dynamics during wound closure in wild type. Notum epithelium expressing mCherry::Moesin, labelling F-actin, and Yki-GFP, labelling Yki. F-actin shown on the left, Yki shown in the middle, and merge shown on the right. Images were acquired using a spinning disk imaging system (Revolution XD; Andor Technology). Frames were taken every 10 secs. Scale bar: 20 µm. (not included in manuscript)

Video S12. Yorkie dynamics during wound closure in Grh KD. Notum epithelium expressing Yki-GFP, labelling Yki, and Grh RNAi. Images were acquired using a spinning disk imaging system (Revolution XD; Andor Technology). Frames were taken every 10 secs. Scale bar: 20 μm. (not included in manuscript)

CHAPTER III

GRAINY HEAD AND CALCIUM REGULATION IN REPAIR:

Nobody puts calcium in the corner

"*So forget any ideas you've got about lost cities, exotic travel, and digging up the world. We do not follow maps to buried treasure, and "X" never, ever marks the spot.*"

Indiana Jones,

in *Indiana Jones and the Last Crusade*

Contents

The author of this thesis performed all the experiments. The RNAi screen was done based on a selection of *Drosophila* Grh targets kindly provided by Christos Samakovlis and Liqun Yao, which resulted from a genome-wide analysis (Yao et al., 2017).

1. Summary

Calcium ions are fast and highly regulated chemical signalling molecules important for several processes in every organism, both at the intra and extracellular level. As maintenance of tissue integrity is crucial, and repair of discontinuities needs to be quickly resolved, calcium signalling is, unsurprisingly, involved in this process as a transcription-independent injury signal. Upon wounding of the pupal notum epithelium, a wave of calcium disperses across the tissue starting from the wound edge. One of the functions of calcium during wound healing is the control of cytoskeletal dynamics, which are of the upmost importance during the characteristic actomyosin polymerization wave formed in response to tissue disruption. Calcium deregulation leads to phenotypically diverse defects in the closure process, likely due to its pleiotropic effects. The epithelial transcription factor Grainy Head (Grh), known to be involved in epithelial maintenance and repair, controls the expression of over a thousand genes, across a span of different developmental contexts. Here, we show that Grh knockdown leads to a dysregulation of calcium dynamics upon wounding. Moreover, we analyse the loss-of-function phenotypes in wound healing of a subset of Grh target genes that can associate with calcium. This analysis sheds new light on the mechanics of the closure process, revealing new players involved in wound healing linked to calcium signalling.

1.1 Keywords

Drosophila, epithelial repair, calcium, grainy head, genetic screen

2. Introduction

Calcium (Ca^{2+}) is an essential ion for the proper function of many biological processes. Not only is it necessary for cell-cell adhesion (Kemler et al., 1989; Kim et al., 2011; Ko et al., 2001), this molecule is also of major importance in several biological processes as diverse as synaptic transmissions, muscle contraction or gene expression regulation across different species (Berridge et al., 2000; Brini et al., 2014; Crabtree, 2001; Szent-Györgyi, 1975). This multitude of functions across species makes calcium an evolutionary conserved signalling molecule (Berridge et al., 2003). Typically it acts locally as an on/off switch in target molecules, by adding positive ion charges to Ca^{2+}-binding proteins, which leads to their rapid conformational change and consequent function (Berridge et al., 2003; Clapham, 2007). High molecular concentrations (~2mM) of calcium in the extracellular space facilitate and accelerate its accessibility (Andrews et al., 2014; McNeil and Kirchhausen, 2005). This is particularly relevant upon stress response events, such as wound healing. Fast signalling processes are of the up most importance in both cell and consequent tissue repair. Calcium has been shown to be linked to plasma membrane repair where physical disruptions lead to calcium influx to the cell through Ca^{2+} transport channels located to the membrane (Andrews et al., 2014; Cheng et al., 2015; McNeil and Kirchhausen, 2005) It has been shown that membrane resealing is impaired in the presence of Ca^{2+} chelators, like ethylene glycol-bis(β-aminoethyl ether)-N,N,N',N'-tetraacetic acid (EGTA) or 1,2-bis(2-aminophenoxy)ethane-N,N,N',N'-tetraacetic acid (BAPTA) (Steinhardt et al., 1994).

Calcium dynamics in wound healing have been studied in several model organisms, such as *Drosophila* (Antunes et al., 2013; Razzell et al., 2013), *C. elegans* (Xu and Chisholm, 2011), *Xenopus* (Bement et al., 1999) and Zebrafish (Yoo et al., 2012), where a rapid increase in intracellular calcium

levels around the wound has been observed. Cytosolic calcium levels are maintained by the capacity of different intracellular organelles to buffer and store calcium, like mitochondria or the endoplasmic reticulum (Fonteriz et al., 2016; Koch, 1990). In *Drosophila* embryos, this calcium signal upon wounding was shown to be important in the activation of reactive oxygen species (ROS) signalling and initiation of the inflammatory response (Razzell et al., 2013).

Calcium signalling and dynamics have also been linked to cytoskeletal rearrangement. A study performed *in vitro* has shown that, in the absence of extracellular calcium, the closure of an actin filament-dependent contractile ring-like structure is impaired (Bement and Capco, 1991). Moreover, calcium levels oscillation at the leading edge of migrating cells correlates with the also oscillatory activity of Rho GTPases responsible for contractility present in the same region, suggesting a cross-talk between these two processes (Clapham, 2007; Machacek et al., 2009; Tsai et al., 2015).

Epithelial wound healing is characterized, in several organisms, by the formation of an actomyosin contractile cable at the wound leading edge responsible for tissue closure in a purse-string movement (Antunes et al., 2013; Bement et al., 1993; Wood et al., 2002). In the *Drosophila* pupal notum epithelium, the rapid expanding calcium wave formed immediately after wounding correlates with the actomyosin and cell constriction flows that follow in the leading edge direction. This behaviour was linked to the regulation of Gelsolin activity, an actin filament severing protein that requires calcium for its activation (Antunes et al., 2013).

As calcium regulation affects tissue contraction and the wound closure process, we decided to investigate whether calcium dynamics are affected in the Grh knockdown (KD) in the *Drosophila* pupal notum epithelium. Moreover, Grh regulates the expression of hundreds of genes, some of which are known to be directly affected by or can affect calcium dynamics, suggesting that Grh function in wound healing (as described in Chapter II of

this study) might be at least in part by the regulation of calcium. To study this, we performed a genetic screen where we analysed the wound healing phenotypes of several Grh target genes known to be associated with calcium.

3. Materials and Methods

3.1 *Drosophila* lines and genetics

Flies were cultured and maintained on standard conditions. F-actin expression in control notum epithelia was assessed by expressing *w;; UAS-mcherry::moesin, pnr-GAL4* (Antunes et al., 2013; Calleja et al., 1996; Millard and Martin, 2008). Intracellular and mitochondrial calcium levels were observed using the genetic probe *UAS-GCaMP3* (Tian et al., 2009) and *UAS-mito-GCaMP3* (Lutas et al., 2012), respectively, crossed with *pnr-GAL4*. For knockdown of specific targets, different *UAS-RNAi* (Dietzl et al., 2007) fly lines from the Transgenic RNAi Project - Bloomington Drosophila Stock Center (Bloomington), Vienna Drosophila Resource Center (VDRC) and National Institute of Genetics (NIG) stated in Table I were crossed with *w;; UAS-mcherry::moesin, pnr-GAL4* for F-actin visualization or *w; UAS-GCaMP3::GFP; pnr-GAL4* for intracellular calcium visualization.

Crosses were performed at 25ºC (crosses with *UAS-RNAi-TK* VDRC control line) or 29ºC (crosses with all RNAi lines in Table I) to maximize RNAi expression and viability using the UAS/GAL4 system (Brand and Perrimon, 1993).

Table I. List of *Drosophila* RNAi lines used in this study.

***Drosophila* stock**	**Stock Center**	**Line reference**
UAS-Abl-RNAi	Bloomington	TRiP RNAi Valium 10 #28325
		TRiP RNAi Valium 20 #41710
UAS-Actn-RNAi	Bloomington	TRiP RNAi Valium 20 #32433

UAS-AnxB9-RNAi	VDRC	KK RNAi #106867
UAS-AnxB11-RNAi	VDRC	KK RNAi #101313
UAS-brat-RNAi	Bloomington	TRiP RNAi Valium 20 #34646
UAS-by-RNAi	Bloomington	TRiP RNAi Valium 20 #38288
UAS-Ca-α1D-RNAi	Bloomington	TRiP RNAi Valium 20 #33413
UAS-CalpC-RNAi	VDRC	KK RNAi #107844
UAS-Calr-RNAi	VDRC	GD RNAi #51271
		GD RNAi #51272
UAS-Cam-RNAi	Bloomington	TRiP RNAi Valium 20 #34609
UAS-CanB-RNAi	Bloomington	TRiP RNAi Valium 10 #27307
UAS-CBP-RNAi	VDRC	KK RNAi #104064
UAS-CG4928-RNAi	VDRC	KK RNAi #103750
UAS-CG9406-RNAi	VDRC	KK RNAi #104832
UAS-CG10126-RNAi	VDRC	KK RNAi #102435
UAS-CG13898-RNAi	VDRC	KK RNAi #100929
UAS-CG17765-RNAi	VDRC	GD RNAi #34404
UAS-CG31475-RNAi	VDRC	KK RNAi #106664
UAS-CG31650-RNAi	VDRC	KK RNAi #100590
UAS-CG32103-RNAi	VDRC	KK RNAi #108078
UAS-Clic-RNAi	VDRC	KK RNAi #1105975
UAS-Crtc-RNAi	Bloomington	TRiP RNAi Valium 10 #28886
UAS-Duox-RNAi	Bloomington	TRiP RNAi Valium 20 #32903

		TRiP RNAi Valium 20 #33975
UAS-Dyb-RNAi	Bloomington	TRiP RNAi Valium 20 #32935
UAS-Dys-RNAi	VDRC	KK RNAi #106401
UAS-Egfr-RNAi	Bloomington	TRiP RNAi Valium 10 #25781
		TRiP RNAi Valium 20 #36770
		TRiP RNAi Valium 20 #36770
UAS-Fim-RNAi	Bloomington	TRiP RNAi Valium 20 #32936
		TRiP RNAi Valium 20 #33977
UAS-ics-RNAi	VDRC	GD RNAi #42188
UAS-Letm1-RNAi	Bloomington	TRiP RNAi Valium 20 #37502
UAS-mey-RNAi	VDRC	KK RNAi #106568
UAS-Nox-RNAi	Bloomington	TRiP RNAi Valium 20 #32433
UAS-pwn-RNAi	VDRC	KK RNAi #101282
UAS-shark-RNAi	Bloomington	TRiP RNAi Valium 10 #25788
UAS-shot-RNAi	Bloomington	TRiP RNAi Valium 10 #28336
UAS-sl-RNAi	Bloomington	TRiP RNAi Valium 20 #32906
UAS-Src42A-RNAi	NIG	7873R-2
UAS-Stat92E-RNAi	Bloomington	TRiP RNAi Valium 20 #33637

3.2 Wounding assay and live imaging

Pupae were staged at 13h after puparium formation (APF) (Bainbridge and Bownes, 1981), mounted and prepared for imaging as previously described (Antunes et al., 2013). Laser wounding and live imaging were performed as previously described (Antunes et al., 2013). Wounds were induced using a MicroPoint (Andor Technology) UV nitrogen-pumped dye laser (435 nm). Live imaging was performed using a Nikon/Andor Revolution spinning disk system with an EMCCD Camera (iXon 897; Andor Technology) at 25ºC or 29ºC, using the iQ software (Andor Technology). Z-stacks were acquired with a Plan Apo VC PFS 60× objective (NA 1.40; Nikon) every 10 seconds, except for the calcium fast imaging which was done every 50 milliseconds.

3.3 Image Analysis

Raw data was processed using Fiji (Schindelin et al., 2012) to obtain maximum intensity projections and orthogonal views. Kymograph were made using a 1 pixel-width line. All stills shown are maximum intensity z-stack projections, except for fast imaging of intracellular calcium, which represent only one focal plane.

4. Results

4.1 Calcium levels during *Drosophila* epithelial wound healing

In *Drosophila* pupal notum epithelial wounding, intracellular calcium levels increase in a wave-like manner, starting from the leading edge of the wound and spreading several cell rows across the tissue right after wounding (Antunes et al., 2013). As calcium is known to change very quickly, we decided to investigate this phenomenon in more detail, by performing live imaging of the pupal notum epithelium during the initial stages of wound closure at higher/faster time resolution than in previous studies (50 milliseconds between frames). We used the previously described genetically encoded calcium sensor GCaMP3, that allows the tracking of rapid changes in cytoplasmic-free calcium concentration (Tian et al., 2009). We observed that the expansion of the calcium wave is not achieved in a constant manner (Fig. 1; Video S1). Immediately upon injury, the first rows of cells around the wound quickly and dramatically increased their intracellular calcium (Fig. 1Aii); during the next 30 seconds (secs), calcium increases progressively in the next 1 to 2 cell rows, spanning across the tissue (Fig. 1Ai-v); between 30 and just before 60 secs after wounding, this calcium accumulation stabilized and did not increase its span over the tissue (red brackets in Fig. 1Aviii). Interestingly, after this time point, we observed fast high intensity calcium flashes around these cells (red arrowheads in Fig. 1Aviii; Video S1), increasing the tissue target range of this wave for 1-2 minutes. After this, calcium sensor intensity progressively decreased, starting from cell rows further away from the wound until the leading edge, accompanied by a decrease in calcium flashes occurrence (Fig. 1Aviii; Video S1).

This two-phase dynamic is only visible in movie analysis with small interval times between frames. These results show that intracellular calcium

concentrations are even more dynamic than previously shown, strengthening its role as one of the first responses to injury.

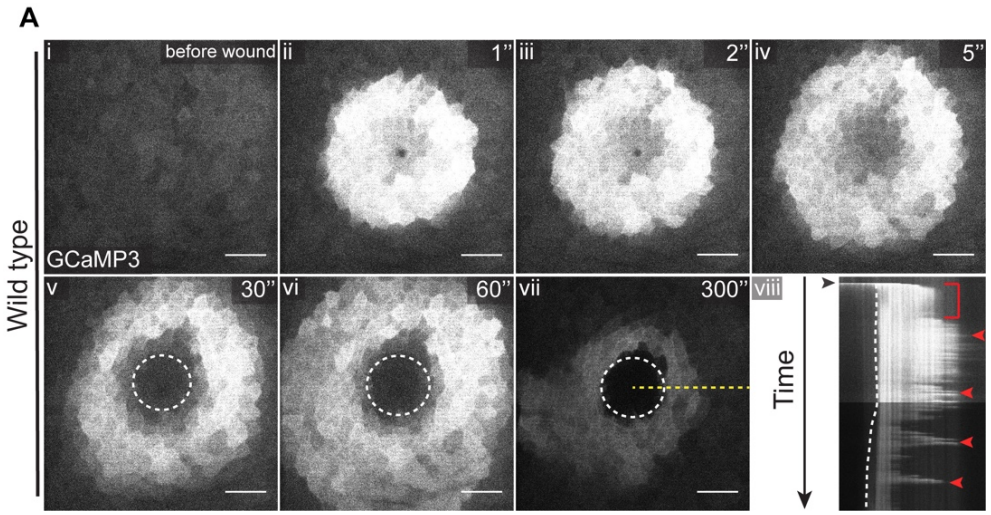

Figure 1. Two-phase dynamics of intracellular calcium signalling upon wounding (**A**) Movie stills of intracellular calcium dynamics during wound closure in wild type pupal notum epithelium expressing UAS-GCaMP3 in wild type (Ai-vii; Video S1) under the control of *pnr*-GAL4 driver. Fast resolution imaging shows a progressive increase of calcium during the first 30 secs after wounding (Avi-v), while calcium spikes only start after 60 secs, after injury, contributing to the calcium signal expansion to the surrounding tissue (Avi). After this, calcium intensity and spike occurrence diminishes (Avii). (Aviii) Kymograph (yellow dashed line in Avii) showing calcium expansion during the first stage of calcium increase (until 30 seconds post wounding) (red brackets in Aviii) followed by the start of the calcium spikes (red arrowheads in Aviii). White dashed lines represent wound margin. Scale bars: 20 μm. n = 4 pupae.

To understand whether this intracellular calcium increase is also associated with organelles that typical store this ion, we looked at mitochondrial calcium changes. Mitochondria are dynamic cellular organelles that can uptake calcium in order to maintain intracellular calcium levels and homeostasis

(Fonteriz et al., 2016; Paupe and Prudent, 2017). Through the expression of GCaMP3 in mitochondria (Lutas et al., 2012), we observed an increase of calcium levels inside these organelles upon wounding (Fig. 2Ai'-iv'), which seems to follow the initial intracellular calcium wave. This pattern resembled the dynamics of this first wave (Fig. 2Ai-iv), although calcium levels inside mitochondria took longer to diminish and stabilize (Fig. 2Aiv,iv').

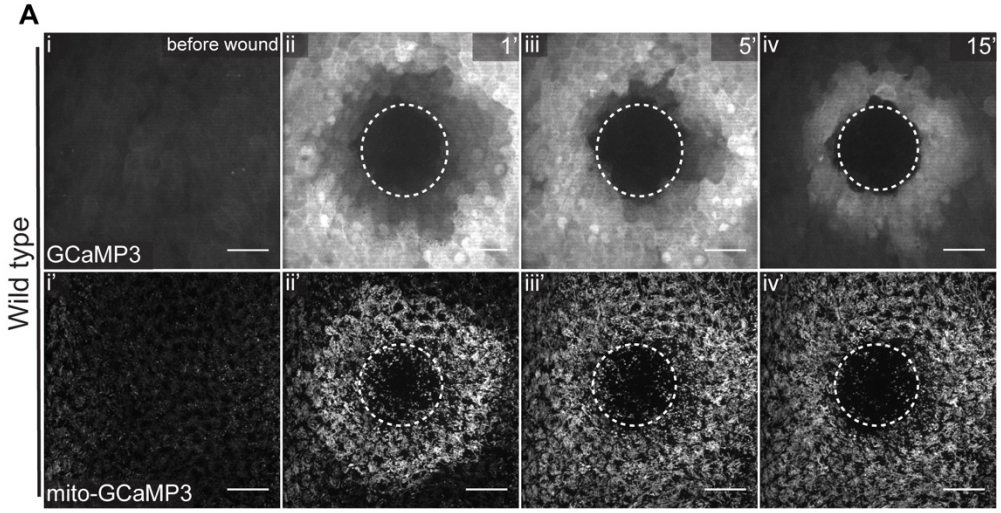

Figure 2. Calcium dynamics inside mitochondria have similar dynamics to intracellular calcium sensor. (**A**) Movie stills of intracellular calcium dynamics during wound closure in wild type pupal notum epithelium expressing UAS-GCaMP3 (Ai-iv; Video S2) or UAS-mito-GCaMP3 (Ai'-iv'; Video S2) under the control of *pnr*-GAL4 driver. Mitochondrial calcium levels exhibit a similar increase to intracellular calcium during the initial seconds of wound closure. White dashed lines represent wound margin. Scale bars: 20 μm. n = 3 pupae per condition.

These results show a new profile for intracellular calcium expansion upon wounding. Moreover, they show conserved dynamics in mitochondrial calcium uptake during epithelial wound healing between species.

4.2 Calcium dynamics are altered in the Grh knockdown

Since Grh KD leads to wound closure failure with an impairment on F-actin dynamics, we decided to analyse how calcium dynamics were affected in this context. As observed in wild type conditions (Fig. 3Ai-iv), intracellular calcium levels increased within the first 5 secs after wounding in the Grh KD. However, after that, calcium levels failed to decrease as detected in the wild type. Instead, calcium levels persisted in a few rows of cells around the wound (Fig. 3Ai'-iv').

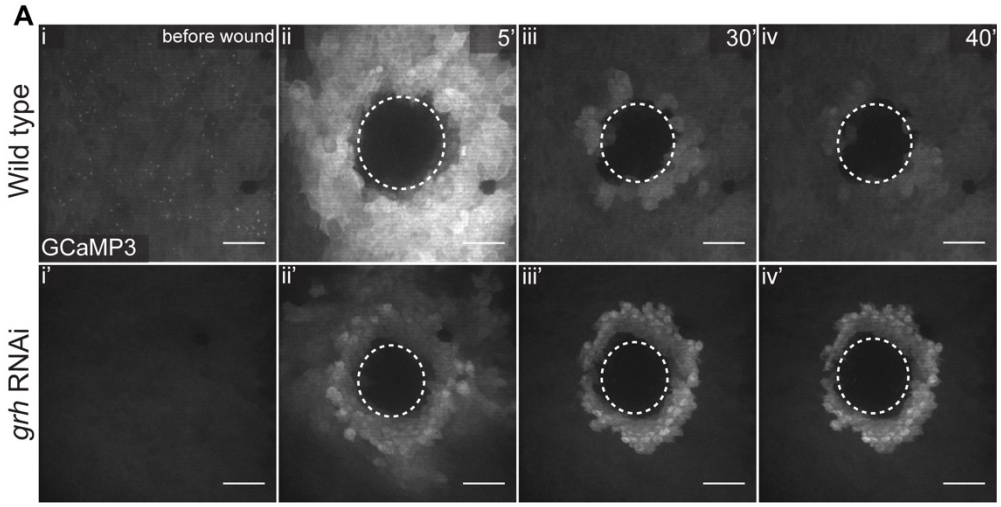

Figure 3. Grh KD leads to dysregulation of intracellular calcium wave upon wounding. (**A**) Movie stills of intracellular calcium dynamics during wound closure in pupal notum epithelia expressing UAS-GCaMP3 in the wild type (Ai-iv; Video S3) and together with UAS-*grh*-RNAi (Ai'-iv'; Video S3) under the control of *pnr*-GAL4 driver. Whereas in the wild type calcium decreases in the tissue around the wound in the wild type (Aiii-iv), in Grh KD we observed a lingering accumulation of intracellular calcium in the tissue (Aiii'-iv'). White dashed lines represent wound margin. Scale bars: 20 μm. n = 3 pupae per condition.

These results show that Grh is involved in the regulation of calcium dynamics upon injury in the notum epithelial cells around the wound.

4.3 Grh activation upon wounding in the *Drosophila* pupal stage

It has been proposed that in Drosophila embryonic wound closure Grh acts through Receptor Tyrosine Kinase (RTK) signalling, involving Src42A and Epidermal Growth Factor Receptor (EGFR)/ERK activation (Geiger et al., 2011; Shilo, 2005; Simon et al., 1985; Takahashi et al., 1996; Tsarouhas et al., 2014). To understand whether Grh regulates calcium dynamics through these pathways, we investigated whether the concentration of this ion changes in EGFR and Src42A loss-of-function in the pupal notum epithelium upon wounding. Since Src42A is also involved in actin cable formation (Tsarouhas et al., 2014), and Grh KD causes the impairment of F-actin wave propagation and ectopic cable formation (described in Chapter II of this study), we also observed RTK KD phenotype in actin cable assembly. Wound healing phenotypes in wild type, Grh KD and RTKs KD were analysed focusing on the resulting phenotype at 60 minutes post wounding, for both calcium and F-actin, at the point when in the wild type process, calcium is already decreased and cable is already formed at the leading edge. Egfr KD leads to mild calcium accumulation and failure to form a proper leading edge actin cable (Fig. 4Aiii,iii'). The same was observed for Src42A KD.

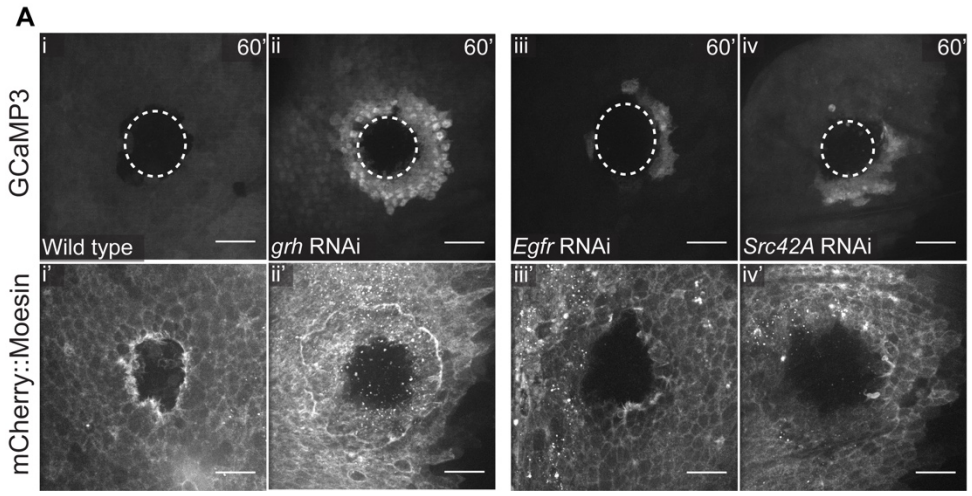

Figure 4. Possible activators of Grh exhibit wound healing phenotypes. (**A**) Movie stills of intracellular calcium, through the expression of UAS-GCaMP3 (Ai-iv) or F-actin dynamics, through the expression of UAS-mCherry::Moesin (Ai'-iv'), in wild type (Ai,i'), UAS-*grh*-RNAi (Aii,ii'), UAS-*Egfr*-RNAi (Aiii,iii') and UAS-*Src42A*-RNAi (Aiv,iv') under the control of *pnr*-GAL4 driver, in pupal notum epithelia. KD of Egfr and Src42A lead to impaired calcium dynamics and F-actin polymerization, although not as strongly as in Grh KD. White dashed lines represent wound margin. Scale bars: 20 μm. n = 3-4 per condition.

Although live imaging analysis of both phenotypes show closure defect phenotypes (Fig. 4), none of them mimics the full extent of Grh KD phenotype. Nonetheless, these results show that, similar to what has been found in embryonic wound closure (Geiger et al., 2011; Tsarouhas et al., 2014), Egfr and Src42A are necessary for proper closure of the pupal notum epithelium upon injury. Furthermore, these signalling pathways might be involved in the regulation of calcium dynamics in this process.

4.4 Grh targets and calcium accumulation

As an epithelial transcription factor, Grh is responsible for the regulation of a vast number of genes involved in several processes in different developmental stages (Wang and Samakovlis, 2012). To better understand how Grh might regulate calcium dynamics, we focused on Grh direct targets. We selected a small subset of direct targets of Grh that are either known modulators of calcium signalling or regulated by calcium. These target genes were kindly provided by Christos Samakovlis and Liqun Yao, from a genome-wide analysis through ChiP-Seq on *grh* mutant embryos (Yao et al., 2017). The chosen target genes, their annotation symbol (Flybase) and previously described function is stated in Table II.

Table II. List of *Drosophila* Grh target genes analysed in the RNAi KD screen. List of selected direct Grh targets selected for a potential role in wound healing. Gene function accessed from current bibliography. *Predicted function based on sequence analysis.

Target Genes	Annotation symbol	Function previously described
Abelson tyrosine kinase (*Abl*)	CG4032	Phosphorylation of cell adhesion and cytoskeletal proteins (Fox and Peifer, 2007)
α-actinin (*Actn*)	CG4376	Actin cross-linking protein (Fyrberg et al., 1998)
Annexin B9 (*AnxB9*)	CG5730	Ca^{2+} and phospholipid-binding protein (Gerke et al., 2005)
Annexin B11 (*AnxB11*)	CG9968	Ca^{2+} and phospholipid-binding protein (Gerke et al., 2005)
brain tumor (*brat*)	CG10719	Tumour suppressor (Sonoda and Wharton, 2001)

blistery (*by*)	CG9379	Tensin homologue; integrin and actin binding (Lee, 2003)
Ca^{2+}-channel protein α_1 subunit D (*Ca-α1D*)	CG4894	Pore-forming α subunit of an L-type voltage-gated Ca^{2+} channel; affects Ca^{2+} influx (Eberl et al., 1998)
Calpain C (*CalpC*)	CG3692	Calcium-dependent cysteine protease (Friedrich et al., 2004)
Calreticulin (*Calr*)	CG9429	Lectin-like chaperone (Michalak et al., 1999)
Calmodulin (*Cam*)	CG8472	Calcium-binding messenger protein (Faas et al., 2011)
Calcineurin B (*CanB*)	CG4209	Regulatory subunit of phosphatase Calcineurin (Sullivan and Rubin, 2002)
sarcoplasmic calcium-binding protein (*CBP*)	CG1435	Transcriptional co-activator (Philip et al., 2015)
CG4928	CG4928	Potassium channel regulator activity*
CG9406	CG9406	Calcium ion binding*
CG10126	CG10126	Calcium ion binding*
CG13898	CG13898	Calcium ion binding*
CG17765	CG17765	Calcium ion binding*
CG31475	CG31475	Calcium ion binding*
CG31650	CG31650	Calcium ion binding*
CG32103	CG32103	Calcium ion binding*
Chloride intracellular channel (*Clic*)	CG10997	Chloride channel (Littler et al., 2008)
CREB-regulated transcription coactivator (*Crtc*)	CG6064	Transcriptional coactivator of cAMP-response element-binding protein (CREB) (Bittinger et al., 2004)

Dual oxidase (*Duox*)	CG3131	Peroxidase (Ha et al., 2005)
Dystrobrevin (*Dyb*)	CG8529	Cytoskeletal protein binding (Jin et al., 2007)
Dystrophin (*Dys*)	CG34157	Cytoskeletal protein binding; establishment of cell polarity (Shcherbata et al., 2007)
Fimbrin (*Fim*)	CG8649	Actin binding protein*
icarus (*ics*)	CG9031	Regulator of integrin-dependent adhesion (Elias et al., 2012)
Leucine zipper and EF-hand containing transmembrane protein 1 (*Letm1*)	CG4589	Calcium:sodium antiporter (Jiang et al., 2009)
morpheyus (*mey*)	CG12063	Membrane component; involved in apical constriction (Fernandes et al., 2010)
NADPH oxidase (*Nox*)	CG34399	Superoxide-generating oxidase (Ritsick et al., 2007)
pawn (*pwn*)	CG11101	Calcium ion binding* (Arruda and Dolph, 2003)
SH2 ankyrin repeat kinase (*shark*)	CG18247	Non-receptor tyrosine kinase of the Syk family (Fernandez et al., 2000)
short stop (*shot*)	CG18076	Spectraplakin; cytoskeletal linker (Roper et al., 2002)
small wing (*sl*)	CG4200	Phosphatidylinositol phospholipase C activity (Mankidy et al., 2003)
Signal-transducer and activator of transcription protein at 92E (*Stat92E*)	CG4257	Transcription factor in the JAK/STAT pathway (Kwon et al., 2000)

All genes were analysed through RNAi KD with wound closure defect and calcium and F-actin dynamics as readout phenotypes. Results were divided in three different categories: no phenotype; inconclusive phenotype; phenotypes both in calcium and F-actin dynamics. Inconclusive means that phenotypes were not reproducible in the majority of the experiments for the given gene. The phenotype for each gene is stated in Table III.

Table III. List of phenotypes observed for the *Drosophila* Grh target genes analysed in the RNAi KD screen. Wound closure phenotype was addressed regarding F-actin (actin wave and actin cable defects) and intracellular calcium dynamics (persistent calcium accumulation) upon wounding, compared to the control. Phenotype categories were established as: Phenotype – defective dynamics in actin and calcium were observed in over 60% of the experiments; Inconclusive – defective dynamics were observed in 25 to 60% of the experiments, with remaining experiments showing no phenotype; No phenotype – defective dynamics were observed in less than 25% of the experiments. At least 4 pupae were imaged for each gene, except in *(n=2).

Gene	Phenotype
Abl	Inconclusive
Actn	No phenotype
AnxB9	Phenotype in calcium and F-actin dynamics
AnxB11	Inconclusive
brat	No phenotype
by	Inconclusive*
Ca-α1D	No phenotype
CalpC	No phenotype
Calr	Inconclusive*

Cam	Phenotype in calcium and F-actin dynamics
CanB	Phenotype in calcium and F-actin dynamics
CBP	Phenotype in calcium and F-actin dynamics
CG4928	Inconclusive
CG9406	Inconclusive
CG10126	Phenotype in calcium and F-actin dynamics
CG13898	Inconclusive
CG17765	No phenotype
CG31475	Inconclusive
CG31650	Inconclusive
CG32103	Inconclusive
Clic	Phenotype in calcium and F-actin dynamics
Crtc	Inconclusive
Duox	No phenotype
Dyb	Inconclusive*
Dys	No phenotype
Fim	No phenotype
ics	No phenotype
Letm1	No phenotype
mey	Phenotype in calcium and F-actin dynamics
Nox	Inconclusive*
pwn	Phenotype in calcium and F-actin dynamics

shark	No phenotype
shot	Phenotype in calcium and F-actin dynamics
sl	No phenotype
Stat92E	Inconclusive

Focusing on the genes that showed phenotype both in calcium and F-actin dynamics, as well as wound closure impairment (Fig. 5), we grouped them as follows according to their previously described functions and structure: *Cam*, *CanB*, *CBP* and *Clic,* which are directly related with calcium signalling; *AnxB9*, *mey*, *pwn* and *shot*, which are related with adhesion or membrane dynamics; and *CG10126*, which is yet not described. Actin wave and cable formation impairment was common to the KD of all these genes (Fig. 5Ai'-xviii'). Calcium accumulation varied from gene to gene (Fig. 5Ai-xviii), with CanB (Fig. 5Av,vi) and Clic (Fig. 5Axi,xii) KD showing a smaller number of cell rows accumulating calcium, relative to other KDs. Nonetheless, calcium accumulation was observed at 60 minutes post wounding in every KD, in this group (Fig. 5Aii,iv,vi,viii,x,xii,xiv,xvi,xviii). AnxB9 (Fig. 5Aii,ii'), CG10126 (Fig. 5Ax,x') and pwn (Fig. 5Axvi,xvi') KD seem to show a slight resemblance to the Grh KD phenotypes at 60 minutes post wounding (Fig. 4Aii,ii'). In these cases, alongside with the persistent calcium accumulation (Fig. 5Aii,x,xvi), we observed a faint actin accumulation between two regions characterized by different F-actin dynamics. Although slightly, this dynamics pattern can be compared with the ectopic actin cable in the Grh KD (Fig. 4Aii') (Video S4).

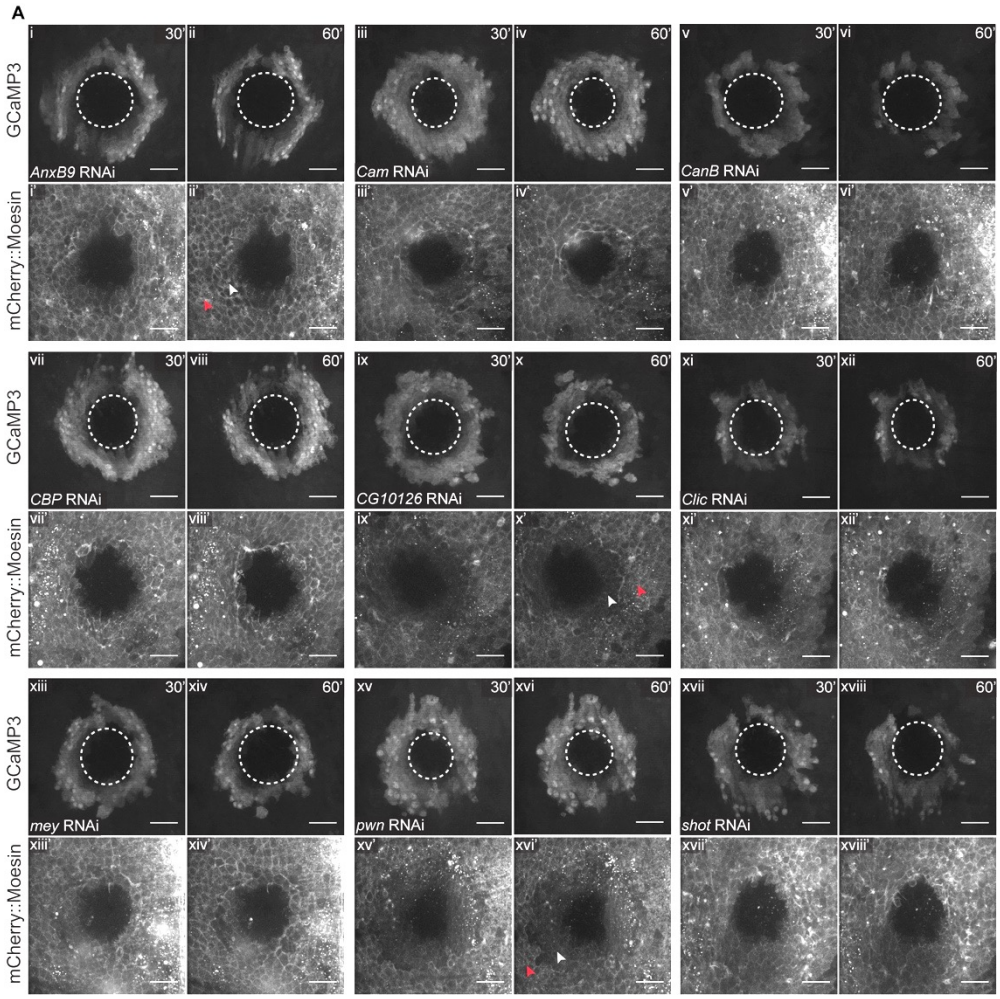

Figure 6. Identification of Grh target genes involved in intracellular calcium and cytoskeletal dynamics upon wounding of the *Drosophila* notum epithelium. (**A**) Movie stills of intracellular calcium, through the expression of UAS-GCaMP3, or F-actin dynamics, through the expression of UAS-mCherry::Moesin, and UAS-RNAi for *AnxB9* (Ai-ii;Ai'-ii'), *Cam* (Aiii-iv;Aiii'-vi'), *CanB* (Aiv-v;Aiv'-v'), *CBP* (Avii-viii; Avii'-viii'), *CG10126* (Aix-x;Aix'-x'), *Clic* (Axi-xii;Axi'-xii'), *mey* (Axiii-xiv;Axiii'-xiv'), *pwn* (Axv-xvi;xv-xv') and *shot* (Axvii-xviii;Axvii'-xviii') under the control of *pnr*-GAL4 driver, in pupal notum epithelia. KD of these genes leads to calcium dynamics deregulation and F-actin polymerization impairment. Red and white arrowheads (Aii',x',xvi') represent different regions separated by a faint actin accumulation

resembling ectopic actin cable in Grh KD (Fig. 4Aii'). White dashed lines represent wound margin. Scale bars: 20 μm. n = 3-4 pupae per condition.

With this RNAi screen, we unveiled new genes involved in *Drosophila* pupal notum epithelium wound healing, involved in calcium and F-actin dynamics regulation.

5. Discussion

Calcium is involved in a myriad of biological processes, spanning from adhesion establishment to neuronal signalling, from muscle contraction to gene regulation, and either cell proliferation or cell death (Berridge et al., 2003; Clapham, 2007; Kim et al., 2011). This versatility comes from its accessibility and fast acting dynamics, which makes it a well conserved second messenger molecule in living organisms (Berridge et al., 2003; Clapham, 2007). Its involvement in tissue repair has been studied across different species (Antunes et al., 2013; Sung et al., 2003; Xu and Chisholm, 2011; Yoo et al., 2012), demonstrating the importance of calcium regulation in this process. Calcium and cytoskeletal dynamics regulation compose the dynamic duo responsible for the onset of the closure process (Antunes et al., 2013). As the first signal induced upon wounding, one of the listed functions proposed for calcium is the activation of molecules that can lead to cytoskeletal rearrangements and tissue contraction (Antunes et al., 2013; Cordeiro and Jacinto, 2013; Tsai et al., 2015; Xu and Chisholm, 2011). Because of this, the deregulation of calcium signalling can lead to irreparable damage on the injured tissue.

5.1 Calcium dynamics as a two-stage expansion process

As one induces a wound in the *Drosophila* epithelial tissue, the first observation is that the rise of intracellular calcium is not limited to the leading edge cells, since it reaches a patch of tissue all around the wound (Antunes et al., 2013; Razzell et al., 2013). The first report of its dynamics in pupal stages has shown a rapid outburst outward of the intensity levels across the tissue, which then comes back to the leading edge, with occasional flashes extending across longer ranges of cells (Antunes et al.,

2013). These flashes have also been described in the *Drosophila* embryo and linked to ROS signalling in order to activate the recruitment of macrophages (called hemocytes in *Drosophila*) to the wound (Razzell et al., 2013). Recently, it has been shown that the calcium spikes, in *Drosophila* wing imaginal discs upon wounding, correlate with the mechanical heterogeneity in the tissue, explained mainly by local cell shape anisotropy (Narciso et al., 2015). This means the mechanics of wound closure might itself regulate the propagation of calcium signalling probably depending on tension cues. This correlates nicely with our observations obtained through fast imaging of calcium dynamics (Fig. 1; Video S1). We showed that the first outburst of calcium inside the cells is actually divided in two stages. In the first stage, the tissue disruption by the wound leads to the increase of intracellular calcium in a few rows of cells across the tissue from the wound site, and progressing slowly on an outward direction during the first 30 seconds after wounding. After it reaches the furthest cell row, the intensity of calcium-sensor levels plateau until around one minute after wounding. Then the second stage initiates, where several random calcium spikes are observed reaching further across the tissue, maintaining the high calcium levels for a couple more minutes. Ultimately, the calcium front restricts its location back to the leading edge, with the number of calcium spikes decreasing. These two stages, one more clearly defined and maintained, and the second one, more stochastic and dynamic might relate to the differences in tension during the first stages after wounding as the tissue acknowledges (first stage) and then accommodates (second stage) the tissue disruption.

We also observed a mitochondrial calcium wave across the tissue (Fig. 2; Video S2). Furthermore, this wave seems to expand following the intracellular calcium one, in accordance with what has been described in *C. elegans* (Xu and Chisholm, 2014). This time shift between both waves nicely correlates to what has been described in homeostatic conditions, where

mitochondria are known to work as storage buffers for increased levels of intracellular calcium to help normalise the levels in the cell, in a conserved manner across species (Fonteriz et al., 2016; Rizzuto et al., 2012). It would be interesting to target the calcium channels in the mitochondria membrane (Paupe and Prudent, 2017). This would help to understand how important is this mitochondrial storage and how much it accounts for the regularization of intracellular calcium levels upon wounding (Fonteriz et al., 2016; Williams et al., 2013). Another interesting point would be to study how this mitochondrial calcium burst affects the mechanisms of fission and fusion of the mitochondria and how important they are in injury response. The actin cytoskeleton is known to interact with mitochondria, in the regulation of their morphology, motility and distribution (Bartolák-Suki et al., 2017; Boldogh and Pon, 2006). Interestingly, this interaction might result in a feedback loop: studies performed in cell culture have shown that, as mitochondria anchor to the cytoskeleton, they can be sensitive to mechanical strain and can function as mechanotransducers by releasing ROS, as a response to this stress stimulus (Ali et al., 2004); in its turn, mitochondria can regulate actin cytoskeleton stiffness, loss of cell polarity or focal adhesion impairment, through the regulation of calcium influx from the cytoplasm (Prudent et al., 2016). Moreover, mitochondria-derived ROS was shown to regulate the activation of Rho kinase and contractility in endothelial smooth muscle cells (Kajimoto et al., 2007). This regulation of Rho GTPases and contractility has also been described in *C. elegans* during wound closure (Xu and Chisholm, 2014). In the future, it would prove useful to integrate all these results in the pupal notum epithelial closure system to decipher the importance of regulating mitochondrial morphology and dynamics during tissue repair.

5.2 Grh and calcium misregulation upon wounding

Since calcium signalling is a *bona fide* first responder in tissue repair, we wanted to understand whether Grh could be involved in regulating calcium dynamics in this process. Grh has been described in several organisms as an acting agent in the regulation of the wound response (Wang and Samakovlis, 2012), either by inducing the transcription of specialized wound response genes (Kim and McGinnis, 2011; Mace et al., 2005) or through homeostatic regulation of the expression of typical epithelial proteins also involved in the closure mechanism (Caddy et al., 2010). Here we show that Grh KD leads to deregulation of calcium dynamics, causing an abnormal and persistent intracellular calcium accumulation in cells around the wound (Fig. 3; Video S3). This is the first observation connecting Grh and calcium. Although transcriptionally Grh regulates a quite extensive list of target genes, one of our hypothesis is that the lingering accumulation of high levels of calcium is associated with the disruption of the cuticle permeability barrier in Grh (Bray and Kafatos, 1991; Mace et al., 2005; Wang and Samakovlis, 2012) (Chapter II of this study, Fig. 2). But this cannot be explained only by a defective permeability barrier, since the primary source of calcium is the extracellular space which is situated below the cuticle barrier. In the future, this hypothesis could be tested by analysing calcium dynamics after wounding KD pupae for Dumpy (dpy), Dopadecarboxilase (Ddc) or krotzkopf verkehrt (kkv), proteins involved in the formation of the *Drosophila* cuticle (Mace et al., 2005; Moussian et al., 2005; Wilkin et al., 2000). Another relevant observation regarding this calcium accumulation phenotype is the range of cells affected by the accumulation. If the permeability barrier was the only factor influencing the calcium accumulation, it would be expected that the whole KD tissue would be affected and not only that particular group of cells close to the wound. Therefore, considering the results of Chapter II in this study regarding the downregulation of E-Cadherin around the wound

(Chapter II – Fig. 4), we suggest that the downregulation of this Adherens Junctions component could lead to a more permissive tissue, where calcium would accumulate. We have tried to test this by wounding E-Cad KD pupae and checking calcium intracellular accumulation dynamics, but unfortunately the data were not conclusive. Nevertheless, this hypothesis deserves to be pursued in future studies.

5.3 Grh and upstream activators

Grh phosphorylation by ERK upon wounding is known to influence the repair process (Kim and McGinnis, 2011; Mace et al., 2005). Although dispensable for homeostatic functions of Grh (Kim and McGinnis, 2011; Wang and Samakovlis, 2012), this post-translational modification is necessary for the activation of wound response genes, such as *Ddc* and *pale* (ple), responsible for cuticular repair (Mace et al., 2005; Pearson et al., 2009; Wang and Samakovlis, 2012). ERK also needs to be activated through phosphorylation prior to Grh phosphorylation, at which point it translocates to the nucleus to phosphorylate target proteins (Geiger et al., 2011; Mace et al., 2005). ERK is known to be phosphorylated by several upstream regulators, such as Egfr (Dieckgraefe and Weems, 1999), including during *Drosophila* wound healing (Geiger et al., 2011; Mace et al., 2005). On the other hand, Scr42A has been described as capable of phosphorylating Grh, independently of ERK (Tsarouhas et al., 2014). To understand whether these kinases could be mediators of calcium and F-actin dynamics during wound healing, we tested whether knocking them down would mimic Grh phenotypes. Our results show that both Egfr and Src42A activation are necessary for proper closure of pupal notum epithelial wounds. Unfortunately, none of these two single KDs were sufficient to mimic the full Grh phenotype (Fig. 4), where calcium accumulation was not as intense and

no ectopic cable was visible in both KDs. This may point to either a combined phosphorylation of Grh by both kinases or to participation of other molecules/targets in mediating the Grh phenotypes. Furthermore, the Grh target Stit, an RTK also described to be involved in ERK and Grh phosphorylation (Wang et al., 2009), did not render a conclusive phenotype. Stit has been linked to the remodelling of the actin cytoskeleton in wound healing and would be of interest to clarify its function in pupal wound healing.

5.4 Grh targets interacting with calcium and their wound healing phenotype

In order to find new potential Grh targets linked to the calcium dynamics phenotype during wounding we performed a small RNAi screen. Our list of 35 potential Grh targets was biased to genes containing calcium binding domains in their structure, which could be involved in calcium signalling pathways or in calcium regulation and interaction. This list was a courtesy of Christos Samakovlis and Liqun Yao (Department of Molecular Biosciences, The Wenner-Gren Institute, Sweden). We proceeded to use the Grh calcium and actin phenotype as a readout to assess if any direct Grh targets were linked to the deregulation of this wound response. From this screen, we identified 9 genes whose KD resulted in persistent intracellular calcium accumulation around the wound (Fig. 6). Moreover, all KDs showed wound closure defects, impairment in actin wave propagation and actin cable formation at the leading edge. This supports the hypothesis that deregulation of calcium dynamics is connected to defects in cytoskeletal rearrangements. Considering the already described functions of the identified genes, we can speculate about their potential function in wound healing. The KD phenotypes for three of these genes were very similar to

the Grh KD (Video S4). One of them, *AnxB9*, has recently been shown to regulate spectrin localization along the baso-lateral membrane and perturb the endosomal system (Tjota et al., 2011). The mislocalization of cell membrane and adhesion components can lead to polarity problems in the cell, which consequently affect cytoskeletal dynamics (Woodham and Machesky, 2014). Moreover, the endosomal machinery is of the upmost importance during wound healing in order to form a proper actin contractile cable (Hunter et al., 2015). The two other genes, *CG10126* and *pwn*, have not been characterized. The *CG10126* is yet to be described. *pwn* is thought to be a large adhesion molecule (Arruda and Dolph, 2003). Both these genes have a somewhat similar KD phenotype to Grh KD, thus it would be interesting to pursue their functional analysis to understand their function in wound healing. Regarding other phenotypes, we identified *Cam*, *CanB* and *CBP*. All three KD phenotype include lingering calcium accumulation around the wound and actin cable formation impairment. These proteins bind directly to Ca^{2+} ions: Cam is an adaptor protein between calcium and other proteins, CanB is as phosphatase involved in TORC signalling and CBP is a co-transcription factor that responds to calcium signalling (Clapham, 2007; Philip et al., 2015). Therefore, their function in wound healing might be extremely diverse. Regarding some negative results, it was rather surprising the absence of phenotype with Duox KD. Duox is responsible for production of hydrogen peroxide, and this has been shown to be important in the detection, regulation and spreading of the wound response across the tissue (Cordeiro and Jacinto, 2013; Juarez et al., 2011; Niethammer et al., 2009). Although its function in wound healing seems to be downstream of calcium activation (Razzell et al., 2013), we did not expect to find that wounds closed despite ROS signalling being potentially affected. This would show that this pathway, although important for the inflammatory response, is not necessary for proper wound closure. Another negative result that might seem surprising was the Shark kinase KD, known to be involved in embryonic dorsal closure by regulating JNK activity (Fernandez et al.,

2000). Dorsal closure and wound closure have been shown to be mechanically similar and have several conserved players (Garcia-Fernandez et al., 2009; Köppen et al., 2006), but unfortunately, we did not observe any phenotype with Shark KD. It would be interesting to test whether, in the pupal notum, JNK is also not involved in wound closure. *mey* and *shot* also encode membrane components. In Chapter II of this study, we show that E-Cad KD leads to defective actin cable formation upon wounding. In this screen, we observed that *mey* and *shot* also presented impaired actin cable formation, along with abnormal calcium accumulation. This strengthens the model where proper cell adhesion structures are necessary for proper contractile dynamics in the mechanism of wound closure. As expected, none of the identified targets fully recapitulated the Grh KD phenotypes. This is probably because Grh, as a master regulator of epithelial maintenance, differentiation and repair, simultaneously regulates several key targets, all important for proper regulation of wound closure dynamics. Moreover, we cannot discard the possibility of false negative results due to poor penetrance of each KD, since RNAi constructs often suffer from different efficiency rates, with low silencing efficacies of specific dsRNA and shRNA molecules. Although an RNAi screen can be very informative, especially regarding genes that induce organism lethality in mutant forms when analysing their function in non-embryonic developmental stages, this system is still based on inducible expression, the UAS/GAL4 system (Brand and Perrimon, 1993), with a certain degree of variability, depending on a tissue restrictive expression driver. Negative results can be rechecked through the co-expression of the Dicer enzyme, to maximize RNAi efficiency in the case of dsRNAs, for example (Dietzl et al., 2007). Also, positive results should be target of further validation, since false positives are less frequent but still possible due to off-target effects caused by similarities between dsRNA sequences. Generation of conditional clonal mutant cells, dominant-negative protein forms or genetic epistatic analysis can be used to validate positive results (Yamamoto-Hino and Goto, 2013).

Despite its limitations, RNAi screens are still very important in the discovery of new players of different biological processes.

Altogether, our results shed new light on calcium dynamics during tissue repair. The new observation of how the calcium wave first expands can lead to interesting studies correlating tissue tension and chemical signalling, as well as the correlation with the mitochondrial calcium wave in this context. Furthermore, our screen analysis has allowed us to propose new Grh effectors involved in the wound healing process. Within the scope of this study, the novel role for Grh in the regulation of calcium dynamics opens a new unexplored field of research for epithelia development and repair.

6. References

Ali, M.H., Pearlstein, D.P., Mathieu, C.E., and Schumacker, P.T. (2004). Mitochondrial requirement for endothelial responses to cyclic strain: implications for mechanotransduction. Am. J. Physiol. Lung Cell. Mol. Physiol. *287*, L486–L496.

Andrews, N.W., Almeida, P.E., and Corrotte, M. (2014). Damage control: Cellular mechanisms of plasma membrane repair. Trends Cell Biol. *24*, 734–742.

Antunes, M., Pereira, T., Cordeiro, J. V., Almeida, L., and Jacinto, A. (2013). Coordinated waves of actomyosin flow and apical cell constriction immediately after wounding. J. Cell Biol. *202*, 365–379.

Arruda, S.E., and Dolph, P.J. (2003). Molecular cloning of the pawn locus from Drosophila melanogaster. Gene *310*, 169–173.

Bainbridge, S.P., and Bownes, M. (1981). Staging the metamorphosis of Drosophila melanogaster. J. Embryol. Exp. Morphol. *66*, 57–80.

Bartolák-Suki, E., Imsirovic, J., Nishibori, Y., Krishnan, R., and Suki, B. (2017). Regulation of mitochondrial structure and dynamics by the cytoskeleton and mechanical factors. Int. J. Mol. Sci. *18*, 7–11.

Bement, W.M., and Capco, D.G. (1991). Analysis of inducible contractile rings suggests a role for protein kinase C in embryonic cytokinesis and wound healing. Cell Motil. Cytoskeleton *20*, 145–157.

Bement, W.M., Forscher, P., and Mooseker, M.S. (1993). A novel cytoskeletal structure involved in purse string wound closure and cell polarity maintenance. J. Cell Biol. *121*, 565–578.

Bement, W.M., Mandato, C.A., and Kirsch, M.N. (1999). Wound-induced assembly and closure of an actomyosin purse string in Xenopus oocytes. Curr. Biol. *9*, 579–587.

Berridge, M.J., Lipp, P., and Bootman, M.D. (2000). The versatility and universality of calcium signalling. Nat. Rev. Mol. Cell Biol. *1*, 11–21.

Berridge, M.J., Bootman, M.D., and Roderick, H.L. (2003). Calcium: Calcium signalling: dynamics, homeostasis and remodelling. Nat. Rev. Mol. Cell Biol. *4*, 517–529.

Bittinger, M., McWhinnie, E., Meltzer, J., Iourgenko, V., Latario, B., Liu, X., Chen, C.H., Song, C., Garza, D., and Labow, M. (2004). Activation of cAMP Response Element-Mediated Gene Expression by Regulated Nuclear Transport of TORC Proteins Mark. Curr. Biol. *14*, 2156–2161.

Boldogh, I.R., and Pon, L.A. (2006). Interactions of mitochondria with the actin cytoskeleton. Biochim. Biophys. Acta - Mol. Cell Res. *1763*, 450–462.

Brand, A.H., and Perrimon, N. (1993). Targeted gene expression as a means of altering cell fates and generating dominant phenotypes. Development *118*, 401–415.

Bray, S.J., and Kafatos, F. (1991). Developmental function of Elf-1: an essential transcription factor during embryogenesis in Drosophila. Genes Dev. *5*, 1672–1683.

Brini, M., Calì, T., Ottolini, D., and Carafoli, E. (2014). Neuronal calcium signaling: Function and dysfunction. Cell. Mol. Life Sci. *71*, 2787–2814.

Caddy, J., Wilanowski, T., Darido, C., Dworkin, S., Ting, S.B., Zhao, Q., Rank, G., Auden, A., Srivastava, S., Papenfuss, T. a, et al. (2010). Epidermal wound repair is regulated by the planar cell polarity signaling pathway. Dev. Cell *19*, 138–147.

Calleja, M., Moreno, E., Pelaz, S., and Morata, G. (1996). Visualization of gene expression in living adult Drosophila. Science *274*, 252–255.

Cheng, X., Zhang, X., Yu, L., and Xu, H. (2015). Calcium signaling in membrane repair. Semin. Cell Dev. Biol. *45*, 24–31.

Clapham, D.E. (2007). Calcium Signaling. Cell *131*, 1047–1058.

Cordeiro, J. V, and Jacinto, A. (2013). The role of transcription-independent damage signals in the initiation of epithelial wound healing. Nat. Rev. Mol. Cell Biol. *14*, 249–262.

Crabtree, G.R. (2001). Calcium, Calcineurin, and the Control of Transcription. J. Biol. Chem. *276*, 2313–2316.

Dieckgraefe, B.K., and Weems, D.M. (1999). Epithelial injury induces Egr-1 and Fos expression by a pathway involving protein kinase C and ERK. Am. J. Physiol. Gastrointest. Liver Physiol. *276*, 322–330.

Dietzl, G., Chen, D., Schnorrer, F., Su, K.-C., Barinova, Y., Fellner, M., Gasser, B., Kinsey, K., Oppel, S., Scheiblauer, S., et al. (2007). A genome-wide transgenic RNAi library for conditional gene inactivation in Drosophila. Nature *448*, 151–156.

Eberl, D.F., Ren, D., Feng, G., Lorenz, L.J., Van Vactor, D., and Hall, L.M. (1998). Genetic and developmental characterization of Dmca1D, a calcium channel alpha1 subunit gene in Drosophila melanogaster. Genetics *148*, 1159–1169.

Elias, M.C., Pronovost, S.M., Cahill, K.J., Beckerle, M.C., Kadrmas, J.L., Alatortsev, V.E., Kramerova, I.A., Frolov, M. V., Lavrov, S.A., Westphal, E.D., et al. (2012). A crucial role for Ras suppressor-1 (RSU-1) revealed when PINCH and ILK binding is disrupted. J. Cell Sci. *125*, 3185–3194.

Faas, G.C., Raghavachari, S., Lisman, J.E., and Mody, I. (2011). Calmodulin as a direct detector of Ca2+ signals. Nat. Neurosci. *14*, 301–304.

Fernandes, I., Chanut-Delalande, H., Ferrer, P., Latapie, Y., Waltzer, L., Affolter, M., Payre, F., and Plaza, S. (2010). Zona pellucida domain proteins remodel the apical compartment for localized cell shape changes. Dev. Cell *18*, 64–76.

Fernandez, R., Takahashi, F., Liu, Z., Steward, R., Stein, D., and Stanley, E.R. (2000). The Drosophila Shark tyrosine kinase is required for embryonic dorsal closure. Genes Dev. *14*, 604–614.

Fonteriz, R., Matesanz-Isabel, J., Arias-del-Val, J., Alvarez-Illera, P., Montero, M., and Alvarez, J. (2016). Modulation of Calcium Entry by Mitochondria. In Calcium Entry Pathways in Non-Excitable Cells., J. Rosado, ed. (Springer International Publishing), pp. 405–421.

Fox, D.T., and Peifer, M. (2007). Abelson kinase (Abl) and RhoGEF2 regulate actin organization during cell constriction in Drosophila. Development *134*, 567–578.

Friedrich, P., Tompa, P., and Farkas, A. (2004). The calpain-system of Drosophila melanogaster: Coming of age. BioEssays *26*, 1088–1096.

Fyrberg, C., Ketchum, A., Ball, E., and Fyrberg, E. (1998). Characterization of Lethal Drosophila melanogaster alpha-Actinin Mutants. Biochem. Genet. *36*, 299–310.

Garcia-Fernandez, B., Campos, I., Geiger, J., Santos, A.C., and Jacinto, A. (2009). Epithelial resealing. Int. J. Dev. Biol. *53*, 1549–1556.

Geiger, J. a, Carvalho, L., Campos, I., Santos, A.C., and Jacinto, A. (2011). Hole-in-one mutant phenotypes link EGFR/ERK signaling to epithelial tissue repair in Drosophila. PLoS One *6*, e28349.

Gerke, V., Creutz, C.E., and Moss, S.E. (2005). Annexins: linking Ca2+ signalling to membrane dynamics. Nat. Rev. Mol. Cell Biol. *6*, 449–461.

Ha, E.-M., Oh, C.-T., Bae, Y.S., and Lee, W.-J. (2005). A Direct Role for Dual Oxidase in Drosophila Gut Immunity. Science *310*, 847–850.

Hunter, M. V., Lee, D.M., Harris, T.J.C., and Fernandez-Gonzalez, R. (2015). Polarized E-cadherin endocytosis directs actomyosin remodeling during embryonic wound repair. J. Cell Biol. *210*, 801–816.

Jiang, D., Zhao, L., and Clapham, D.E. (2009). Genome-Wide RNAi Screen Identifies Letm1 as a Mitochondrial Ca2+/H+ Antiporter. Science *326*, 144–147.

Jin, H., Tan, S., Hermanowski, J., Böhm, S., Pacheco, S., McCauley, J.M., Greener, M.J., Hinits, Y., Hughes, S.M., Sharpe, P.T., et al. (2007). The dystrotelin, dystrophin and dystrobrevin superfamily: new paralogues and old isoforms. BMC Genomics *8*, 19.

Juarez, M.T., Patterson, R. a, Sandoval-Guillen, E., and McGinnis, W. (2011). Duox, Flotillin-2, and Src42A are required to activate or delimit the spread of the transcriptional response to epidermal wounds in Drosophila. PLoS Genet. *7*, e1002424.

Kajimoto, H., Hashimoto, K., Bonnet, S.N., Haromy, A., Harry, G., Moudgil, R., Nakanishi, T., Rebeyka, I., Thébaud, B., Michelakis, E.D., et al. (2007). Oxygen activates the rho/rho-kinase pathway and induces RhoB and ROCK-1 expression in human and rabbit ductus arteriosus by increasing mitochondria-derived reactive oxygen species: A newly recognized mechanism for sustaining ductal constriction. Circulation *115*, 1777–1788.

Kemler, R., Ozawa, M., and Ringwald, M. (1989). Calcium-dependent cell adhesion molecules. Curr. Opin. Cell Biol. *1*, 892–897.

Kim, M., and McGinnis, W. (2011). Phosphorylation of Grainy head by ERK is essential for wound-dependent regeneration but not for development of an epidermal barrier. Proc. Natl. Acad. Sci. U. S. A. *108*, 650–655.

Kim, S.A., Tai, C.-Y., Mok, L.-P., Mosser, E.A., and Schuman, E.M. (2011). Calcium-dependent dynamics of cadherin interactions at cell-cell junctions. Proc. Natl. Acad. Sci. *108*, 9857–9862.

Ko, K.S., Arora, P.D., Bhide, V., Chen, A., and McCulloch, C.A. (2001). Cell-cell adhesion in human fibroblasts requires calcium signaling. J. Cell Sci. *114*, 1155–1167.

Koch, G.L. (1990). The endoplasmic reticulum and calcium storage. Bioessays *12*, 527–531.

Köppen, M., Fernández, B.G., Carvalho, L., Jacinto, A., and Heisenberg, C.-P. (2006). Coordinated cell-shape changes control epithelial movement in zebrafish and Drosophila. Development *133*, 2671–2681.

Kwon, E.J., Park, H.S., Kim, Y.S., Oh, E.J., Nishida, Y., Matsukage, A., Yoo, M.A., and Yamaguchi, M. (2000). Transcriptional regulation of the Drosophila raf proto-oncogene by drosophila STAT during development and in immune response. J. Biol. Chem. *275*, 19824–19830.

Lee, S.B. (2003). blistery encodes Drosophila tensin protein and interacts with integrin and the JNK signaling pathway during wing development. Development *130*, 4001–4010.

Littler, D.R., Harrop, S.J., Brown, L.J., Pankhurst, G.J., Mynott, A. V., Luciani, P., Mandyam, R.A., Mazzanti, M., Tanda, S., Berryman, M.A., et al. (2008). Comparison of vertebrate and invertebrate CLIC proteins: The crystal structures of Caenorhabditis elegans EXC-4 and Drosophila melanogaster DmCLIC. Proteins Struct. Funct. Genet. *71*, 364–378.

Lutas, A., Wahlmark, C.J., Acharjee, S., and Kawasaki, F. (2012). Genetic analysis in Drosophila reveals a role for the mitochondrial protein p32 in synaptic transmission. G3 (Bethesda). *2*, 59–69.

Mace, K.A., Pearson, J.C., and McGinnis, W. (2005). An epidermal barrier wound repair pathway in Drosophila is mediated by grainy head. Science *308*, 381–385.

Machacek, M., Hodgson, L., Welch, C., Elliott, H., Pertz, O., Nalbant, P., Abell, A., Johnson, G.L., Hahn, K.M., and Danuser, G. (2009). Coordination of Rho GTPase activities during cell protrusion. Nature *461*, 99–103.

Mankidy, R., Hastings, J., and Thackeray, J.R. (2003). Distinct phospholipase Ca2+-dependent signaling pathways in the Drosophila eye

and wing are revealed by a new small wing allele. Genetics *164*, 553–563.

McNeil, P.L., and Kirchhausen, T. (2005). An emergency response team for membrane repair. Nat. Rev. Mol. Cell Biol. *6*, 499–505.

Michalak, M., Corbett, E.F., Mesaeli, N., Nakamura, K., and Opas, M. (1999). Calreticulin: one protein, one gene, many functions. Biochem. J. *344 Pt 2*, 281–292.

Millard, T.H., and Martin, P. (2008). Dynamic analysis of filopodial interactions during the zippering phase of Drosophila dorsal closure. Development *135*, 621–626.

Moussian, B., Schwarz, H., Bartoszewski, S., and Nüsslein-Volhard, C. (2005). Involvement of chitin in exoskeleton morphogenesis in Drosophila melanogaster. J. Morphol. *264*, 117–130.

Narciso, C., Wu, Q., Brodskiy, P., Garston, G., Baker, R., Fletcher, A., and Zartman, J. (2015). Patterning of wound-induced intercellular Ca 2+ flashes in a developing epithelium. Phys. Biol. *12*, 56005.

Niethammer, P., Grabher, C., Look, A.T., and Mitchison, T.J. (2009). A tissue-scale gradient of hydrogen peroxide mediates rapid wound detection in zebrafish. Nature *459*, 996–999.

Paupe, V., and Prudent, J. (2017). New insights into the role of mitochondrial calcium homeostasis in cell migration. Biochem. Biophys. Res. Commun. *in press.*

Pearson, J.C., Juarez, M.T., Kim, M., Drivenes, Ø., and McGinnis, W. (2009). Multiple transcription factor codes activate epidermal wound-response genes in Drosophila. Proc. Natl. Acad. Sci. U. S. A. *106*, 2224–2229.

Philip, P., Boija, A., Vaid, R., Churcher, A.M., Meyers, D.J., Cole, P.A., Mannervik, M., and Stenberg, P. (2015). CBP binding outside of promoters and enhancers in Drosophila melanogaster. Epigenetics Chromatin *8*, 48.

Prudent, J., Popgeorgiev, N., Gadet, R., Deygas, M., Rimokh, R., and Gillet, G. (2016). Mitochondrial Ca2+ uptake controls actin cytoskeleton dynamics during cell migration. Sci. Rep. *6*, 36570.

Razzell, W., Evans, I.R., Martin, P., and Wood, W. (2013). Calcium Flashes Orchestrate the Wound Inflammatory Response through DUOX Activation and Hydrogen Peroxide Release. Curr. Biol. *23*, 424–429.

Ritsick, D.R., Edens, W.A., Finnerty, V., and Lambeth, J.D. (2007). Nox regulation of smooth muscle contraction. Free Radic. Biol. Med. *43*, 31–38.

Rizzuto, R., De Stefani, D., Raffaello, A., and Mammucari, C. (2012). Mitochondria as sensors and regulators of calcium signalling. Nat. Rev. Mol. Cell Biol. *13*, 566–578.

Roper, K., Gregory, S.L., and Brown, N.H. (2002). The "Spectraplakins": cytoskeletal giants with characteristics of both spectrin and plakin families. J. Cell Sci. *115*, 4215–4225.

Schindelin, J., Arganda-Carreras, I., Frise, E., Kaynig, V., Longair, M., Pietzsch, T., Preibisch, S., Rueden, C., Saalfeld, S., Schmid, B., et al. (2012). Fiji: an open-source platform for biological-image analysis. Nat. Methods *9*, 676–682.

Shcherbata, H.R., Yatsenko, A.S., Patterson, L., Sood, V.D., Nudel, U., Yaffe, D., Baker, D., and Ruohola-Baker, H. (2007). Dissecting muscle and neuronal disorders in a Drosophila model of muscular dystrophy. EMBO J. *26*, 481–493.

Shilo, B.-Z. (2005). Regulating the dynamics of EGF receptor signaling in space and time. Development *132*, 4017–4027.

Simon, M.A., Drees, B., Kornberg, T., and Bishopts, J.M. (1985). The Nucleotide Sequence and the Tissue-Specific Expression of Drosophila c-src. *42*, 831–840.

Sonoda, J., and Wharton, R.P. (2001). Drosophila Brain Tumor is a

translational repressor Drosophila. Genes Dev. *15*, 762–773.

Steinhardt, R.A., Bi, G., and Alderton, J.M. (1994). Cell Membrane Resealing by a Vesicular Mechanism Similar to Neurotransmitter Release Author (s): Richard A . Steinhardt , Guoqiang Bi and Janet M . Alderton Published by : American Association for the Advancement of Science Stable URL : http://www.jstor. Science (80-.). *263*, 390–393.

Sullivan, K.M.C., and Rubin, G.M. (2002). The Ca2+-calmodulin-activated protein phosphatase calcineurin negatively regulates Egf receptor signaling in Drosophila development. Genetics *161*, 183–193.

Sung, Y.J., Sung, Z., Ho, C.L., Lin, M. Te, Wang, J.S., Yang, S.C., Chen, Y.J., and Lin, C.H. (2003). Intercellular calcium waves mediate preferential cell growth toward the wound edge in polarized hepatic cells. Exp. Cell Res. *287*, 209–218.

Szent-Györgyi, A.G. (1975). Calcium regulation of muscle contraction. Biophys. J. *15*, 707–723.

Takahashi, F., Endo, S., Kojima, T., and Saigo, K. (1996). Regulation of cell-cell contacts in developing Drosophila eyes by Dsrc41, a new, close relative of vertebrate c-src. Genes Dev. *10*, 1645–1656.

Tian, L., Hires, S.A., Mao, T., Huber, D., Chiappe, M.E., Chalasani, S.H., Petreanu, L., Akerboom, J., McKinney, S.A., Schreiter, E.R., et al. (2009). Imaging neural activity in worms, flies and mice with improved GCaMP calcium indicators. Nat. Methods *6*, 875–881.

Ting, S.B., Caddy, J., Wilanowski, T., Auden, A., Cunningham, J.M., Elias, P.M., Holleran, W.M., and Jane, S.M. (2005). The Epidermis of Grhl3-Null Mice Displays Altered Lipid Processing and Cellular Hyperproliferation Stephen. Organogenesis *2*, 33–35.

Tjota, M., Lee, S.-K., Wu, J., Williams, J. a, Khanna, M.R., and Thomas, G.H. (2011). Annexin B9 binds to β(H)-spectrin and is required for

multivesicular body function in Drosophila. J. Cell Sci. *124*, 2914–2926.

Tsai, F., Kuo, G., Chang, S., and Tsai, P. (2015). Ca 2 + Signaling in Cytoskeletal Reorganization, Cell Migration, and Cancer Metastasis. Biomed Res. Int. *2015*, 409245.

Tsarouhas, V., Yao, L., and Samakovlis, C. (2014). Src kinases and ERK activate distinct responses to Stitcher receptor tyrosine kinase signaling during wound healing in Drosophila. J. Cell Sci. *127*, 1829–1839.

Wang, S., and Samakovlis, C. (2012). Grainy head and its target genes in epithelial morphogenesis and wound healing. In Current Topics in Developmental Biology, S. Plaza, and F. Payre, eds. (Amsterdam: Elsevier Inc.), pp. 35–63.

Wang, S., Tsarouhas, V., Xylourgidis, N., Sabri, N., Tiklová, K., Nautiyal, N., Gallio, M., and Samakovlis, C. (2009). The tyrosine kinase Stitcher activates Grainy head and epidermal wound healing in Drosophila. Nat. Cell Biol. *11*, 890–895.

Wilkin, M.B., Becker, M.N., Mulvey, D., Phan, I., Chao, A., Cooper, K., Chung, H., Campbell, I.D., Baron, M., Macintyre, R., et al. (2000). Drosophila Dumpy is a gigantic extracellular protein required to maintain tension at epidermal – cuticle attachment sites. Curr. Biol. *10*, 559–567.

Williams, G.S.B., Boyman, L., Chikando, A.C., Khairallah, R.J., and Lederer, W.J. (2013). Mitochondrial calcium uptake. Proc. Natl. Acad. Sci. *110*, 10479–10486.

Wood, W., Jacinto, A., Grose, R., Woolner, S., Gale, J., Wilson, C., and Martin, P. (2002). Wound healing recapitulates morphogenesis in Drosophila embryos. Nat. Cell Biol. *4*, 907–912.

Woodham, E.F., and Machesky, L.M. (2014). Polarised cell migration: Intrinsic and extrinsic drivers. Curr. Opin. Cell Biol. *30*, 25–32.

Xu, S., and Chisholm, A.D. (2011). A Gα(q)-Ca(2+) Signaling Pathway

Promotes Actin-Mediated Epidermal Wound Closure in C. elegans. Curr. Biol. *21*, 1960–1967.

Xu, S., and Chisholm, A.D. (2014). C. elegans Epidermal Wounding Induces a Mitochondrial ROS Burst that Promotes Wound Repair. Dev. Cell *31*, 48–60.

Yamamoto-Hino, M., and Goto, S. (2013). In Vivo RNAi-based screens: Studies in model organisms. Genes (Basel). *4*, 646–665.

Yao, L., Wang, S., Orzechowski-Westholm, J., Dai, Q., Matsuda, R., Hosono, C., Bray, S., Lai, E.C., and Samakovlis, C. (2017). Genome-wide identification of Grainy head targets in Drosophila reveals regulatory interactions with the POU-domain transcription factor, Vvl. Development *144*, 3145–3155.

Yoo, S.K., Freisinger, C.M., Lebert, D.C., and Huttenlocher, A. (2012). Early redox, Src family kinase, and calcium signaling integrate wound responses and tissue regeneration in zebrafish. J. Cell Biol. *199*, 225–234.

7. Acknowledgements

I would like to thank Christos Samakovlis and Liqun Yao for sharing unpublished data; Lara Carvalho and Anabela Bensimon-Brito for helpful discussions; TRiP at Harvard Medical School (NIH/NIGMS R01-GM084947), VDRC and NIG for providing transgenic RNAi fly stocks used in this study and the Bloomington Stock Center for other *Drosophila* lines.

8. Supplementary Data

8.1 Video Legends

Video S1. Two-phase dynamics of intracellular calcium signalling upon wounding. Wild type notum epithelium expressing UAS-GCaMP3, labelling intracellular calcium, under the control of *pnr*-GAL4 driver. Images were acquired using a spinning disk imaging system (Revolution XD; Andor Technology). Frames were taken every 50 ms. Scale bar: 20 μm.

Video S2. Intracellular and mitochondrial calcium dynamics upon wounding. Wild type notum epithelia expressing UAS-GCaMP3, labelling intracellular calcium, shown on the left, and UAS-mito-GCaMP3, labelling mitochondrial calcium, shown on the right, under the control of *pnr*-GAL4 driver. Images were acquired using a spinning disk imaging system (Revolution XD; Andor Technology). Frames were taken every 10 secs. Scale bar: 20 μm.

Video S3. Intracellular calcium dynamics in wild type and Grh KD. Notum epithelia expressing UAS-GCaMP3, shown on the left, and together with UAS-*grh*-RNAi, shown on the right, labelling intracellular under the control of pnr-GAL4 driver. Images were acquired using a spinning disk imaging system (Revolution XD; Andor Technology). Frames were taken every 10 secs. Scale bar: 20 μm.

Video S4. Intracellular calcium and F-actin dynamics in AnxB9, CG10126 and pwn KD. Notum epithelia expressing UAS-GCaMP3 (upper panels), labelling intracellular calcium, or UAS-mCherry::Moesin (lower panels), labelling F-actin, together with UAS-*AnxB9*-RNAi, shown on the left, or together with UAS-*CG10126*-RNAi, show in the middle, or together with UAS-*pwn*-RNAi, shown on the right, under the control of pnr-GAL4 driver. Images were acquired using a spinning disk imaging system (Revolution XD; Andor Technology). Frames were taken every 10 secs. Scale bar: 20 μm.

CHAPTER IV

GRAINYHEAD-LIKE GENES IN ZEBRAFISH DEVELOPMENT AND WOUND HEALING:

Diving into the vertebrate world

"*Just keep swimming. Just keep swimming. Just keep swimming, swimming, swimming. What do we do? We swim, swim.*"

Dory,
in *Finding Nemo*

Contents

The author of this thesis performed most of the experiments. Analysis of *grainyhead-like* genes during development was done in collaboration with Ana Sofia Brandão and Anabela Bensimon-Brito. Ana Farinho performed the sample cuts for cryosections preparation. Data analysis was done by the author of this thesis together with Ana Sofia Brandão and Anabela Bensimon-Brito.

1. Summary

The ability to maintain a well-controlled epithelial barrier is fundamental for an organism to survive, a function imperative to all species from invertebrates to vertebrates. The *grainy head* gene family is already linked to both epithelial permeability regulation and to the establishment of cell polarity. This is achieved mainly through the regulation of expression of different adhesion molecules, like Adherens and Occluding Junctions. In vertebrates, this family is represented by up to four genes. Here, we characterize the expression patterns of *grainyhead-like* (*grhl*) genes during Zebrafish development, to understand the spatial and temporal distribution of the different transcription factors included in this family.

Moreover, using laser-based tissue wounding, live imaging and knockdown via morpholino technology, we studied the role of *grhl* genes during the repair of vertebrate simple epithelia. For this, we focused on repair of the surface epithelium of the zebrafish embryo, Enveloping Layer (EVL), the first epithelium formed during development. We show that *grhl* genes are important for proper stability of the tissue upon wounding. Their knockdown leads to a delay of the wound healing process, which can be related to deregulation of cytoskeletal and junctional components. Our observations strengthen the importance of the *grainy head* gene family in regulating epithelial maintenance in homeostatic and repair conditions.

1.1 Keywords

Zebrafish, *grainyhead-like*, embryogenesis, repair, epithelial junctions.

2. Introduction

Epithelia are the principal physical barriers protecting living organisms and their organs from the surrounding environment (Moussian and Uv, 2005). The maintenance of epithelial tissues requires robust response that can ensure their integrity in a variety of biological situations (Guillot and Lecuit, 2013). The regulation of this process and maintenance of the organism barrier has been linked to a tight regulation of intercellular junctions, namely Adherens Junctions (AJs) and Occluding Junctions. These are responsible for the assembly of a ion- and size-selective barrier, crucial for the physical separation of organs and communication between them (Niessen, 2007). Occluding Junctions are a type of structure that includes invertebrate Septate Junctions (SJs) and vertebrate Tight Junctions (TJs). Both are key components in forming a diffusion barrier that prevents exchange of water and solutes between adjacent cells (Furuse and Tsukita, 2006). Two groups of proteins are involved in the TJ complex: transmembrane proteins, which bridge the intercellular space and create a paracellular seal (e.g. Claudins and Occludin) and peripheral proteins, which assemble at the cytoplasmic surface of the junctional site and serve as a scaffold for the link between membrane and cytoskeleton (e.g. ZOs and Par-3) (Bauer et al., 2011). Drosophila homologues of vertebrate Claudins localize to SJs, being also required for SJ formation and function (Furuse and Tsukita, 2006). On the other hand, SJs and TJs show significant differences in their structure and cellular localization: TJs localize apically to the adherens junctions, whereas SJs are basal and contain proteins that are not found in TJs, such as the adhesion molecule Neurexin-IV and the FERM domain protein Coracle (Furuse and Tsukita, 2006).

One of the gene family commonly associated with TJ/SJ regulation is the *grainy head* (*grh*) family. Grh proteins are predominantly expressed in ectoderm-derived epithelia during early development, and are widely

conserved during evolution. In addition, these proteins are known to be involved in development and maturation of epithelia, in maintaining epidermal barrier integrity, organogenesis and wound repair (Paré et al., 2012; Traylor-Knowles et al., 2010; Wang and Samakovlis, 2012). Firstly discovered in *Drosophila* (Bray et al., 1989; Moussian and Uv, 2005; Wang and Samakovlis, 2012), *grh* is involved the regulation of SJ components (Narasimha et al., 2008) and maintenance of the paracellular permeability barrier (Hemphälä et al., 2003; Narasimha et al., 2008; Wang and Samakovlis, 2012). Moreover, it is shown to be important for the activation of wound response genes during epithelial repair (Geiger et al., 2011; Kim and McGinnis, 2011). The vertebrate homologues of the *Drosophila grh,* the *grainyhead-like* (*grhl)* genes, share a certain degree of conservation at sequence and function level (Moussian and Uv, 2005; Paré et al., 2012; Wang and Samakovlis, 2012). In mammalians, there are three *grhl* genes – *grhl1*, *grhl2* and *grhl3*. Mammalian *grhl1* and *grhl2* have been shown to be linked to the regulation of expression of different junctional components like desmosomal cadherin (Wilanowski et al., 2008) or *claudin-4* (*cldn-4*) and *e-cadherin* (*e-cad*), important components of TJs and AJs, respectively (Werth et al., 2010). Mice lacking *grhl3* have compromised skin barrier function and deficient wound repair, presenting defects in keratin cross-linking (Ting et al., 2005; Boglev et al., 2011). These results point to the conserved role of *grhl* in the regulation of cellular junctional complexes and epithelial maintenance. *grhl* genes have been shown to have cooperative roles and overlapping expression patterns during several processes of development opening a possibility for redundancy in some of the processes in which they are involved. However, they can also have specific target genes during different stages of the organism development (Ting et al., 2003; Rifat et al., 2010; Boglev et al., 2011).

Zebrafish (*Danio rerio*) is a widely used model organism, suitable for the study of multiple processes of vertebrate development. During the first

stages of development, the Zebrafish embryo is composed of a yolk cell and two cell types (blastoderm): the embryonic enveloping cell layer (EVL) and the deep cells (DCs). While the DCs give rise to all three germ layers of the embryo and consequent adult organism, the EVL, the first tissue being formed in the embryo, will later define the most outer layer of the embryonic, larval and adult epidermis (periderm). The EVL, a simple squamous epithelium, constitutes the epidermis, along with the basal layer. Zebrafish early development relies on tightly orchestrated morphogenetic movements. Just three hours post fertilization (hpf), the EVL spreads over the DCs and yolk, with its cells becoming progressively thinner and longer until they engulf the whole embryo in the vegetal pole, closing the epithelial gap, in a movement called epiboly (Solnica-Krezel, 2006). Moreover, simple epithelial tissues have an extraordinary capacity to close small discontinuities rapidly and efficiently through a resealing mechanism to prevent disruption of the permeability barrier, without leaving any scar tissue. This process seems to be conserved across species and involves the assembly of a contractile actomyosin purse-string, which is fundamental for proper tissue repair (Antunes et al., 2013; Bement et al., 1993; Carvalho et al., 2014; Garcia-Fernandez et al., 2009; Köppen et al., 2006; Mateus et al., 2012; Wood et al., 2002).

In Zebrafish, the *grhl* gene family is represented by four different genes: *grhl1, grhl2a*, *grhl2b* and *grhl3* (Wang and Samakovlis, 2012). Studies regarding functions of these genes are sparse, focusing on *in situ* hybridization for characterization of expression patterns and function analysis through morpholino knockdown technology (Heasman, 2002). Regarding *grhl1*, this gene has been shown to be important for the specification of epidermal cell lineages and differentiation of specific cells, the ionocytes (important for active ion transport and osmoregulation), during the maturation of the epidermal tissue (Janicke et al., 2010). Furthermore, *grhl1* and *grhl3* seem to have cooperative functions in periderm

differentiation (de la Garza et al., 2012). Grhl2b has been shown to be involved in otic development through the regulation of the adhesion molecules Epcam and Claudin B in the apical junctional complexes, leading to abnormal otic epithelial cells. This defect correlates with a single nucleotide polymorphism found in the human *GRHL-2* gene associated with age-related hearing loss. Interestingly, human GRHL-2 expression seems to be sufficient to rescue the phenotype in Zebrafish otic epithelial cells (Han et al., 2011; Wang and Samakovlis, 2012). This points to a possible functional conservation between species. In addition, *grhl2b* has been linked to maintenance and folding of the Midbrain-Hindbrain Boundary (MHB), where its loss leads loss of MHB markers and apoptosis (Dworkin et al., 2012). Although these studies show possible conserved functions for each of these genes, it is still important to understand their expression pattern in Zebrafish epithelial development. The EVL, as an extremely amenable tissue to live imaging, is a perfect candidate to address the importance of the *grhl* genes, not only in the formation and maturation of vertebrate epithelial tissues during development, but also in the epithelial repair process. For this, we characterized the expression pattern of the different *grhl* genes present in the first stages of Zebrafish development and its importance in wound healing of simple epithelial sheets in the vertebrate context.

3. Materials and Methods

3.1 Ethics Statement

All experiments involving animals were approved by the Animal User and Ethical Committees at Instituto Medicina Molecular (IMM), Instituto Gulbenkian Ciência (IGC) and Centro de Estudos de Doenças Crónicas (CEDOC), according to European Union directives and Portuguese law (Directive 2010/63/EU and Decreto-Lei 113/2013).

3.2 Zebrafish lines and maintenance

All Zebrafish lines used were maintained in a re-circulating system with a 14/10 hours light/dark cycle at 28°C. Embryos were obtained from crosses between wild type (AB strain), *Tg(ßactin:mgfp)* (Cooper et al., 2005), here referred as *ras:GFP*, *Tg(col2a1aBAC:mcherry)* (Hammond and Schulte-Merker, 2009), here referred as *col2:mCherry*, Tg(*2.2shh:gfp:ABC#15*) (Shkumatava et al., 2004), here referred as *shh:GFP*, and *Tg(SAGFF(LF)53A:gfp)* (Zebrafish Gene Trap and Enhancer Trap Database, Kawakami Lab), here referred as *SAGFF53A:GFP.* Mating pairs were put together overnight in crossing boxes. Embryos were collected the following day and kept in E3 embryo medium at 28ºC during the experimental procedure in order to follow specific developmental stages.

3.3 Immunofluorescence

Immunofluorescence protocol performed as follows (adapted from Neugebauer et al., 2009): Zebrafish wild type (AB strain), *shh:GFP* and *SAGFF53A:GFP* embryos were collected at different developmental stages during embryogenesis (50%-60% epiboly, 24hpf and 48hpf) for characterization of *grhl* genes expression; wild type (AB strain) for characterization of *grhl* morpholino oligonucleotides (MOs) (Heasman, 2002) injected embryos; and *ras:GFP* embryos (24hpf) for ERK activation assay upon wounding. Embryos were dechorionated either manually with forceps or through the incubation (5-10 minutes) in a solution of 1mg/ml pronase protease from *Streptomyces griseus* (Calbiochem) diluted in E3 embryo medium, followed by several washes with E3 embryo medium. For all experiments, embryos were fixed at 4ºC overnight (ON) in 2% or 4% paraformaldehyde solution prepared in phosphate-buffered saline (PBS), depending if dechorionation was done prior or posterior to fixation. In the following day, embryos were transferred to 100% Methanol (MeOH) (Merck) and stored at -20ºC, ON or until used. Subsequently, embryos were gradually rehydrated in series of MeOH/PBS, followed by several washes in a PBT solution (0.1% Triton X-100 in PBS) and washed once in PBS. Embryos were then incubated for 7 minutes in acetone at -20ºC, washed in a PBDX solution (0.1% Triton- X100, 1% DMSO (Sigma) and 1% Bovine Serum Albumin (BSA; Sigma) in PBS diluted in MiliQ water) during 20 minutes and incubated for 4 hours (h) in a blocking solution (1% goat serum in PBDX) at room temperature. Embryos were then incubated ON with the primary antibodies diluted in blocking solution at 4ºC. For this, several dilutions were tested. The optimal dilutions of the antibodies seem to be dependent, mainly, on the developmental stage analysed. After ON incubation, embryos were washed several times from 2h-4h in PBDX solution and incubated ON with secondary antibodies and/or with phalloidin

(1:200, conjugated with Alexa Fluor 488 or 594, Invitrogen) diluted in blocking solution, at 4ºC. Embryos were then washed for 20 minutes in PBT 0.3% (0.3% Triton in PBS), followed by 30 minutes wash in PBS. Embryos were then incubated in a 4',6-Diamidino-2-Phenylindole (DAPI, Sigma) solution (1 µm/ml, diluted in PBS) for 15 minutes for nuclei labelling (Kapuscinski, 1995). After this final incubation, embryos were washed during 2h in PBS and mounted in mounting medium (80% Glycerol, 2% DABCO (Sigma) diluted in PBS). Immunofluorescence was also performed in cryosections of wild type embryos. Axial sections were cut at 12µm using a Microm cryostat and maintained at -20°C. The sections were thawed 15 minutes at room temperature, washed twice in PBS at 37°C for 10 minutes and washed once in 0.1M glycine (Sigma) in PBS for 10 minutes. Sections were then incubated in acetone as previously described and followed the same protocol. DAKO Fluorescent Mounting Media (Agilent) was used to prepare samples for imaging. In embryos/cryosections labelled with phalloidin, no MeOH transfer was done, proceeding to the following steps of the protocol. All antibodies and dilutions used in this study are stated in Table I.

Table I. List of antibodies. Primary and secondary antibodies used in this study, with respective host organism, dilution and company which they were acquired from. *Different dilutions used with cryosections, whole mount epiboly and whole mount 24-48hpf, respectively. **Antigen sequence available at company website.

Antibody	Host	Dilution	Company
Anti-Grhl1** (SAB2100971)	Rabbit	1:100/1:500/1:1000*	Sigma
Anti-Grhl2** (HPA004820)	Rabbit	1:100/1:500/1:1000*	Sigma
Anti-Grhl3** (AV39489)	Rabbit	1:100/1:500/1:1000*	Sigma
Anti-E-Cadherin	Mouse	1:200	BD Transduction

			Labs
Anti-Col2	Mouse	1:200	DSHC
Anti-pERK1/2	Rabbit	1:100	Cell Signaling
Anti-ZO1	Mouse	1:100	Invitrogen
Anti-Clnd1	Rabbit	1:200	Invitrogen
Anti-GFP	Rabbit	1:100	Invitrogen
Alexa 488 anti-rabbit	Goat	1:500	Invitrogen
Alexa 488 anti-mouse	Goat	1:500	Invitrogen
Alexa 568 anti-rabbit	Goat	1:500	Invitrogen
Alexa 568 anti-mouse	Goat	1:500	Invitrogen
Alexa 633 anti-mouse	Goat	1:500	Invitrogen

3.4 Image acquisition and analysis

Imaging of immunolabelled samples was performed using a confocal laser-scanning microscope (LSM710; Carl Zeiss), through a Pan-NeoFluar 10x (N.A. 0.3; Zeiss) and a C-Apochromat 40x water (N.A. 1.2; Zeiss) objectives. Images were analysed using Fiji (ImageJ NIH) (Schindelin et al., 2012). All stills shown are maximum intensity z-stack projections, except when noted.

3.5 Fluorescence-activated cell sorting (FACS)

To specifically isolate notochord cells, we used the *col2:mcherry* transgenic line. *col2:mcherry* embryos were dechorionated and allowed to develop until 24hpf in E3 embryo medium at 28ºC. Embryos were then sacrificed and dissociated by maceration and manual pipetting in PBS supplemented with 0.1% liberase (Roche). Samples were kept at 28ºC for 30 minutes, with

constant mixing. Cell suspension was filtered through a Partec CellTrics 30µm filter (Sysmex) and centrifuged for 5 minutes at 300*g*, at 4ºC. Posteriorly, 10% fetal bovine serum (FBS) diluted in PBS was added to the cells. Cells were sorted in a MoFlo high speed cell sorter (Beckman Coulter, Fort Collins, USA) equipped with a 488 nm laser (200 mW air-cooled Sapphire, Coherent) for scatter measurements and a 561 nm laser (50 mW DPSS, CrystaLaser) for mCherry excitation. mCherry was detected using a 630/75 nm bandpass emission filter. To separate cells according to mCherry expression non-labeled wild type AB embryos at the same developing stage were used as a negative control. Gating strategy was chosen with a maximum of stringency to avoid cross contamination between positive and negative populations. The instrument was run at a constant pressure of 207 kPa (30 psi) with a 100 µm nozzle and frequency of drop formation of approximately 40 kHz. Positive fluorescent cells were selected and collect directly into RTL buffer (RNeasy micro Kit, Qiagen) and stored at -80ªC for RNA extraction. Four independent cell sorting collections were done, each varying between 12 500 and 30 000 cells collected.

3.6 Total RNA isolation and quantitative realtime PCR (qPCR)

For the analysis of *grhl* genes expression during early development, wild type (AB strain) embryos were collected at several developmental stages (6, 12, 24, 48 and 72 hpf) and dechorionated with pronase treatment previously described. RNA extraction was performed with Trizol reagent (Invitrogen) followed by DnaseI (Roche) treatment according to the manufacturer's protocol. Total RNA (1 µg) was reverse-transcribed using the 1st Strand cDNA Synthesis Kit for PCR (Roche). Quantitative real-time PCR (qPCR) was performed by using the Fast Green Master Mix (Roche) and the Roche LightCycler 480 system. Program conditions were as follows: 15 minutes at

95°C followed by 55 amplification cycles, each cycle for 30 seconds at 95°C and 15 seconds at 68°C. Normalization of gene expression value was done regarding the *elongation factor 1α* (*ef1α*) housekeeping gene expression levels and the fold change was calculated through the ΔΔCT method (Livak and Schmittgen, 2001). Three biological replicates and two technical replicates were analysed for each condition. Primers were the following:

ef1α Fwd -5′- ACGCCCTCCTGGCTTTCACCC -3′;

ef1α Rev -5′- TGGGACGAAGGCAACACTGGC -3′;

grhl1 Fwd -5′- CGACAAGGGTGCCGAGC -3′;

grhl1 Rev -5′- GAGCGGCACCTTGACATCTG -3′;

grhl2a Fwd -5′- GCCTACTACGCCTGCGGCT -3′;

grhl2a Rev-5′- CCTTGTTGGCCCCGGTCT -3′;

grhl2b Fwd -5′- GCGGCAAAAGCAGGGC -3′;

grhl2b Rev -5′- GTGCTGGCGGGAGTGC -3′;

grhl3 Fwd -5′- GCTGTGGCCTGGTACCCC -3′;

grhl3 Rev -5′- GCGGGGTTGTTTGCATGG -3′.

Results were analysed in GraphPad Prism software using two-tailed, non-parametric unpaired Mann-Whitney tests.

To analyse the expression of *grhl2a* and *grhl2b* in Col2 positive cells, previously sorted cells were thawed at room temperature and RNA extraction was performed with the RNeasy micro Kit (Qiagen) following the manufacturer's protocol. Total RNA (50ng) was reverse transcribed and qPCR analysis performed using the protocols described above. Used primers are also stated above.

3.7 Microinjection of Zebrafish embryos

Wild type one-cell stage embryos (AB strain) were injected with 50 pg of Utrophin-GFP mRNA for fluorescent labelling of F-actin as previously described (Barth and Wilson, 1995). For mRNA synthesis, the vector pcs2-utrophin-GFP (Burkel et al., 2007) was linearized with the restriction enzyme NotI (Fermentas). Transcription was achieved using the SP6 mMESSAGE mMACHINE High Yield Capped RNA Transcription Kit (Ambion). Microinjection was performed using a PV-820 Pico-injector (World Precision Instruments) and a Narashige micromanipulator. In addition to Utrophin-GFP mRNA, the following MOs were also injected for each knockdown experimental condition: grhl2bATGBlock-MO (5'-TCT TAC TGT CTG TCT CCT GTG ACAT-3'); grhl3ATGBlock-MO (5'-TGA GAC CCT CAA TCT CCT TGG TCAT-3'); standard negative control-MO (5'- CCT CTT ACC TCA GTT ACA ATT TATA -3').

3.8 Live imaging

Live imaging was performed in dechorionated wild type (AB strain) embryos undergoing epiboly (50%-60% epiboly stage), previously injected with Utrophin-GFP mRNA and control / *grhl2b* / *grhl3* MOs. Embryos were mounted in silicon rings filled with 1% low melting agarose (Sigma) diluted in E3 embryo medium. Live imaging was performed using a Nikon/Andor Revolution spinning disk system with an EMCCD Camera (iXon 897; Andor Technology) at 28ºC, using the iQ software (Andor Technology). Z-stacks were acquired with a Plan Fluor 40x oil objective (N.A. 1.30; Nikon) every 10 seconds.

3.9 Wound healing assay

Wounding assay for posterior tissue fixation was performed through UV laser ablation in a Zeiss 5 Live confocal microscope (W Plan-Apochromat 20x water dipping objective: N.A. 1.00) or through mechanical wounding (using a tungsten needle under a stereoscope).

Wounding assay performed during live imaging experiments was performed 1-3 minutes after the beginning of each movie, using a MicroPoint (Andor Technology) UV nitrogen-pumped dye laser (435 nm).

3.10 Statistical and sequence analysis

Statistical analysis was performed using Prism (GraphPad Software). Error bars in graphs correspond to the standard deviation. Sequence analysis and alignments were done on CLC Sequence Viewer 7 (Qiagen), using peptide sequences from Ensembl: Grhl1 - ENSDARP00000124180; Grhl2a - ENSDARP00000125051; Grhl2b - ENSDARP00000124302; Grhl3 - ENSDARP00000097661 (Gap open cost 10 and Gap extension cost 1).

4. Results

4.1 Characterization of *grainyhead-like* genes during Zebrafish early development

The formation and maturation of the first protective barrier in Zebrafish embryos coincides with the start of epiboly. The EVL proceeds to cover the whole embryo and yolk, creating a thin permeability layer that will then develop into the larval epidermis. Until 72 hpf, the epidermis is formed by two layers of epithelial tissues: a more basal layer and an outer superficial layer, called peridermis. The latter is of extreme importance for the structural integrity of the organism, as well as for the control of permeability in the aqueous environment (Fukazawa et al., 2010). In order to characterize the expression pattern of *grhl* genes during early development, we started by quantifying the mRNA levels for all four *grhl* genes during the first 72 hpf in order to understand the variations during the formation and maturation of the epithelium (Fig.1). We decided to compare all values against 6hpf, which corresponds to the time point described for maternal-to-zygotic transition (MZT), when the embryo activates transcription of the genes necessary for its development, and not relying solely on maternal contribution (Langley et al., 2014). From this point on, we observed a reduction in the transcript levels in all *grhl* genes, except *grhl2b,* which showed a slight variation at 24hpf but then stabilized until 72 hpf. *grhl1* although decreased compared to 6hpf levels, showed a slight increase the following stages as well as *grhl2a*. In contrast, *grhl3* seems to show a slight but steady decreased along these early stages.

These results suggest an early requirement for most *grhl* genes and a potential involvement of grhl2b with later developmental processes.

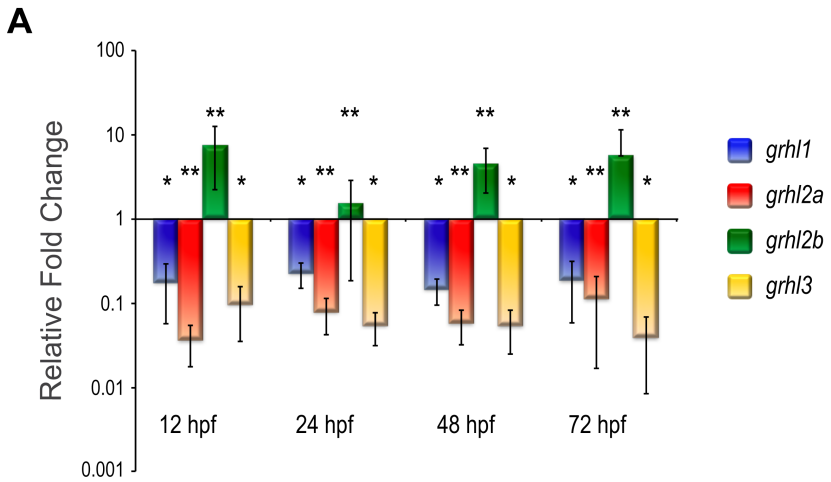

Figure 1. Relative expression levels of different *grhl* transcripts during embryonic and larval development. qPCR quantification of *grhl* mRNA levels in wild type (AB strain) embryos and larvae, at different hours post fertilization, relative to each *grhl* mRNA levels at 6 hpf. All *grhl* genes have an early peak of expression (6 hpf), opposing to *grhl2b,* which is transcriptionally upregulated from 12 hpf onwards. *P value<0.05; **P value<0.005; two tailed, non-parametric unpaired Mann-Whitney test. Error bars represent standard deviation.

In order to understand the protein dynamics at a cellular level, we decided to analyse the localization all Grhl TFs by immunofluorescence in embryos during epiboly, 24 hpf and 48 hpf. This complements previous published studies focusing on mRNA expression pattern analysis during embryonic development for each *grhl* gene, through *in situ* hybridization (Dworkin et al., 2012; Janicke et al., 2010; de la Garza et al., 2012). We made use of commercially available antibodies, already tested in cell culture or mice. Although the sequences are not similar between species, there is a high degree of conservation between *grhl* genes. By analysing the antigen sequence for each antibody (Supplementary Data – Sequence alignment), we decided to test them in Zebrafish, keeping in mind that there is only one Grhl2 in mammals, while in Zebrafish there is a duplicated form. The

alignment analysis seems to show a higher similarity with Grhl2b (Fig. S3), which also is concordant with what is known for the encoding sequence of the *GRHL2* and both *grhl2* Zebrafish genes (Dworkin et al., 2012). Furthermore, based on our sequence alignment analysis, the Grhl3 antibody might be also recognizing Grhl1 (Fig. S5). For the purpose of this study we will now consider Grhl2 for both Grhl2a and Grhl2b, regarding protein localization assessment.

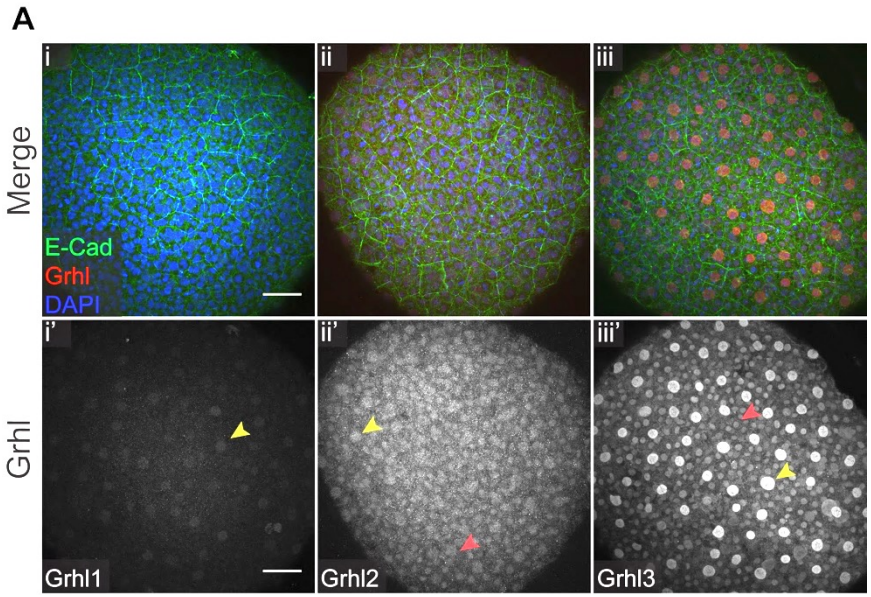

Figure 2. Grhl protein localization during epiboly. Representative immunofluorescence images with anti-Grhl1/2/3 antibodies in wild type embryos during epiboly (6-8hpf) (Ai'-iii'). Cell membranes are labelled with anti-E-Cad and the nuclei with DAPI (Ai-iii). All Grhl proteins can be detected during epiboly in the EVL nuclei (yellow arrowheads), although at different intensity levels. Grhl2 and 3 are also present in the Deep Cells (DC) (red arrowheads). Scale bars: 40μm. n = 3-4 embryos per condition.

During epiboly, all Grhl are present in the embryo, with Grhl1 being localized to the EVL, while both Grhl2 and Grhl3 are also present in the Deep Cells (Fig. 2) These results are consistent with mRNA expression data already

published (de la Garza et al., 2012). EVL nuclei are in the most superficial layer of cells and are bigger then the DCs nuclei, which makes them easily distinguishable. Grhl3 seems to have increased levels compared to the other Grhl proteins (Fig. 2Aiii'), in line with results already published that show more *grhl3* expression at this developmental stage (de la Garza et al., 2012).

At 24hpf, Grhl1 intensity levels seems to increase, comparing to epiboly levels (Fig. 3 and Fig. 2Ai'), with a localization pattern restricted to the peridermis nuclei (Fig. 3Aii,ii'). This is also supported by our previous qPCR results (Fig. 1), where we observe an increase in transcript levels between 12 and 24hpf.

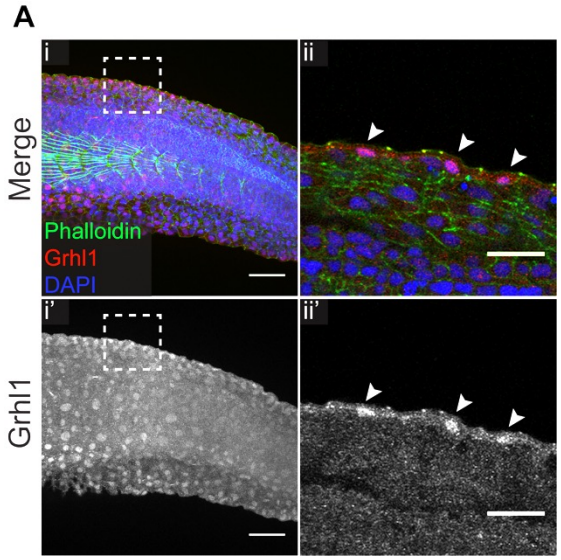

Figure 3. Grhl1 protein localization in the epidermis at 24hpf. Representative immunofluorescence images with anti-Grhl1 (Ai') in 24hpf wild type embryos, also labelled with DAPI and Phalloidin, for F-actin visualization (Ai-iii). Insets of the regions in dashed square lines, show a single image in the z plane. Arrowheads point to nuclei labelled with DAPI and Grhl1 (Aii,Aii'), in the peridermis. Grhl1 seems to be restricted to these cells, with its levels increasing relative to epiboly (compare to Figure 2Ai'). Scale bars: 40μm and 5μm in insets. n = 3-4 embryos per condition.

Regarding Grhl2 (a or b), the expression pattern at 24hpf is rather surprising. Although we did not observe Grhl2 at the epidermal level, we

identified a very specific pattern at the notochord level (Fig. 4). Three cell populations can be morphologically distinguished: a single line with more cuboidal shape nuclei (dashed arrows in Fig. 4) on top of a tubular structure identified as the notochord (arrowheads in Fig. 4); very long and squeezed nuclei within the notochord; and another line of linearly positioned nuclei below the notochord (arrows in Fig. 4), but in this case more elongated in the anterior-posterior axis (Fig. 4A). In order to clearly identify the different cell types, we took advantage of the *shh* reporter line (Blagden et al., 1997) and the enhancer trap line *SAGFF53A* (Figure 4B), which are expressed in the notochord, floor plate and hypochord. Immunostainings in embryos from these lines allowed us to confirm that Grhl2 protein can be detected in the nuclei of the floor plate cells (dashed arrow in Fig. 4Ai', 4Bi',ii'), in the notochord cells (arrow head in Fig. 4Ai', 4Bi',ii') and in the hypochord cells (arrow in Fig. 4Ai', 4Bi',ii'). Their characteristic position and morphology can be observed either in longitudinal or sagittal views of the larvae (Fig. 4A-C).

The notochord originates from the embryonic shield (Oppenheimer, 1936), a mesodermal-derived originated organ, formed in the initial stages of gastrulation. The notochord is known to endure high hydrostatic pressure and to share many components common to epithelia (Stemple 2005). It is formed by two types of cells: large vacuolated cells called chordocytes, and an epithelial cell sheath of cells called chordoblasts, that can later differentiate into chordocytes (Tong et al., 2013). Grhl2 is localized in the nucleus of both these cell types. Another set of cells positive for Grhl2 are situated on top of the notochord named the floor plate cells. These cells are organized along the anterior-posterior axis, positioned at the ventral midline of the neural tube, where they have important functions in the establishment of the neuronal network (Placzek and Briscoe, 2005). The last population of Grhl2-positive cells are the hypochord cells. The hypochord also originates from mesodermal cells, forming a chain of cells below the latter referred

structure. This structure is important for the development and positioning of the dorsal aorta (Eriksson and Löfberg, 2000).

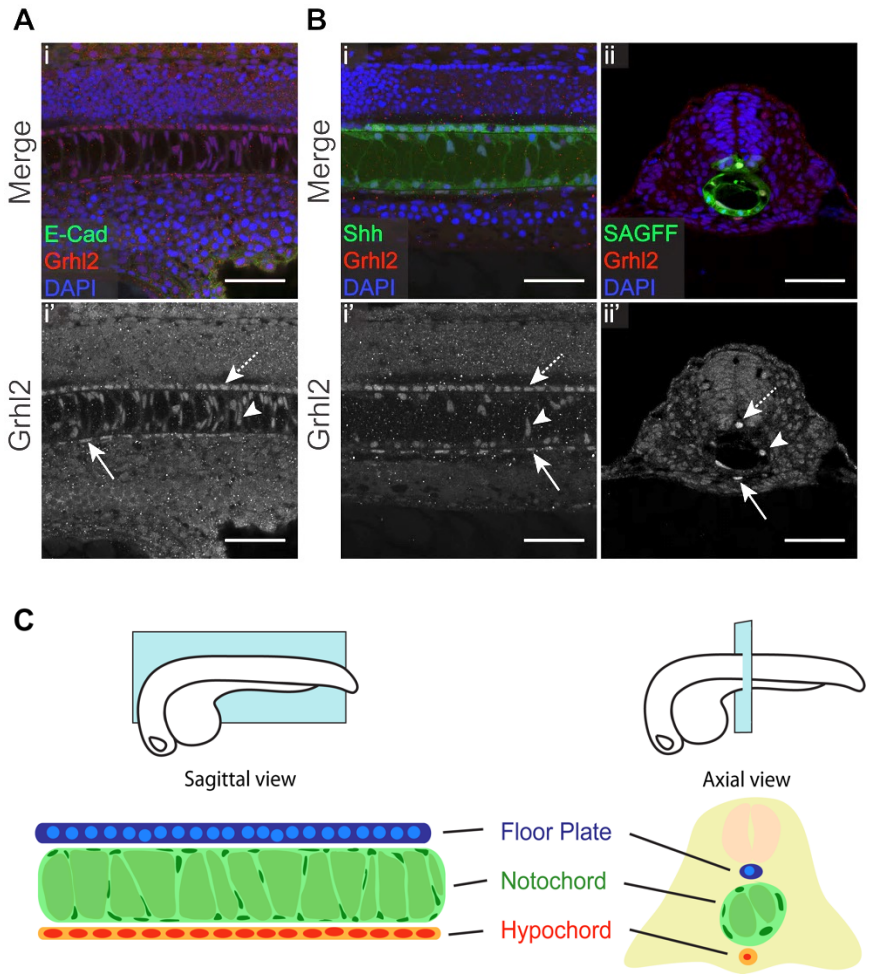

Figure 4. Grhl2 protein localization at 24hpf is restricted to the notochord. (**A**) Representative immunofluorescence images with anti-Grhl2 (Ai') in 24 hpf wild type larvae, also labelled with DAPI and anti-E-Cad (Ai-i'). (**B**) Representative immunofluorescence images with anti-Grhl2 in *shh*:GFP larvae (Bi') and *SAGFF53A:GFP* 24hpf larvae in sagittal and axial sections, respectively (Bii'), also labelled with DAPI and anti-GFP (Bi-i'). *shh:GFP* and *SAGFF53A:GFP* are expressed in the notochord, floor plate and hypochord (Bi-ii). Arrows and arrowheads point to nuclei co-labelled with DAPI and Grhl2 (Ai'; Bi'-ii') in the floor plate (dashed arrow), the notochord cells (arrowhead) and the hypochord (arrow) (Ai'; Bi'-ii'). All images represent a single image in the z plane. Scale bars: 40μm. n = 3-4 embryos per

condition. (**C**) Schematic representation of the floor plate, notochord and hypochord in sagittal and axial views, identified in the immunolabelled images in A and B.

Grhl3 is restricted to the peridermis at 24hpf just as Grhl1, although intensity levels seem to be lower (Fig. 5 and Fig. 1). These results are supported by our mRNA quantifications (Fig. 1). The co-localization of Grhl1 and Grhl3 suggests that they may be working together in the establishment of the peridermis. This is in accordance with published results, showing that Grhl1 and Grhl3 have a conserved role in the formation and maintenance of the permeability barrier and outer epithelium across species (de la Garza et al., 2012; Ting et al., 2005).

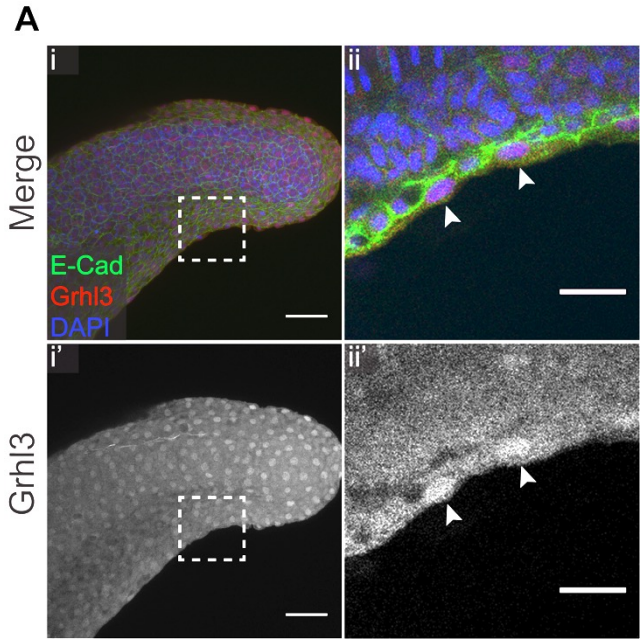

Figure 5. Grhl3 protein localization in the epidermis at 24hpf. Representative immunofluorescence images with anti-Grhl3 (Ai') in 24 hpf wild type embryos, also labelled with DAPI and anti-E-Cad (Ai-iii). Insets of the regions in dashed square lines, show a single image in the z plane. Arrowheads point to nuclei co-labelled with DAPI and Grhl3 (Aii,ii') in the peridermis. Scale bars: 40μm and 5μm in insets. n = 3-4 embryos per condition.

The pattern of expression of all Grhl remains the same at 48hpf, although Grhl1 seems to slightly increase and Grhl2 and Grhl3 seem to decrease (Fig. 6). Although this is not visible in our qPCR results (Fig. 1), we have to

reinforce the fact that this protein localization analysis is a qualitative assessment which may not demonstrate the full expression of the Grhl proteins due to protein stability.

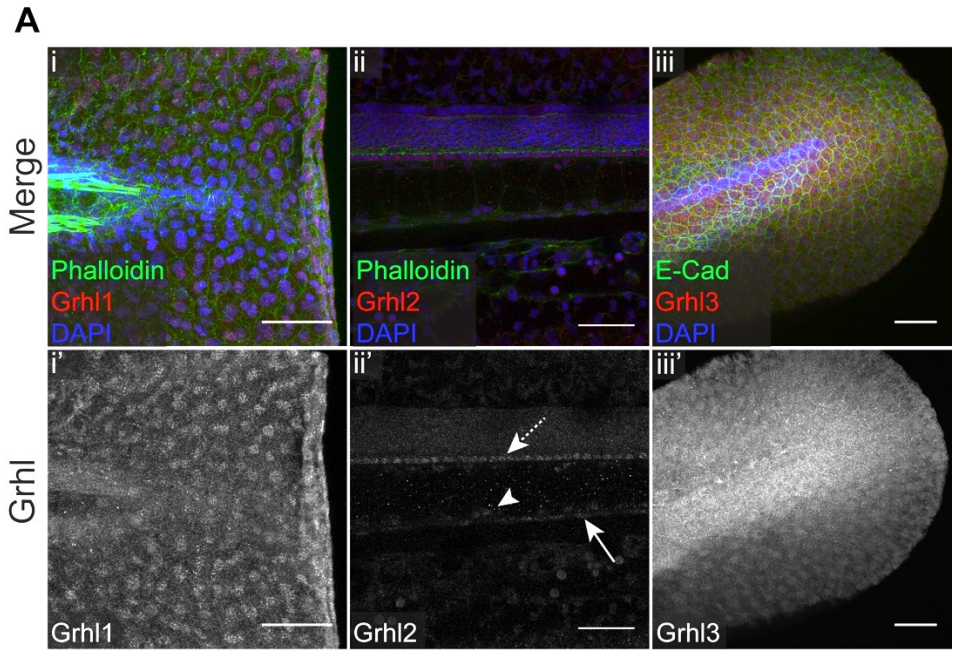

Figure 6. Grhl protein localization at 48hpf. Representative immunofluorescence images with anti-Grhl1/2/3 (Ai',ii',iii') in 48 hpf wild type larvae, also labelled with DAPI and Phalloidin, for F-actin visualization or anti-E-Cad (Ai-iii), for epidermal cell membrane. Grhl1 and Grhl3 localize to the periderm as at 24 hpf. Grhl2 remains in the notochord, but at lower levels (compare to Figure 4Ai'). Arrows and arrowhead point to nuclei labelled with Grhl2 (Aii') in the floor plate (dashed arrow), the notochord cells (arrowhead) and the hypochord (arrow). Images Grhl1 and 3 represent maximum intensity projections and for Grhl2 represent a single image in the z plane. Scale bars: 40μm and 5μm in insets. n = 3-4 embryos per condition.

Due to the impossibility of distinguishing between the two Grhl2 Zebrafish proteins through immunofluorescence, we decided to address *grhl2a* and

grhl2b transcript levels in one of the specific set of cells in which we observed Grhl2 localization, the chordocytes. For that, we made use of the *col2:mCherry* transgenic fish, labelling *collagen2a* expressing cells in the notochord, more specifically the chordocytes (Hammond and Schulte-Merker, 2009). In order to allow extraction of mRNA from this subset of cells, we isolated them through FACS. Unfortunately, the amount of extracted mRNA was not sufficient to detect expression for both genes.

Overall, our observations show a common localization pattern for each Grhl, strengthening their role in the formation and maturation of the Zebrafish epidermis. Additionally, we bring new evidences that support an unknown function for Grhl2 in the formation and maturation of non-ectodermal derived tissues, such as the notochord, floor plate and hypochord.

4.2 Junctional components are affected by *grhl* knockdown during EVL formation

Due to Grhl restricted pattern of expression and from what is already known regarding epithelial development and the *grhl* gene family, we decided to knockdown (KD) the expression of two of the *grhl* genes to analyse their importance in the formation and development of the EVL. Since *grhl1* showed a diminished expression at the first stages of development, more specifically during epiboly, we decided to focus in *grhl2b*, due to its higher similarity with the mammalian *GRHL2*, and *grhl3*. We knockdown both genes through MOs injection at one-cell stage embryos. Both morpholinos targeted the ATG site. We initially injected 2ng and 4ng of both MOs to achieve an efficient knockdown for both genes. However, embryos were highly affected when injected with 4ng, thus we carried our experiments with 2ng injections. The *grhl2b* MO had been previously described (Dworkin et al., 2012), to induce a specific phenotype of the midbrain-hindbrain

boundary, unrelated to EVL formation or development. Since *grhl* genes are frequently described to alter the expression of junctional components (Boglev et al., 2011; Narasimha et al., 2008; Ting et al., 2005; Wang and Samakovlis, 2012; Werth et al., 2010), we started by analysing the presence and localization of three different junctional proteins and actin. For that we performed immunofluorescence in embryos during epiboly and observed the distribution of these proteins (Fig. 7). In *grhl2b* MO injected embryos, development is not delayed when compared with embryos injected with control MO. Additionally, F-actin levels do not seem to be affected, with the formation of the characteristic actin cable at the EVL leading edge (Fig 7Ai'',ii''). However, E-Cad seems to be highly reduced in these morphants (Fig. 7Aii'). In *grhl3* morphants, E-Cad is present but F-actin seems slightly reduced (Fig. 7Aiii,iii',iii''). Regarding ZO-1 and Cldn1, TJ components, both are present in *grhl2b* morphants, with Cldn1 levels being more intense compared to the control embryos (Fig. 7B).

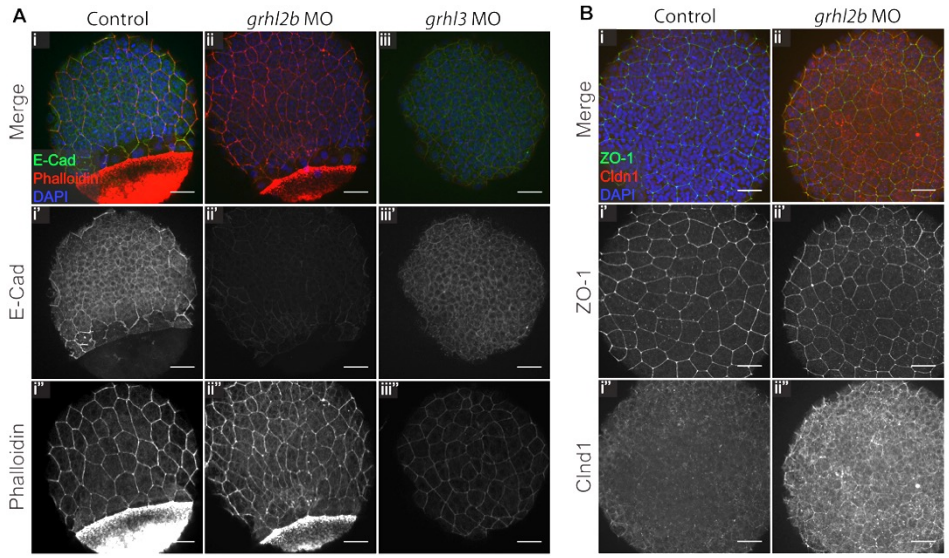

Figure 7. Junctional components in *grhl2b and grhl3* morphants during epiboly. (**A**) Representative immunofluorescence images of anti-E-Cad (Ai'-iii') with DAPI and Phalloidin

(Ai''-iii''), for F-actin visualization, in wild type embryos injected with 2ng standard control MO (Ai,i',i'') and with 2ng of *grhl2* (Aii,ii',ii'') or *grhl3* (Aiii,iii',iii'') MOs. Grhl2b KD seems to lead to E-Cad depletion, while Grhl3 KD shows a decrease in F-actin levels. (**B**) Representative immunofluorescence images with anti-ZO1 (Bi'-ii') and anti-Cldn1 (Bi''-ii'') with DAPI in wild type embryos injected with 2ng standard control MO (Bi,i',i'') and embryos injected with 2ng of *grhl2* MO (Bii,ii',ii''). While ZO-1 levels do not seem to suffer any perturbation in Grhl2b KD, Cldn1 seems increased when compared with the control experiment. Scale bars: 40μm. n = 3-4 embryos per condition.

These results suggest a conserved role for the regulation of junctional component expression by the *grhl* gene family.

4.3 Wound healing during Zebrafish Epiboly

The study of EVL formation and development also requires looking at its capability of to repair discontinuities. As mentioned before, simple squamous epithelia are able to close wounds quickly and in a scar-free manner (Antunes et al., 2013; Wood et al., 2002). It has also been shown that Zebrafish fin fold regeneration includes a first stage of wound closure through the formation of an actomyosin contractile cable (Mateus et al., 2012), as described in *Drosophila*. The regeneration process entails more complex processes and different levels of regulation, regarding different cell populations. In the case of the Zebrafish embryo epithelium, the EVL, no regeneration occurs during laser ablation, with its repair relying solely on the contractile purse string closure of the actomyosin cable. To analyse the wound repair process in the newly formed EVL, we used a same setup already used in our lab to induce wounds in the *Drosophila* epithelia. One-cell stage embryos were injected with Utrophin-GFP mRNA, to track F-actin dynamics, mounted in agarose, to allow epiboly to proceed while imaging,

and then wounded and imaged in high-speed resolution (Fig. 8Ai-iv' and Video S1). In this vertebrate system wound repair resembles nicely his invertebrate counterpart (Fig. 8), with the formation of the actin cable at the wound leading edge (Fig. 8Aiii,iii'). The difference relies on the time frame between the two systems: while the *Drosophila* epithelium (embryonic or pupal) take around 2,5 hours to close the wound, in the Zebrafish embryo the process takes only 15 minutes (Fig. 8Aiv,iv'). This can be due to the lower number of cells affected upon wounding, since the cell size is bigger in the vertebrate system, but it can also be linked to adaptive evolution since in the aqueous environment, the permeability barrier is of the upmost importance. In the case of cytoskeletal dynamics, Zebrafish EVL repair is more related to *Drosophila* embryonic repair (Wood et al., 2002) since we cannot distinguish an actin polymerization wave, like the one on the *Drosophila* pupal repair process (Antunes et al., 2013). An added value of this assay is the size of the cells at the leading edge that make this assay perfect to observe processes at the sub cellular level, with a clear resolution in the apical area of each cell.

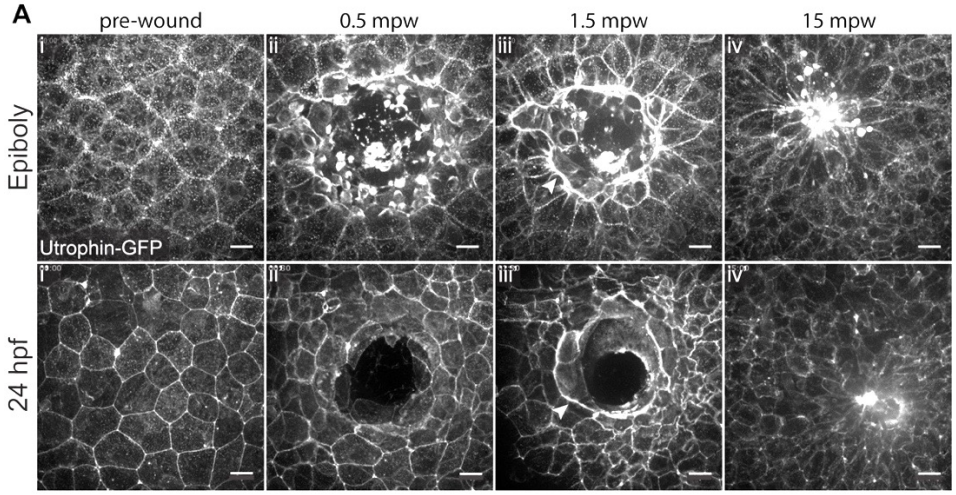

Figure 8. Actin dynamics during wound closure in Zebrafish embryos. Movie stills of the wound closure process during epiboly (Ai-iv) and at 24hpf (Ai'-iv'), in the EVL. Wild type

embryos were injected with 50pg Utrophin-GFP mRNA, to allow the visualization of F-actin dynamics. During epiboly, wound was induced in the animal pole, while at 24hpf the wound was targeted in the yolk sac of each animal. In both developmental stages, an actin cable (arrowheads) is quickly formed at the leading edge of the wound (Aiii,iii') and the wound is fully closed at 15 minutes post wounding (Aiv,iv') (Video S1). Scale bar: 20 μm. n = 4 embryos per condition.

Wounding the EVL above the yolk sac at 24hpf, results in the same closure dynamics (Fig. 8Ai'-iv' and Video S1), with a slight increase in speed that can result from the absence of the DCs below possibly dragging the tissue and increasing the friction between the cell layers.

The establishment of this new assay will facilitate the live imaging analysis of cellular machinery and dynamics during vertebrate wound healing.

4.4 Grhl are important for proper regulation of the epithelial repair process

As the *Drosophila grh* was shown to be important for wound healing and proper epithelial repair, we wanted to address *grhl* genes importance and conservation in the similar vertebrate process. Using our newly established wounding system during Zebrafish epiboly, we decided to wound *grhl2b* and *grhl3* morphant embryos, to analyse their phenotype. We have previously described in Chapter II of this study, how *Drosophila* Grh was regulating pupal epithelium repair, through the proper regulation of epithelial identity markers and their dynamics upon wounding. In that system, we have demonstrated Grh represses E-Cad. In our Zebrafish model, *grhl2b* morphant characterization showed a decrease in this AJ component, pointing to opposite regulatory functions. This has also been shown in mice

(Werth et al., 2010), indicating a relevant difference of regulation between invertebrate and vertebrates. E-Cad is a major player of cell junctions regulation and epithelial stability and in *Drosophila*, the loss of E-Cad upon wounding leads to an impairment in the formation of a proper actin cable at the leading edge (Chapter II of this study). Therefore, we started by wounding *grhl2b* morphants to address their phenotype. In *Drosophila*, the loss of E-Cad upon wounding leads to an impairment in the formation of a proper actin cable at the leading edge of the gap. In *grhl2b* morphants, in which we showed a decrease in intensity levels of E-Cad (Fig. 7Aii'), F-actin levels at the leading edge cable seem lower and the wound closure takes slightly longer (Fig. 9Ai'-iii'), compared to the control (Fig. 9Ai-iii). Regarding *grhl3* morphants, which did not show differences in E-Cad but instead in cortical F-actin, wound closure takes twice as long as the control embryo repair (Fig. 9Ai''-iv''), assembling a faint cable that seems to lack the proper contractile ability to maintain the leading edge cohere and strong enough to propel closure at the desired rate (Video S2).

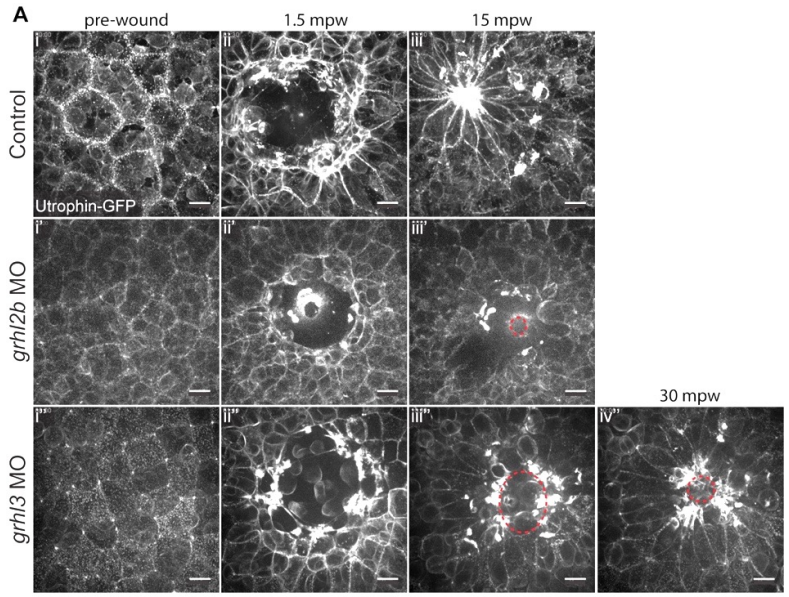

Figure 9. Closure dynamics in *grhl2b* and *grhl3* morphant embryos. (**A**) Movie stills of the wound closure process during epiboly in the EVL over the animal pole of embryos

injected with 50pg Utrophin-GFP mRNA, to allow the visualization of F-actin dynamics (Video S2). Control embryos were additionally injected with 2ng standard control MO (Ai-iii). *grhl2b* (Ai'-iii') and *grhl3* (Ai''-iv'') morphants were also injected with 2ng of each respective MO. Closure in *grhl* KD took longer than control conditions, with the *grhl3* taking double the time to complete full closure. Red dashed lines show wound leading edge. Scale bar: 20 μm. n= 3-4 embryos per condition.

Our observations point to a common cytoskeletal and junctional regulation during wound repair.

Preliminary results with double morphants for these genes lead to closure impairment and structural disintegration of the tissue upon wounding (data not shown), which might indicate a possible redundancy in the *grhl* gene family for specific functions, such as regulation of epithelial repair.

4.5 ERK phosphorylation upon wounding might point to a conserved activation of Grhl during the repair process

Transcription factors can suffer post-translational modifications in order to adjust their activating or repressing function to regulate the transcription of other genes. The *Drosophila* Grh is one of these transcription factors. With over a thousand target genes (Yao et al., 2017), Grh can work as an activator or repressor according to different development stages. Moreover this switch in function can be regulated through Grh phosphorylation by Extracellular signal-regulated Kinase (ERK) (Liaw et al., 1995), which happens in the context of wound healing. Grh phosphorylation is essential for the transcription of wound response genes important for *Drosophila* cuticle repair (Geiger et al., 2011; Kim and McGinnis, 2011; Mace et al., 2005), although it does not seem to be necessary for epidermal barrier

establishment (Kim and McGinnis, 2011). ERK itself is dually phosphorylated upon wounding to activate the MAP Kinase signalling cascade (Dieckgraefe and Weems, 1999; Mace et al., 2005; Wang et al., 2009). Although ERK phosphorylation upon wounding can definitely be a conserved mechanism across species, this has not been shown in Zebrafish. Furthermore, the link between ERK activation and Grh phosphorylation as only been addressed in *Drosophila*. Recently, a study has hypothesized the involvement of Grhl2b in different functions during Midbrain-Hindbrain Boundary patterning as result of a post-translational modification by ERK phosphorylation (Dworkin et al., 2012). Here we show that ERK is phosphorylated quickly upon wounding, both in laser induced wounds or by mechanical puncture of the animal (Fig. 10, arrowheads).

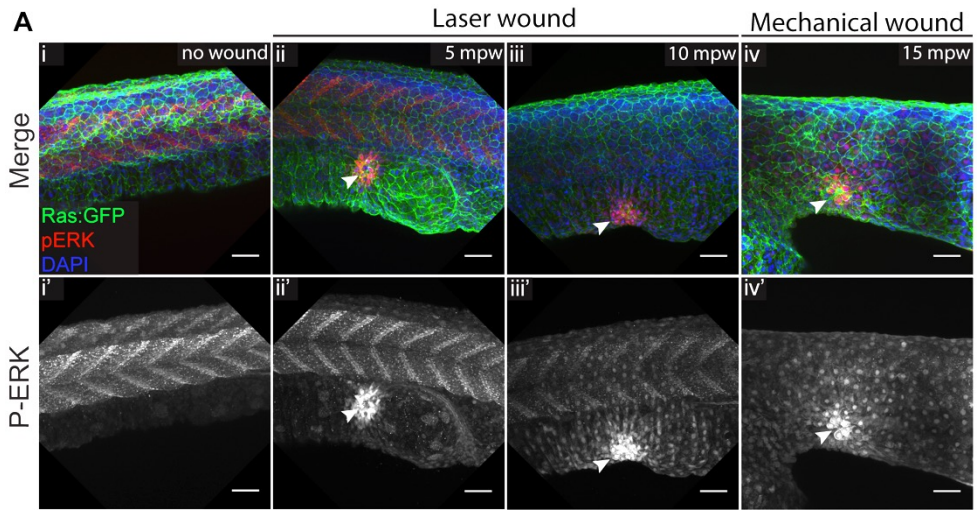

Figure 10. Localization of phospho-ERK1/2 in wounded 24hpf embryos. Representative immunofluorescence images of RAS-GFP embryos labelled with pERK (Ai'-iv'), anti-GFP and DAPI (merge in Ai-iv): not wounded (Ai,i'), 5 (Aii,ii') and 10 (Aiii,iii') minutes post wounding with laser ablation system, and 15 minutes post wounding with mechanical wounding setup (Aiv,iv'). Since mechanical wounds were bigger, they took longer to close, hence the 5 minutes difference from the laser ablation closure time. Wounds were performed in the yolk extension below the trunk of each animal. White arrowheads indicate wound site. Scale bars: 40µm. n = 3-4 embryos per condition.

This analysis was done in 24hpf embryos for two reasons: since the wounding assay was performed in living embryos that would be later collected and fixed for immunostaining, 24 hpf are easier to orient correctly in E3 embryo medium, allowing for a methodical wound approach, either by UV laser ablation with a dipping lens or manual puncture, without the need to embed the animal in agarose; furthermore, manual puncture is more easily attained in more resistant 24 hpf embryos, since embryos during epiboly still display uncovered yolk regions that are extremely sensitive to mechanical pressure. Our data shows a strong and accentuated activation of ERK at the leading edge of the wound. Although the MAP Kinase signalling pathway is involved in other signalling processes in response to stress, these results can suggest a possible regulation of Grhl activity upon wounding, to modulate and refine the immediate necessary functions for Grhl in a stress response condition.

5. Discussion

The importance of Grhl Transcription Factors during epithelial maintenance and repair has been a subject of several studies in invertebrate and vertebrate research. Its roles in junctional component regulation and activation of wound repair related genes have been shown across different species (Kim and McGinnis, 2011; Mace et al., 2005; Ting et al., 2005; Wang and Samakovlis, 2012; Werth et al., 2010). With this study, we aimed at a more comprehensive and thorough characterization of Grhl localization and requirement during development and wound healing in Zebrafish, a key vertebrate model.

5.1 Grhl characterization during Zebrafish development

Our data show that all four *grhl* genes are expressed in the first stages of embryonic and larval development (Fig. 1). Although their expression progressively changes after maternal-to-zygotic transition, all four genes could be detected at 6 hpf, suggesting a role from early developmental stages. Particularly, all genes except *grhl2b*, show a slow and progressive decrease in expression from 6 hpf onward. This might be due to the specific cellular distribution of each gene after blastula stages. Although there are no specific antibodies for Zebrafish Grhl proteins, we proceeded the protein localization assessment using antibodies that recognize its human orthologs, keeping in mind the limitations of these tools. Due to the similarity and conservation between sequences of each *grhl* gene with its human orthologs, we tested whether GRHL1, GRHL2 and GRHL3 antibodies raised against the human protein would recognize the Zebrafish proteins. Regarding GRHL2, since mammalians only have one *GRHL2* gene, we could not distinguish between Zebrafish Grhl2a and 2b. Nevertheless, *GRHL2* shows more similarities with *grhl2b* (Dworkin et al., 2012) and the

antibody epitope seems to be more conserved with this protein sequence (Supplementary Data – Fig. S3), therefore suggesting that we are detecting Grhl2b. Further validation of the antibodies is needed to clarify which of the two proteins is responsible for the localization pattern we observed.

During EVL formation and maturation, spanning from epiboly until 48hpf, Grhl1 and Grhl3 show similar localization patterns, although their intensity levels seem to counterbalance each other. As Grhl1 increases its intensity through time, localizing to the EVL cells in epiboly and the peridermis from 24hpf onward (Figs. 2, 3 and 6), Grhl3 seems to progressively lose intensity from epiboly to the subsequent stages (Figs. 2, 5 and 6). Although our mRNA quantification analysis does not show this relation, this is consistent with published *in situ* hybridization analysis for both genes (Janicke et al., 2010; de la Garza et al., 2012). One difference in their localization pattern regards the DCs during epiboly, where Grhl3 is present but not Grhl1 (Fig. 2). Another caveat of these results is the fact that the immunofluorescence analysis is not a quantitative assay, and these observations need to be complemented with Western Blot analysis in order to analyse quantities of expressed protein. Nonetheless, the restricted and similar localization pattern for both proteins in the early precursors of the ectoderm in embryonic (EVL) and ectoderm-derived tissue (peridermis), may point to a cooperative and/or redundant role in the establishment of the primary epithelial barrier, an important and highly regulated feature in all organisms (Wang and Samakovlis, 2012).

The most surprising and not yet reported result of this study was the localization pattern observed for Grhl2 at 24 and 48 hpf (Figs. 4 and 6). Grhl are considered to be *bona fide* epithelial transcription factors, by regulating genes responsible for epithelial identity and maintenance. They have been described in neuronal cell populations (Almeida and Bray, 2005; Pyrgaki et al., 2011), but in both cases, all *grhl* expressing cells are mostly related to ectoderm-derived tissues (Bray and Kafatos, 1991; Wang and Samakovlis,

2012), although non-ectodermal expression has been shown in mice (Auden et al., 2006). In the Zebrafish developing embryo and larva, Grhl2 appears nuclear localized in three sets of cells: the floor plate, notochord cells and the hypochord (Fig. 4 and 6). With an important structural and patterning function, the notochord is an essential structure in vertebrate development. Its central position according to the dorso-ventral axis is of extreme importance given its role in secreting factors necessary for specifying cell fates or controlling symmetry aspects. Its composition is similar to cartilage and it is the backbone of the skeletal embryonic structure (Stemple, 2005). All three cell types positive for Grhl2 derive from mesodermal cells, and the notochord and floor plate cells specifically derive from the dorsal organizer of the Zebrafish embryo, the embryonic shield (Eriksson and Löfberg, 2000; Oppenheimer, 1936; Placzek and Briscoe, 2005). In fact, Grhl2 was localized to the DCs as well during epiboly, being present in these precursor cells (Fig. 2). The floor plate is described as the key organizer of the Central Nervous System, regulating the specification of neuroepithelial, neuronal and glial cell fates in adjacent tissues by the secretion of specific morphogens (Placzek and Briscoe, 2005). In *Drosophila*, *grh* has been shown to be important in the signalling cascade leading to neuroblast differentiation (Almeida and Bray, 2005). Since we show that Grhl2 is localized in the floor plate cells, this might point to a conserved function in neuronal specification between *Drosophila* and Zebrafish for this gene family. Regarding the notochord, although it is linked with important patterning functions, one of its main characteristics is being associated with a structural role (Stemple, 2005). The localization of Grhl2 in the notochord cells can also be of extreme importance for its maintenance and development, due to the tight barrier regulation that these cells need. The notochord cells progenitor originates from the dorsal organizer and, depending on Notch signalling, will then differentiate in chordocytes or chordoblasts (Yamamoto et al., 2010). The chordocytes are the notochord structural cells that develop big inflated vacuoles within them, in order to

increase the hydrostatic pressure necessary to form a strong although flexible axis for the development and locomotion of the organism (Tong et al., 2013). Around these cells there is a layer of epithelial sheath cells, the chordoblasts, that along with the Extracellular Matrix layer covering the outside of the notochord, the floor plate and the hypochord provide the structural stability necessary to keep the hydrostatic pressure in check (Stemple, 2005; Tong et al., 2013). Problems in vacuole formation and maintenance lead to defective notochord maturation and defective skeletal structures in the adult organism (Ellis et al., 2013). The expression of *grhl2* in these cells might be important for epithelial differentiation cues, to form the fully differentiated notochord cells, and also for the possible regulation of junctional complexes in the formation of the vacuolated cells, which need to be tightly controlled in order to maintain their structural integrity. Lastly, the expression of *grhl2* in the hypochord cells might also be related to its epithelial-like characteristics. The hypochord is transient structure important for the formation and maturation of the dorsal aorta (Eriksson and Löfberg, 2000), possibly providing, as previously referred, structural support for the dorso-ventral axis of the embryo/larva. During its formation, the hypochord cells form a basal lamina characteristic of epithelial cell differentiation, which can lead to the description of the hypochord as an epithelial rod (Löfberg and Collazo, 1997). This differentiation could be due to the expression of *grhl2* in these cells, as it functions as an epidermal differentiation transcription factor. The fact that all these subsets of cells derive from mesodermal tissue is also in line with our data of Grhl2 localization in the DCs during epiboly (Fig. 2), which account for the mesoderm precursors in the embryo gastrula. These preliminary findings open an exciting new field of study for *grhl* genes during the formation of the structural axis of the Zebrafish embryo. Anabela Bensimon-Brito has already generated CRISPR/Cas9 (Hwang et al., 2013; Jinek et al., 2012) mutants for both *grhl2a* and *grhl2b*, that can now be used for the characterization and full description of these genes function in these tissues.

Since our study was focused in simple epithelia formation, and considering our observations regarding the localization of Grhl proteins, we decided to analyse the phenotype of *grhl2b* and *grhl3* knockdown morphants during the first stages of development, focusing on the EVL. Our choice for *grhl2b* was due to its sequence similarity with mammalian *GRHL2*. In order to understand if these genes might be important for the regulation of junctional complexes during epithelial barrier formation, we decided to address AJs and TJs levels and localization in these morphants. Studies in Zebrafish, as well as in cell culture and in other vertebrates, have shown that *grhl* genes are important for specific functions in organ formation, commonly associated with deregulations in junctional components (Han et al., 2011; Senga et al., 2012; Tanimizu and Mitaka, 2013; Wang and Samakovlis, 2012; Wilanowski et al., 2008). Here we show, in accordance with what has been observed in other vertebrate systems, that *grhl2b* might be responsible for the regulation of E-Cad levels during epiboly (Fig. 7). This deregulation might be important in the development of a functional epithelial barrier, required for the defence of this organism against the surrounding environment. Moreover, *grhl3* knockdown seemed to interfere with F-actin levels, also in line with what has been published (Caddy et al., 2010). Since this deregulation does not affect the morphogenetic process and development, we can assume that an increase in the knockdown levels or complete knockout of this gene could render stronger phenotypes, but this would not be viable for our subsequent wound repair study. Despite this, we also need to take into account how a functional compensation by all four *grhl* genes may occur, masking phenotypes and KD effects.

5.2 Grhl are involved in Zebrafish Wound Healing

Our study of epithelial wound healing has focused on simple epithelia which heal in a scar-free manner through the assembly of a contractile cable at the leading edge, allowing a purse-string driven closure (Garcia-Fernandez et al., 2009). The Zebrafish embryo and its simple epithelial layer EVL present the best live imaging approach for the study of cellular dynamics during this process in vertebrates. We set up an assay where cell shape analysis and cytoskeletal dynamics is easily observed upon laser wounding of the epithelium (Fig. 8). Moreover, in Zebrafish, this process is much quicker than in its invertebrate counterpart (Antunes et al., 2013; Wood et al., 2002), with the formation of the actin cable immediately after wounding and gap closure being achieved within 15 minutes in the wild type embryos (Fig. 8). This assay has the potential to be a convenient and reliable tool for vertebrate wound repair studies, since live high resolution imaging is directly attained and genetic expression during the first stages of embryonic development can be easily manipulated. Furthermore, this assay can be also used to address epithelial repair in two-layered stratified epithelium of the larval Zebrafish, as the closure dynamics are similar.

With this setup established, we then analysed the importance of *grhl* genes in wound repair. Although this gene family had already been linked to defects in epithelial repair (Caddy et al., 2010; Ting et al., 2005), our data allows the live *in vivo* analysis of the process and phenotype in the knockdown morphants. Our preliminary data has shown that, despite both morphants showing delay in closure during epiboly, *grhl3* seems to have a stronger phenotype than *grh2b*, leading to two-fold increase in the closure time (Fig. 9). In both cases, we could observe contractile instability at the leading edge, which is probably associated to a misregulation of F-actin. With these results, we propose that *grhl3* has a more prominent role in EVL stability, which is consistent with its protein expression patterns in the EVL cells. On the other hand, *grhl2b* phenotype was milder despite its importance for the regulation of E-Cad, a key component of epithelial

stability during epithelial repair (*shg/e-cad* KD in *Drosophila* epithelial repair leads to defective closure and altered cytoskeletal dynamics – Chapter II of this study). This might point to functional redundancy either in *grhl* regulation of junctions or the junctional components functions in epithelial repair. Another interesting observation made in this study, is that the ERK signalling pathway is activated upon wounding (Fig. 10). Beside this signalling cascade regulating several processes during wound repair, one of the known functions of phosphorylated ERK in *Drosophila* wound healing is the phosphorylation of Grh. This phosphorylation culminates in the activation of other specific wound response genes by Grhl (Kim and McGinnis, 2011). Thus, the observed activation of ERK pathway during Zebrafish wound healing might also modulate Grhl function. This would be an interesting research focus in the future as this possible conserved role of ERK could account for regulatory differences between homeostasis and repair of the EVL. Moreover, it could show Grhl phosphorylation by ERK upon wounding to be another conserved characteristic in the *grh* gene family between vertebrates and invertebrates. More analysis is required to address this modulation.

Taken together, our data suggest that *grhl* genes are involved in epithelial formation and maintenance, even in non-ectodermal derived tissues, uncovering possible new functions in structural maintenance of the organism. Moreover, our preliminary data also indicates a conserved role for *grhl* in wound repair regulation of simple embryonic epithelia.

6. References

Almeida, M.S., and Bray, S.J. (2005). Regulation of post-embryonic neuroblasts by Drosophila Grainyhead. Mech. Dev. *122*, 1282–1293.

Antunes, M., Pereira, T., Cordeiro, J. V., Almeida, L., and Jacinto, A. (2013). Coordinated waves of actomyosin flow and apical cell constriction immediately after wounding. J. Cell Biol. *202*, 365–379.

Auden, A., Caddy, J., Wilanowski, T., Ting, S.B., Cunningham, J.M., and Jane, S.M. (2006). Spatial and temporal expression of the Grainyhead-like transcription factor family during murine development. Gene Expr. Patterns *6*, 964–970.

Bauer, H.C., Traweger, A., Zweimueller-Mayer, J., Lehner, C., Tempfer, H., Krizbai, I., Wilhelm, I., and Bauer, H. (2011). New aspects of the molecular constituents of tissue barriers. J. Neural Transm. *118*, 7–21.

Bement, W.M., Forscher, P., and Mooseker, M.S. (1993). A novel cytoskeletal structure involved in purse string wound closure and cell polarity maintenance. J. Cell Biol. *121*, 565–578.

Blagden, C.S., Currie, P.D., Ingham, P.W., and Hughes, S.M. (1997). Notochord induction of zebrafish slow muscle mediated by Sonic hedgehog. Genes Dev. *11*, 2163–2175.

Boglev, Y., Wilanowski, T., Caddy, J., Parekh, V., Auden, A., Darido, C., Hislop, N.R., Cangkrama, M., Ting, S.B., and Jane, S.M. (2011). The unique and cooperative roles of the Grainy head-like transcription factors in epidermal development reflect unexpected target gene specificity. Dev. Biol. *349*, 512–522.

Bray, S.J., and Kafatos, F. (1991). Developmental function of Elf-1: an essential transcription factor during embryogenesis in Drosophila. Genes Dev. *5*, 1672–1683.

Bray, S.J., Burke, B., Brown, N.H., and Hirsh, J. (1989). Embryonic

expression pattern of a family of Drosophila proteins that interact witn a central nervous system regulatory element. Genes Dev. *1019*, 1130–1145.

Caddy, J., Wilanowski, T., Darido, C., Dworkin, S., Ting, S.B., Zhao, Q., Rank, G., Auden, A., Srivastava, S., Papenfuss, T. a, et al. (2010). Epidermal wound repair is regulated by the planar cell polarity signaling pathway. Dev. Cell *19*, 138–147.

Carvalho, L., Jacinto, A., and Matova, N. (2014). The Toll/NF-κB signaling pathway is required for epidermal wound repair in Drosophila. Proc. Natl. Acad. Sci. U. S. A. *111*, E5373-82.

Cooper, M.S., Szeto, D.P., Sommers-Herivel, G., Topczewski, J., Solnica-Krezel, L., Kang, H.C., Johnson, I., and Kimelman, D. (2005). Visualizing morphogenesis in transgenic zebrafish embryos using BODIPY TR methyl ester dye as a vital counterstain for GFP. Dev. Dyn. *232*, 359–368.

Dieckgraefe, B.K., and Weems, D.M. (1999). Epithelial injury induces Egr-1 and Fos expression by a pathway involving protein kinase C and ERK. Am. J. Physiol. Gastrointest. Liver Physiol. *276*, 322–330.

Dworkin, S., Darido, C., Georgy, S.R., Wilanowski, T., Srivastava, S., Ellett, F., Pase, L., Han, Y., Meng, A., Heath, J.K., et al. (2012). Midbrain-hindbrain boundary patterning and morphogenesis are regulated by diverse grainy head-like 2-dependent pathways. Development *536*, 525–536.

Ellis, K., Bagwell, J., and Bagnat, M. (2013). Notochord vacuoles are lysosome-related organelles that function in axis and spine morphogenesis. J. Cell Biol. *200*, 667–679.

Eriksson, J., and Löfberg, J. (2000). Development of the hypochord and dorsal aorta in the zebrafish embryo (Danio rerio). J. Morphol. *244*, 167–176.

Fukazawa, C., Santiago, C., Park, K.M., Deery, W.J., De, S.G., Canny, T., Holterhoff, C.K., and Wagner, D.S. (2010). poky/chuk/ikk1 is required for

differentiation of the zebrafish embryonic epidermis. Dev. Biol. *346*, 272–283.

Furuse, M., and Tsukita, S. (2006). Claudins in occluding junctions of humans and flies. Trends Cell Biol. *16*, 181–188.

Garcia-Fernandez, B., Campos, I., Geiger, J., Santos, A.C., and Jacinto, A. (2009). Epithelial resealing. Int. J. Dev. Biol. *53*, 1549–1556.

Geiger, J., Carvalho, L., Campos, I., Santos, A.C., and Jacinto, A. (2011). Hole-in-one mutant phenotypes link EGFR/ERK signaling to epithelial tissue repair in Drosophila. PLoS One *6*, e28349.

Guillot, C., and Lecuit, T. (2013). Mechanics of Epithelial Tissue Homeostasis and Morphogenesis. Science *340*, 1185–1189.

Hammond, C.L., and Schulte-Merker, S. (2009). Two populations of endochondral osteoblasts with differential sensitivity to Hedgehog signalling. Development *136*, 3991–4000.

Han, Y., Mu, Y., Li, X., Xu, P., Tong, J., Liu, Z., Ma, T., Zeng, G., Yang, S., Du, J., et al. (2011). Grhl2 deficiency impairs otic development and hearing ability in a zebrafish model of the progressive dominant hearing loss DFNA28. Hum. Mol. Genet. *20*, 3213–3226.

Heasman, J. (2002). Morpholino Oligos: Making Sense of Antisense? Dev. Biol. *243*, 209–214.

Hemphälä, J., Uv, A., Cantera, R., Bray, S., and Samakovlis, C. (2003). Grainy head controls apical membrane growth and tube elongation in response to Branchless/FGF signalling. Development *130*, 249–258.

Hwang, W.Y., Fu, Y., Reyon, D., Maeder, M.L., Shengdar, Q., Sander, J.D., Peterson, R.T., Yeh, J.J., and Keith, J. (2013). Efficient In Vivo Genome Editing Using RNA-Guided Nucleases Woong. Nat. Biotechnol. *31*, 227–229.

Janicke, M., Renisch, B., and Hammerschmidt, M. (2010). Zebrafish grainyhead-like1 is a common marker of different non-keratinocyte epidermal cell lineages, which segregate from each other in a Foxi3-dependent manner. Int. J. Dev. Biol. *54*, 837–850.

Jinek, M., Chylinski, K., Fonfara, I., Hauer, M., Doudna, J.A., and Charpentier, E. (2012). A Programmable Dual-RNA–Guided DNA Endonuclease in Adaptive Bacterial Immunity. Science *337*, 816–822.

Kapuscinski, J. (1995). DAPI: a DNA-Specific Fluorescent Probe. Biotech. Histochem. *70*, 220–233.

Kim, M., and McGinnis, W. (2011). Phosphorylation of Grainy head by ERK is essential for wound-dependent regeneration but not for development of an epidermal barrier. Proc. Natl. Acad. Sci. U. S. A. *108*, 650–655.

Köppen, M., Fernández, B.G., Carvalho, L., Jacinto, A., and Heisenberg, C.-P. (2006). Coordinated cell-shape changes control epithelial movement in zebrafish and Drosophila. Development *133*, 2671–2681.

de la Garza, G., Schleiffarth, J.R., Dunnwald, M., Mankad, A., Weirather, J.L., Bonde, G., Butcher, S., Mansour, T. a, Kousa, Y. a, Fukazawa, C.F., et al. (2012). Interferon Regulatory Factor 6 Promotes Differentiation of the Periderm by Activating Expression of Grainyhead-Like 3. J. Invest. Dermatol. *133*, 68–77.

Langley, A.R., Smith, J.C., Stemple, D.L., and Harvey, S.A. (2014). New insights into the maternal to zygotic transition. Development *141*, 3834–3841.

Liaw, G.J., Rudolph, K.M., Huang, J.D., Dubnicoff, T., Courey, A.J., and Lengyel, J.A. (1995). The torso response element binds GAGA and NTF-1/Elf-1, and regulates tailless by relief of repression. Genes Dev. *9*, 3163–3176.

Livak, K.J., and Schmittgen, T.D. (2001). Analysis of relative gene

expression data using real-time quantitative PCR and the 2(-Delta Delta C(T)) Method. Methods *25*, 402–408.

Löfberg, J., and Collazo, A. (1997). Hypochord, an enigmatic embryonic structure: Study of the axolotl embryo. J. Morphol. *232*, 57–66.

Mace, K.A., Pearson, J.C., and McGinnis, W. (2005). An epidermal barrier wound repair pathway in Drosophila is mediated by grainy head. Science *308*, 381–385.

Mateus, R., Pereira, T., Sousa, S., de Lima, J.E., Pascoal, S., Saúde, L., and Jacinto, A. (2012). In vivo cell and tissue dynamics underlying zebrafish fin fold regeneration. PLoS One *7*, e51766.

Moussian, B., and Uv, A.E. (2005). An ancient control of epithelial barrier formation and wound healing. BioEssays *27*, 987–990.

Narasimha, M., Uv, A., Krejci, A., Brown, N.H., and Bray, S.J. (2008). Grainy head promotes expression of septate junction proteins and influences epithelial morphogenesis. J. Cell Sci. *121*, 747–752.

Neugebauer, J.M., Amack, J.D., Peterson, A.G., Bisgrove, B.W., and Yost, H.J. (2009). FGF signalling during embryo development regulates cilia length in diverse epithelia. Nature *458*, 651–654.

Niessen, C.M. (2007). Tight junctions/adherens junctions: basic structure and function. J. Invest. Dermatol. *127*, 2525–2532.

Oppenheimer, J. (1936). Transplantation experiments on Developing Teleosts (Fundulus and Perca). J. Exp. Zool. *72*, 409–437.

Paré, A., Kim, M., Juarez, M.T., Brody, S., and McGinnis, W. (2012). The functions of Grainy Head-like proteins in animals and fungi and the evolution of apical extracellular barriers. PLoS One *7*, e36254.

Placzek, M., and Briscoe, J. (2005). The floor plate: multiple cells, multiple signals. Nat. Rev. Neurosci. *6*, 230–240.

Pyrgaki, C., Liu, A., and Niswander, L. (2011). Grainyhead-like 2 regulates neural tube closure and adhesion molecule expression during neural fold fusion. Dev. Biol. *353*, 38–49.

Rifat, Y., Parekh, V., Wilanowski, T., Hislop, N.R., Auden, A., Ting, S.B., Cunningham, J.M., and Jane, S.M. (2010). Regional neural tube closure defined by the Grainy head-like transcription factors. Dev. Biol. *345*, 237–245.

Schindelin, J., Arganda-Carreras, I., Frise, E., Kaynig, V., Longair, M., Pietzsch, T., Preibisch, S., Rueden, C., Saalfeld, S., Schmid, B., et al. (2012). Fiji: an open-source platform for biological-image analysis. Nat. Methods *9*, 676–682.

Senga, K., Mostov, K.E., Mitaka, T., Miyajima, A., and Tanimizu, N. (2012). Grainyhead-like 2 regulates epithelial morphogenesis by establishing functional tight junctions through the organization of a molecular network among claudin3, claudin4, and Rab25. Mol. Biol. Cell *23*, 2845–2855.

Shkumatava, A., Fischer, S., Müller, F., Strahle, U., and Neumann, C.J. (2004). Sonic hedgehog, secreted by amacrine cells, acts as a short-range signal to direct differentiation and lamination in the zebrafish retina. Development *131*, 3849–3858.

Solnica-Krezel, L. (2006). Gastrulation in zebrafish - all just about adhesion? Curr. Opin. Genet. Dev. *16*, 433–441.

Stemple, D.L. (2005). Structure and function of the notochord: an essential organ for chordate development. Development *132*, 2503–2512.

Tanimizu, N., and Mitaka, T. (2013). Role of grainyhead-like 2 in the formation of functional tight junctions. Tissue Barriers *1*, e23495.

Ting, S.B., Wilanowski, T., Auden, A., Hall, M., Voss, A.K., Thomas, T., Parekh, V., Cunningham, J.M., and Jane, S.M. (2003). Inositol- and folate-resistant neural tube defects in mice lacking the epithelial-specific factor

Grhl-3. Nat. Med. *9*, 1513–1519.

Ting, S.B., Caddy, J., Hislop, N., Wilanowski, T., Auden, A., Zhao, L.-L., Ellis, S., Kaur, P., Uchida, Y., Holleran, W.M., et al. (2005). A homolog of Drosophila grainy head is essential for epidermal integrity in mice. Science *308*, 411–413.

Tong, X., Xia, Z., Zu, Y., Telfer, H., Hu, J., Yu, J., Liu, H., Zhang, Q., Sodmergen, Lin, S., et al. (2013). NGS (Notochord Granular Surface) gene encodes a novel type of intermediate filament family protein essential for notochord maintenance in Zebrafish. J. Biol. Chem. *288*, 2711–2720.

Traylor-Knowles, N., Hansen, U., Dubuc, T.Q., Martindale, M.Q., Kaufman, L., and Finnerty, J.R. (2010). The evolutionary diversification of LSF and Grainyhead transcription factors preceded the radiation of basal animal lineages. BMC Evol. Biol. *10*, 101.

Wang, S., and Samakovlis, C. (2012). Grainy head and its target genes in epithelial morphogenesis and wound healing. (Amsterdam: Elsevier).

Wang, S., Tsarouhas, V., Xylourgidis, N., Sabri, N., Tiklová, K., Nautiyal, N., Gallio, M., and Samakovlis, C. (2009). The tyrosine kinase Stitcher activates Grainy head and epidermal wound healing in Drosophila. Nat. Cell Biol *11*, 890–895.

Werth, M., Walentin, K., Aue, A., Schönheit, J., Wuebken, A., Pode-Shakked, N., Vilianovitch, L., Erdmann, B., Dekel, B., Bader, M., et al. (2010). The transcription factor grainyhead-like 2 regulates the molecular composition of the epithelial apical junctional complex. Development *137*, 3835–3845.

Wilanowski, T., Caddy, J., Ting, S.B., Hislop, N.R., Cerruti, L., Auden, A., Zhao, L.-L., Asquith, S., Ellis, S., Sinclair, R., et al. (2008). Perturbed desmosomal cadherin expression in grainy head-like 1-null mice. EMBO J. *27*, 886–897.

Wood, W., Jacinto, A., Grose, R., Woolner, S., Gale, J., Wilson, C., and Martin, P. (2002). Wound healing recapitulates morphogenesis in Drosophila embryos. Nat. Cell Biol. *4*, 907–912.

Yamamoto, M., Morita, R., Mizoguchi, T., Matsuo, H., Isoda, M., Ishitani, T., Chitnis, A.B., Matsumoto, K., Crump, J.G., Hozumi, K., et al. (2010). Mib-Jag1-Notch signalling regulates patterning and structural roles of the notochord by controlling cell-fate decisions. Development *137*, 2527–2537.

Yao, L., Wang, S., Orzechowski-Westholm, J., Dai, Q., Matsuda, R., Hosono, C., Bray, S., Lai, E.C., and Samakovlis, C. (2017). Genome-wide identification of Grainy head targets in Drosophila reveals regulatory interactions with the POU-domain transcription factor, Vvl. Development *144*, 3145–3155.

7. Acknowledgements

I would like to thank Anabela Bensimon-Brito and Ana Sofia Brandão for the contribution to the experimental work and helpful discussions; the Fish Facility technicians at IMM, IGC and CEDOC (Lara M. Carvalho, Aida Barros, Maysa Franco, Fábio Valério e Petra Pintado) for support with animal care; Ana Farinho for the Histology work; Cláudia Andrade, Cláudia Bispo and the Flow Cytometry Facility at IGC for help with the cell sorting experiment; the Imaging Facilities at IGC and IMM.

8. Supplementary Data

8.1 Video Legends

Video S1. Closure dynamics in wild type zebrafish embryos. EVL epithelium in Zebrafish embryos injected with 50pg Utrophin-GFP, labelling F-actin, during wound healing. Epiboly stage, wounded in the animal pole, on the left and 24hpf, wounded over the yolk on the right. Images were acquired using a spinning disk imaging system (Revolution XD; Andor Technology). Frames were taken every 10 secs. Scale bar: 20 μm.

Video S2. Closure dynamics during epiboly in *grhl* morphants. EVL epithelium over the animal pole of Zebrafish embryos injected with 50pg Utrophin-GFP, labelling F-actin, during wound healing. Embryo injected with 2ng standard control morpholino on the left, *grhl2b* morphant injected with 2ng morpholino in the middle, and and *grhl3* morphant injected with 2ng morpholino on the right. Images were acquired using a spinning disk imaging system (Revolution XD; Andor Technology). Frames were taken every 10 secs. Scale bar: 20 μm.

8.2 Sequence alignment

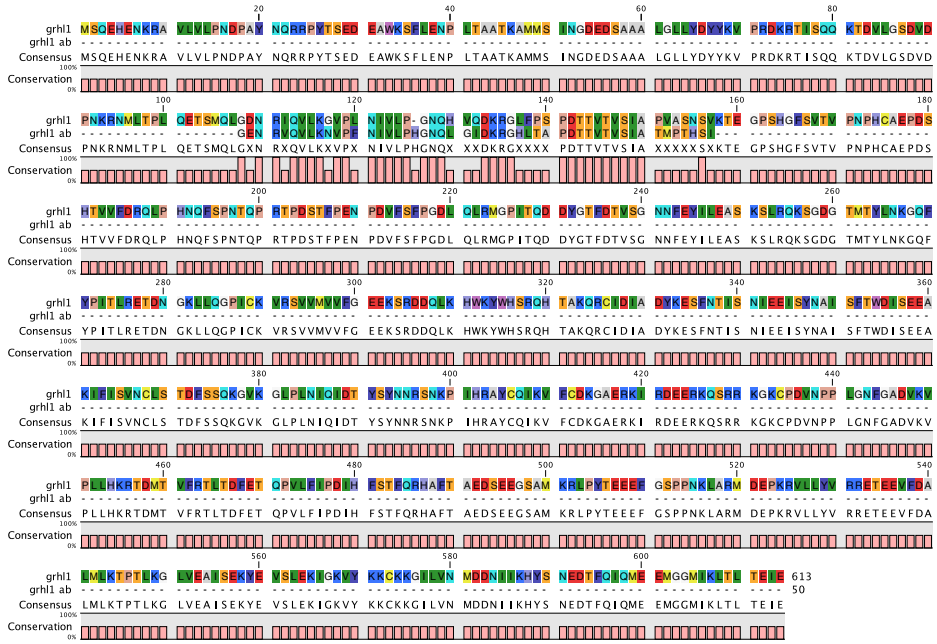

Figure S1. Peptide Sequence alignment between zGrhl1 and anti-Grhl1 antigen.

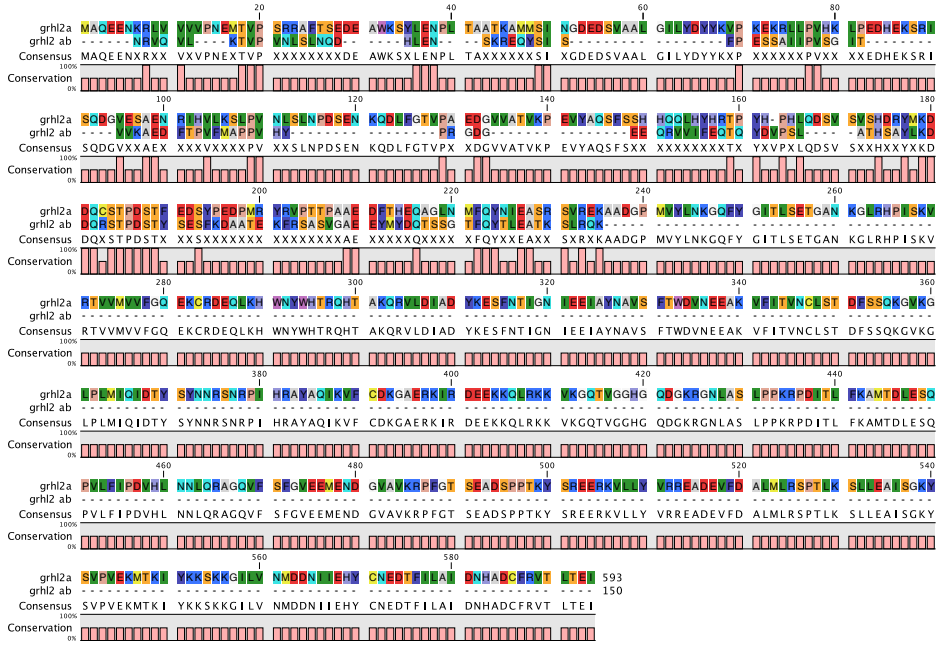

Figure S2. Peptide Sequence alignment between zGrhl2a and anti-Grhl2 antigen.

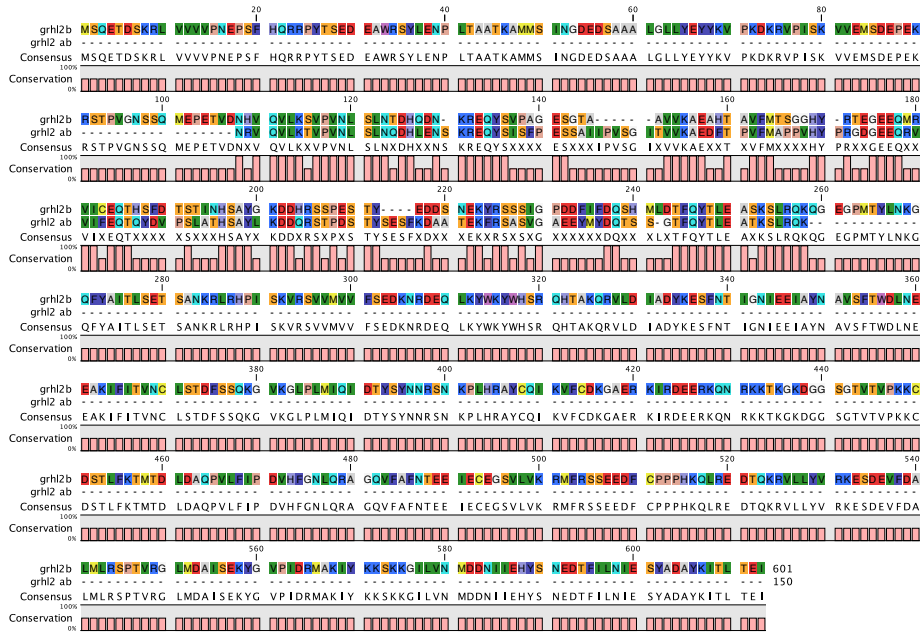

Figure S3. Peptide Sequence alignment between zGrhl2b and anti-Grhl2 antigen.

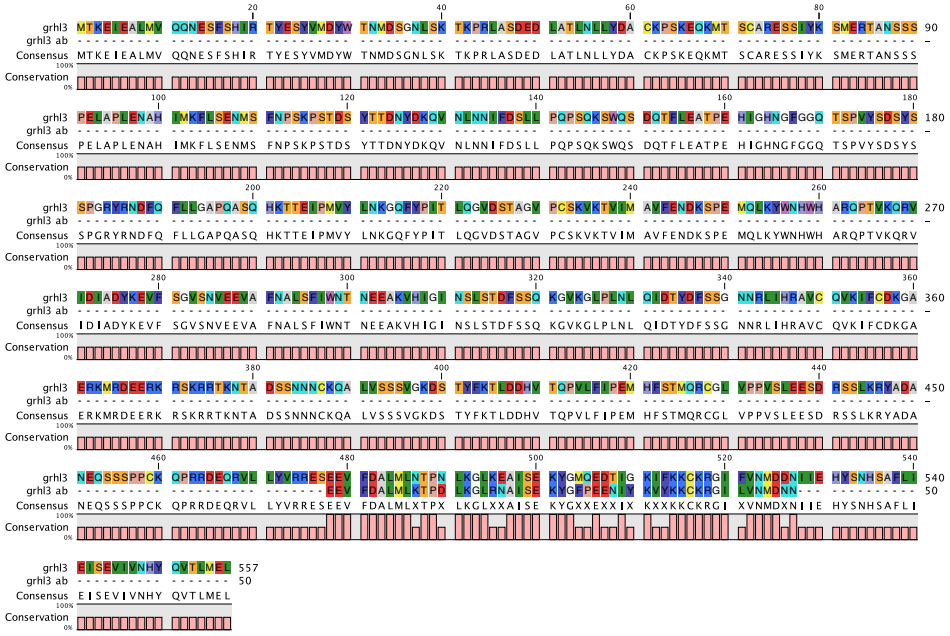

Figure S4. Peptide Sequence alignment between zGrhl3 and anti-Grhl3 antigen.

CHAPTER V

General Discussion:

Integrating Knowledge

“ *Never tell me the odds!* ”

Han Solo,

in *Star Wars: Episode V - The Empire Strikes Back*

Contents

A coordinated sequence of cellular events is the core of the wound repair process. Sensing the stress, reorganizing structure, and activating specialized molecular players, need to be tightly regulated for an efficient recovery of tissue integrity. This applies to simple epithelia or to more complex epidermal tissues. In recent years, this field of study has thrived with the use of several model systems across different species. The major goal is to understand how cells, and ultimately the tissues, cope with and respond to aggression and injury infliction. Although, from a biomedical point of view, the unravelling of the mechanisms of repair of complex stratified epithelia is the ultimate goal, the molecular basis of tissue repair is more accessible through the analysis of simple epithelia. This is due to the conservation of the molecular players and processes of wound healing across different species. Adding to this, simple epithelia are capable of restoring tissue integrity in a scar-free manner. This might prove valuable for the understanding and future manipulation of scar formation in the vertebrate repair process. With this work, focused on simple epithelia and purse string closure, I analysed the role of Grainy head (Grh), a transcription factor associated with epithelial formation and development, in the process of wound repair. I show how Grh can be involved in the several levels of regulation of the wound healing protocol of simple epithelia. These findings complement the already described functions for Grh in wound response gene activation and cuticle repair (Kim and McGinnis, 2011; Mace et al., 2005), cementing its role as a master regulator of epithelial maintenance.

Adhesion and cytoskeletal reorganization promote tissue integrity and identity

This study shows that Grh regulates the expression and dynamics of E-Cad during both early and late stages of wound response in the *Drosophila* pupal notum epithelium. Adhesion complexes can act as mechanical sensing hubs with a tight link to the cytoskeleton (Martin et al., 2010; Michael and Yap, 2013; Sawyer et al., 2009), mutually regulating each other (Borghi and Nelson, 2009; Smutny et al., 2010). Upon wounding, there is an imperative need for a high turnover and downregulation of E-Cad, not only to accommodate cell shape changes, but also for the regulation of the actomyosin cytoskeleton (Carvalho et al., 2014; Hunter et al., 2015; Matsubayashi et al., 2015). In the pupal notum epithelium, the tissue displacement resultant from the injury leads to the possible dilution of the cadherin complexes along the stretched membranes (Antunes et al., 2013). Downregulation of E-Cad is required at the leading edge for the accumulation of the actomyosin filaments and the formation of the supracellular cable (Carvalho et al., 2014; Hunter et al., 2015). This redistribution of E-Cad along the membrane might be essential for the propagation of the actomyosin flow in the pupal epithelium. Previous studies have also shown that differential distribution and downregulation of E-Cad along the membrane are important for the directionality and polarization of contractile actomyosin flows within the cell driving cellular rearrangements (Pinheiro et al., 2017; Rauzi et al., 2010). The actomyosin flow generated upon wounding of the pupal epithelium can be a tissue level version of this behaviour. Our work has shown that overall downregulation of E-Cad levels leads to the impairment of this flow, showing the need to tightly control the levels of adhesion to promote the essential cytoskeletal reorganization. Moreover, we propose that E-Cad regulation is achieved by Grh. We show that Grh transcriptionally represses the expression of *e-cad* in homeostatic

conditions, situation that is counteracted in the wound response. This differential regulation might result from context specific partners of Grh activity. Grh has been shown to interact or compete with other transcription factors to differentially regulate gene expression (Wang and Samakovlis, 2012). In this study, we propose a new regulatory interaction for Grh upon wounding. As Dorsal (Dl) is activated upon wounding, promoting cortical E-Cad downregulation, Grh represses (or inhibits) this effector of the Toll/NF-κB signalling pathway, in order to control E-Cad downregulation to the minimum required. In the absence of Grh, this downregulation escalates, leading to exacerbated depletion of E-Cad through Dl. This results in profound defects in the cytoskeleton dynamics and cellular behaviour. This adhesion deregulation, adding to other phenotypes resultant of Grh KD, leads to loss of cortical stability and epithelial identity. These characteristics are common to Epithelia-Mesenchymal Transition (EMT). Our model allowed us to observe the cellular transitions that lead to a mesenchymal-like state around the wound, in the absence of Grh. Nevertheless, the interaction between Grh and Dl needs to be further addressed, to understand its biochemical nature and if post-translational modifications in the Grh protein can trigger it. One hypothesis is this interaction may be driven by the phosphorylation of Grh by ERK upon wounding, that is also important for the wound response genes activation (Kim and McGinnis, 2011). This post-translational modification might induce the direct binding of Grh to Dl to repress Dl activity.

The most phenotypically intriguing characteristic of the Grh knockdown (KD) phenotype is the displacement of the actomyosin cable away from the leading edge. This might be explained by the abrupt change in the adhesion characteristics of the tissue surrounding the wound. Supracellular cables are also found in areas between differential adhesion, like compartment boundaries (Röper, 2013) or when adhesion is downregulated in patches of mutant cells (Ho et al., 2010; Sarpal et al., 2012; Wei et al., 2005). This

correlates with the delocalization of the actomyosin cable in the Grh KD upon wounding, since it localizes at the boundary where E-Cad depletion starts. Hence, the site of ectopic cable formation may be related to the limit of tissue responsiveness to the wound. Although several mechanosensing and mechanotransduction processes have been studied across different systems and developmental processes (Petridou et al., 2017), what determines the range of the wound response in the *Drosophila* notum epithelium is still not understood. Calcium is one of the factors potentially associated with the extent of response activation within the tissue.

Calcium and the start of wound healing

Increased intracellular calcium is the first documented event resulting from epithelial injury (Cordeiro and Jacinto, 2013; Sonnemann and Bement, 2011). It represents a conserved method across species to rapidly signal the existence of a wound to the surrounding tissue (Razzell et al., 2013; Xu and Chisholm, 2011; Yoo et al., 2012). In the *Drosophila* pupa notum epithelium, this increase originates from the wound site and extends to several cell rows across the tissue, dependent on wound size. This leads to the initiation of a sequential series of flows essential for closure in this system (Antunes et al., 2013). In this study, we brought new insights to calcium dynamics upon wounding, showing that the initial steps of calcium increase are actually divided in two stages: a first abrupt increase of calcium within the cells, as fast as 50 milliseconds after wounding, followed by a second expansion characterized by apparently stochastic calcium flashes. The initial outburst that occurs during the 30 to 60 seconds after wounding might be a direct consequence of the tissue displacement, probably due to mechanical response to tension disruption. The second calcium expansion may be linked to cell-to-cell communication mechanisms (Narciso et al., 2015), amplifying the calcium signalling through biochemical processes.

Nevertheless, this correlation needs to be further analysed. In addition, this study shows that the calcium wave is also visible across the mitochondrial population of the cells affected by tissue displacement. This observation was also made in *C. elegans* (Xu and Chisholm, 2014), suggesting that mitochondria might be involved in wound healing in a conserved manner.

In this study, we show that Grh KD leads to deregulation of calcium dynamics upon wounding, with cells accumulating intracellular calcium for a long period of time. As a transcription factor, Grh regulates hundreds of genes involved in several processes in the epithelial cell (Yao et al., 2017). Among them are several genes linked to calcium regulation. This study is thus the first evidence that Grh regulates calcium dynamics, by unveiling new target genes that affect calcium dynamics upon wounding. This opens exciting new lines of study, to understand the functions of these new effectors on calcium dynamics. Moreover, we show that the deregulation of calcium in the KD of the target genes is concomitant with alterations in the cytoskeletal dynamics and actin cable formation, leading to closure defects. Calcium increase in wound healing is intimately linked to cytoskeletal rearrangement (Antunes et al., 2013; Clark et al., 2009). In the *Drosophila* pupal notum, calcium is important for the activation of Gelsolin, an actin-severing protein that promotes the increase of the monomeric pool of actin to use in the following round of high polymerization levels during wound closure (Antunes et al., 2013). Accumulation of high levels of calcium in the Grh KD might lead to a constant activation of Gelsolin, which could be one of the reasons for the abnormal actin polymerization in the cells around the wound. Due to the pleiotropic effect of calcium in the cellular environment, this may not be the only aspect interfering with proper cytoskeletal dynamics. Taking this into account, we should consider the effects of the E-Cad depletion referred previously, resultant of Dl misregulation. It is necessary to note that calcium dynamics does not only affect cytoskeletal reorganization. Calcium might also regulate NF-κB pathway activity

(Lilienbaum and Israel, 2003; Tabary et al., 2006). In this study, our proposed hyperactivation of Dorsal (Dl), the pathway effector, results from the deregulation of Dl transcripts in the absence of Grh, pointing to a repression activity of Grh over Dl. Additionally, Dl activation might be exacerbated by the deregulation of calcium dynamics. High levels of calcium lead to destabilization of Cactus, the Dl inhibitor, and consequent activation of the pathway (Kubota and Gay, 1995). These different regulatory levels might explain the phenotype severity of the Grh KD. Hence, the novel role for Grh in the regulation of calcium dynamics opens a new unexplored field of research in epithelia development and repair.

Altogether, by showing the importance of Grh in regulating calcium, adhesion and cytoskeletal dynamics, and considering the already described functions of this TF in epithelial barrier restoration (Kim and McGinnis, 2011; Mace et al., 2005), this study heightens the role of Grh as a master regulator of the stress response and epithelial identity during *Drosophila* epithelial wound healing.

New functions for Grainy head in vertebrate development and wound repair

In order to complement the study of simple epithelial wound repair, we decided to explore the possible roles of the *grainyhead-like* (*grhl*) genes in a vertebrate system. For that, we used Zebrafish, focusing on embryonic development and the formation and repair of its simple epithelia. All four *grhl* genes show a high degree of conservation regarding its invertebrate homologue (Janicke et al., 2010). In this study, we characterize the expression of the different *grhl* genes during the first 48 hours post fertilization. We identified for the first time the presence of a Grhl protein in the notochord, floor plate and hypochord, important organs for the axis and

structural support of the developing Zebrafish larva (Stemple, 2005). Although unexpected, since none of these three organs are ectodermal-derived, the expression of Grhl2 correlates with the phenotypic epithelial characteristics of these cells. The notochord conveys the structural rigidity for the developmental of the Zebrafish larva, while the skeletal structures are not fully formed. In order to sustain the swimming movements essential for the survival of the animal, the notochord cells are subjected to internal hydrostatic pressure (Ellis et al., 2013; Stemple, 2005), where regulation of adhesion might play an essential role. The expression of adhesion molecules, like desmosomal cadherins, have been observed in the notochord (Goonesinghe et al., 2012), which may contribute to the referred structural regulation. Interestingly, one of the Grhl TFs has been shown to regulate desmosomal cadherin expression in mice (Wilanowski et al., 2008), which suggests a similar possible function of Grhl expression in the Zebrafish notochord. With the generation of the *grhl2* zebrafish mutants, it would be interesting to further address this new role of Grh in vertebrate organogenesis.

We also observed the deregulation of adhesion molecules in the simple vertebrate epithelia, upon KD of Grhl expression, which correlates with the proposed function of Grhl proteins in vertebrate development (Werth et al., 2010; Yu et al., 2006). This deregulation might be important in the context of wound repair. To address this, we setup a new wound healing model in Zebrafish simple epithelia. This allowed us to take advantage of live imaging of cellular dynamics to analyse the contribution of Grhl TFs to the process of wound healing in simple vertebrate epithelia. Although preliminary, our results show alterations in contractile cable formation and delay in the repair process in the absence of one of the Grhl TFs. This is in line with what is published in other vertebrate systems, such as *Xenopus* and mice (Caddy et al., 2010; Ting et al., 2005). Despite being the first observed evidence of the contribution of Grhl TFs to Zebrafish wound repair, the functional

mechanism of action stills needs to be dissected in future studies. Furthermore, in addition to the KD experiments, the now available mutant Zebrafish lines will provide a more accurate understanding of the role for these genes.

Main conclusions

Taken together, the results of this study show important roles for Grh in wound repair: regulation of adhesion and cytoskeletal dynamics in early and later stages of the wound healing process; control of cortical stability and epithelial identity through maintenance of adhesion integrity; the regulation of intracellular calcium dynamics and consequent reorganization of the actin cytoskeleton. By unveiling new functions and partners for Grh in epithelial formation and repair, complemented by the existing reports throughout several animal species, we can propose the Grh TFs family as master regulators of epidermal tissue stability and important managers of the stress response mechanism.

Future perspectives

Targeting Calcium

Calcium signalling and dynamics consitute one of the first signals upon wounding, and one of the most intriguing aspects of wound repair. Although several studies have shown its importance and downstream targets (Lansdown, 2002; Moe et al., 2015), the rapid increase, decrease and source of this calcium fluctuation still need to be comprehensively addressed and understood. Despite a few studies regarding internal calcium

storages (Xu and Chisholm, 2014), cell-to-cell propagation of calcium molecules through gap junctions (Narciso et al., 2015; Razzell et al., 2013; Solan and Lampe, 2016) and regulation of cytoskeletal dynamics by calcium modulation (Antunes et al., 2013), the regulation of proper tissue closure modulated by these processes still needs to be further addressed. Since calcium has been shown to improve wound healing, understanding the mechanism by which this happens might prove to be of great importance to applied biomedical studies (Lansdown, 2002). One hypothesis for calcium modulation might be interfering with internal calcium storages, such as mitochondria. These organelles are known to respond morphologically to mechanical stimuli, through fission and fusion processes, that consequently influence the release or uptake of intracellular calcium. Moreover, mitochondria and actin cytoskeleton have been shown to interact (Bartolák-Suki et al., 2017; Prudent et al., 2016). The relevance of these interactions and dynamic morphology chenages has not yet been addressed in the process of wound repair and might prove to be important in the whole regulatory chain of the closure process.

Toll receptors and wound healing

Toll-like receptors are commonly linked to the activation of the inflammatory response in response triggered by microorganisms aggression (Chen and DiPietro, 2017; Dasu and Isseroff, 2012; Hultmark, 2003; Matova and Anderson, 2006), but their functions are not only confined to the immune response. In *Drosophila,* the differential expression of Toll-like receptors was shown to regulate actomyosin-driven junctional remodelling during morphogenetic cellular rearrangements (Paré et al., 2014). Additionally, they regulate adhesion dynamics through the activation of the NF-κB factor Dl (Carvalho et al., 2014). In this study, we propose a novel interaction

between Grh and Dl in the regulation of the wound response. Supporting our model, the Toll/NF-κB pathway was recently shown to regulate the expression of the same wound response genes as Grh to promote epithelial barrier repair (Capilla et al., 2017). Further assessment of the biochemical nature of the interaction between Grh and NF-κb would be useful to clarify the cross talk between these two main regulatory pathways in wound healing. Additionally, the study of this interaction in the vertebrate tissue would be of high biomedical relevance, as they could be possible therapeutical targets to resolve of tissue injuries.

Wound healing and EMT – an entry point for cancer

In this study, we show that Grh depletion leads to the upregulation of mesenchymal markers normally repressed in epithelial tissues. Upon wounding, the loss of junctional E-Cad in cells around the wound seems to make them lose their apical cortical stability. These cells then acquire mesenchymal morphological characteristics, like cell rounding and filopodia emission, in a process resembling EMT (Nieto et al., 2016). This transformation of cellular identity can occur during the development of an organism, but it is also commonly associated with cancerous and invasive phenotypes (Baum et al., 2008; Moustakas and de Herreros, 2017). During the re-epithelialization stages of wound healing in complex epithelia, cells need to convert from a sedentary to a proliferative and migratory profile, through the process of EMT (Leopold et al., 2012). Interestingly, the deregulation in the control of this process can result in abnormal scaring or even cancer (Dvorak, 1986). In vertebrates, Grh has been proposed to be important in the modulation of this process (Cieply et al., 2012, 2013). In invertebrate simple epithelia repair, due to the lack of proliferation necessary for wound closure, this topic was never addressed. Also, the rapid

reorganization of the cytoskeleton in order to quickly close the wound might be preventing this transition. But in the absence of Grh and consequent cytoskeletal deregulation, EMT might be the solution the tissue finds to survive. It would be interesting to address this through the full characterization of the protein signature of these cells to understand if invertebrate and vertebrate epithelial repair have more in common than what is assumed so far.

Zebrafish embryonic and larval epithelia in wound repair

Vertebrate wound healing models are commonly associated with complex epithelia (Dorsett-Martin and Wysocki, 2008; Dunn et al., 2013). Adult Zebrafish has emerged in the wound repair field as a good model system to analyse scar-free skin repair due to its high regenerative capacity (Richardson et al., 2013). Although this system can be useful for more comprehensive analysis of the several stages of the repair program, it is very amenable to live imaging of cellular dynamics. Zebrafish embryonic and larval epithelia bridge this gap to help understand the basis of the cellular changes. In this study, we establish a new model system for vertebrate epithelial repair, useful for the analysis of several parameters of wound closure using a live imaging approach. Furthermore, we show that the repair mechanism is conserved in both simple embryonic and larval two-layer stratified epithelia. Therefore, the larval tissue might also prove to be a useful alternative to embryonic and adult epithelia. Despite the obvious necessity to further analyse the role of Grhl TFs in vertebrate simple epithelia, these Zebrafish systems will be useful for the analysis of the interaction between Grhl TFs and the NF-κB pathway and to assess the conservation of this process across species.

References

Antunes, M., Pereira, T., Cordeiro, J. V., Almeida, L., and Jacinto, A. (2013). Coordinated waves of actomyosin flow and apical cell constriction immediately after wounding. J. Cell Biol. *202*, 365–379.

Bartolák-Suki, E., Imsirovic, J., Nishibori, Y., Krishnan, R., and Suki, B. (2017). Regulation of mitochondrial structure and dynamics by the cytoskeleton and mechanical factors. Int. J. Mol. Sci. *18*, 7–11.

Baum, B., Settleman, J., and Quinlan, M.P. (2008). Transitions between epithelial and mesenchymal states in development and disease. Semin. Cell Dev. Biol. *19*, 294–308.

Borghi, N., and Nelson, J.W. (2009). Intercellular Adhesion in Morphogenesis. Molecular and Biophysical Considerations. In Current Topics in Developmental Biology, T. Lecuit, ed. (Elsevier Inc.), pp. 1–32.

Caddy, J., Wilanowski, T., Darido, C., Dworkin, S., Ting, S.B., Zhao, Q., Rank, G., Auden, A., Srivastava, S., Papenfuss, T. a, et al. (2010). Epidermal wound repair is regulated by the planar cell polarity signaling pathway. Dev. Cell *19*, 138–147.

Capilla, A., Karachentsev, D., Patterson, R.A., Hermann, A., Juarez, M.T., and McGinnis, W. (2017). Toll pathway is required for wound-induced expression of barrier repair genes in the *Drosophila* epidermis. Proc. Natl. Acad. Sci. *114*, E2682–E2688.

Carvalho, L., Jacinto, A., and Matova, N. (2014). The Toll/NF-κB signaling pathway is required for epidermal wound repair in Drosophila. Proc. Natl. Acad. Sci. U. S. A. *111*, E5373-82.

Chen, L., and DiPietro, L.A. (2017). Toll-Like Receptor Function in Acute Wounds. Adv. Wound Care *6*, 344–355.

Cieply, B., Riley, P., Pifer, P.M., Widmeyer, J., Addison, J.B., Ivanov, A. V,

Denvir, J., and Frisch, S.M. (2012). Suppression of the Epithelial-Mesenchymal Transition by Grainyhead-Like-2. Cancer Res. *72*, 2440–2453.

Cieply, B., Farris, J., Denvir, J., Ford, H.L., and Frisch, S.M. (2013). Epithelial-mesenchymal transition and tumor suppression are controlled by a reciprocal feedback loop between ZEB1 and Grainyhead-like-2. Cancer Res. *73*, 6299–6309.

Clark, A.G., Miller, A.L., Vaughan, E., Yu, H.-Y.E., Penkert, R., and Bement, W.M. (2009). Integration of single and multicellular wound responses. Curr. Biol. *19*, 1389–1395.

Cordeiro, J. V, and Jacinto, A. (2013). The role of transcription-independent damage signals in the initiation of epithelial wound healing. Nat. Rev. Mol. Cell Biol. *14*, 249–262.

Dasu, M.R., and Isseroff, R.R. (2012). Toll-like receptors in wound healing: location, accessibility, and timing. J. Invest. Dermatol. *132*, 1955–1958.

Dorsett-Martin, W. a., and Wysocki, A.B. (2008). Rat Models of Skin Wound Healing. Sourceb. Model. Biomed. Res. 631–638.

Dunn, L., Prosser, H.C.G., Tan, J.T.M., Vanags, L.Z., Ng, M.K.C., and Bursill, C.A. (2013). Murine Model of Wound Healing. J. Vis. Exp. *75*, e50265.

Dvorak, H.F. (1986). Tumors: wounds that do not heal. Similarities between tumor stroma generation and wound healing. N. Engl. J. Med. *315*, 1650–1659.

Ellis, K., Bagwell, J., and Bagnat, M. (2013). Notochord vacuoles are lysosome-related organelles that function in axis and spine morphogenesis. J. Cell Biol. *200*, 667–679.

Goonesinghe, A., Luan, X.-M., Hurlstone, A., and Garrod, D. (2012). Desmosomal cadherins in zebrafish epiboly and gastrulation. BMC Dev.

Biol. *12*.

Ho, Y.-H., Lien, M.-T., Lin, C.-M., Wei, S.-Y., Chang, L.-H., and Hsu, J.-C. (2010). Echinoid regulates Flamingo endocytosis to control ommatidial rotation in the Drosophila eye. Development *137*, 745–754.

Hultmark, D. (2003). Drosophila immunity: Paths and patterns. Curr. Opin. Immunol. *15*, 12–19.

Hunter, M. V., Lee, D.M., Harris, T.J.C., and Fernandez-Gonzalez, R. (2015). Polarized E-cadherin endocytosis directs actomyosin remodeling during embryonic wound repair. J. Cell Biol. *210*, 801–816.

Janicke, M., Renisch, B., and Hammerschmidt, M. (2010). Zebrafish grainyhead-like1 is a common marker of different non-keratinocyte epidermal cell lineages, which segregate from each other in a Foxi3-dependent manner. Int. J. Dev. Biol. *54*, 837–850.

Kim, M., and McGinnis, W. (2011). Phosphorylation of Grainy head by ERK is essential for wound-dependent regeneration but not for development of an epidermal barrier. Proc. Natl. Acad. Sci. U. S. A. *108*, 650–655.

Kubota, K., and Gay, N.J. (1995). Calcium destabilises Drosophila cactus protein and dephosphorylates the dorsal transcription factor. Biochem. Biophys. Res. Commun. *214*, 1191–1196.

Lansdown, A.B.G. (2002). Calcium: A potential central regulator in wound healing in the skin. Wound Repair Regen. *10*, 271–285.

Leopold, P.L., Vincent, J., and Wang, H. (2012). A comparison of epithelial-to-mesenchymal transition and re-epitheliazation. Semin. Cancer Biol. *22*, 471–483.

Lilienbaum, A., and Israel, A. (2003). From Calcium to NF- B Signaling Pathways in Neurons. Mol. Cell. Biol. *23*, 2680–2698.

Mace, K.A., Pearson, J.C., and McGinnis, W. (2005). An epidermal barrier

wound repair pathway in Drosophila is mediated by grainy head. Science *308*, 381–385.

Martin, A.C., Gelbart, M., Fernandez-Gonzalez, R., Kaschube, M., and Wieschaus, E.F. (2010). Integration of contractile forces during tissue invagination. J. Cell Biol. *188*, 735–749.

Matova, N., and Anderson, K. V (2006). Rel/NF-kappaB double mutants reveal that cellular immunity is central to Drosophila host defense. Proc. Natl. Acad. Sci. U. S. A. *103*, 16424–16429.

Matsubayashi, Y., Coulson-Gilmer, C., and Millard, T.H. (2015). Endocytosis-dependent coordination of multiple actin regulators is required for wound healing. J. Cell Biol. *210*, 419–433.

Michael, M., and Yap, A.S. (2013). The regulation and functional impact of actin assembly at cadherin cell-cell adhesions. Semin. Cell Dev. Biol. *24*, 298–307.

Moe, A.M., Golding, A.E., and Bement, W.M. (2015). Cell healing: Calcium, repair and regeneration. Semin. Cell Dev. Biol. *45*, 18–23.

Moustakas, A., and de Herreros, A.G. (2017). Epithelial–mesenchymal transition in cancer. Mol. Oncol. *9*, 715–717.

Narciso, C., Wu, Q., Brodskiy, P., Garston, G., Baker, R., Fletcher, A., and Zartman, J. (2015). Patterning of wound-induced intercellular Ca 2+ flashes in a developing epithelium. Phys. Biol. *12*, 56005.

Nieto, M.A., Huang, R.Y.Y.J., Jackson, R.A.A., and Thiery, J.P.P. (2016). Emt: 2016. Cell *166*, 21–45.

Paré, A.C., Vichas, A., Fincher, C.T., Mirman, Z., Farrell, D.L., Mainieri, A., and Zallen, J. a. (2014). A positional Toll receptor code directs convergent extension in Drosophila. Nature *515*, 523–527.

Petridou, N.I., Spiró, Z., and Heisenberg, C.-P. (2017). Multiscale force

sensing in development. Nat. Cell Biol. *19*, 581–588.

Pinheiro, D., Hannezo, E., Herszterg, S., Bosveld, F., Gaugue, I., Balakireva, M., Wang, Z., Cristo, I., Rigaud, S.U., Markova, O., et al. (2017). Transmission of cytokinesis forces via E-cadherin dilution and actomyosin flows. Nature *545*, 103–107.

Prudent, J., Popgeorgiev, N., Gadet, R., Deygas, M., Rimokh, R., and Gillet, G. (2016). Mitochondrial Ca2+ uptake controls actin cytoskeleton dynamics during cell migration. Sci. Rep. *6*, 36570.

Rauzi, M., Lenne, P.-F., and Lecuit, T. (2010). Planar polarized actomyosin contractile flows control epithelial junction remodelling. Nature *468*, 1110–1114.

Razzell, W., Evans, I.R., Martin, P., and Wood, W. (2013). Calcium Flashes Orchestrate the Wound Inflammatory Response through DUOX Activation and Hydrogen Peroxide Release. Curr. Biol. *23*, 424–429.

Richardson, R., Slanchev, K., Kraus, C., Knyphausen, P., Eming, S., and Hammerschmidt, M. (2013). Adult zebrafish as a model system for cutaneous wound healing research. J. Invest. Dermatol. *133*, 1655–1665.

Röper, K. (2013). Supracellular actomyosin assemblies during development. Bioarchitecture *3*, 45–49.

Sarpal, R., Pellikka, M., Patel, R.R., Hui, F.Y.W., Godt, D., and Tepass, U. (2012). Mutational analysis supports a core role for Drosophila α-Catenin in adherens junction function. J. Cell Sci. *125*, 233–245.

Sawyer, J.K., Harris, N.J., Slep, K.C., Gaul, U., and Peifer, M. (2009). The Drosophila afadin homologue Canoe regulates linkage of the actin cytoskeleton to adherens junctions during apical constriction. J. Cell Biol. *186*, 57–73.

Smutny, M., Cox, H.L., Leerberg, J.M., Kovacs, E.M., Conti, M.A., Ferguson, C., Hamilton, N.A., Parton, R.G., Adelstein, R.S., and Yap, A.S. (2010).

Myosin II isoforms identify distinct functional modules that support integrity of the epithelial zonula adherens. Nat. Cell Biol. *12*, 696–702.

Solan, J.L., and Lampe, P.D. (2016). Kinase programs spatiotemporally regulate gap junction assembly and disassembly: Effects on wound repair. Semin. Cell Dev. Biol. *50*, 40–48.

Sonnemann, K.J., and Bement, W.M. (2011). Wound repair: toward understanding and integration of single-cell and multicellular wound responses. Annu. Rev. Cell Dev. Biol. *27*, 237–263.

Stemple, D.L. (2005). Structure and function of the notochord: an essential organ for chordate development. Development *132*, 2503–2512.

Tabary, O., Boncoeur, E., De Martin, R., Pepperkok, R., Clément, A., Schultz, C., and Jacquot, J. (2006). Calcium-dependent regulation of NF-κB activation in cystic fibrosis airway epithelial cells. Cell. Signal. *18*, 652–660.

Ting, S.B., Caddy, J., Hislop, N., Wilanowski, T., Auden, A., Zhao, L.-L., Ellis, S., Kaur, P., Uchida, Y., Holleran, W.M., et al. (2005). A homolog of Drosophila grainy head is essential for epidermal integrity in mice. Science *308*, 411–413.

Wang, S., and Samakovlis, C. (2012). Grainy head and its target genes in epithelial morphogenesis and wound healing. In Current Topics in Developmental Biology, S. Plaza, and F. Payre, eds. (Amsterdam: Elsevier Inc.), pp. 35–63.

Wei, S.-Y., Escudero, L.M., Yu, F., Chang, L.-H., Chen, L.-Y., Ho, Y.-H., Lin, C.-M., Chou, C.-S., Chia, W., Modolell, J., et al. (2005). Echinoid is a component of adherens junctions that cooperates with DE-Cadherin to mediate cell adhesion. Dev. Cell *8*, 493–504.

Werth, M., Walentin, K., Aue, A., Schönheit, J., Wuebken, A., Pode-Shakked, N., Vilianovitch, L., Erdmann, B., Dekel, B., Bader, M., et al. (2010). The transcription factor grainyhead-like 2 regulates the molecular

composition of the epithelial apical junctional complex. Development *137*, 3835–3845.

Wilanowski, T., Caddy, J., Ting, S.B., Hislop, N.R., Cerruti, L., Auden, A., Zhao, L.-L., Asquith, S., Ellis, S., Sinclair, R., et al. (2008). Perturbed desmosomal cadherin expression in grainy head-like 1-null mice. EMBO J. *27*, 886–897.

Xu, S., and Chisholm, A.D. (2011). A Gα(q)-Ca(2+) Signaling Pathway Promotes Actin-Mediated Epidermal Wound Closure in C. elegans. Curr. Biol. *21*, 1960–1967.

Xu, S., and Chisholm, A.D. (2014). C. elegans Epidermal Wounding Induces a Mitochondrial ROS Burst that Promotes Wound Repair. Dev. Cell *31*, 48–60.

Yao, L., Wang, S., Orzechowski-Westholm, J., Dai, Q., Matsuda, R., Hosono, C., Bray, S., Lai, E.C., and Samakovlis, C. (2017). Genome-wide identification of Grainy head targets in Drosophila reveals regulatory interactions with the POU-domain transcription factor, Vvl. Development *144*, 3145–3155.

Yoo, S.K., Freisinger, C.M., LeBert, D.C., and Huttenlocher, a. (2012). Early redox, Src family kinase, and calcium signaling integrate wound responses and tissue regeneration in zebrafish. J. Cell Biol. *199*, 225–234.

Yu, Z., Lin, K.K., Bhandari, A., Spencer, J. a, Xu, X., Wang, N., Lu, Z., Gill, G.N., Roop, D.R., Wertz, P., et al. (2006). The Grainyhead-like epithelial transactivator Get-1/Grhl3 regulates epidermal terminal differentiation and interacts functionally with LMO4. Dev. Biol. *299*, 122–136.